Molecular Drivers of Pediatric Acute Lymphoblastic Leukemia

Toward targeted therapy for children with ALL

Roel Polak

Molecular drivers of pediatric acute lymphoblastic leukemia; toward targeted therapy for children with ALL.

ISBN: 978-94-6233-805-0

Cover design: Roel Polak
Layout: Gildeprint, Enschede, The Netherlands
Printing: Gildeprint, Enschede, The Netherlands

The work described in this thesis was performed at the Department of Hematology and the Department of Pediatric Oncology of the Erasmus University Medical Center, Rotterdam, the Netherlands. The work was funded by KIKA (Children Cancer Free), KWF Kankerbestrijding (Dutch Cancer Society), and SKOCR.

Printing of this thesis was financially supported by SKOCR.

Molecular Drivers of Pediatric Acute Lymphoblastic Leukemia

Toward targeted therapy for children with ALL

Moleculaire determinanten van acute lymfatische leukemie bij kinderen;
op weg naar therapie op maat voor kinderen met ALL

Proefschrift

ter verkrijging van de graad van doctor aan de
Erasmus Universiteit Rotterdam
op gezag van de
rector magnificus

Prof.dr. H.A.P. Pols

en volgens besluit van het College voor Promoties.
De openbare verdediging zal plaatsvinden op
woensdag 22 november 2017 om 09:30 uur

door

Roel Polak
geboren te Alkmaar

Erasmus University Rotterdam

PROMOTIECOMMISSIE

Promotoren:	Prof.dr. M.L. den Boer
	Prof.dr. R. Pieters
Overige leden:	Prof.dr. P.J. Coffer
	Prof.dr. B. Löwenberg
	Prof.dr. S.S. Sleijfer
Copromotoren:	Dr. M. Buitenhuis
	Dr. M.B. Bierings

Voor mijn ouders
Voor Merel

TABLE OF CONTENTS

Chapter 1

Introduction

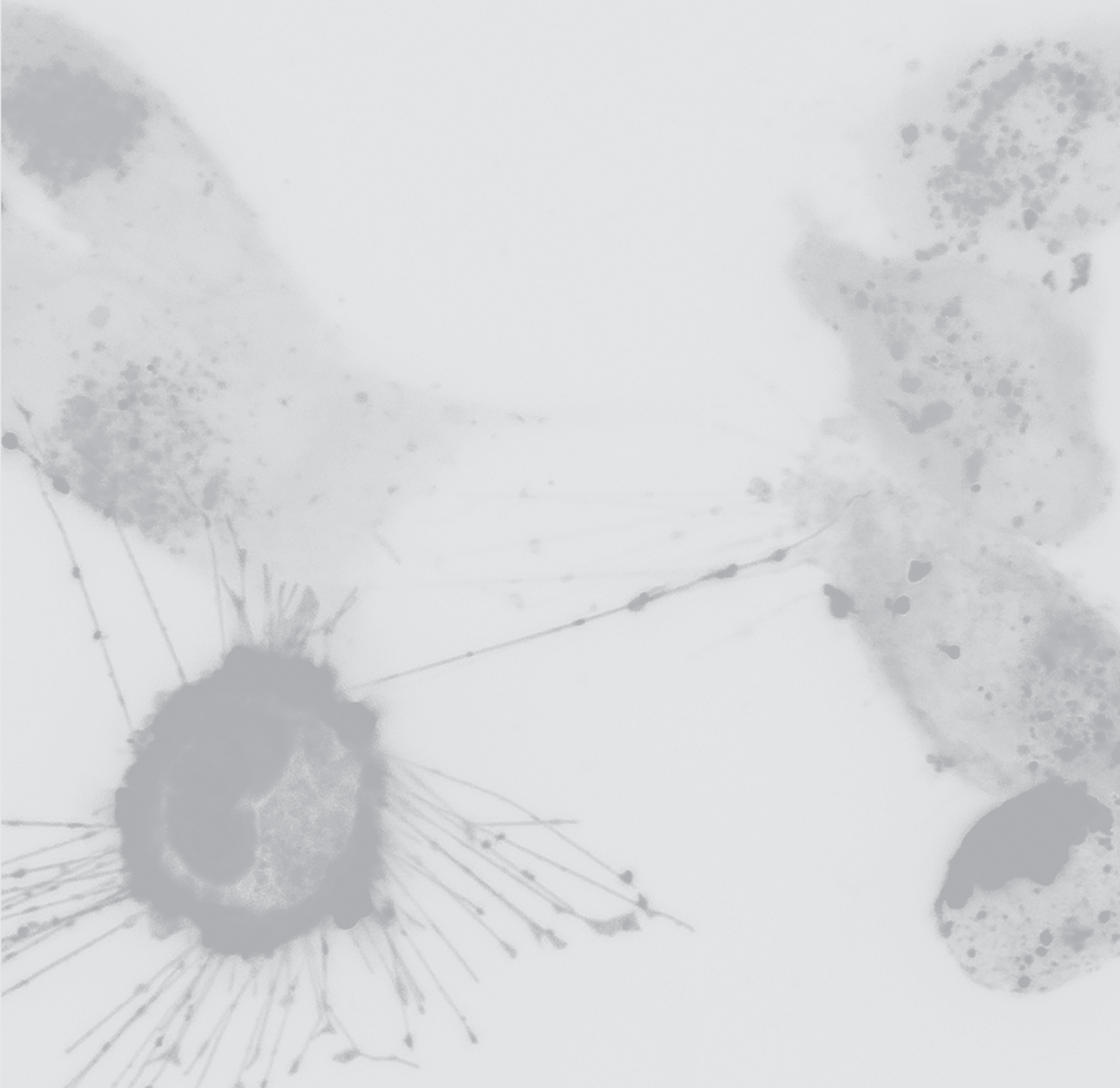

HEMATOPOIESIS

Hematopoiesis (from ancient Greek: αιμα, 'blood' and ποιεω 'to make') is the process that generates new blood cells. This complex process takes place in the bone marrow and is carefully organized and strictly regulated by growth factors and transcription factors (Figure 1). Hematopoietic stem cells (HSCs) are responsible for the continuous generation and maintenance of diverse types of mature blood cells (or lineages) that exert distinct important functions[1]. Red blood cells or erythrocytes (from: ερυθρος, 'red', κυτος, 'vessel/cell') are required for the transportation of oxygen from the lungs throughout the body. Platelets or thrombocytes (from: θρομβος, 'clot') are, together with coagulation factors, responsible for the process of blood clotting. White blood cells or leukocytes (from: λευκος, 'white') play a critical role in the host defense mechanism against pathogens. To warrant these pivotal processes, approximately 200 billion erythrocytes, 100 billion leukocytes and 100 billion thrombocytes are produced in adults every day[2]. Since mature blood cells are predominantly short-lived, HSCs are required to replenish this system. Therefore, HSCs produce multilineage progenitors that, in turn, produce lineage-committed precursors[3,4] (Figure 1). Rare long-term HSCs (LT-HSC) reside at the top of this hierarchy. These cells give rise to the more frequent short-term HSC (ST-HSC)[5]. Both types of HSCs have the unique capacity to maintain themselves through self-renewal and at the same time generate more mature progeny through differentiation, a process called asymmetrical cell division[3,5,6]. LT-HSCs are mainly quiescent and are capable of securing hematopoiesis throughout life. ST-HSCs are the drivers of daily hematopoietic replenishment and have a more restricted ability to self-renew (less than 8 weeks)[3]. ST-HSC can undergo differentiation into a multipotent progenitor (MPP) that, in turn, gives rise to the progenitors of the two main lineages of hematopoiesis: the common lymphoid progenitor (CLP)[7] and the common myeloid progenitor (CMP)[8]. The CLP generates lymphoid precursors that produce B cells, T cells and Natural Killer (NK) cells. The CMP can differentiate toward a granulocyte-macrophage progenitor (GMP), giving rise to precursors of monocytes/macrophages, neutrophils, eosinophils and basophils, and a megakaryocyte-erythroid progenitor (MEP), giving rise to precursors of erythrocytes and megakaryocytes. This continuous process of self-renewal and differentiation is activated or accelerated if the demand for blood cells increases (e.g. during infection or after blood loss), and is tightly controlled by lineage-specific hematopoietic cytokines and intracellular activation of lineage-specific transcription factors (Figure 1).

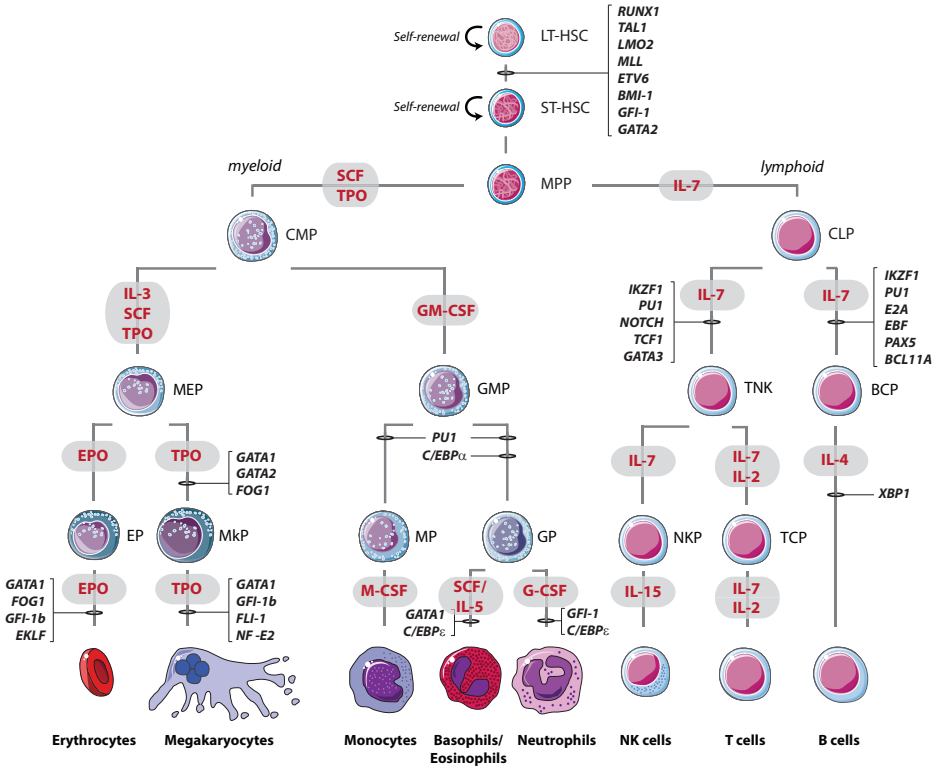

Figure 1. Schematic representation of hematopoiesis.
Blood cell development is a strictly orchestrated process progressing from the hematopoietic stem cell toward differentiated blood cells. This figure shows a schematic representation of this process. It includes the cytokines that support survival, proliferation and differentiation at several stages during hematopoiesis (red text in gray background) and depicts at which stage of hematopoiesis transcription factor are essential for further differentiation (determined by conditional knockout models)[2,4]. Abbreviations: LT-HSC, long-term hematopoietic stem cell; ST-HSC, short-term hematopoietic stem cell; MPP, multipotent progenitor; CMP, common myeloid progenitor; CLP, common lymphoid progenitor; MEP, megakaryocyte-erythroid progenitor; GMP, granulocyte-macrophage progenitor; TNK, T cell and NK cell progenitor; BCP, B cell progenitor; EP, erythroid progenitor; MkP, megakaryocyte progenitor; MP, monocyte progenitor; GP, granulocyte progenitor; NKP, NK cell progenitor; TCP, T cell progenitor; SCF, stem cell factor; TPO, thrombopoietin; IL, interleukin; GM-CSF, granulocyte macrophage colony stimulating factor; EPO, erythropoietin; M-CSF; macrophage colony stimulating factor; G-CSF, granulocyte colony stimulating factor.

ACUTE LEUKEMIA AND LEUKEMOGENESIS

Leukemia (from: λευκος, 'white' and αιμα 'blood') is a type of cancer that is characterized by an accumulation of immature, abnormal hematopoietic progenitors in the bone marrow. In contrast to healthy progenitors, these leukemic progenitors are highly proliferative and proliferate independently of the demand of blood cells. Further, the differentiation capacity of leukemic cells is impaired, while self-renewal capacity is still present. The initiation and development of leukemia,

or leukemogenesis, is an 'evolutionary' process in which multiple independent aberrations accumulate in a pre-leukemic cell. These aberrations affect genetic or epigenetic regulators of important cellular processes. Genetic alterations are mostly caused by chromosomal aberrations and gene mutations. Epigenetic modifications are driven by regulators of DNA methylation, histone modification, and by microRNAs[9]. The multitude of genetic and epigenetic hits driving leukemia makes this disease very heterogeneous.

Leukemia is classified based on the speed of disease progression (acute versus chronic) and the affected lineage of hematopoiesis (myeloid or lymphoid). Acute leukemia is characterized by the accumulation of highly proliferative leukemic progenitor cells that have completely lost their capacity to differentiate. In contrast, chronic leukemia has a slow onset and progression, and is defined by the accumulation of more mature progenitors that still have partial differentiation capacity. Since leukemia can originate from both myeloid and lymphoid progenitors, acute leukemia is classified as either acute myeloid leukemia (AML)[10,11] or acute lymphoblastic leukemia (ALL)[12-14]. These types of acute leukemia comprise multiple heterogeneous malignancies driven by distinct pathogenic mechanisms. Despite the genetic heterogeneity of acute leukemia, the clinical features at diagnosis are highly similar. Due to the proliferation of immature progenitors in the bone marrow, patients with acute leukemia develop pancytopenia (from: παν, 'all' and κυτος, 'vessel/cell' and πενια, 'deficiency'). These patients have a shortage of functional erythrocytes (anemia), leukocytes (leukopenia), and thrombocytes (thrombocytopenia). These deficiencies result in weakness, fatigue and paleness (anemia), induced vulnerability for infections (leukopenia), and bleeding tendency shown by easy bruising, formation of hemorrhages and/or the presence of petechiae or ecchymoses (thrombocytopenia). Furthermore, patients can suffer from bone pains, anorexia, headaches, and abdominal discomfort. The prevalence and prognosis of patients with acute leukemia differ between subtypes. AML is the most common subtype of acute leukemia in adults, with a prevalence of 3.8 cases per 100.000 and a median age of onset of approximately 70 years[11]. ALL is the most common form of cancer in children with an incidence rate of 1 per 20.000 children. In the Netherlands, every year ~150 children are newly diagnosed with leukemia, of which 125 children with ALL and 25 children with AML. Sixty percent of all patients with ALL are children with an average age of onset between 2-5 years[12-14]. The prognosis of patients with acute leukemia is affected by multiple factors, including age at diagnosis, white blood cell count at diagnosis, initial response to chemotherapy, the type of acute leukemia (AML versus ALL), and the genetic abnormalities that characterize the leukemia[10-14]. This thesis focuses on the most common pediatric malignancy: acute lymphoblastic leukemia.

PEDIATRIC ACUTE LYMPHOBLASTIC LEUKEMIA

Overall survival rates of pediatric acute lymphoblastic leukemia (ALL) have increased steadily over the last five decades[12-18]. While chances of survival in the early sixties were approximately 10%, currently most children (more than 85%) with ALL are cured[12-19]. This remarkable increase is mostly due to optimization of multi-agent chemotherapeutic drug regimens combined with risk-directed therapy protocols, and increased standards of supportive care[17-19]. An essential step in this progress was the cytogenetic and molecular characterization of common abnormalities in pediatric ALL subtypes and the subsequent assessment of the risk of relapse for these subgroups. This characterization also facilitated better minimal residual disease monitoring, which is essential for risk stratification and the early detection of relapsed disease.

Genetic subclassification and prognostic significance

Pediatric ALL can be subdivided in leukemia originating from a B cell progenitor (B-cell precursor ALL, or BCP-ALL) and leukemia originating from the T cell lineage (T-ALL). BCP-ALL is the most frequent pediatric ALL, representing approximately 85% of pediatric ALL cases. During the last decades, pediatric ALL has been investigated extensively, resulting in the discovery of major BCP-ALL and T-ALL subtypes with distinct molecular drivers and associated prognoses (Figure 2).

Good prognostic BCP-ALL subgroups

The most recurrent alterations in pediatric BCP-ALL are translocation t(12;21)(p13;q22) and hyperdiploidy[20]. These alterations are believed to be initial events in leukemogenesis that occur years before leukemia initiation and are even occurring *in utero*, since their presence has been shown in neonatal blood spots on Guthrie cards[21]. Both subgroups have an excellent prognosis. Hyperdiploidy, the presence of more than 50 chromosomes per leukemic cell, is present in approximately 25% of pediatric patients with BCP-ALL. The overall event-free survival of children within this subgroup is almost 90%[12,22,23]. Among patients with hyperdiploidy, the presence of extra copies of chromosome 4, 10 or 17 has been associated with an even more favorable prognosis, while trisomy of chromosome 5 confers poorer outcome[22]. Translocation t(12;21)(p13;q22), resulting in the *ETV6-RUNX1* fusion gene, is present in approximately 25% of pediatric BCP-ALL patients and is therewith the most common fusion gene in childhood cancer[24-26]. ETV6-RUNX1 positive BCP-ALL is a subgroup with overall good prognostic features (event-free survival rates of 85%-95%)[23,27]. In this group, a wide variety of additional genetic aberrations further affect prognosis, including deletion of the second *ETV6* gene, duplication of *RUNX1*,

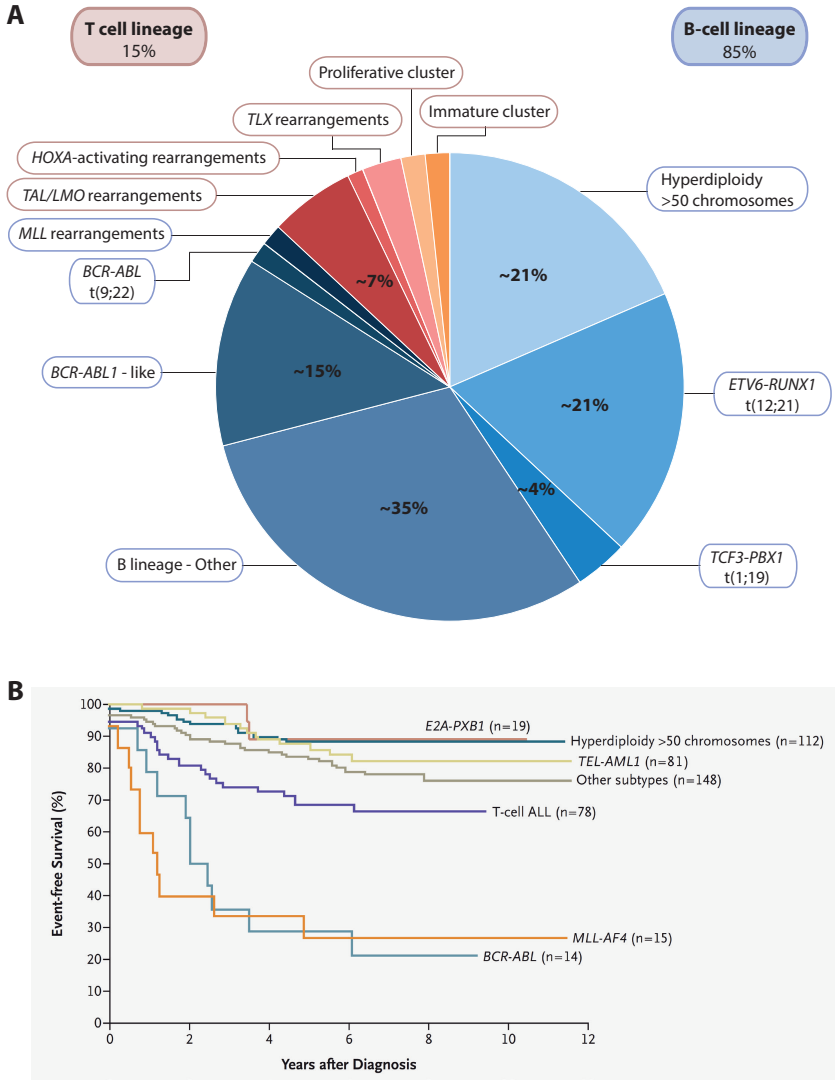

Figure 2. Major BCP-ALL and T-ALL subtypes have distinct molecular drivers and associated prognoses.
(A) BCP-ALL can be subdivided in 7 clusters comprising 85% of all pediatric ALL patients. T-ALL can be subdivided in 5 clusters comprising 15% of all pediatric ALL patients. (B) Prognosis of different subtypes BCP-ALL and T-ALL differs significantly. Figure 2B is adapted from Pui *et al.* [13].

and an extra der(21)t(12;21). Both ETV6-RUNX1 positive ALL without an additional genetic aberration and ETV6-RUNX1 positive ALL with der(21)t(12;21) duplication confer poorer outcome (5 year disease-free survival of less than 80%)[27]. Another good prognostic BCP-ALL subgroup includes patients with a t(1;19)(q23;p13.3) induced *TCF3-PBX1* (or *E2A-PBX1*) fusion gene. This subgroup comprises 2-5% of

BCP-ALL patients and has excellent prognostic features (>95% event free survival)[23]. Together, these three subtypes of BCP-ALL have more than 90% 5 years event-free survival. This excellent prognosis is mainly due to a good response to commonly used chemotherapeutics[23,28,29].

Poor prognostic BCP-ALL subgroups

BCP-ALL patients with the *BCR-ABL1* fusion gene (2% of BCP-ALL), *BCR-ABL*1like gene expression profiles (15-20%), *MLL*-rearrangements (2%), and hypodiploidy (1%) have a poor prognosis, exhibiting average event-free survival rates lower than 50%. The incidence of translocation t(9;22)(q34;q11), resulting in the *BCR-ABL1* fusion gene, increases with age: while this fusion is present in only 2% of pediatric ALL patients, this percentage increases to 25% in adult ALL patients. This subgroup is characterized by a high frequency of RAG-mediated deletions of *Ikaros (IKZF1)*, a transcription factor that plays an important role in normal B cell development (see Figure 1)[30,31]. Recently, the introduction of targeted therapy directed against the fusion protein (tyrosine kinase inhibitors, such as Imatinib) has improved the prognosis of this subgroup dramatically[18,32-36]. Addition of Imatinib to treatment protocols has resulted in an increase of the event-free survival rates of pediatric BCR-ABL1 positive ALL from ~35% to > 70%[35,37].

The *MLL*-rearranged BCP-ALL subgroup comprises translocations involving the *MLL* gene on chromosome 11q23, and more than 50 different fusion partners. The most frequent *MLL* translocations are: t(4;11), resulting in *MLL-AF4*, t(11;19), resulting in *MLL-ENL*, and t(9;11), resulting in *MLL-AF9*. These *MLL*-rearrangements mainly occur in infants (present in 80% of infants with ALL) and induce the development of an ALL subtype with less favorable prognosis due to therapy resistance[38].

Extensive gene expression profiling of BCP-ALL patients recently revealed a new BCP-ALL subtype with unfavorable outcome that has a gene expression profile similar to *BCR-ABL1* positive patients: BCR-ABL-like ALL[39-41]. More than 80% of patients with such a *BCR-ABL1*-like signature display abnormalities in genes that are important for B-cell differentiation, including *IKZF1, PAX5* and *EBF1* (see Figure 1)[40,41]. Both the *BCR-ABL1*-like signature and *IKZF1* deletion are independent prognostic factors predicting poor outcome of pediatric ALL.

T-ALL

T-ALL represents approximately 15% of pediatric ALL cases and can be subdivided in five distinct subgroups based on the most recurrent genetic abnormalities, namely the TAL/LMO subgroup (comprised of oncogenic rearrangements of *TAL* or *LMO* genes), the HOXA subgroup (comprised of *HOXA*-activating rearrangements), the TLX subgroup (comprised of oncogenic rearrangement of *TLX1* or *TLX3*), the early/

immature subgroup (comprised of e.g. *MEF2C*-activating rearrangements), and the proliferative subgroup (comprised of e.g. *NKX2*-activating rearrangements)[42]. The prognosis for children with T-ALL remains inferior compared to BCP-ALL. In recent treatment protocols, the 5-year event free survival rate of T-ALL patients is around 80% [19,20,23]. The early/immature subgroup, also known as early T-cell precursor (ETP) leukemia, is a T-ALL subgroup associated with a poor prognosis[43-45]. The prognostic relevance of the other distinct subgroups is still largely unknown, and varies per treatment protocol[20].

Targeting leukemia-specific aberrations

Treatment of ALL has been optimized by using the above-described prognostic information in the risk stratification and subsequent therapy schedules of patients. This approach has led to significant increase in survival of pediatric ALL patients. However, the functional role of the subtype-specific aberrations is largely unknown. A better understanding of the cellular processes affected by these genetic abnormalities will provide insight into the prognostic features of a specific subgroup and might enable targeting of the molecular drivers of ALL. In the first part of this thesis, we attempt to identify the molecular effectors of ETV6-RUNX1 positive BCP-ALL.

ETV6-RUNX1 POSITIVE ACUTE LYMPHOBLASTIC LEUKEMIA

The t(12;21)(p13;q22) rearrangement fuses the 5' non-DNA binding region of the ETS family transcription factor *ETV6* (*TEL*) to almost the entire *RUNX1* (*AML1*) locus[46], resulting in the formation of the ETV6-RUNX1 fusion protein (also known as TEL-AML1)[24,25]. Both fusion partners (ETV6 and RUNX1) are important regulators of hematopoiesis.

ETV6

The *ETV6* gene is a member of a large family of ETS-domain transcription factors that are important regulators of proliferation, differentiation and apoptosis[47,48]. ETV6 is a ubiquitously expressed protein that is comprised of 3 major domains (Figure 3). The pointed domain (PD) is important for nuclear export of ETV6[49], transcriptional repression[50,51], heterodimerization[52], and oligo-homodimerization[53]. The repression domain is essential for sequence-specific transcriptional repression of target genes[54]. The ETS domain is involved in DNA binding and is important for protein-protein interactions[48]. Genetic mutations in *ETV6* have frequently been observed in leukemia, suggesting an important role for ETV6 in regulation of hematopoiesis[55].

Indeed, analysis of mouse chimeras with *ETV6-/-* embryonic stem cells revealed that ETV6 function is essential for both normal hematopoiesis in the bone marrow and survival of HSCs[56]. Therefore, it is not surprising that in addition to ETV6-RUNX1, other ETV6 related fusion proteins (including ETV6-PDGFRβ[57], ETV6-ABL[58], and ETV6-JAK2[59]) have been identified in hematological malignancies.

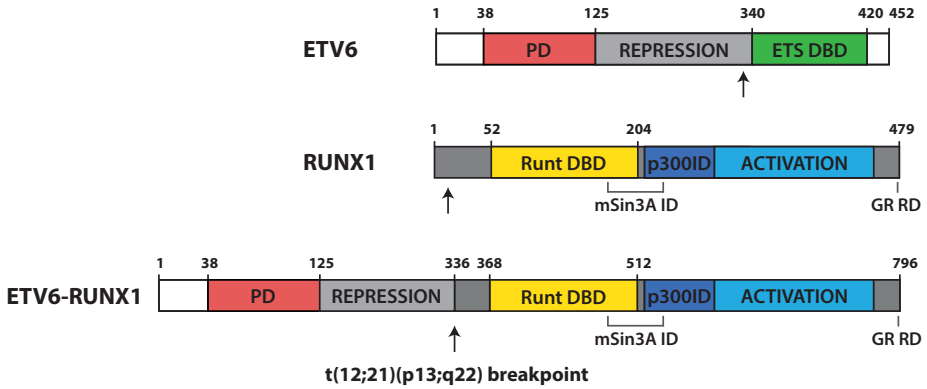

Figure 3. Schematic representation of ETV6, RUNX1 and the ETV6-RUNX1 fusion protein.
Translocation (12;21) fuses the 5′ non-DNA binding region of ETV6 to almost the entire RUNX1 locus. Numbers represent amino acids flanking the major domains of the proteins. Abbreviations: PD, oligomerization pointed domain; DBD, DNA binding domain; p300ID, histone acetyl transferase p300 interaction domain; mSin3A ID, corepressor mSin3a interaction domain; GR RD, Groucho-related corepressor domain. Adapted from Zelent *et al.*[46].

RUNX1

The transcription factor RUNX1 (Runt-related protein 1), also known as AML1 (acute myeloid leukemia 1) and CBFα (Core binding factor α), is considered to be a key regulator of hematopoiesis. It has, for example, been demonstrated that RUNX1 plays a critical role in regulation of definitive hematopoiesis during embryogenesis[60]. In addition, conditional deletion of RUNX1 in adult mice revealed that RUNX1 also plays an important role in regulation of adult hematopoiesis. These mice exhibit reduced megakaryocyte differentiation and a block in lymphocyte development[61]. Furthermore, RUNX1 also negatively regulates the number of quiescent HSCs, suggesting that RUNX1 plays an important role in regulation of HSC maintenance[62]. RUNX1 regulates hematopoiesis via transcriptional inhibition of, for example, $p21^{WAF/CIP}$ and induction of a large number of specific target genes, including Myeloperoxidase, M-CSFR, IL-3R, Neutrophil elastase, Granzyme B, T-cell receptors, and B-cell receptors[63]. The transcriptional activity of RUNX1 depends on the association with CBFβ. CBFβ itself does not bind to the DNA but enhances the DNA-binding ability of RUNX1 and protects it from ubiquitin-mediated proteolysis[64]. It has been demonstrated that mice expressing mutated CBFβ exhibit a phenotype

similar to RUNX1 deficient mice, indicating that CBFβ is essential for RUNX1 function *in vivo*[65]. Taken together, the observed hematopoietic defects in RUNX1 and CBFβ deficient mice demonstrate the importance of correct regulation of RUNX1 transcriptional activity in healthy hematopoietic cells. Chromosomal translocations involving RUNX1 have been identified in a large proportion of pediatric leukemias. In addition to the ETV6-RUNX1 fusion protein, more than a dozen chromosomal translocations have been found that involve RUNX1. For example, the t(8;21)(q22;q22) translocation, resulting in expression of the RUNX1-RUNX1T1 fusion protein, occurs in 12–30% of pediatric AML patients[66,67].

ETV6-RUNX1

The ETV6-RUNX1 fusion product combines the pointed domain of ETV6 with all functional domains of RUNX1 (Figure 3)[46]. Similar to RUNX1, ETV6-RUNX1 transcriptional activity depends on binding to CBFβ[68]. ETV6-RUNX1 can act as a dominant-negative protein. ETV6-RUNX1 can form an inhibitory complex through recruitment of histone deacetylases (HDAC) by ETV6 and mSin3a by RUNX1[46,69]. Like RUNX1-RUNX1T1, ETV6-RUNX1 is thought to have higher affinity for multiple AML binding sites, resulting in abrogation of the transcriptional activity of endogenous RUNX1[46,69]. However, experiments performed with transgenic mice expressing ETV6-RUNX1 under its endogenous promoter revealed different phenotypes compared to RUNX1 deficient mice. Whereas expression of ETV6-RUNX1 induced the number of LT-HSCs, RUNX1 deficiency resulted in reduced LT-HSC levels[61,62,70]. Further, chromatin immunoprecipitation in a murine cell line model revealed that, although ETV6-RUNX1 predominantly binds DNA through the Runt DNA binding domain, it also binds multiple ETV6-RUNX1 specific promoter regions[71]. This suggests that ETV6-RUNX1 not only functions as a dominant-negative protein for RUNX1 transcriptional activity, but also regulates ETV6-RUNX1 specific target genes (Figure 4). The molecular mechanisms underlying the emergence and maintenance of ETV6-RUNX1 positive BCP-ALL remain to be investigated, although previous research has unraveled drivers of this ALL subtype. Previous reports revealed that enhanced levels of STAT3, heat-shock proteins, Survivin, Has-mir-125b-2, the erythropoietin receptor, and cytoskeleton regulatory genes as well as aberrant regulation of the TGFβ pathway or the interferon α/β pathway are important for ETV6-RUNX1 positive BCP-ALL[68,72-80].

The ETV6-RUNX1 fusion protein induces a silent pre-leukemic clone that requires additional genetic hits for the transition to leukemia[70,81-85]. These pre-leukemic ETV6-RUNX1 positive HSCs have a high proliferation rate, still possess self-renewal properties, and are capable of contributing to hematopoiesis. However, they fail to outcompete normal HSCs[70,84,86]. In case of leukemia development, this early genetic

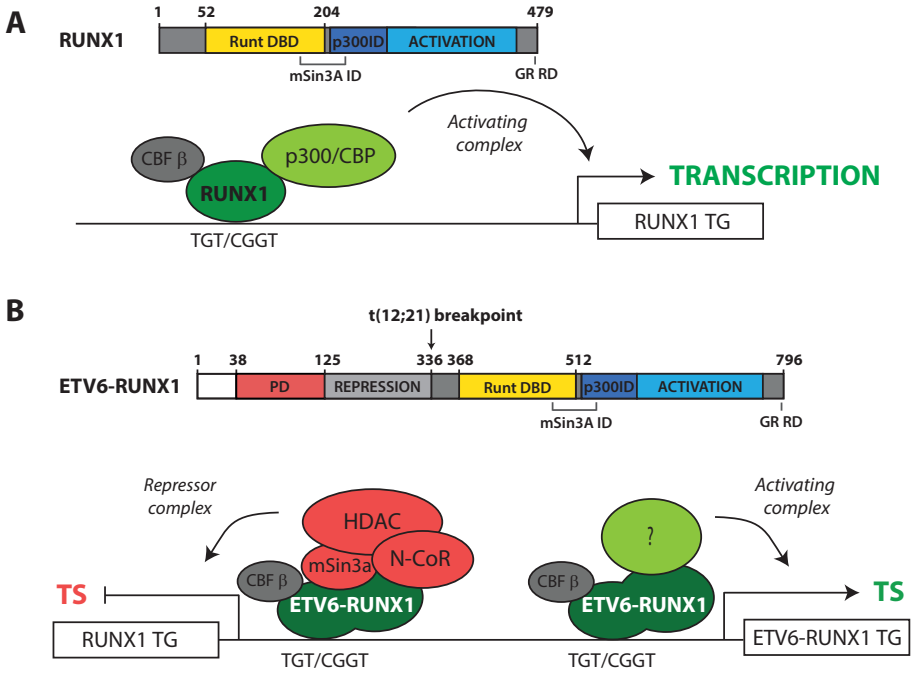

Figure 4. Model for the transcriptional mechanisms by which ETV6-RUNX changes gene expression in pre-leukemic cells.
(A) RUNX1 is known to start transcription of target genes by reversing mSin3a/histone deacetylase (HDAC) binding and subsequent association with an activating complex including the histone acetyl transferases p300 and CREB-binding protein (CBP). (B) ETV6-RUNX1 functions as a dominant-negative protein repressing native RUNX1 protein targets through strong binding of a repressor complex consisting of corepressor mSin3a, nuclear receptor corepressor 1 (N-CoR) and histone deacetylase (HDAC) (left). However, recent data suggests that ETV6-RUNX1 also binds ETV6-RUNX1 specific promoter regions and can activate transcription of these genes important for ETV6-RUNX1 function.

lesion is followed by a small number of 'driver' copy number alterations, which are predominantly directed to genes regulating normal B cell differentiation[87,88]. These alterations are acquired independently and without preferential order, thereby generating a dynamic clonal architecture[87]. This genetic variation implies that targeted therapy in ETV6-RUNX1 positive ALL should be directed to (targets of) initial lesions that are present in all subclones, such as ETV6-RUNX1. This concept is further supported by the observation that ETV6-RUNX1 positive cell lines are highly dependent on the expression of the fusion protein for their survival[75,89]. To date, ETV6-RUNX1 positive cells cannot be selectively targeted or sensitized to conventional chemotherapy. For the development of novel targeted therapies with less short-term and long-term side effects, it is therefore important to identify the molecular pathways induced by the ETV6-RUNX1 fusion protein. **Chapter 3 and 4** of this thesis are dedicated to find such targets.

HEALTHY AND LEUKEMIC BONE MARROW MICROENVIRONMENT

In addition to molecular events that drive leukemogenesis and are intrinsically important for the leukemic cell, increasing evidence suggests that also the microenvironment plays an essential role in leukemogenesis and maintenance of leukemia.

The healthy bone-marrow microenvironment

Hematopoietic stem and progenitor cells (HSPCs) reside in the bone marrow microenvironment, a complex ecosystem comprised of several specialized cell types. This microenvironment, or niche, regulates HSCs in line with the need for specific blood cells, offers relative hypoxia and is important for stemness of HSCs[90]. Bone marrow niche cells, including mesenchymal stromal cells (MSCs), endothelial cells (ECs), megakaryocytes (MKs) and osteoblasts (OBs) directly or indirectly regulate HSC function by either secreting soluble supportive factors, or expressing cell-bound signaling molecules[91-93]. Bone marrow niche cells produce numerous growth factors, including stem cell factor (SCF), transforming growth factor β (TGFβ), thrombopoietin (TPO), Interleukin-7 (IL-7), and erythropoietin (EPO). These factors are either important regulators of HSC quiescence or drive the proliferation and differentiation of HSCs toward a certain hematopoietic lineage. Furthermore, niche cells produce chemokines essential for homing toward and anchoring in the niche, including stromal cell-derived factor 1 (SDF1 or CXCL12). Recently, analysis of conditional knock-out mouse models has provided a better understanding of the role of different stromal compartments in regulation of HSC function and the production of the above-mentioned factors. Vascular ECs, which form the blood vessels of the bone marrow, express factors regulating HSC function including SCF and CXCL12, both important for HSC maintenance[94-96], NOTCH ligands, important for HSC self-renewal[97], and E-selectin, important for HSC proliferation[98], indicating that these cells are important instructors of HSCs. In addition, mature megakaryocytes are often found in close proximity to HSCs within the bone marrow niche[99,100]. These blood platelet progenitors secrete growth factors important for HSC quiescence (e.g. TPO[101], CXCL4[100], and TGFβ[99]) and, in stress conditions, produce growth factors for HSC proliferation (e.g. FGF1[99]). By far the best-studied bone marrow niche cells are MSCs, multipotent adult stromal cells for the mesenchymal lineage. These cells can differentiate toward the osteogenic (bone), chondrogenic (cartilage) and adipocytic (fat) lineages[102]. Bone marrow MSCs surround the ECs of the arterioles and sinusoid vessels. In murine bone marrow, it has become evident that various MSC populations exist that all are important for

HSC function. Important markers for murine MSC populations are Nestin[103], NG2[104], Leptin receptor (LEP-R)[105], PDGFRA, CD150, and Sca-1[106,107]. While these populations all have MSC characteristics and express HSC-supportive factors, including SCF and CXCL12, they are localized at different regions of the bone marrow and differentially affect HSCs[93]. While, NG2 positive MSCs are mainly located around arterioles and co-localize with quiescent HSCs, LEP-R positive MSCs are located peri-sinusoidal and co-localize with proliferating HSCs[104]. Another specific subset of MSCs highly expresses CXCL12 (CXCL12-abundant reticular (CAR) cells) and is

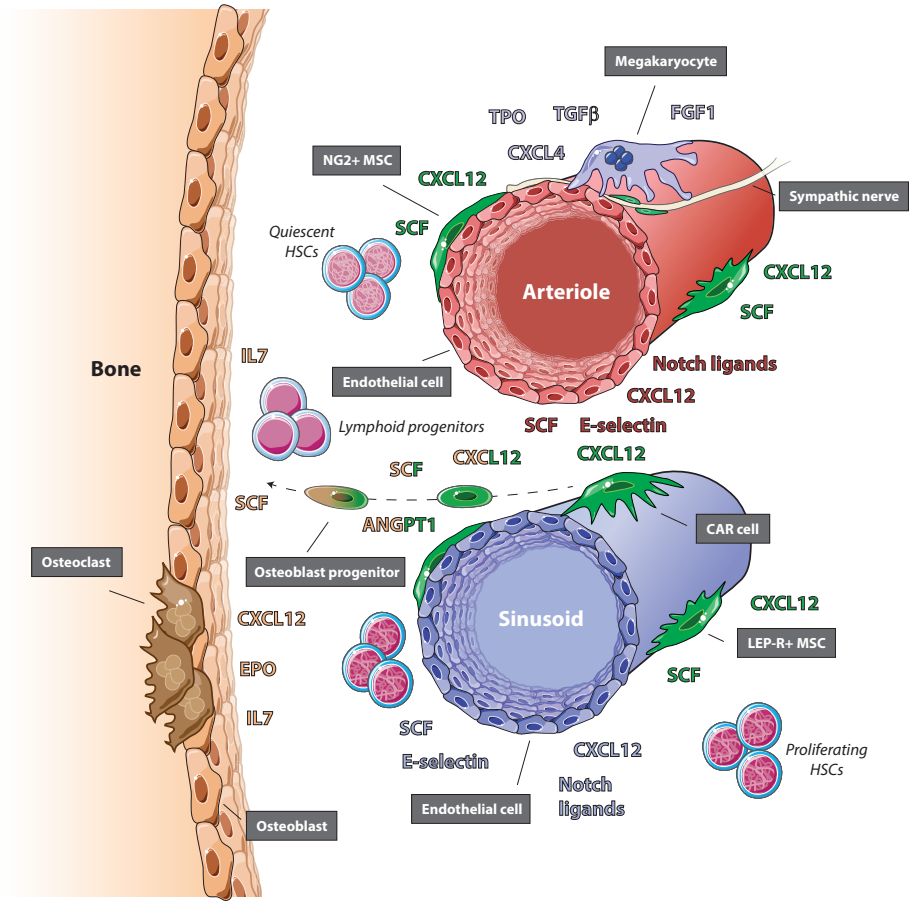

Figure 5. Model for the healthy bone marrow microenvironment.
Hematopoietic stem cells reside in the bone marrow microenvironment, where they are maintained by several specialized supporting cells[93]. This model shows a selection of cellular subsets that have been shown to be important for murine hematopoiesis[91]. The cytokines and growth factors that are produced by these cells are color-coded. See main text for more details (paragraph 5.1). Abbreviations: HSC, hematopoietic stem cell; MSC, mesenchymal stromal cell, NG2, neural/glial antigen 2; LEP-R, leptin receptor, CAR, CXCL12-abundant reticular cell; SCF, stem cell factor; EPO, erythropoietin; TPO, thrombopoietin, FGF1, fibroblast growth factor 1; TGFβ, transforming growth factor beta; CXCL, chemokine C-X-C motif ligand; IL, interleukin; ANGPT1, angiopoietin 1.

shown to be important in regulation of HSC proliferation[108]. A substantial fraction of CAR cells are osteoblastic progenitor cells, a more differentiated subset of MSCs[109]. These cells also express important factors for HSCs, including CXCL12, SCF and ANGPT1[106,109], and are important for the proliferation of lymphoid and common myeloid progenitors[110]. Furthermore, mature osteoblasts have been shown to secrete IL-7 and to be essential for maintenance and proliferation of B cell progenitors[95,96,111]. This suggests that specialized compartments exist within the bone marrow niche, differentially regulating quiescence, proliferation and differentiation of HSPCs.

In contrast to our understanding of the functional role of these stromal subsets on murine HSPCs, the role of human stromal subsets within the bone marrow is poorly understood. Human HSPCs are localized within the trabecular region of the bone and mainly co-localize with MSCs expressing HSC-supportive factors[107,112-114]. In addition, MSCs, ECs, and osteoblastic progenitors all can support the maintenance and proliferation of HSPCs *in vitro*[115], suggesting that also in the human bone marrow these cells play an essential role in HSPC regulation.

The leukemic bone marrow microenvironment

Like healthy HSPCs, leukemic cells reside in the local microenvironment of the bone marrow. By using similar homing and anchoring signals, including E-selectin and CXCL12, leukemic cells create a leukemic niche that interferes with normal HSPC function[116-118]. Furthermore, in comparison to healthy HSPCs, leukemic cells are less dependent on niche signals for their survival and proliferation, making them strong invaders[119-121]. The invasion of leukemic cells was shown to remodel the human bone marrow niche by impairing angiogenesis and inducing bone loss[122]. Several mouse models have provided further insight into the changes in bone marrow stromal cells after leukemogenesis. For example, BCR-ABL1 positive CML cells have been shown to down-regulate CXCL12 production in bone marrow stromal cells, which directly impaired normal HSC maintenance[109,123], and to up-regulate platelet growth factor (PLGF) secretion by stroma, directly inducing CML cell proliferation[124]. In addition, Jak2^{V617F} myelodysplastic syndrome (MDS) cells and MLL-AF9 AML cells were shown to induce neuropathy in bone marrow, thereby affecting the activity and maintenance of normal MSC subsets, which in turn led to accelerated disease development[125,126]. Human MDS cells have also been shown to up-regulate important regulators of fibrosis (e.g. LIF and VEGF) in bone marrow stromal cells, which were in turn important for MDS cell survival in a xenograft mouse model[127].

Leukemia-induced changes of the microenvironment appear to be important for initiation, maintenance and progression of disease. In addition, healthy hematopoietic cells could be transformed to MDS cells in a deficient microenvironment[128-132]. Similarly, activation of an oncogene or oncogenic pathway, e.g. activation of

β-catenin, in stromal cells could initiate leukemogenesis[131-133]. To date, it is not clear whether such mutations also occur in human disease.

The leukemic microenvironment not only induces leukemogenesis as described above, it also protects leukemic cells from elimination by immune responses and chemotherapeutic agents, and can facilitate the development of drug resistance[134-137]. Several studies report the induction of resistance to both classical chemotherapeutic agents and newly developed targeted therapies (such as tyrosine kinase inhibitors) by the tumor microenvironment[137-143]. The disruption of the leukemic niche is therefore considered a promising new therapeutic strategy[95,117,144-151].

Approaches to disrupt the leukemic niche

Targeting the leukemic niche can be approached in several ways. The most explored option is the reduction of leukemic cell homing to and anchoring in the niche. Pioneer studies using granulocyte colony stimulating factor (G-CSF) showed that addition of growth factors to conventional chemotherapy can enhance therapy efficiency[152]. G-CSF was later shown to decrease CXCL12 levels in the bone marrow, resulting in mobilization of stem cells[153]. More recently, several pre-clinical studies used CXCR4 inhibition as a means to disrupt the leukemic niche. Stromal-derived factor-1 (SDF-1/CXCL12) is a chemoattractant that is actively produced by MSCs, ECs and osteoblasts in the bone marrow. CXCL12 binds to the CXCR4 receptor, which is highly expressed on HSCs and leukemic cells. Blocking CXCR4/CXCL12 interaction with CXCR4 antagonists leads to mobilization of leukemic cells, increased sensitivity to therapeutic agents, and prolonged survival in mouse models[146,147,150,151,154-159]. Phase 1/2 clinical trials have shown the feasibility of using CXCR4 antagonists during chemotherapeutic treatment[160-164]. However, growth factor priming (with G-CSF/GM-CSF) in more than 4000 AML patients has not resulted in overall improved survival rates[165]. In addition, recent data argues that leukemic stem cells are not mobilized by CXCR4 inhibition[166], suggesting that CXCR4 inhibition is not sufficient to completely disrupt leukemic niches. Furthermore, CXCR4 inhibition does not only interrupt the leukemic, but also the healthy hematopoietic niche[167,168].

An alternative approach to disrupt the leukemic niche, is the inhibition of communication between leukemic cells and their stromal counterparts. Several communication mechanisms between leukemic cells and stromal niche cells are known to be important for their interaction, including integrin signaling, cytokine and chemokine signaling, and extracellular vesicle signaling[141]. However, the mechanisms underlying the crosstalk within the leukemic niche and consequently how this communication drives leukemic cell survival and chemotherapy resistance remains poorly understood. Recently, tunneling nanotubes (TNTs), or membrane nanotubes, have been described as a novel mode of communication between

eukaryotic cells[169-173]. These intercellular membrane conduits have been observed in several cell types, complex tissues, and organisms[172,174-176] and facilitate the transport of several types of cargo[171,172,177-179]. The pathophysiological importance of TNTs has been well established in the field of immunology, since it has been shown that prions and HIV-1 particles use TNTs to promote disease spread[173,180]. TNTs have also been observed between cancer cells[173,179,181,182]. However, the presence of TNTs within the leukemic niche and hence their role in crosstalk within this niche has not been addressed. Importantly, the functional role of TNTs in leukemic cell survival and drug resistance is currently unknown.

SCOPE AND OUTLINE OF THIS THESIS

New treatment regimens increasingly aim to target specific intrinsic characteristics and extrinsic signals important for leukemia. This approach has for example led to the successful development of targeted inhibitors, such as imatinib and dasatinib, that drastically improved the outcome of BCR-ABL1 positive leukemia patients[19,31-35]. However, the majority of pediatric patients with leukemia are still treated with non-specific classic chemotherapy regimens. Twenty percent of pediatric ALL cases relapse due to resistance to this therapy[183,184], while long-term side effects of treatment remain considerable[97,185,186]. This thesis aims to identify leukemia-specific processes that can be used to target leukemic cells or the leukemic microenvironment.

The first part of this thesis focuses on cellular processes that are driven by initial mutations present in (pre-) leukemic cells in order to better understand leukemogenesis and leukemia. Further, we aim to inhibit these biological processes in order to selectively target leukemic cells.

In **chapter 2,** we focus on one of the most important intracellular signaling programs in human cells: the PI3K/PKB signaling pathway. We review the role of this signaling pathway in normal and malignant hematopoiesis and summarize the efforts to target this pathway in order to improve therapy of leukemia patients.

In **chapter 3 and 4**, we focus on the cellular processes that are affected by the ETV6-RUNX1 fusion protein. We studied the effects of ectopic expression of ETV6-RUNX1 in healthy hematopoietic progenitor cells and found that ETV6-RUNX1 induces pro-proliferative, pro-survival, and pro-migratory signaling pathways. In **chapter 3,** we describe the enhanced expression of the class-III phosphoinositide 3-kinase Vps34 in ETV6-RUNX1 positive ALL. Vps34 is an important regulator of autophagy, and was found to be important for proliferation and survival of ETV6-RUNX1 positive ALL cells. This chapter further describes the pre-clinical

evaluation of autophagy inhibition as targeted therapy for ETV6-RUNX1 positive leukemia. In **chapter 4,** we describe the importance of Leukemia-Associated Rho guanine exchange factor (LARG) and RhoA in the pro-migratory phenotype induced by ETV6-RUNX1. This chapter aims to target these cell-intrinsic mediators of ETV6-RUNX1 positive leukemic cell migration in order to develop strategies that target leukemic cell migration without affecting the migration of healthy hematopoietic cells.

The leukemic microenvironment protects leukemic cells from elimination by classic and targeted therapy. The second part of this thesis aims to better understand the dynamic crosstalk between leukemic cells and human bone marrow-derived stromal cells in order to find novel ways to disrupt this leukemic niche.

Chapter 5 describes the discovery of tunneling nanotube signaling as communication mechanism between leukemic cells and mesenchymal stromal cells. We investigate the functional consequence of the inhibition of TNT signaling on cell survival and drug resistance of leukemic cells. In **chapter 6**, we evaluate whether leukemic cells modify MSC-mediated production of chemokines to create a leukemic niche. We investigate how this modified MSC secretome affects migration of leukemic cells, healthy hematopoietic progenitors, and MSCs. Furthermore, we aim to identify alternative candidate factors for leukemic niche disruption.

Finally, the results outlined in this thesis are discussed in **chapter 7** and summarized in **chapter 9.**

REFERENCES

1. Orkin, S.H. Diversification of haematopoietic stem cells to specific lineages. *Nature reviews. Genetics* **1**, 57-64 (2000).
2. Kaushansky, K. Lineage-specific hematopoietic growth factors. *N Engl J Med* **354**, 2034-2045 (2006).
3. Reya, T., Morrison, S.J., Clarke, M.F. & Weissman, I.L. Stem cells, cancer, and cancer stem cells. *Nature* **414**, 105-111 (2001).
4. Orkin, S.H. & Zon, L.I. Hematopoiesis: an evolving paradigm for stem cell biology. *Cell* **132**, 631-644 (2008).
5. Morrison, S.J. & Weissman, I.L. The long-term repopulating subset of hematopoietic stem cells is deterministic and isolatable by phenotype. *Immunity* **1**, 661-673 (1994).
6. Huntly, B.J. & Gilliland, D.G. Leukaemia stem cells and the evolution of cancer-stem-cell research. *Nat Rev Cancer* **5**, 311-321 (2005).
7. Kondo, M., Weissman, I.L. & Akashi, K. Identification of clonogenic common lymphoid progenitors in mouse bone marrow. *Cell* **91**, 661-672 (1997).
8. Akashi, K., Traver, D., Miyamoto, T. & Weissman, I.L. A clonogenic common myeloid progenitor that gives rise to all myeloid lineages. *Nature* **404**, 193-197 (2000).
9. Chen, J., Odenike, O. & Rowley, J.D. Leukaemogenesis: more than mutant genes. *Nat Rev Cancer* **10**, 23-36 (2010).
10. Lowenberg, B., Downing, J.R. & Burnett, A. Acute myeloid leukemia. *N Engl J Med* **341**, 1051-1062 (1999).
11. Estey, E. & Dohner, H. Acute myeloid leukaemia. *Lancet* **368**, 1894-1907 (2006).
12. Pui, C.H., Robison, L.L. & Look, A.T. Acute lymphoblastic leukaemia. *Lancet* **371**, 1030-1043 (2008).
13. Pui, C.H., Relling, M.V. & Downing, J.R. Acute lymphoblastic leukemia. *N Engl J Med* **350**, 1535-1548 (2004).
14. Inaba, H., Greaves, M. & Mullighan, C.G. Acute lymphoblastic leukaemia. *Lancet* **381**, 1943-1955 (2013).
15. Pui, C.H. & Evans, W.E. Acute lymphoblastic leukemia. *N Engl J Med* **339**, 605-615 (1998).
16. Pui, C.H. & Evans, W.E. Drug therapy - Treatment of acute lymphoblastic leukemia. *New England Journal of Medicine* **354**, 166-178 (2006).
17. Pieters, R. & Carroll, W.L. Biology and treatment of acute lymphoblastic leukemia. *Hematol Oncol Clin North Am* **24**, 1-18 (2010).
18. Bhojwani, D. & Pui, C.H. Relapsed childhood acute lymphoblastic leukaemia. *Lancet Oncol* **14**, e205-217 (2013).
19. Pui, C.H. & Evans, W.E. Treatment of acute lymphoblastic leukemia. *N Engl J Med* **354**, 166-178 (2006).
20. Meijerink, J.P., den Boer, M.L. & Pieters, R. New genetic abnormalities and treatment response in acute lymphoblastic leukemia. *Seminars in hematology* **46**, 16-23 (2009).
21. Greaves, M. Infection, immune responses and the aetiology of childhood leukaemia. *Nat Rev Cancer* **6**, 193-203 (2006).
22. Heerema, N.A., *et al.* Prognostic impact of trisomies of chromosomes 10, 17, and 5 among children with acute lymphoblastic leukemia and high hyperdiploidy (> 50 chromosomes). *J Clin Oncol* **18**, 1876-1887 (2000).

23. Pieters, R., *et al.* Successful Therapy Reduction and Intensification for Childhood Acute Lymphoblastic Leukemia Based on Minimal Residual Disease Monitoring: Study ALL10 From the Dutch Childhood Oncology Group. *J Clin Oncol* **34**, 2591-2601 (2016).
24. Romana, S.P., *et al.* The t(12;21) of acute lymphoblastic leukemia results in a tel-AML1 gene fusion. *Blood* **85**, 3662-3670 (1995).
25. Shurtleff, S.A., *et al.* TEL/AML1 fusion resulting from a cryptic t(12;21) is the most common genetic lesion in pediatric ALL and defines a subgroup of patients with an excellent prognosis. *Leukemia* **9**, 1985-1989 (1995).
26. Golub, T.R., *et al.* Fusion of the TEL gene on 12p13 to the AML1 gene on 21q22 in acute lymphoblastic leukemia. *Proc Natl Acad Sci U S A* **92**, 4917-4921 (1995).
27. Stams, W.A., *et al.* Incidence of additional genetic changes in the TEL and AML1 genes in DCOG and COALL-treated t(12;21)-positive pediatric ALL, and their relation with drug sensitivity and clinical outcome. *Leukemia* **20**, 410-416 (2006).
28. Kaspers, G.J., *et al.* Favorable prognosis of hyperdiploid common acute lymphoblastic leukemia may be explained by sensitivity to antimetabolites and other drugs: results of an in vitro study. *Blood* **85**, 751-756 (1995).
29. Ramakers-van Woerden, N.L., *et al.* TEL/AML1 gene fusion is related to in vitro drug sensitivity for L-asparaginase in childhood acute lymphoblastic leukemia. *Blood* **96**, 1094-1099 (2000).
30. Mullighan, C.G., *et al.* BCR-ABL1 lymphoblastic leukaemia is characterized by the deletion of Ikaros. *Nature* **453**, 110-114 (2008).
31. van der Veer, A., *et al.* IKZF1 status as a prognostic feature in BCR-ABL1-positive childhood ALL. *Blood* **123**, 1691-1698 (2014).
32. Thompson, C.B. Attacking cancer at its root. *Cell* **138**, 1051-1054 (2009).
33. Druker, B.J., *et al.* Efficacy and safety of a specific inhibitor of the BCR-ABL tyrosine kinase in chronic myeloid leukemia. *N Engl J Med* **344**, 1031-1037 (2001).
34. Zwaan, C.M., *et al.* Dasatinib in children and adolescents with relapsed or refractory leukemia: results of the CA180-018 phase I dose-escalation study of the Innovative Therapies for Children with Cancer Consortium. *J Clin Oncol* **31**, 2460-2468 (2013).
35. Schultz, K.R., *et al.* Improved early event-free survival with imatinib in Philadelphia chromosome-positive acute lymphoblastic leukemia: a children's oncology group study. *J Clin Oncol* **27**, 5175-5181 (2009).
36. Goldman, J.M. & Melo, J.V. Chronic myeloid leukemia--advances in biology and new approaches to treatment. *N Engl J Med* **349**, 1451-1464 (2003).
37. Biondi, A., *et al.* Imatinib after induction for treatment of children and adolescents with Philadelphia-chromosome-positive acute lymphoblastic leukaemia (EsPhALL): a randomised, open-label, intergroup study. *Lancet Oncol* **13**, 936-945 (2012).
38. Pieters, R., *et al.* A treatment protocol for infants younger than 1 year with acute lymphoblastic leukaemia (Interfant-99): an observational study and a multicentre randomised trial. *Lancet* **370**, 240-250 (2007).
39. van der Veer, A., *et al.* Independent prognostic value of BCR-ABL1-like signature and IKZF1 deletion, but not high CRLF2 expression, in children with B-cell precursor ALL. *Blood* **122**, 2622-2629 (2013).
40. Den Boer, M.L., *et al.* A subtype of childhood acute lymphoblastic leukaemia with poor treatment outcome: a genome-wide classification study. *Lancet Oncol* **10**, 125-134 (2009).

41. Mullighan, C.G., *et al.* Deletion of IKZF1 and prognosis in acute lymphoblastic leukemia. *N Engl J Med* **360**, 470-480 (2009).
42. Homminga, I., *et al.* Integrated transcript and genome analyses reveal NKX2-1 and MEF2C as potential oncogenes in T cell acute lymphoblastic leukemia. *Cancer Cell* **19**, 484-497 (2011).
43. Coustan-Smith, E., *et al.* Early T-cell precursor leukaemia: a subtype of very high-risk acute lymphoblastic leukaemia. *Lancet Oncol* **10**, 147-156 (2009).
44. Haydu, J.E. & Ferrando, A.A. Early T-cell precursor acute lymphoblastic leukaemia. *Curr Opin Hematol* **20**, 369-373 (2013).
45. Jain, N., *et al.* Early T-cell precursor acute lymphoblastic leukemia/lymphoma (ETP-ALL/LBL) in adolescents and adults: a high-risk subtype. *Blood* **127**, 1863-1869 (2016).
46. Zelent, A., Greaves, M. & Enver, T. Role of the TEL-AML1 fusion gene in the molecular pathogenesis of childhood acute lymphoblastic leukaemia. *Oncogene* **23**, 4275-4283 (2004).
47. Sementchenko, V.I. & Watson, D.K. Ets target genes: past, present and future. *Oncogene* **19**, 6533-6548 (2000).
48. Sharrocks, A.D. The ETS-domain transcription factor family. *Nat Rev Mol Cell Biol* **2**, 827-837 (2001).
49. Wood, L.D., Irvin, B.J., Nucifora, G., Luce, K.S. & Hiebert, S.W. Small ubiquitin-like modifier conjugation regulates nuclear export of TEL, a putative tumor suppressor. *Proc Natl Acad Sci U S A* **100**, 3257-3262 (2003).
50. Fenrick, R., *et al.* Both TEL and AML-1 contribute repression domains to the t(12;21) fusion protein. *Mol Cell Biol* **19**, 6566-6574 (1999).
51. Uchida, H., *et al.* Three distinct domains in TEL-AML1 are required for transcriptional repression of the IL-3 promoter. *Oncogene* **18**, 1015-1022 (1999).
52. Baker, D.A., Mille-Baker, B., Wainwright, S.M., Ish-Horowicz, D. & Dibb, N.J. Mae mediates MAP kinase phosphorylation of Ets transcription factors in Drosophila. *Nature* **411**, 330-334 (2001).
53. Kim, C.A., *et al.* Polymerization of the SAM domain of TEL in leukemogenesis and transcriptional repression. *The EMBO journal* **20**, 4173-4182 (2001).
54. Lopez, R.G., *et al.* TEL is a sequence-specific transcriptional repressor. *J Biol Chem* **274**, 30132-30138 (1999).
55. Rubnitz, J.E., Pui, C.H. & Downing, J.R. The role of TEL fusion genes in pediatric leukemias. *Leukemia* **13**, 6-13 (1999).
56. Wang, L.C., *et al.* The TEL/ETV6 gene is required specifically for hematopoiesis in the bone marrow. *Genes Dev* **12**, 2392-2402 (1998).
57. Golub, T.R., Barker, G.F., Lovett, M. & Gilliland, D.G. Fusion of PDGF receptor beta to a novel ets-like gene, tel, in chronic myelomonocytic leukemia with t(5;12) chromosomal translocation. *Cell* **77**, 307-316 (1994).
58. Papadopoulos, P., Ridge, S.A., Boucher, C.A., Stocking, C. & Wiedemann, L.M. The novel activation of ABL by fusion to an ets-related gene, TEL. *Cancer Res* **55**, 34-38 (1995).
59. Lacronique, V., *et al.* A TEL-JAK2 fusion protein with constitutive kinase activity in human leukemia. *Science* **278**, 1309-1312 (1997).
60. Okuda, T., van Deursen, J., Hiebert, S.W., Grosveld, G. & Downing, J.R. AML1, the target of multiple chromosomal translocations in human leukemia, is essential for normal fetal liver hematopoiesis. *Cell* **84**, 321-330 (1996).
61. Ichikawa, M., *et al.* AML1/Runx1 negatively regulates quiescent hematopoietic stem cells in adult hematopoiesis. *J Immunol* **180**, 4402-4408 (2008).

62. Ichikawa, M., *et al.* AML-1 is required for megakaryocytic maturation and lymphocytic differentiation, but not for maintenance of hematopoietic stem cells in adult hematopoiesis. *Nat Med* **10**, 299-304 (2004).
63. Kurokawa, M. AML1/Runx1 as a versatile regulator of hematopoiesis: regulation of its function and a role in adult hematopoiesis. *International journal of hematology* **84**, 136-142 (2006).
64. Kurokawa, M. & Hirai, H. Role of AML1/Runx1 in the pathogenesis of hematological malignancies. *Cancer science* **94**, 841-846 (2003).
65. Wang, Q., *et al.* The CBFbeta subunit is essential for CBFalpha2 (AML1) function in vivo. *Cell* **87**, 697-708 (1996).
66. Erickson, P., *et al.* Identification of breakpoints in t(8;21) acute myelogenous leukemia and isolation of a fusion transcript, AML1/ETO, with similarity to Drosophila segmentation gene, runt. *Blood* **80**, 1825-1831 (1992).
67. Xiao, Z., *et al.* Molecular characterization of genomic AML1-ETO fusions in childhood leukemia. *Leukemia* **15**, 1906-1913 (2001).
68. Roudaia, L., *et al.* CBFbeta is critical for AML1-ETO and TEL-AML1 activity. *Blood* **113**, 3070-3079 (2009).
69. Hiebert, S.W., *et al.* The t(12;21) translocation converts AML-1B from an activator to a repressor of transcription. *Mol Cell Biol* **16**, 1349-1355 (1996).
70. Schindler, J.W., *et al.* TEL-AML1 corrupts hematopoietic stem cells to persist in the bone marrow and initiate leukemia. *Cell Stem Cell* **5**, 43-53 (2009).
71. Linka, Y., *et al.* The impact of TEL-AML1 (ETV6-RUNX1) expression in precursor B cells and implications for leukaemia using three different genome-wide screening methods. *Blood Cancer J* **3**, e151 (2013).
72. Mangolini, M., *et al.* STAT3 mediates oncogenic addiction to TEL-AML1 in t(12;21) acute lymphoblastic leukemia. *Blood* **122**, 542-549 (2013).
73. Torrano, V., Procter, J., Cardus, P., Greaves, M. & Ford, A.M. ETV6-RUNX1 promotes survival of early B lineage progenitor cells via a dysregulated erythropoietin receptor. *Blood* **118**, 4910-4918 (2011).
74. Diakos, C., *et al.* TEL-AML1 regulation of survivin and apoptosis via miRNA-494 and miRNA-320a. *Blood* **116**, 4885-4893 (2010).
75. Diakos, C., *et al.* RNAi-mediated silencing of TEL/AML1 reveals a heat-shock protein- and survivin-dependent mechanism for survival. *Blood* **109**, 2607-2610 (2007).
76. Gefen, N., *et al.* Hsa-mir-125b-2 is highly expressed in childhood ETV6/RUNX1 (TEL/AML1) leukemias and confers survival advantage to growth inhibitory signals independent of p53. *Leukemia* **24**, 89-96 (2010).
77. Palmi, C., *et al.* Cytoskeletal Regulatory Gene Expression and Migratory Properties of B Cell Progenitors are Affected by the ETV6-RUNX1 Rearrangement. *Mol Cancer Res* (2014).
78. Ford, A.M., *et al.* The TEL-AML1 leukemia fusion gene dysregulates the TGF-beta pathway in early B lineage progenitor cells. *J Clin Invest* **119**, 826-836 (2009).
79. Inthal, A., *et al.* Role of the erythropoietin receptor in ETV6/RUNX1-positive acute lymphoblastic leukemia. *Clin Cancer Res* **14**, 7196-7204 (2008).
80. de Laurentiis, A., Hiscott, J. & Alcalay, M. The TEL-AML1 fusion protein of acute lymphoblastic leukemia modulates IRF3 activity during early B-cell differentiation. *Oncogene* (2015).

81. Ford, A.M., *et al.* Origins of "late" relapse in childhood acute lymphoblastic leukemia with TEL-AML1 fusion genes. *Blood* **98**, 558-564 (2001).
82. Kuster, L., *et al.* ETV6/RUNX1-positive relapses evolve from an ancestral clone and frequently acquire deletions of genes implicated in glucocorticoid signaling. *Blood* **117**, 2658-2667 (2011).
83. Tsuzuki, S., Seto, M., Greaves, M. & Enver, T. Modeling first-hit functions of the t(12;21) TEL-AML1 translocation in mice. *Proc Natl Acad Sci U S A* **101**, 8443-8448 (2004).
84. Hong, D., *et al.* Initiating and cancer-propagating cells in TEL-AML1-associated childhood leukemia. *Science* **319**, 336-339 (2008).
85. van der Weyden, L., *et al.* Modeling the evolution of ETV6-RUNX1-induced B-cell precursor acute lymphoblastic leukemia in mice. *Blood* **118**, 1041-1051 (2011).
86. Castor, A., *et al.* Distinct patterns of hematopoietic stem cell involvement in acute lymphoblastic leukemia. *Nat Med* **11**, 630-637 (2005).
87. Anderson, K., *et al.* Genetic variegation of clonal architecture and propagating cells in leukaemia. *Nature* **469**, 356-361 (2011).
88. Mullighan, C.G., *et al.* Genome-wide analysis of genetic alterations in acute lymphoblastic leukaemia. *Nature* **446**, 758-764 (2007).
89. Fuka, G., *et al.* Silencing of ETV6/RUNX1 abrogates PI3K/AKT/mTOR signaling and impairs reconstitution of leukemia in xenografts. *Leukemia* **26**, 927-933 (2012).
90. Spencer, J.A., *et al.* Direct measurement of local oxygen concentration in the bone marrow of live animals. *Nature* **508**, 269-273 (2014).
91. Schepers, K., Campbell, T.B. & Passegue, E. Normal and Leukemic Stem Cell Niches: Insights and Therapeutic Opportunities. *Cell Stem Cell* **16**, 254-267 (2015).
92. Kfoury, Y. & Scadden, D.T. Mesenchymal Cell Contributions to the Stem Cell Niche. *Cell Stem Cell* **16**, 239-253 (2015).
93. Morrison, S.J. & Scadden, D.T. The bone marrow niche for haematopoietic stem cells. *Nature* **505**, 327-334 (2014).
94. Ding, L., Saunders, T.L., Enikolopov, G. & Morrison, S.J. Endothelial and perivascular cells maintain haematopoietic stem cells. *Nature* **481**, 457-462 (2012).
95. Ding, L. & Morrison, S.J. Haematopoietic stem cells and early lymphoid progenitors occupy distinct bone marrow niches. *Nature* **495**, 231-235 (2013).
96. Greenbaum, A., *et al.* CXCL12 in early mesenchymal progenitors is required for haematopoietic stem-cell maintenance. *Nature* **495**, 227-230 (2013).
97. Butler, J.M., *et al.* Endothelial cells are essential for the self-renewal and repopulation of Notch-dependent hematopoietic stem cells. *Cell Stem Cell* **6**, 251-264 (2010).
98. Winkler, I.G., *et al.* Vascular niche E-selectin regulates hematopoietic stem cell dormancy, self renewal and chemoresistance. *Nat Med* **18**, 1651-1657 (2012).
99. Zhao, M., *et al.* Megakaryocytes maintain homeostatic quiescence and promote post-injury regeneration of hematopoietic stem cells. *Nat Med* **20**, 1321-1326 (2014).
100. Bruns, I., *et al.* Megakaryocytes regulate hematopoietic stem cell quiescence through CXCL4 secretion. *Nat Med* **20**, 1315-1320 (2014).
101. Nakamura-Ishizu, A., Takubo, K., Fujioka, M. & Suda, T. Megakaryocytes are essential for HSC quiescence through the production of thrombopoietin. *Biochemical and biophysical research communications* **454**, 353-357 (2014).
102. Dominici, M., *et al.* Minimal criteria for defining multipotent mesenchymal stromal cells. The International Society for Cellular Therapy position statement. *Cytotherapy* **8**, 315-317 (2006).

103. Mendez-Ferrer, S., *et al.* Mesenchymal and haematopoietic stem cells form a unique bone marrow niche. *Nature* **466**, 829-834 (2010).
104. Kunisaki, Y., *et al.* Arteriolar niches maintain haematopoietic stem cell quiescence. *Nature* **502**, 637-643 (2013).
105. Zhou, B.O., Yue, R., Murphy, M.M., Peyer, J.G. & Morrison, S.J. Leptin-receptor-expressing mesenchymal stromal cells represent the main source of bone formed by adult bone marrow. *Cell Stem Cell* **15**, 154-168 (2014).
106. Winkler, I.G., *et al.* Bone marrow macrophages maintain hematopoietic stem cell (HSC) niches and their depletion mobilizes HSCs. *Blood* **116**, 4815-4828 (2010).
107. Pinho, S., *et al.* PDGFRalpha and CD51 mark human nestin+ sphere-forming mesenchymal stem cells capable of hematopoietic progenitor cell expansion. *The Journal of experimental medicine* **210**, 1351-1367 (2013).
108. Sugiyama, T., Kohara, H., Noda, M. & Nagasawa, T. Maintenance of the hematopoietic stem cell pool by CXCL12-CXCR4 chemokine signaling in bone marrow stromal cell niches. *Immunity* **25**, 977-988 (2006).
109. Schepers, K., *et al.* Myeloproliferative neoplasia remodels the endosteal bone marrow niche into a self-reinforcing leukemic niche. *Cell Stem Cell* **13**, 285-299 (2013).
110. Omatsu, Y., *et al.* The essential functions of adipo-osteogenic progenitors as the hematopoietic stem and progenitor cell niche. *Immunity* **33**, 387-399 (2010).
111. Wu, J.Y., *et al.* Osteoblastic regulation of B lymphopoiesis is mediated by Gs{alpha}-dependent signaling pathways. *Proc Natl Acad Sci U S A* **105**, 16976-16981 (2008).
112. Guezguez, B., *et al.* Regional localization within the bone marrow influences the functional capacity of human HSCs. *Cell Stem Cell* **13**, 175-189 (2013).
113. Flores-Figueroa, E., Varma, S., Montgomery, K., Greenberg, P.L. & Gratzinger, D. Distinctive contact between CD34+ hematopoietic progenitors and CXCL12+ CD271+ mesenchymal stromal cells in benign and myelodysplastic bone marrow. *Laboratory investigation; a journal of technical methods and pathology* **92**, 1330-1341 (2012).
114. Li, H., *et al.* Low/negative expression of PDGFR-alpha identifies the candidate primary mesenchymal stromal cells in adult human bone marrow. *Stem cell reports* **3**, 965-974 (2014).
115. Taichman, R.S. Blood and bone: two tissues whose fates are intertwined to create the hematopoietic stem-cell niche. *Blood* **105**, 2631-2639 (2005).
116. Colmone, A., *et al.* Leukemic cells create bone marrow niches that disrupt the behavior of normal hematopoietic progenitor cells. *Science* **322**, 1861-1865 (2008).
117. Sipkins, D.A., *et al.* In vivo imaging of specialized bone marrow endothelial microdomains for tumour engraftment. *Nature* **435**, 969-973 (2005).
118. Yilmaz, O.H., *et al.* Pten dependence distinguishes haematopoietic stem cells from leukaemia-initiating cells. *Nature* **441**, 475-482 (2006).
119. Santaguida, M., *et al.* JunB protects against myeloid malignancies by limiting hematopoietic stem cell proliferation and differentiation without affecting self-renewal. *Cancer Cell* **15**, 341-352 (2009).
120. Krause, D.S., *et al.* Differential regulation of myeloid leukemias by the bone marrow microenvironment. *Nat Med* **19**, 1513-1517 (2013).
121. Lane, S.W., *et al.* Differential niche and Wnt requirements during acute myeloid leukemia progression. *Blood* **118**, 2849-2856 (2011).
122. Duhrsen, U. & Hossfeld, D.K. Stromal abnormalities in neoplastic bone marrow diseases. *Annals of hematology* **73**, 53-70 (1996).

123. Zhang, B., *et al.* Altered microenvironmental regulation of leukemic and normal stem cells in chronic myelogenous leukemia. *Cancer Cell* **21**, 577-592 (2012).
124. Schmidt, T., *et al.* Loss or inhibition of stromal-derived PlGF prolongs survival of mice with imatinib-resistant Bcr-Abl1(+) leukemia. *Cancer Cell* **19**, 740-753 (2011).
125. Arranz, L., *et al.* Neuropathy of haematopoietic stem cell niche is essential for myeloproliferative neoplasms. *Nature* **512**, 78-81 (2014).
126. Hanoun, M., *et al.* Acute myelogenous leukemia-induced sympathetic neuropathy promotes malignancy in an altered hematopoietic stem cell niche. *Cell Stem Cell* **15**, 365-375 (2014).
127. Medyouf, H., *et al.* Myelodysplastic Cells in Patients Reprogram Mesenchymal Stromal Cells to Establish a Transplantable Stem Cell Niche Disease Unit. *Cell Stem Cell* (2014).
128. Walkley, C.R., Shea, J.M., Sims, N.A., Purton, L.E. & Orkin, S.H. Rb regulates interactions between hematopoietic stem cells and their bone marrow microenvironment. *Cell* **129**, 1081-1095 (2007).
129. Walkley, C.R., *et al.* A microenvironment-induced myeloproliferative syndrome caused by retinoic acid receptor gamma deficiency. *Cell* **129**, 1097-1110 (2007).
130. Kim, Y.W., *et al.* Defective Notch activation in microenvironment leads to myeloproliferative disease. *Blood* **112**, 4628-4638 (2008).
131. Raaijmakers, M.H., *et al.* Bone progenitor dysfunction induces myelodysplasia and secondary leukaemia. *Nature* **464**, 852-857 (2010).
132. Wang, L., *et al.* Notch-dependent repression of miR-155 in the bone marrow niche regulates hematopoiesis in an NF-kappaB-dependent manner. *Cell Stem Cell* **15**, 51-65 (2014).
133. Kode, A., *et al.* Leukaemogenesis induced by an activating beta-catenin mutation in osteoblasts. *Nature* **506**, 240-244 (2014).
134. Arai, F., *et al.* Tie2/angiopoietin-1 signaling regulates hematopoietic stem cell quiescence in the bone marrow niche. *Cell* **118**, 149-161 (2004).
135. Fujisaki, J., *et al.* In vivo imaging of Treg cells providing immune privilege to the haematopoietic stem-cell niche. *Nature* **474**, 216-219 (2011).
136. Nakasone, E.S., *et al.* Imaging tumor-stroma interactions during chemotherapy reveals contributions of the microenvironment to resistance. *Cancer Cell* **21**, 488-503 (2012).
137. McMillin, D.W., *et al.* Tumor cell-specific bioluminescence platform to identify stroma-induced changes to anticancer drug activity. *Nat Med* **16**, 483-489 (2010).
138. McMillin, D.W., Negri, J.M. & Mitsiades, C.S. The role of tumour-stromal interactions in modifying drug response: challenges and opportunities. *Nat Rev Drug Discov* **12**, 217-228 (2013).
139. Straussman, R., *et al.* Tumour micro-environment elicits innate resistance to RAF inhibitors through HGF secretion. *Nature* **487**, 500-504 (2012).
140. Wilson, T.R., *et al.* Widespread potential for growth-factor-driven resistance to anticancer kinase inhibitors. *Nature* **487**, 505-509 (2012).
141. Konopleva, M.Y. & Jordan, C.T. Leukemia stem cells and microenvironment: biology and therapeutic targeting. *J Clin Oncol* **29**, 591-599 (2011).
142. Pallasch, C.P., *et al.* Sensitizing protective tumor microenvironments to antibody-mediated therapy. *Cell* **156**, 590-602 (2014).
143. Manshouri, T., *et al.* Bone marrow stroma-secreted cytokines protect JAK2(V617F)-mutated cells from the effects of a JAK2 inhibitor. *Cancer Res* **71**, 3831-3840 (2011).
144. Jin, L., Hope, K.J., Zhai, Q., Smadja-Joffe, F. & Dick, J.E. Targeting of CD44 eradicates human acute myeloid leukemic stem cells. *Nat Med* **12**, 1167-1174 (2006).

145. Matsunaga, T., *et al.* Interaction between leukemic-cell VLA-4 and stromal fibronectin is a decisive factor for minimal residual disease of acute myelogenous leukemia. *Nat Med* **9**, 1158-1165 (2003).
146. Nervi, B., *et al.* Chemosensitization of acute myeloid leukemia (AML) following mobilization by the CXCR4 antagonist AMD3100. *Blood* **113**, 6206-6214 (2009).
147. Tavor, S., *et al.* CXCR4 regulates migration and development of human acute myelogenous leukemia stem cells in transplanted NOD/SCID mice. *Cancer Res* **64**, 2817-2824 (2004).
148. Zeng, Z., *et al.* Targeting the leukemia microenvironment by CXCR4 inhibition overcomes resistance to kinase inhibitors and chemotherapy in AML. *Blood* **113**, 6215-6224 (2009).
149. Tabe, Y., *et al.* Activation of integrin-linked kinase is a critical prosurvival pathway induced in leukemic cells by bone marrow-derived stromal cells. *Cancer Res* **67**, 684-694 (2007).
150. Burger, J.A. & Peled, A. CXCR4 antagonists: targeting the microenvironment in leukemia and other cancers. *Leukemia* **23**, 43-52 (2009).
151. Juarez, J., Bradstock, K.F., Gottlieb, D.J. & Bendall, L.J. Effects of inhibitors of the chemokine receptor CXCR4 on acute lymphoblastic leukemia cells in vitro. *Leukemia* **17**, 1294-1300 (2003).
152. Lowenberg, B., *et al.* Effect of priming with granulocyte colony-stimulating factor on the outcome of chemotherapy for acute myeloid leukemia. *N Engl J Med* **349**, 743-752 (2003).
153. Petit, I., *et al.* G-CSF induces stem cell mobilization by decreasing bone marrow SDF-1 and up-regulating CXCR4. *Nat Immunol* **3**, 687-694 (2002).
154. Burger, M., *et al.* Small peptide inhibitors of the CXCR4 chemokine receptor (CD184) antagonize the activation, migration, and antiapoptotic responses of CXCL12 in chronic lymphocytic leukemia B cells. *Blood* **106**, 1824-1830 (2005).
155. Juarez, J., *et al.* CXCR4 antagonists mobilize childhood acute lymphoblastic leukemia cells into the peripheral blood and inhibit engraftment. *Leukemia* **21**, 1249-1257 (2007).
156. Tavor, S., *et al.* The CXCR4 antagonist AMD3100 impairs survival of human AML cells and induces their differentiation. *Leukemia* **22**, 2151-5158 (2008).
157. Azab, A.K., *et al.* CXCR4 inhibitor AMD3100 disrupts the interaction of multiple myeloma cells with the bone marrow microenvironment and enhances their sensitivity to therapy. *Blood* **113**, 4341-4351 (2009).
158. Parameswaran, R., Yu, M., Lim, M., Groffen, J. & Heisterkamp, N. Combination of drug therapy in acute lymphoblastic leukemia with a CXCR4 antagonist. *Leukemia* **25**, 1314-1323 (2011).
159. O'Callaghan, K., *et al.* Targeting CXCR4 with cell-penetrating pepducins in lymphoma and lymphocytic leukemia. *Blood* **119**, 1717-1725 (2012).
160. Uy, G.L., *et al.* A phase 1/2 study of chemosensitization with the CXCR4 antagonist plerixafor in relapsed or refractory acute myeloid leukemia. *Blood* **119**, 3917-3924 (2012).
161. Fierro, F.A., *et al.* Combining SDF-1/CXCR4 antagonism and chemotherapy in relapsed acute myeloid leukemia. *Leukemia* **23**, 393-396 (2009).
162. Borthakur, G. BL-8040, a Peptidic CXCR4 Antagonist, Induces Leukemia Cell Death and Specific Leukemia Cell Mobilization in Relapsed/Refractory Acute Myeloid Leukemia Patients in an Ongoing Phase IIa Clinical Trial. *ASH abstract 950* (2014).
163. Becker, P.S. Targeting the CXCR4 Pathway: Safety, Tolerability and Clinical Activity of Ulocuplumab (BMS-936564), an Anti-CXCR4 Antibody, in Relapsed/Refractory Acute Myeloid Leukemia. *ASH Abstract 386* (2014).

164. Cooper, T.M. Chemosensitization and Mobilization Of AML/ALL/MDS With Plerixafor (AMD 3100), a CXCR4 Antagonist: A Phase I Study Of Plerixafor + Cytarabine and Etoposide In Pediatric Patients With Acute Leukemia and MDS. *ASH Abstract 2680* (2013).
165. Ottmann, O.G., Bug, G. & Krauter, J. Current status of growth factors in the treatment of acute myeloid and lymphoblastic leukemia. *Seminars in hematology* **44**, 183-192 (2007).
166. Heuser, M., *et al.* Priming reloaded? *Blood* **114**, 925-926; author reply 926-927 (2009).
167. Aiuti, A., Webb, I.J., Bleul, C., Springer, T. & Gutierrez-Ramos, J.C. The chemokine SDF-1 is a chemoattractant for human CD34+ hematopoietic progenitor cells and provides a new mechanism to explain the mobilization of CD34+ progenitors to peripheral blood. *The Journal of experimental medicine* **185**, 111-120 (1997).
168. Peled, A., *et al.* Dependence of human stem cell engraftment and repopulation of NOD/SCID mice on CXCR4. *Science* **283**, 845-848 (1999).
169. Chauveau, A., Aucher, A., Eissmann, P., Vivier, E. & Davis, D.M. Membrane nanotubes facilitate long-distance interactions between natural killer cells and target cells. *Proc Natl Acad Sci U S A* **107**, 5545-5550 (2010).
170. Onfelt, B., Nedvetzki, S., Yanagi, K. & Davis, D.M. Cutting edge: Membrane nanotubes connect immune cells. *J Immunol* **173**, 1511-1513 (2004).
171. Rainy, N., *et al.* H-Ras transfers from B to T cells via tunneling nanotubes. *Cell Death Dis* **4**, e726 (2013).
172. Rustom, A., Saffrich, R., Markovic, I., Walther, P. & Gerdes, H.H. Nanotubular highways for intercellular organelle transport. *Science* **303**, 1007-1010 (2004).
173. Sowinski, S., *et al.* Membrane nanotubes physically connect T cells over long distances presenting a novel route for HIV-1 transmission. *Nat Cell Biol* **10**, 211-219 (2008).
174. Chinnery, H.R., Pearlman, E. & McMenamin, P.G. Cutting edge: Membrane nanotubes in vivo: a feature of MHC class II+ cells in the mouse cornea. *J Immunol* **180**, 5779-5783 (2008).
175. Marzo, L., Gousset, K. & Zurzolo, C. Multifaceted roles of tunneling nanotubes in intercellular communication. *Front Physiol* **3**, 72 (2012).
176. Seyed-Razavi, Y., Hickey, M.J., Kuffova, L., McMenamin, P.G. & Chinnery, H.R. Membrane nanotubes in myeloid cells in the adult mouse cornea represent a novel mode of immune cell interaction. *Immunol Cell Biol* **91**, 89-95 (2013).
177. Watkins, S.C. & Salter, R.D. Functional connectivity between immune cells mediated by tunneling nanotubules. *Immunity* **23**, 309-318 (2005).
178. Arkwright, P.D., *et al.* Fas stimulation of T lymphocytes promotes rapid intercellular exchange of death signals via membrane nanotubes. *Cell Res* **20**, 72-88 (2010).
179. Pasquier, J., *et al.* Different modalities of intercellular membrane exchanges mediate cell-to-cell p-glycoprotein transfers in MCF-7 breast cancer cells. *J Biol Chem* **287**, 7374-7387 (2012).
180. Gousset, K., *et al.* Prions hijack tunnelling nanotubes for intercellular spread. *Nat Cell Biol* **11**, 328-336 (2009).
181. Pasquier, J., *et al.* Preferential transfer of mitochondria from endothelial to cancer cells through tunneling nanotubes modulates chemoresistance. *J Transl Med* **11**, 94 (2013).
182. Lou, E., *et al.* Tunneling nanotubes provide a unique conduit for intercellular transfer of cellular contents in human malignant pleural mesothelioma. *PLoS One* **7**, e33093 (2012).
183. Pui, C.H., Carroll, W.L., Meshinchi, S. & Arceci, R.J. Biology, risk stratification, and therapy of pediatric acute leukemias: an update. *J Clin Oncol* **29**, 551-565 (2011).
184. Nguyen, K., *et al.* Factors influencing survival after relapse from acute lymphoblastic leukemia: a Children's Oncology Group study. *Leukemia* **22**, 2142-2150 (2008).

185. Robison, L.L. Late effects of acute lymphoblastic leukemia therapy in patients diagnosed at 0-20 years of age. *Hematology Am Soc Hematol Educ Program* **2011**, 238-242 (2011).
186. Oeffinger, K.C., Nathan, P.C. & Kremer, L.C. Challenges after curative treatment for childhood cancer and long-term follow up of survivors. *Hematol Oncol Clin North Am* **24**, 129-149 (2010).

Chapter 2

The PI3K/PKB signaling module as key regulator of hematopoiesis: implications for therapeutic strategies in leukemia

Roel Polak[1] and Miranda Buitenhuis[1,2]

[1]*Department of Hematology, Erasmus MC, Rotterdam, the Netherlands.*
[2]*Erasmus MC Stem Cell Institute for Regenerative Medicine, Erasmus MC, Rotterdam, the Netherlands*

Blood. 2012 Jan 26;119(4):911-23

ABSTRACT

An important mediator of cytokine signaling implicated in regulation of hematopoiesis is the PI3K/protein kinase B (PKB/c-Akt) signaling module. Constitutive activation of this signaling module has been observed in a large group of leukemias. Because activation of this signaling pathway has been demonstrated to be sufficient to induce hematologic malignancies and is thought to correlate with poor prognosis and enhanced drug resistance, it is considered to be a promising target for therapy. A high number of pharmacologic inhibitors directed against either individual or multiple components of this pathway have already been developed to improve therapy. In this review, the safety and efficacy of both single and dual-specificity inhibitors will be discussed as well as the potential of combination therapy with either inhibitors directed against other signal transduction molecules or classic chemotherapy.

PI3K plays a critical role in both HSC maintenance and lineage development

The PI3K family consists of 3 distinct subclasses of which, to date, only the class I isoforms have been implicated in regulation of hematopoiesis. Three distinct catalytic class IA isoforms have been identified: p110α, p110β, and p110δ[1]. These isoforms are predominantly activated by protein tyrosine kinases and form heterodimers with a group a regulatory adapter molecules, including p85α, p85β, p50α, p55α, and p55γ[1]. In addition, a single-class 1B isoform termed p110γ has been described, which can be specifically activated by G-protein coupled receptors and associates with a p101 regulatory molecule[1]. The most important substrate for these class I PI3Ks is phosphatidylinositol 4,5 bisphosphate [PI(4,5)P_2] which can be phosphorylated at the D3 position of the inositol ring on extracellular stimulation, resulting in the formation of phosphatidylinositol 3,4,5 trisphosphate [PI(3,4,5)P_3][1] (Figure 1). The activity of PI3K can be inhibited by phosphate and tensin homologue (PTEN), a ubiquitously expressed tumor suppressor protein that can dephosphorylate PIP_3, resulting in the formation of PI(4,5)P_2[1,2]. Similarly, SH2-containing inositol-5′-phosphatase 1 (SHIP1), a protein predominantly expressed in hematopoietic cells, can hydrolyze PIP_3 to generate PI(3,4)P_2[1,2]. Although both PTEN and SHIP1 act on the main product of PI3K, PI(3,4,5)P_3, the generated products PI(3,4)P_2 and PI(4,5)P_2 both act as discrete second messengers activating distinct downstream events[2]. Recently, pleckstrin homology (PH) domain leucine-rich repeat protein phosphatase (PHLPP) was found to terminate PKB signaling by directly dephosphorylating and inactivating PKB[3]. However, a role for PHLPP in regulation of hematopoiesis remains to be determined. Inositol 1,3,4,5-tetrakiphosphate [Ins(1,3,4,5)P4], which is generated from inositol 1,4,5-triphosphate [Ins(1,4,5)P3] by inositol triphosphate 3-kinase B (InsP3KB), is considered to be a fourth negative regulator of the PI3K/PKB signaling module. The activity of downstream effectors of PI3K, including PKB, can be abrogated because of binding of PI(3,4,5)P_3-specific pleckstrin homology (PH) domains to Ins(1,3,4,5)P4[4]. Since the identification of PI3K, it has become evident that it plays an essential role in proliferation, survival, and differentiation of many different cell types. Correct regulation of the activity of PI3K has been demonstrated to be essential for maintenance of hematopoietic stem cells using PTEN- and SHIP1-deficient mice that displayed constitutive activation of PI3K activity. In those mice, an initial expansion of HSCs could be observed that was followed by a depletion of long-term repopulating HSCs[5]. The role of class I PI3K isoforms in lineage development has been investigated in more detail. Combined deletion of p85α, p55α, and p50α has, for example, resulted in a complete block in B lymphocyte development[6]. Similarly, introduction of a mutated, catalytically inactive p110δ (p110δ^{D910A}) in the normal p110δ locus also resulted in a block in early B lymphocyte development, whereas T-cell development was unaffected[7]. These results indicate that PI3K activity is

essential for normal B lymphocyte development. In addition, conditional deletion of either PTEN or SHIP1 in adult HSCs, resulting in activation of the PI3K pathway, not only reduced the level of B-lymphocytes but also enhanced the level of myeloid cells[8,9]. Furthermore, enhanced levels of megakaryocyte progenitors have been observed in SHIP1-deficient mice[10]. In time, both PTEN- and SHIP1-deficient mice developed a myeloproliferative disorder that progressed to leukemia[8,9]. In PTEN heterozygote (+/−) SHIP null (−/−) mice, a more severe myeloproliferative phenotype, displayed by reduced erythrocyte and platelet numbers and enhanced white blood cell counts including elevated levels of neutrophils and monocytes in the peripheral blood, could be observed[11]. Recently, a shorter SHIP1 isoform (s-SHIP1), which is transcribed from an internal promoter in the SHIP1 gene, has also been implicated in positive regulation of lymphocyte development during hematopoiesis[12]. Pharmacologic inhibition of PI3K activity in human umbilical cord blood-derived $CD34^+$ HSCs and progenitor cells revealed that inhibition of the activity of PI3K is sufficient to completely abrogate both proliferation and differentiation of eosinophil and neutrophil progenitors eventually leading to cell death[13]. Finally, mice deficient for InsP3KB, resulting in an induction of PKB activity, display higher levels of granulocyte-macrophage progenitors and mature neutrophils in the bone marrow[14] and dramatically reduced levels of mature $CD4^+$ and $CD8^+$ T lymphocytes[15]. Together, these studies suggest that correct temporal regulation of PI3K activity is critical for both HSC maintenance and regulation of lineage development.

PKB is an important mediator of PI3K in regulation of hematopoiesis

An important mediator of PI3K signaling is protein kinase B (PKB/c-akt). Whereas PKB is cytosolic in unstimulated cells, PI3K-mediated activation of PKB requires translocation of PKB to the membrane. $PI(3,4,5)P_3$, which is generated by PI3K, serves as an anchor for PH domain–containing proteins in the membrane, including PKB[16]. Activation of PKB requires phosphorylation on both Thr^{308} in the activation loop, by phosphoinositide-dependent kinase 1 (PDK1) and Ser^{473}, within the carboxyl-terminal hydrophobic motif, by the MTORC2 complex that consists of multiple proteins, including mTOR, Rictor, mLST8, DEPTOR, Sin1, and PROTOR[17] (Figure 1).

Three highly homologous PKB isoforms have been described to be expressed in mammalian cells: PKBα, PKBβ, and PKBγ. PKB has been demonstrated to play an important role in regulation of cell survival and proliferation in a large variety of cell types[18]. Analysis of HSCs derived from PKBα/PKBβ double-knockout mice revealed that PKB plays an important role in maintenance of long-term repopulating HSCs. These PKBα/PKBβ double-deficient HSCs were found to persist in the G_0 phase of the cell cycle, suggesting that the functional defects observed in these mice with regard

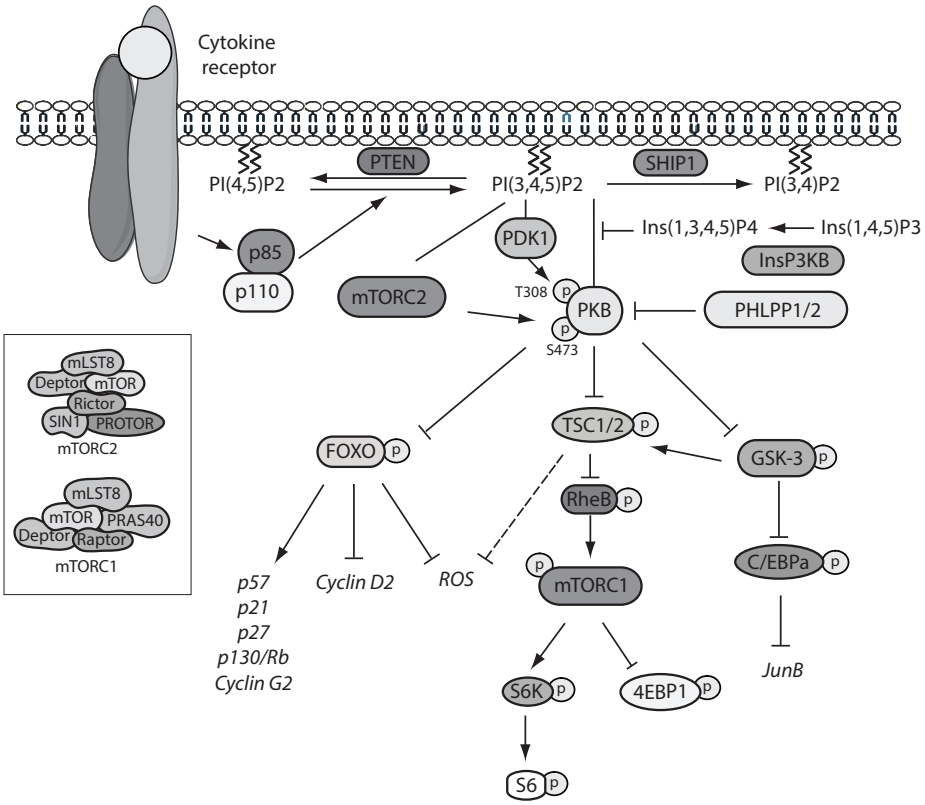

Figure 1. Schematic representation of the PI3K/PKB signaling module.
Activation of PI3K by receptor stimulation results in the production of PtdIns(3,4,5)P_3 at the plasma membrane. PKB subsequently translocates to the plasma membrane where it is phosphorylated by PDK1 and the mTORC2 complex. On phosphorylation, PKB is released into the cytoplasm where it can both inhibitory phosphorylate multiple substrates, including FoxO transcription factors and GSK-3, and induce the activity of other substrates, such as mTOR as part of the mTORC1 complex. Negative regulators of the PI3K/PKB signaling module include PTEN, SHIP1, Ins(1,3,4,5)P4, and PHLPP1/2.

to long-term hematopoiesis were caused by enhanced quiescence[19]. In contrast, loss of only one of the isoforms only minimally affected HSCs[19]. In addition, ectopic expression of constitutively active PKB in mouse HSCs conversely resulted in transient expansion and increased cycling of HSCs, followed by apoptosis and expansion of immature progenitors in BM and spleen, which was also associated with impaired engraftment[20]. In addition to HSC maintenance, PKB also plays a critical role in the regulation of cell fate decisions during hematopoietic lineage development. High PKB activity in human umbilical cord blood-derived hematopoietic progenitors was, for example, found to promote neutrophil and monocyte differentiation and to inhibit B lymphocyte development, whereas reduction of PKB activity has been demonstrated to be required for optimal eosinophil maturation[13]. In addition, PKB

plays an important role in regulation of proliferation and survival, but not maturation, of human dendritic cell (DC) progenitors[21]. The development of a myeloproliferative disease, characterized by extramedullary hematopoiesis in liver and spleen, and lymphoblastic thymic T-cell lymphoma in the majority of mice transplanted with mouse bone marrow cells ectopically expressing constitutively active PKB further demonstrates the importance for correct regulation of PKB activity in HSCs and progenitor cells[20]. In addition, recent findings suggest that constitutive activation of PKBβ is sufficient to accelerate MYC-induced T-cell acute lymphoblastic leukemia (T-ALL) in zebrafish[22]. Furthermore, analysis of mice deficient for both PKBα and PKBβ, but not single knockout mice, revealed that the generation of marginal zone and B1 B cells and the survival of mature follicular B cells also depend on correct regulation of PKB activity[23].

Downstream effectors of PKB differentially regulate hematopoiesis

Multiple PKB substrates have been identified, including members of the FoxO subfamily of forkhead transcription factors FoxO1, FoxO3, and FoxO4, the serine/threonine kinase glycogen synthase kinase-3 (GSK-3), and the serine/threonine kinase mammalian target of rapamycin (mTOR) as part of the MTORC1 complex, which also includes the regulatory associated protein of mTOR (Raptor; Figure 1)[18]. FoxO transcription factors, which are inhibitory phosphorylated by PKB[18], are known to play an important role in regulation of proliferation and survival of various cell types. In addition, these transcription factors play an important role in HSC maintenance, which has been demonstrated by conditional deletion of FoxO1, FoxO3, and FoxO4 in the adult hematopoietic system[24]. An initial expansion of HSCs has been observed in those mice, which correlated with an HSC-specific up-regulation of cyclin D2 and down-regulation of cyclin G2, p130/Rb, p27, and p21[24]. After this initial expansion, a reduction in HSC numbers was observed, resulting in a defective long-term repopulating capacity[24]. Similarly, competitive repopulation experiments revealed that deletion of FoxO3 alone is also sufficient to impair long-term reconstitution[25]. In addition, in aging mice deficient for FoxO3, the frequency of HSCs was increased compared with wild-type littermate controls[25]. Both mouse models have also been used to examine the role of FoxO transcription factors in lineage development. Conditional deletion of FoxO1, FoxO3, and FoxO4 resulted in enhanced levels of myeloid cells and decreased numbers of peripheral blood lymphocytes under normal conditions. In time, these mice developed leukocytosis characterized by a relative neutrophilia and lymphopenia[24]. In contrast, in FoxO3-deficient mice, neutrophilia only developed during aging and under myelosuppressive stress conditions[26]. Although deletion of FoxO3 alone was not sufficient to induce neutrophilia, ectopic expression of a constitutively active, nonphosphorylatable, FoxO3 mutant in mouse

hematopoietic progenitors did result in a decrease in the formation of both myeloid and erythroid colonies[27], suggesting that FoxO3 does play an important role in lineage development. Modulation of the activity of either PKB or FoxO transcription factors has been observed to alter the level of reactive oxygen species (ROS). Although ROS levels are reduced in PKBα/β-deficient mice[19], increased levels have been observed in mice deficient for FoxO[25]. Increasing the ROS levels in PKBα/β-deficient mice was sufficient to rescue differentiation defects, but not impair long-term hematopoiesis[19]. Reducing the ROS levels in FoxO-deficient mice with N-acetyl-L-cysteine, an antioxidative agent, was sufficient to abrogate the enhanced levels of proliferation and apoptosis in FoxO-deficient HSCs and to restore the reduced colony-forming ability of these cells[24]. These studies demonstrate that correct regulation of ROS by FoxO transcription factors is essential for normal hematopoiesis.

Recent findings have demonstrated that correct regulation of the activity of GSK-3, which is inhibitory phosphorylated by PKB[18], is also essential for HSC maintenance. A reduction in long-term, but not short-term, repopulating HSCs has, for example, been observed in GSK3-deficient mice[28]. In addition, disruption of GSK-3 activity in mice with a pharmacologic inhibitor or shRNAs has been shown to transiently induce expansion of both HSCs and progenitor cells followed by exhaustion of long-term repopulation HSCs[28,29]. An acceleration of neutrophil and megakaryocyte recovery could be observed after transplantation of mice treated with a GSK-3 inhibitor, suggesting a role for GSK-3 in lineage development[29]. Indeed, ex vivo experiments with human hematopoietic progenitors revealed that GSK-3 can enhance eosinophil differentiation and inhibit neutrophil development at least in part via regulation of C/EBPα, a key regulator of hematopoiesis[13].

A third, important mediator of PI3K/PKB signaling is mTOR[18]. In contrast to GSK-3 and FoxO transcription factors, which are inhibitory phosphorylated by PKB, the activity of mTOR is positively regulated by PKB. Inhibition of the GTPase activating protein Tuberous sclerosis protein 2 (TSC2)/TSC1 complex by PKB results in accumulation of GTP-bound Rheb and subsequent activation of mTOR[30]. In addition, because rapamycin was sufficient to revert the HSC phenotype of mice in which GSK-3 was depleted, it is probable that mTOR is an important effector of GSK-3[28]. Conditional deletion of TSC1 in mice, resulting in activation of mTOR, has been demonstrated to enhance the percentage of cycling HSCs and to reduce the self-renewal capacity of HSCs in serial transplantation assays[31]. In addition, treatment of PTEN-deficient mice with rapamycin appears to be sufficient to revert the HSC phenotype in those mice, indicating that mTORC1 is an important mediator of PI3K in regulation of HSC proliferation[32]. In addition, deletion of TSC1 has been demonstrated to induce ROS levels in HSCs. *In vivo* treatment of TSC1-deficient mice with an ROS antagonist restored HSC numbers and function[31], suggesting that

TSC1, similar to FoxO transcription factors, regulates HSC numbers at least in part via ROS. Although mice deficient of TSC1 also display reduced granulocyte and lymphocyte numbers, this is probably because of reduced progenitor proliferation. In contrast to PKB, which regulates both proliferation and differentiation of myeloid progenitors[13], mTOR primarily regulates expansion of hematopoietic progenitors, as was demonstrated for, for example, granulocyte progenitors[33] and progenitors for interstitial DCs and Langerhans cells[21]. Although the molecular mechanisms underlying mTOR-mediated regulation of lineage development are largely unknown, it has recently been demonstrated that mTOR decreases the ratio of wild-type C/EBPα (C/EBPαp42) and truncated C/EBPαp30, which is generated by alternative translation initiation, resulting in high levels of the smaller p30 C/EBPα isoform[34], which inhibits trans-activation of C/EBPα target genes in a dominant-negative manner and binds to the promoters of a unique set of target genes to suppress their transcription.

Together, these studies show that FoxO transcription factors GSK-3 and mTOR are all important mediators of PI3K in terms of HSC maintenance and lineage development.

Deregulated PI3K/PKB signaling in malignant hematopoiesis

The studies described in the first three sections of this review clearly demonstrate that deregulation of the PI3K/PKB signaling module dramatically affects hematopoiesis resulting in the development of hematologic malignancies. To investigate whether, in patients, the development of leukemia can be caused by aberrant regulation of this signaling module, research has focused on identifying mutations in PI3K and upstream and downstream regulators of this molecule (Figure 2). Constitutive activation of class I PI3K isoforms has been observed in a high percentage of patients with acute[35,36] and chronic leukemia[37]. In contrast to the expression of p110α, β, and γ, which is only up-regulated in leukemic blasts of some patients, p110δ expression appears to be consistently up-regulated in cells from patients with either acute myeloid leukemia (AML) or acute promyelocytic leukemia[36,38]. Activating mutations in the kinase domain (H1047R) and helical domain (E545A) of p110α have been detected in a wide variety of human solid tumors[39]. The latter has also been detected in acute leukemia, albeit in a very low percentage (1 of 88)[39]. In addition, another activating helical domain mutation (E545G) has recently been detected in a chronic myeloid leukemia (CML) cell line[40]. Furthermore, both activating mutations in p110α (PIK3CA) and in-frame insertions/deletions in the PI3K regulatory subunit p85α (PIK3R1) have been observed in a low number of pediatric T-ALL patients (both 2 of 44)[41]. In a small group of myelodysplastic syndrome (MDS) patients, however, the above described mutations could not be detected[42].

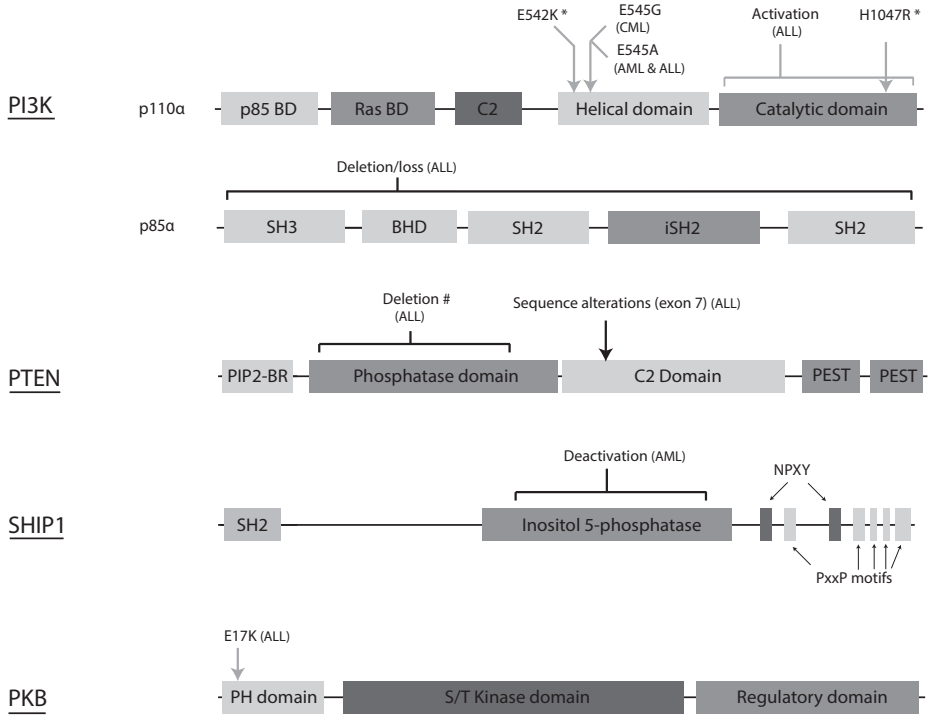

Figure 2. Schematic representation of the known mutations in the PI3K/PKB signaling module in leukemia.

Aberrant regulation of the PI3K/PKB signaling module has been found in a large group of patients with leukemia. However, only few mutations are known to directly affect hematopoiesis. Mutations indentified in leukemic cells are indicated above the linear (unscaled) representations of PI3K, SHIP, PTEN, and PKB. Grey arrows/lines indicate activating mutations; black arrows, inactivating mutations/deletions. *Mutations found in AML and ALL cell lines. **Mutation found in CML cell line. #Mutations inducing leukemia in mouse model. BD indicates binding domain; C2, C2 domain (putative membrane binding domain); SH2, Src homology 2 region (tyrosine-phosphorylated residue binding region); BHD, Bcr homology domain; SH3, Src homology 3 region (proline-rich protein-protein interaction region); and BR, binding region.

Importantly, ectopic expression of mutated p110α has been demonstrated to be sufficient to induce leukemia in a mouse transplantation model[43]. Alternatively, constitutive activation of PI3K may also be caused by either aberrant expression or activation of PTEN. Reduced expression of PTEN has, for example, been observed in different types of leukemia. Although analysis of both myeloid leukemic cell lines and primary AML blasts indicates that PTEN mutations are rare in AML[44,45], both homozygous and heterozygous deletion of PTEN as well as nonsynonymous sequence alterations in exon 7 have been detected in approximately 15% and 25% of T-ALL patients, respectively[41]. In addition, analysis of primary T-ALL cells revealed that, as a result of mutation-induced alternative splicing, full-length SHIP1

expression is often low or undetectable[46]. In addition, an inactivating mutation in the phosphatase domain of SHIP1 has also been detected in primary AML blasts[47].

Although constitutive activation of PKB, resulting in enhanced survival signals[48-50], has been demonstrated in a significant fraction of AML[51,52] and chronic lymphoid leukemia (CLL) patients[50,53,54], until recently, no PKB mutations were found in patients with leukemia. However, an activating mutation in the pleckstrin homology domain of PKB (E17K) has recently been detected in various solid tumors[55] and one pediatric T-ALL patient[41]. In contrast, this mutation could not be detected in a several cohorts of CLL[56,57], CML[58], and AML patients[57,59], suggesting that this particular mutation is very rare. However, transplantation of mice with bone marrow cells ectopically expressing this E17K mutation was sufficient to induce leukemia[55]. Although mutations in mTOR have thus far not been described in hematologic malignancies, a recent study has identified several mTOR mutations in solid tumors[60]. Interestingly, 2 single amino acid mutations, S2215Y and R2505P, identified in large intestine adenocarcinoma and renal cell carcinoma, respectively, appear to induce constitutive activation of mTOR, even under nutrient starvation conditions[60].

In addition to mutations in the PI3K signaling module itself, mutations in cytokine receptors, including constitutive activation of FMS-like tyrosine kinase 3 (FLT3) by internal tandem duplication (Flt3-ITD)[61] and mutation in c-Kit[43,62] have been described to affect PI3K signaling in hematologic malignancies. In addition to these tyrosine kinase receptors, the activity of the PI3K/PKB pathway can also be enhanced by several fusion proteins, including Bcr-Abl[63], which can be detected in virtually all patients with CML and in a subset of patients with ALL[64]. The mechanisms underlying Bcr-Abl–mediated activation of the PI3K/PKB signaling pathway have been investigated extensively. Coimmunoprecipitation experiments revealed that Bcr-Abl associates with Shc[65], which subsequently binds to the p85α subunit of PI3K[66] resulting in activation. In addition, expression of Bcr-Abl has been shown to reduce the levels of PHLPP1 and PHLPP2, which are negative regulators of PKB phosphorylation[67], and to up-regulate the level of p110γ[68]. Bcr-Abl has also been shown to indirectly induce the activity of the PI3K/PKB signaling module by, for example, increasing the level of Nox-4–generated ROS resulting in inhibition of PP1a, a negative regulator of PI3K/PKB[69].

Other potential regulators of PI3K often mutated or aberrantly expressed in leukemia include Ras[1], Evi1[70], PP2A[52], and casein kinase 2 (CK2)[35]. Inhibition of CK2 has been shown to reduce the activity of the PI3K/PKB signaling module by dephosphorylation and activation of PTEN, resulting in induction of apoptosis in primary CLL cells *in vitro*[71,72]. Interestingly, in a subset of MDS patients, it was demonstrated that deletion of glutathione S-transferase θ can result in the

generation of a DNA sequence homologous to mTOR, thereby inducing the activity of downstream effectors of mTOR in a PI3K/PKB-independent manner. Inhibition of mTOR in these cells was sufficient to induce apoptosis[73,74].

It is evident that the activity of the PI3K/PKB signaling module is regulated by various extracellular factors, suggesting that deregulation of the production of those factors by components of the microenvironment could also result in aberrant hematopoiesis. Several studies have revealed that the microenvironment of CLL patients constitutively activates PI3K in leukemic cells, induces proliferation and survival of CLL cells, and contributes to the resistance of leukemic cells to cytotoxic agents[75-80]. Inhibition of the PI3K/PKB signaling pathway was shown to be sufficient to induce apoptosis in CLL cells[75,76]. In addition, the migratory capacity of primary CLL cells has been demonstrated to be enhanced by CX3CL1 in an autocrine manner[78]. Constitutive release of soluble CX3CL1 by CLL cells results in a PKB-dependent up-regulation of CXCR4, a chemokine receptor that is important for CLL cell migration[78].

Although the studies described in this section clearly demonstrate that constitutive activation of the PI3K/PKB signaling module can result in the development of leukemia, enhanced FoxO activity has also been observed in 40% of the AML patients[81]. Similarly, enhanced FoxO activity could also be observed in MLL-AF9–induced AML in a mouse model[81]. Activation of PKB or deletion of FoxO1/3/4 was sufficient to reduce leukemic cell growth, suggesting that inactivation of the PI3K/PKB signaling module contributes to the development of MLL-AF9–induced leukemia[81]. Together, these studies demonstrate that, in addition to constitutive activation of the PI3K/PKB signaling pathway, inactivation of this module can also result in the development of leukemia.

Prognosis of leukemia with activated PI3K/PKB signaling

Because the PI3K/PKB signaling module is aberrantly regulated in many patients with leukemia, the question was raised whether the level of PI3K/PKB activation in leukemic blasts could be used as a prognostic marker. Mouse transplantation studies with blasts from pediatric de novo B-ALL patients revealed that a rapid induction of leukemia correlates with enhanced mTOR activity in the leukemic blasts[82]. In addition, comparison of pediatric T-ALL patients revealed that the survival rate of patients positively correlates with the level of PTEN[83]. Similar observations were made in a different cohort of pediatric T-ALL patients, in which PTEN deletions correlated with early treatment failure in T-ALL[41]. Furthermore, constitutive activation of the PI3K pathway, as measured by enhanced FoxO3 expression[84] or phosphorylation[85], enhanced levels of phosphorylated, and therefore inactive, PTEN[86] or enhanced levels of phosphorylated PKB[52,87] is also considered to be an independent adverse

prognostic factor in AML patients. Similarly, in MDS, activation of the PI3K/PKB pathway has only been detected in high-risk MDS, but not in low-risk MDS patients[88,89], suggesting that high PKB activity may also be an adverse prognostic factor for MDS.

In contrast, Tamburini et al suggest that enhanced PKB phosphorylation positively correlates with the survival of AML patients[90]. Although the short-term survival rate (within 12 months) appeared to be slightly lower in the group displaying high PKB phosphorylation compared with the group with low levels of phosphorylated PKB, both the long-term survival and relapse-free survival were significantly enhanced[90]. Except for this last study, all other studies suggest that enhanced PI3K/PKB activity correlates with reduced survival rate in both ALL and AML patients.

The molecular mechanisms underlying this reduced prognosis are, thus far, incompletely understood. However, a reduced apoptotic response has been observed in AML blasts displaying enhanced PI3K/PKB activation[91]. In addition, PI3K has been demonstrated to induce expression of the multidrug resistance-associated protein 1, a member of the ATP-binding cassette membrane transporters that functions as a drug efflux pump[92], suggesting that high PI3K activity induces drug resistance. The observation that high levels of multidrug resistance-associated protein 1 correlate with enhanced drug resistance in AML cells and poor prognosis supports that hypothesis[93].

PI3K/PKB signaling as a therapeutic target in leukemia

Because aberrant regulation of the PI3K signaling module has frequently been observed in leukemic cells, PI3K and its downstream effectors are considered to be promising targets for therapy (Figure 3; Table 1). The functionality of LY294002 and wortmannin, 2 well-known PI3K inhibitors that prevent ATP to bind to and activate PI3K, has for example been investigated extensively. Preclinical experiments indicate that both LY294002 and wortmannin induce apoptosis in leukemic cells and rescue drug sensitivity. However, it has also been demonstrated that both inhibitors are detrimental for normal cells[13,94]. In addition, both inhibitors exhibit little specificity within the PI3K family and inhibit the activity of other kinases, including CK2 and smMLCK, respectively[95]. Recently, several novel PI3K inhibitors, including S14161[96], the p110α-selective inhibitor AS702630[97], the p110β-selective inhibitor TGX-115[36], and the p110δ inhibitors IC87114[36,38] and CAL-101[80,98-100] have been discovered that also appear to affect proliferation and survival of leukemic blasts. It has, for example, been demonstrated that IC87114 reduces proliferation and survival of both AML blasts[38] and acute promyelocytic leukemia cells[36] without affecting the proliferation of normal hematopoietic progenitors[38]. For CAL-101, a dual mechanism of action

has been revealed in patients with CLL. CAL-101 both decreases the survival of CLL cells directly and abrogates cellular interactions between CLL cells components of the tissue microenvironment[98,100]. Phase 1 or 2 clinical trials (NCT00710528 and NCT01090414) have therefore been initiated to examine the efficacy of CAL-101 as a therapeutic agent in CLL.

Research has also focused on the development of pharmacologic compounds that inhibit PKB. One such compound is perifosine, a synthetic alkylphosphocholine with oral bioavailability that inhibits PKB phosphorylation by competitive interaction with its PH domain and promotes degradation of PKB, mTOR, Raptor, Rictor, p70S6K, and 4E-BP1[101]. It has been demonstrated that this compound induces apoptosis in multidrug-resistant human T-ALL cells and primary AML cells[102,103] but does not affect normal $CD34^+$ hematopoietic progenitor cells[103]. The efficacy of perifosine in treatment of different types of leukemia is currently examined in several phase 2 clinical trials (NCT00391560 and NCT00873457). Phosphatidylinositol ether lipid analogs inhibit PKB activity in a similar manner compared with perifosine. Treatment of HL60 cells with phosphatidylinositol ether lipid analogs resulted in inhibition of proliferation and sensitization to chemotherapeutic agents in concentrations that did not affect proliferation of normal hematopoietic progenitors[104]. Another specific PKB inhibitor (AKT-I-1/2 inhibitor) has been demonstrated to efficiently reduce colony formation in high-risk AML samples[52] and induces apoptosis in primary CLL cells[105]. The PKB inhibitor triciribine (API-2), a purine analog, has been demonstrated to interact with the PH domain of PKB and can thus prevent association of PKB with $PI(3,4,5)P_3$. In T-ALL cell lines, API-2 has been demonstrated to induce cell cycle arrest and apoptosis[106]. The safety of this inhibitor is currently examined in a phase 1 clinical trial in patients with advanced hematologic malignancies (NCT00363454). Recently, a novel specific PKB inhibitor termed AiX has been demonstrated to preferentially induce apoptosis in CLL cells with a normal immunoglobulin status that correlates with poor clinical outcome[107].

Rapamycin and its analogs RAD001 (everolimus), CCI-779 (temsirolimus), AP23573 (deforolimus), and RAD001[108,109] inhibit the mTORC1 complex by association with FKBP-12, which abrogates the association of Raptor with mTOR[110]. The efficacy of these compounds as therapeutic drugs has been examined in various preclinical and clinical studies for a wide range of malignancies. Although both rapamycin and its analog CCI-779 exhibit strong anti–tumor capacities *in vitro*[82,111,112], only a partial response was observed in clinical trials with rapamycin[112] or its analog AP23573 in hematologic malignancies[113]. The observed induction of PKB activity in AML blasts treated with rapamycin or AP23573 may explain the limited therapeutic effects of these compounds[114]. Furthermore, experiments with PTEN-deficient mice revealed that withdrawal of rapamycin results in a rapid reinduction of leukemia

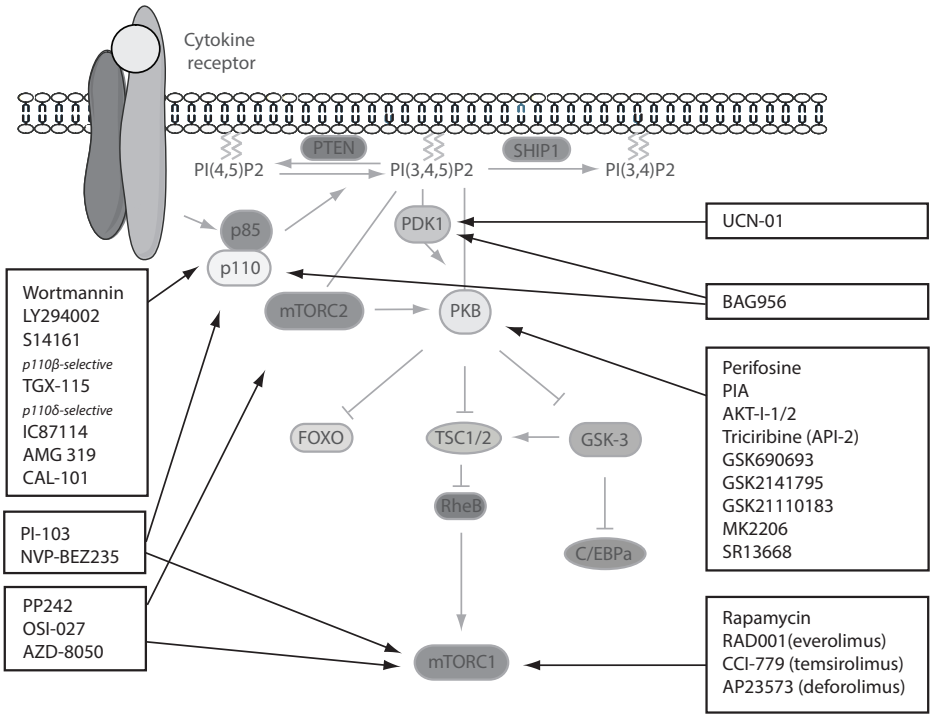

Figure 3. Schematic representation of the PI3K/PKB signaling module and the available inhibitors inhibiting this pathway.

Several inhibitors have been developed to inhibit aberrant regulation of the PI3K/PKB signaling module in leukemia. These inhibitors target single or multiple proteins in the pathway. Black boxes represent groups of similar inhibitors; and black arrows, the specific target of the inhibitors.

and death in the majority of mice, which is probably because of failure to eliminate the leukemic stem cell population[115]. In a subset of CLL patients, RAD-001 displays a modest antitumor activity[116]. In addition, treatment of CLL patients with RAD-001 results in mobilization of malignant cells from the protective nodal masses into the peripheral blood[116]. As an alternative, ATP-competitive mTOR inhibitors have recently been generated that inhibit the activity of both mTORC1 and mTORC2[117]. Compared with rapamycin, the mTORC 1/2 inhibitor PP242 more efficiently reduced the development of leukemia in mice transplanted with primary ALL blasts or preleukemic thymocytes overexpressing PKB[117], while inducing less adverse effects on proliferation and function of normal lymphocytes[117,118]. Similarly, OSI-027, another mTORC1/2 inhibitor[118], has been demonstrated to exhibit anti–leukemic effects in both Ph^+ ALL and CML cells[119], and, compared with rapamycin, to efficiently suppress proliferation of AML cell lines[120].

Table 1. Inhibitors of the PI3K/PKB signaling pathway.

Target	Compound	Effect		Leukemia	Clinical Trials (phase)	Reference(s)
		In vitro	*In vivo*			
PI3K	Wortmannin	+	-			147,148
	LY294002	+	-			37,148-150
	AS702630	+	-			105
	S14161	+	+			96
p110β	TGX-115	+	-			36,105
p110δ	IC87114	+	-			36,38,105,145
	AMG 319	-	-	CLL and ALL	NCT01300026 (I)	
	CAL-101	+ +	+ +	CLL and AML CLL and AML	NCT01090414 (I) NCT00710528 (I)	80,99,100 80,99,100
PDK1	UCN-01	+	-			122
PKB	Perifosine	+ -	- -	RRL CLL	NCT00391560 (II) NCT00873457 (II)	101-103
	PIA	+	-			104
	A-443654	+	-			53
	AiX	+	-			107
	AKT-I-1/2	+	-			52,53
	Triciribine (API-2)	+	-		NCT00363454 (I)	106
	GSK690693	+	-		NCT00493818 (I)	151
	MK2206	-	-	RRL AML	NCT01231919 (I) NCT01253447 (II)	
	SR13668	-	-		NCT00896207 (I)	
	GSK2141795	-	-		NCT00920257 (I)	
	GSK21110183	-	-	RRL	NCT00881946 (I/II)	
mTOR	Rapamycin	+ + +	+ + +	ALL ALL and AML CML	NCT00795886 (II) NCT00068302 (I) (II)	112,152,153 112,152,153 154,155
	RAD001	+ + +	+ + +	AML and MDS B-CLL CLL	NCT00636922 (I/II) (II) (II)	138 109 116
	CCI-779	+ + + +	+ + + +	ALL CLL RRL CLL	(II) NCT00290472 (II) NCT00084916 (II) NCT00084474 (II)	156
	AP23573	-	-	AML RRL	(II) NCT00086125 (II)	113
	PP242	+	+			117,118,157
	OSI-027	+	-			118-120
	AZD-8050	+	-			118
PI3K/mTOR	PI-103	+	+			76,126,127,158
PI3K/mTOR	NVP-BEZ235	+	+			123-125
PI3K/PDK1	BAG956	+	+			121
PKB/PDK1/Flt3	KP372-1	+	-			128

RRL indicates relapsed and refractory leukemia.

Dual inhibition of the PI3K/PKB pathway

Although the single-specificity inhibitors do affect the survival of leukemic cells, their effect in patients appears to be modest. The efficacy of combination therapy using multiple inhibitors directed against different intermediates of the PI3K signaling module is therefore also under investigation. Combined inhibition of mTOR and p110δ with RAD001 and IC87114, respectively, has for example been demonstrated to synergistically reduce proliferation of AML blasts[114]. Similarly, combining the PI3K/PDK1 inhibitor BAG956 with RAD001 also resulted in a synergistic reduction in tumor volume in a mouse model transplanted with BCR-ABL–expressing cells[121]. Finally, the efficacy of a novel combination regimen, including both perifosine and UCN-01 (NCT00301938), a PDK1 inhibitor that is known to induce apoptosis in AML cells *in vitro*[122], is currently examined in a phase 1 trial.

To further optimize inhibition of the PI3K signaling module, dual-specificity inhibitors have also been generated (Table 1). Recently, NVP-BEZ235, an orally bioavailable imidazoquinoline derivative that inhibits the activity of both PI3K and mTOR by binding to their ATP-binding pocket, has been identified[123]. This compound significantly reduced proliferation and survival in both primary T-ALL[124] and AML cells[125] as well as leukemic cell lines[124,125] without affecting the clonogenic capacity of normal hematopoietic progenitors[125]. Another potent dual inhibitor for both class I PI3K isoforms and mTORC1 is PI-103, a synthetic small molecule of the pyridofuropyrimidine class. PI-103 has been demonstrated to reduce proliferation and survival of cells from T-ALL[126], AML[127], and CLL patients[76] and appears to exhibit a stronger anti–leukemic activity compared with both rapamycin[126] and the combination of RAD001 and IC87114[127]. Importantly, although PI-103 reduces proliferation of normal hematopoietic progenitors, survival is not affected[127]. A dual PI3K/PDK1 inhibitor called BAG956 has also recently been described. Although this compound can inhibit proliferation of BCR-ABL and FLT3-ITD–expressing cells, its anti–leukemic capacity is reduced compared with RAD001[121]. In addition to these 3 dual-specificity inhibitors, KP372-1, a multiple kinase inhibitor capable of inhibiting PKB, PDK1, and FLT3, has been generated[128]. It has been demonstrated that KP372-1 can induce apoptosis in primary AML cells and leukemic cell lines without affecting the survival of normal hematopoietic progenitors[128].

Optimization of treatment strategies with combination therapy

Leukemogenesis involves aberrant regulation of various signal transduction pathways, including, but not limited to, the PI3K signaling module. Simultaneous targeting of multiple aberrantly regulated signal transduction pathways is therefore considered to be a promising therapeutic strategy (Tables 2 and 3). Histone deacetylase inhibitors have, for example, emerged as a promising class of anti–tumor

agents. Although, in mouse models, the histone deacetylase inhibitor MS-275 only partially inhibited leukemic cells, combined administration of MS-275 and RAD001 potentiated the effect of both inhibitors individually both *in vitro* and *in vivo*[129]. Synergistic negative effects on proliferation and survival of leukemic cell lines have also been observed after coadministration of histone deacetylase inhibitors and perisofine[130]. Although proteosome inhibitors are considered to be a new class of therapeutic agents, treatment of pediatric and adult B-ALL patients with such an inhibitor (bortezomib) was not sufficient to induce a robust anti–tumor response[131]. Experiments in leukemic cell lines and primary cells from B-ALL patients revealed that, whereas MG132, a proteosome inhibitor, and RAD001 alone only modestly reduce cell viability, combined inhibition of proteosomes and mTOR significantly enhanced cell death[132]. In addition to proteosome inhibitors, the efficacy of specific tyrosine kinase inhibitors, including inhibitors of Flt3, Abl, and c-Kit, has been investigated in preclinical and clinical models. Combined inhibition of tyrosine kinases and the PI3K/PKB pathway resulted in a synergistically enhanced anti–leukemia effect in ALL and AML cells[121] compared with the individual inhibitors. Phase 1 or 2 clinical trials have therefore been initiated to investigate the synergistic effects of combined inhibition of PI3K/PKB and Flt3 (NCT00819546) or c-Kit (NCT00762632). The occurrence of clinical resistance to STI-571 is a major problem

Table 2. Combination regimens with single specificity inhibitors.

Target	Compound	Combination regimens	Effects		Leukemia	Clinical trials (phase)	Reference(s)
			In vitro	*In vivo*			
PI3K	Wortmannin	ATRA (DA)	+	-			159
		Imatinib (Bcr-Abl TKI)	+	-			141
	LY294002	Apigenin (CK2 I)	+	-			160
		ATRA (DA)	+	-			159
		Imatinib (Bcr-Abl TKI)	+	-			141
		Arsenic trioxide	+	-			161
p110δ	IC87114	VP16 (CT)	+	-			145
	CAL-101	Lenalidomide	+	-			99
		CT & mAb CD20	+	-	CLL	NCT01088048 (I)	
		Rituximab	+	-	CLL	NCT01203930 (II)	
PDK1	UCN-01	Ara-C (CT)	+	-	AML	(II)	146
		Cytarabine (CT)	-	-	AML and MDS	NCT00004263 (I)	
		Fludarabine (CT)	-	-	RRL	NCT00019838 (I)	
	OSU-03012	Imatinib (Bcr-Abl TKI)	+	-			140
PP2A	Forskolin	Idarubicine/Ara-C	+	-			162
PKB	Perifosine	UCN-01	-	-	RRL	NCT00301938 (I)	
		HDAC I	+	-			130
		TRAIL (AI)	+	-			163
		Etoposide (CT	+	-			103
	PIA	CT	+	-			104
	Triciribine	Cytarabine (CT)	+	-			106
	MK2206	Rituximab (mAb CD20)	-	-	CLL	NCT01369849 (I/II)	
		Arsenic trioxide	+	-			161

Table 2. Combination regimens with single specificity inhibitors. (*continued*)

Target	Compound	Combination regimens	Effects		Leukemia	Clinical trials (phase)	Reference(s)
			In vitro	*In vivo*			
mTOR	Rapamycin	UCN-01	+	-			122
		3-BrOP (glycolysis I)	+	-			164
		Imatinib (Bcr-Abl TKI)	+	-			139
		Notch I	+	-			165
		Erlotinib (EGFR-TKI)	+	-			166
		Curcumin	+	-			167
		Dexamethason	+	-			168,169
		Etoposide (CT)	+	+			144
		Decatibine (CT)	-	-	AML	NCT00861874 (I)	
		Aracytin (CT)	-	-	AML	NCT00235560 (II)	
		Methotrexate (CT)	+	+	ALL and CLL	NCT01162551 (II)	111
		Anthracyclin (CT)	+	-			170
		Daunorubicine (CT)	+	-			171
		CT	+	-	ALL and CML	NCT00776373 (I/II)	152
			+	-	AML	NCT01184898 (I/II)	152
			+	-	AML and CML	NCT00780104 (I/II)	152
	RAD001	IC87114	+	-			114
		BAG956	+	+			121
		Bortezomib (PI)	+	-			132
		MS-275 (HDAC I)	+	+			129
		PKC412 (Flt3 TKI)	-	-	AML and MDS	NCT00819546 (I)	
		Imatinib (Bcr-Abl TKI)	+	-	CML	NCT00093639 (I/II)	139
			+	-	CML	NCT01188889 (I/II)	139
		Nilotinib (c-Kit-TKI)	-	-	AML	NCT00762632 (I/II)	
		Alemtuzumab (mAb	-	-	CLL	NCT00935792 (I/II)	
		CD52)	+	+			172
		ATRA (DA)	+	-			132,149
		Ara-C (CT)	+	+			173
		Vincristine (CT)	-	-	AML	NCT00544999 (I)	
		CT	-	-	AML	NCT01154439 (I)	
	CCI-779	Methotrexate (CT)	+	+			111
		Clofarabine (CT)	-	-	AML	NCT00775593 (II)	
		STI-571 (Bcr-Abl TKI)	-	-	CML	NCT00101088 (I)	
	PP242	Vincristine (CT)	+	-			118
	OSI-027	STI-571 (Bcr-Abl TKI)	+	-			119
	GILZ	STI-571 (Bcr-Abl TKI)	+	-			137

DA indicates differentiating agents; TKI, tyrosine kinase inhibitor; I, inhibitor; CT, chemotherapy; AI, apoptosis inducer; RRL, relapsed and refractory leukemia; and PI, proteasome inhibitor.

Table 3. Combination regimens with dual specificity inhibitors.

Target	Compound	Combination regimens	Effects		Clinical trials (phase)	Reference(s)
			In vitro	*In vivo*		
PI3K/mTOR	PI-103	Nutlin-3 (MDM2-I)	+	-		158
		STI-571 (Bcr-Abl-TKI)	+	-		142
		Arsenic disulfide	+	-		174
		Vincristine (CT)	+	-		126
		Fludarabine (CT)	+	-		76
PI3K/mTOR	NVP-BEZ235	CT	+	-		124
PI3K/PDK1	BAG956	STI-571 (Bcr-Abl-TKI)	+	+		121
		Rapamycin / RAD-001	+	-		121
		PKC412 (Flt3 TKI)	+	+		121

I indicates inhibitor; TKI, tyrosine kinase inhibitor; and CT, chemotherapy

for CML patients. Although the most common mechanisms of induction of resistance are mutations or alterations in the Bcr-Abl gene[133], a STI-571–induced compensatory PKB/mTor activation has also been described as a potential mechanism for the persistence of Bcr-Abl-positive cells in STI-571–treated patients[134-136]. A combination of pharmacologic compounds inhibiting the PI3K/PKB pathway and STI-571 has been shown to be effective in cells from STI-571–resistant CML patients[119,121,137-142]. Several phase 1 or 2 clinical trials have therefore been initiated to determine the effectiveness of such a combination therapy in STI-571–resistant CML patients (NCT01188889, NCT00093639, and NCT00101088).

Chemotherapy has been shown to be effective in a subset of patients. However, incomplete remission and the development of a refractory disease have been observed in many patients with acute leukemia[143]. To optimize treatment, chemotherapy could potentially be combined with specific pharmacologic inhibitors (Table 2). Coadministration of mTOR inhibitors with different types of chemotherapeutic drugs, including etoposide, Ara-C, cytarabine, and dexamethasone, has, for example, been demonstrated to induce synergistic anti–leukemia effects in cells from AML patients[144] and ALL patients[111,132]. Several phase 1 or 2 clinical trials have therefore been initiated to investigate and optimize the synergistic effect of mTOR inhibitors and chemotherapeutic drugs in patients (NCT00544999, NCT01184898, NCT00780104, NCT01162551, and NCT00776373, NCT00861874, NCT00235560, and NCT01154439). In addition, synergistic effects have been observed in AML cells after coadministration of chemotherapeutic agents with IC87114[145], UCN-01[146], or triciribine[106]. Similar results were obtained in T-ALL cells when combining the dual-specificity inhibitors PI-103 and NVP-BEZ235 with chemotherapy[124,126]. Finally, inhibition of the activity of p110δ with CAL-101 was shown to be sufficient to abrogate lenalidomide-induced activation of primary CCL cells[99]. In addition to the clinical trials focusing on CAL-101 alone, the efficacy of a combination regimen with both CAL-101 and lenalidomide is therefore also under investigation in phase 1 or 2 clinical trials (NCT01203930 and NCT0108848).

Future perspectives

During the last 2 decades, it has become clear that the PI3K/PKB signal transduction pathway plays an important role in both normal and malignant hematopoiesis. As discussed in "Derequlated P13K/PKB signaling in malignant hematopoiesis", aberrant regulation of this signaling module has been observed in a large group of acute leukemias. Although mutations in PI3K, PKB, or the upstream regulators PTEN and SHIP1 have been detected in cells from patients with leukemia, these mutations appear to be rare. These mutations can therefore not account for the large incidence of constitutive activation of PI3K in patients with leukemia. In contrast,

several oncogenic fusion proteins and mutated tyrosine kinase receptors have been demonstrated to induce hematologic malignancies by constitutive activation of the PI3K/PKB signaling module. Because PI3K is frequently activated in leukemia and activation of this molecule is thought to correlate with poor prognosis and drug resistance, it is considered to be a promising target for therapy. A high number of pharmacologic inhibitors directed against both individual and multiple components of this pathway have already been developed to improve therapy. Although the single-specificity inhibitors do affect the survival of leukemic cells, their effect in patients appears to be modest. This can be explained by both inhibitor-induced abrogation of negative feedback loops and alternative mechanisms of activation of downstream effectors of PI3K/PKB. Although further research is required to examine the safety and efficacy of the dual-specificity inhibitors, these compounds appear to possess more promising anti–leukemic activities compared with single-specificity inhibitors. In addition, to further optimize therapeutic regimens, research has focused on coadministration of inhibitors of the PI3K signaling module with either classic chemotherapy or inhibitors directed against other signal transduction molecules. The *in vitro* studies and mouse transplantation experiments described herein strongly suggest that both strategies could indeed be used to improve current therapeutic regimens in specific patient groups.

Inhibition of aberrantly regulated intracellular signal transduction pathways provides an important means to improve therapeutic regimens for patients with leukemia. Because the PI3K/PKB signaling pathway appears to be highly deregulated in a large number of patients with leukemia, this pathway is considered to be a promising target for therapy. Compared with targeting individual components of the PI3K/PKB signaling module alone, either abrogating this pathway at multiple levels using dual-specificity inhibitors or combining pathway specific inhibitors with classic regimens appears to be a more effective therapeutic strategy for patients with leukemia. Further research is therefore warranted to examine the safety and efficacy of these regimens in leukemia patients.

Authorship

Contribution: R.P. and M.B. wrote the manuscript.

Conflict-of-interest disclosure: The authors declare no competing financial interests.

Acknowledgements

R.P. was supported by KiKa (Children Cancer Free grant).

The authors apologize that, because of space restrictions, some references to original papers may not have been included in this review.

REFERENCES

1. Vanhaesebroeck, B., Guillermet-Guibert, J., Graupera, M. & Bilanges, B. The emerging mechanisms of isoform-specific PI3K signalling. *Nat Rev Mol Cell Biol* **11**, 329-341 (2010).
2. Buitenhuis, M. & Coffer, P.J. The role of the PI3K-PKB signaling module in regulation of hematopoiesis. *Cell Cycle* **8**, 560-566 (2009).
3. Brognard, J., Sierecki, E., Gao, T. & Newton, A.C. PHLPP and a second isoform, PHLPP2, differentially attenuate the amplitude of Akt signaling by regulating distinct Akt isoforms. *Mol Cell* **25**, 917-931 (2007).
4. Jia, Y., *et al.* Inositol 1,3,4,5-tetrakisphosphate negatively regulates phosphatidylinositol-3,4,5-trisphosphate signaling in neutrophils. *Immunity* **27**, 453-467 (2007).
5. Helgason, C.D., Antonchuk, J., Bodner, C. & Humphries, R.K. Homeostasis and regeneration of the hematopoietic stem cell pool are altered in SHIP-deficient mice. *Blood* **102**, 3541-3547 (2003).
6. Fruman, D.A., *et al.* Hypoglycaemia, liver necrosis and perinatal death in mice lacking all isoforms of phosphoinositide 3-kinase p85 alpha. *Nat Genet* **26**, 379-382 (2000).
7. Okkenhaug, K., *et al.* Impaired B and T cell antigen receptor signaling in p110delta PI 3-kinase mutant mice. *Science* **297**, 1031-1034 (2002).
8. Zhang, J., *et al.* PTEN maintains haematopoietic stem cells and acts in lineage choice and leukaemia prevention. *Nature* **441**, 518-522 (2006).
9. Helgason, C.D., *et al.* Targeted disruption of SHIP leads to hemopoietic perturbations, lung pathology, and a shortened life span. *Genes Dev* **12**, 1610-1620 (1998).
10. Perez, L.E., Desponts, C., Parquet, N. & Kerr, W.G. SH2-inositol phosphatase 1 negatively influences early megakaryocyte progenitors. *PLoS One* **3**, e3565 (2008).
11. Moody, J.L., Xu, L., Helgason, C.D. & Jirik, F.R. Anemia, thrombocytopenia, leukocytosis, extramedullary hematopoiesis, and impaired progenitor function in Pten+/-SHIP-/- mice: a novel model of myelodysplasia. *Blood* **103**, 4503-4510 (2004).
12. Nguyen, N.Y., *et al.* An ENU-induced mouse mutant of SHIP1 reveals a critical role of the stem cell isoform for suppression of macrophage activation. *Blood* **117**, 5362-5371 (2011).
13. Buitenhuis, M., *et al.* Protein kinase B (c-akt) regulates hematopoietic lineage choice decisions during myelopoiesis. *Blood* **111**, 112-121 (2008).
14. Jia, Y., *et al.* Inositol trisphosphate 3-kinase B (InsP3KB) as a physiological modulator of myelopoiesis. *Proc Natl Acad Sci U S A* **105**, 4739-4744 (2008).
15. Pouillon, V., *et al.* Inositol 1,3,4,5-tetrakisphosphate is essential for T lymphocyte development. *Nat Immunol* **4**, 1136-1143 (2003).
16. Burgering, B.M. & Coffer, P.J. Protein kinase B (c-Akt) in phosphatidylinositol-3-OH kinase signal transduction. *Nature* **376**, 599-602 (1995).
17. Oh, W.J. & Jacinto, E. mTOR complex 2 signaling and functions. *Cell Cycle* **10**, 2305-2316 (2011).
18. Manning, B.D. & Cantley, L.C. AKT/PKB signaling: navigating downstream. *Cell* **129**, 1261-1274 (2007).
19. Juntilla, M.M., *et al.* AKT1 and AKT2 maintain hematopoietic stem cell function by regulating reactive oxygen species. *Blood* **115**, 4030-4038 (2010).
20. Kharas, M.G., *et al.* Constitutively active AKT depletes hematopoietic stem cells and induces leukemia in mice. *Blood* **115**, 1406-1415 (2010).

21. van de Laar, L., *et al.* Human CD34-derived myeloid dendritic cell development requires intact phosphatidylinositol 3-kinase-protein kinase B-mammalian target of rapamycin signaling. *J Immunol* **184**, 6600-6611 (2010).
22. Gutierrez, A., *et al.* Pten mediates Myc oncogene dependence in a conditional zebrafish model of T cell acute lymphoblastic leukemia. *J Exp Med* **208**, 1595-1603 (2011).
23. Calamito, M., *et al.* Akt1 and Akt2 promote peripheral B-cell maturation and survival. *Blood* **115**, 4043-4050 (2010).
24. Tothova, Z., *et al.* FoxOs are critical mediators of hematopoietic stem cell resistance to physiologic oxidative stress. *Cell* **128**, 325-339 (2007).
25. Miyamoto, K., *et al.* Foxo3a is essential for maintenance of the hematopoietic stem cell pool. *Cell Stem Cell* **1**, 101-112 (2007).
26. Miyamoto, K., *et al.* FoxO3a regulates hematopoietic homeostasis through a negative feedback pathway in conditions of stress or aging. *Blood* **112**, 4485-4493 (2008).
27. Engstrom, M., Karlsson, R. & Jonsson, J.I. Inactivation of the forkhead transcription factor FoxO3 is essential for PKB-mediated survival of hematopoietic progenitor cells by kit ligand. *Exp Hematol* **31**, 316-323 (2003).
28. Huang, J., *et al.* Pivotal role for glycogen synthase kinase-3 in hematopoietic stem cell homeostasis in mice. *J Clin Invest* **119**, 3519-3529 (2009).
29. Trowbridge, J.J., Xenocostas, A., Moon, R.T. & Bhatia, M. Glycogen synthase kinase-3 is an in vivo regulator of hematopoietic stem cell repopulation. *Nat Med* **12**, 89-98 (2006).
30. Sengupta, S., Peterson, T.R. & Sabatini, D.M. Regulation of the mTOR complex 1 pathway by nutrients, growth factors, and stress. *Mol Cell* **40**, 310-322 (2010).
31. Chen, C., *et al.* TSC-mTOR maintains quiescence and function of hematopoietic stem cells by repressing mitochondrial biogenesis and reactive oxygen species. *J Exp Med* **205**, 2397-2408 (2008).
32. Yilmaz, O.H., *et al.* Pten dependence distinguishes haematopoietic stem cells from leukaemia-initiating cells. *Nature* **441**, 475-482 (2006).
33. Geest, C.R., Zwartkruis, F.J., Vellenga, E., Coffer, P.J. & Buitenhuis, M. Mammalian target of rapamycin activity is required for expansion of CD34+ hematopoietic progenitor cells. *Haematologica* **94**, 901-910 (2009).
34. Fu, C.T., *et al.* An evolutionarily conserved PTEN-C/EBPalpha-CTNNA1 axis controls myeloid development and transformation. *Blood* **115**, 4715-4724 (2010).
35. Silva, A., *et al.* PTEN posttranslational inactivation and hyperactivation of the PI3K/Akt pathway sustain primary T cell leukemia viability. *J Clin Invest* **118**, 3762-3774 (2008).
36. Billottet, C., Banerjee, L., Vanhaesebroeck, B. & Khwaja, A. Inhibition of class I phosphoinositide 3-kinase activity impairs proliferation and triggers apoptosis in acute promyelocytic leukemia without affecting atra-induced differentiation. *Cancer Res* **69**, 1027-1036 (2009).
37. Ringshausen, I., *et al.* Constitutively activated phosphatidylinositol-3 kinase (PI-3K) is involved in the defect of apoptosis in B-CLL: association with protein kinase Cdelta. *Blood* **100**, 3741-3748 (2002).
38. Sujobert, P., *et al.* Essential role for the p110delta isoform in phosphoinositide 3-kinase activation and cell proliferation in acute myeloid leukemia. *Blood* **106**, 1063-1066 (2005).
39. Lee, J.W., *et al.* PIK3CA gene is frequently mutated in breast carcinomas and hepatocellular carcinomas. *Oncogene* **24**, 1477-1480 (2005).
40. Quentmeier, H., Eberth, S., Romani, J., Zaborski, M. & Drexler, H.G. BCR-ABL1-independent PI3Kinase activation causing imatinib-resistance. *J Hematol Oncol* **4**, 6 (2011).

41. Gutierrez, A., *et al.* High frequency of PTEN, PI3K, and AKT abnormalities in T-cell acute lymphoblastic leukemia. *Blood* **114**, 647-650 (2009).
42. Machado-Neto, J.A., *et al.* Screening for hotspot mutations in PI3K, JAK2, FLT3 and NPM1 in patients with myelodysplastic syndromes. *Clinics (Sao Paulo)* **66**, 793-799 (2011).
43. Horn, S., *et al.* Mutations in the catalytic subunit of class IA PI3K confer leukemogenic potential to hematopoietic cells. *Oncogene* **27**, 4096-4106 (2008).
44. Liu, T.C., *et al.* Mutation analysis of PTEN/MMAC1 in acute myeloid leukemia. *Am J Hematol* **63**, 170-175 (2000).
45. Aggerholm, A., Gronbaek, K., Guldberg, P. & Hokland, P. Mutational analysis of the tumour suppressor gene MMAC1/PTEN in malignant myeloid disorders. *Eur J Haematol* **65**, 109-113 (2000).
46. Lo, T.C., *et al.* Inactivation of SHIP1 in T-cell acute lymphoblastic leukemia due to mutation and extensive alternative splicing. *Leuk Res* **33**, 1562-1566 (2009).
47. Luo, J.M., *et al.* Possible dominant-negative mutation of the SHIP gene in acute myeloid leukemia. *Leukemia* **17**, 1-8 (2003).
48. Longo, P.G., *et al.* The Akt/Mcl-1 pathway plays a prominent role in mediating antiapoptotic signals downstream of the B-cell receptor in chronic lymphocytic leukemia B cells. *Blood* **111**, 846-855 (2008).
49. Cuni, S., *et al.* A sustained activation of PI3K/NF-kappaB pathway is critical for the survival of chronic lymphocytic leukemia B cells. *Leukemia* **18**, 1391-1400 (2004).
50. Schade, A.E., Powers, J.J., Wlodarski, M.W. & Maciejewski, J.P. Phosphatidylinositol-3-phosphate kinase pathway activation protects leukemic large granular lymphocytes from undergoing homeostatic apoptosis. *Blood* **107**, 4834-4840 (2006).
51. Min, Y.H., *et al.* Constitutive phosphorylation of Akt/PKB protein in acute myeloid leukemia: its significance as a prognostic variable. *Leukemia* **17**, 995-997 (2003).
52. Gallay, N., *et al.* The level of AKT phosphorylation on threonine 308 but not on serine 473 is associated with high-risk cytogenetics and predicts poor overall survival in acute myeloid leukaemia. *Leukemia* **23**, 1029-1038 (2009).
53. Zhuang, J., *et al.* Akt is activated in chronic lymphocytic leukemia cells and delivers a pro-survival signal: the therapeutic potential of Akt inhibition. *Haematologica* **95**, 110-118 (2010).
54. Schade, A.E., Wlodarski, M.W. & Maciejewski, J.P. Pathophysiology defined by altered signal transduction pathways: the role of JAK-STAT and PI3K signaling in leukemic large granular lymphocytes. *Cell Cycle* **5**, 2571-2574 (2006).
55. Carpten, J.D., *et al.* A transforming mutation in the pleckstrin homology domain of AKT1 in cancer. *Nature* **448**, 439-444 (2007).
56. Mahmoud, I.S., *et al.* The transforming mutation E17K/AKT1 is not a major event in B-cell-derived lymphoid leukaemias. *Br J Cancer* **99**, 488-490 (2008).
57. Zenz, T., *et al.* Chronic lymphocytic leukaemia and acute myeloid leukaemia are not associated with AKT1 pleckstrin homology domain (E17K) mutations. *Br J Haematol* **141**, 742-743 (2008).
58. He, Y., *et al.* Chronic myeloid leukemia and BCR/ABL signal pathways are not associated with AKT1 pleckstrin homology domain (E17K) mutations. *Eur J Haematol* **84**, 87-88 (2010).
59. Tibes, R., *et al.* PI3K/AKT pathway activation in acute myeloid leukaemias is not associated with AKT1 pleckstrin homology domain mutation. *Br J Haematol* **140**, 344-347 (2008).
60. Sato, T., Nakashima, A., Guo, L., Coffman, K. & Tamanoi, F. Single amino-acid changes that confer constitutive activation of mTOR are discovered in human cancer. *Oncogene* **29**, 2746-2752 (2010).

61. Brandts, C.H., *et al.* Constitutive activation of Akt by Flt3 internal tandem duplications is necessary for increased survival, proliferation, and myeloid transformation. *Cancer Res* **65**, 9643-9650 (2005).
62. Hashimoto, K., *et al.* Necessity of tyrosine 719 and phosphatidylinositol 3′-kinase-mediated signal pathway in constitutive activation and oncogenic potential of c-kit receptor tyrosine kinase with the Asp814Val mutation. *Blood* **101**, 1094-1102 (2003).
63. Skorski, T., *et al.* Transformation of hematopoietic cells by BCR/ABL requires activation of a PI-3k/Akt-dependent pathway. *EMBO J* **16**, 6151-6161 (1997).
64. Clark, S.S., *et al.* Expression of a distinctive BCR-ABL oncogene in Ph1-positive acute lymphocytic leukemia (ALL). *Science* **239**, 775-777 (1988).
65. Harrison-Findik, D., Susa, M. & Varticovski, L. Association of phosphatidylinositol 3-kinase with SHC in chronic myelogeneous leukemia cells. *Oncogene* **10**, 1385-1391 (1995).
66. Ren, S.Y., Xue, F., Feng, J. & Skorski, T. Intrinsic regulation of the interactions between the SH3 domain of p85 subunit of phosphatidylinositol-3 kinase and the protein network of BCR/ABL oncogenic tyrosine kinase. *Exp Hematol* **33**, 1222-1228 (2005).
67. Hirano, I., *et al.* Depletion of Pleckstrin homology domain leucine-rich repeat protein phosphatases 1 and 2 by Bcr-Abl promotes chronic myelogenous leukemia cell proliferation through continuous phosphorylation of Akt isoforms. *J Biol Chem* **284**, 22155-22165 (2009).
68. Hickey, F.B. & Cotter, T.G. BCR-ABL regulates phosphatidylinositol 3-kinase-p110gamma transcription and activation and is required for proliferation and drug resistance. *J Biol Chem* **281**, 2441-2450 (2006).
69. Naughton, R., Quiney, C., Turner, S.D. & Cotter, T.G. Bcr-Abl-mediated redox regulation of the PI3K/AKT pathway. *Leukemia* **23**, 1432-1440 (2009).
70. Yoshimi, A., *et al.* Evi1 represses PTEN expression and activates PI3K/AKT/mTOR via interactions with polycomb proteins. *Blood* **117**, 3617-3628 (2011).
71. Martins, L.R., *et al.* Targeting CK2 overexpression and hyperactivation as a novel therapeutic tool in chronic lymphocytic leukemia. *Blood* **116**, 2724-2731 (2010).
72. Martins, L.R., *et al.* On CK2 regulation of chronic lymphocytic leukemia cell viability. *Mol Cell Biochem* **356**, 51-55 (2011).
73. Maeda, Y., *et al.* Mutant type glutathione S-transferase theta 1 gene homologue to mTOR in myelodysplastic syndrome: possible clinical application of rapamycin. *Leuk Lymphoma* **44**, 1179-1185 (2003).
74. Maeda, Y., *et al.* Relationship between expression of mutant type glutathione S-transferase theta-1 gene and reactivity of rapamycin in myelodysplastic syndrome. *Hematology* **14**, 266-270 (2009).
75. Shehata, M., *et al.* Reconstitution of PTEN activity by CK2 inhibitors and interference with the PI3-K/Akt cascade counteract the antiapoptotic effect of human stromal cells in chronic lymphocytic leukemia. *Blood* **116**, 2513-2521 (2010).
76. Niedermeier, M., *et al.* Isoform-selective phosphoinositide 3′-kinase inhibitors inhibit CXCR4 signaling and overcome stromal cell-mediated drug resistance in chronic lymphocytic leukemia: a novel therapeutic approach. *Blood* **113**, 5549-5557 (2009).
77. Buchner, M., *et al.* Spleen tyrosine kinase inhibition prevents chemokine- and integrin-mediated stromal protective effects in chronic lymphocytic leukemia. *Blood* **115**, 4497-4506 (2010).
78. Ferretti, E., *et al.* A novel role of the CX3CR1/CX3CL1 system in the cross-talk between chronic lymphocytic leukemia cells and tumor microenvironment. *Leukemia* **25**, 1268-1277 (2011).

79. Ding, W., *et al.* Bi-directional activation between mesenchymal stem cells and CLL B-cells: implication for CLL disease progression. *Br J Haematol* **147**, 471-483 (2009).
80. Lannutti, B.J., *et al.* CAL-101, a p110delta selective phosphatidylinositol-3-kinase inhibitor for the treatment of B-cell malignancies, inhibits PI3K signaling and cellular viability. *Blood* **117**, 591-594 (2011).
81. Sykes, S.M., *et al.* AKT/FOXO signaling enforces reversible differentiation blockade in myeloid leukemias. *Cell* **146**, 697-708 (2011).
82. Meyer, L.H., *et al.* Early relapse in ALL is identified by time to leukemia in NOD/SCID mice and is characterized by a gene signature involving survival pathways. *Cancer Cell* **19**, 206-217 (2011).
83. Jotta, P.Y., *et al.* Negative prognostic impact of PTEN mutation in pediatric T-cell acute lymphoblastic leukemia. *Leukemia* **24**, 239-242 (2010).
84. Santamaria, C.M., *et al.* High FOXO3a expression is associated with a poorer prognosis in AML with normal cytogenetics. *Leuk Res* **33**, 1706-1709 (2009).
85. Kornblau, S.M., *et al.* Highly phosphorylated FOXO3A is an adverse prognostic factor in acute myeloid leukemia. *Clin Cancer Res* **16**, 1865-1874 (2010).
86. Cheong, J.W., *et al.* Phosphatase and tensin homologue phosphorylation in the C-terminal regulatory domain is frequently observed in acute myeloid leukaemia and associated with poor clinical outcome. *Br J Haematol* **122**, 454-456 (2003).
87. Kornblau, S.M., *et al.* Simultaneous activation of multiple signal transduction pathways confers poor prognosis in acute myelogenous leukemia. *Blood* **108**, 2358-2365 (2006).
88. Follo, M.Y., *et al.* The Akt/mammalian target of rapamycin signal transduction pathway is activated in high-risk myelodysplastic syndromes and influences cell survival and proliferation. *Cancer Res* **67**, 4287-4294 (2007).
89. Nyakern, M., *et al.* Frequent elevation of Akt kinase phosphorylation in blood marrow and peripheral blood mononuclear cells from high-risk myelodysplastic syndrome patients. *Leukemia* **20**, 230-238 (2006).
90. Tamburini, J., *et al.* Constitutive phosphoinositide 3-kinase/Akt activation represents a favorable prognostic factor in de novo acute myelogenous leukemia patients. *Blood* **110**, 1025-1028 (2007).
91. Rosen, D.B., *et al.* Distinct patterns of DNA damage response and apoptosis correlate with Jak/Stat and PI3kinase response profiles in human acute myelogenous leukemia. *PLoS One* **5**, e12405 (2010).
92. Tazzari, P.L., *et al.* Multidrug resistance-associated protein 1 expression is under the control of the phosphoinositide 3 kinase/Akt signal transduction network in human acute myelogenous leukemia blasts. *Leukemia* **21**, 427-438 (2007).
93. Mahadevan, D. & List, A.F. Targeting the multidrug resistance-1 transporter in AML: molecular regulation and therapeutic strategies. *Blood* **104**, 1940-1951 (2004).
94. Gunther, R., Abbas, H.K. & Mirocha, C.J. Acute pathological effects on rats of orally administered wortmannin-containing preparations and purified wortmannin from Fusarium oxysporum. *Food Chem Toxicol* **27**, 173-179 (1989).
95. Davies, S.P., Reddy, H., Caivano, M. & Cohen, P. Specificity and mechanism of action of some commonly used protein kinase inhibitors. *Biochem J* **351**, 95-105 (2000).
96. Mao, X., *et al.* A small-molecule inhibitor of D-cyclin transactivation displays preclinical efficacy in myeloma and leukemia via phosphoinositide 3-kinase pathway. *Blood* **117**, 1986-1997 (2011).

97. de Frias, M., *et al.* Isoform-selective phosphoinositide 3-kinase inhibitors induce apoptosis in chronic lymphocytic leukaemia cells. *Br J Haematol* **150**, 108-111 (2010).
98. Herman, S.E., *et al.* Phosphatidylinositol 3-kinase-delta inhibitor CAL-101 shows promising preclinical activity in chronic lymphocytic leukemia by antagonizing intrinsic and extrinsic cellular survival signals. *Blood* **116**, 2078-2088 (2010).
99. Herman, S.E., *et al.* The role of phosphatidylinositol 3-kinase-delta in the immunomodulatory effects of lenalidomide in chronic lymphocytic leukemia. *Blood* **117**, 4323-4327 (2011).
100. Hoellenriegel, J., *et al.* The phosphoinositide 3'-kinase delta inhibitor, CAL-101, inhibits B-cell receptor signaling and chemokine networks in chronic lymphocytic leukemia. *Blood* **118**, 3603-3612 (2011).
101. Fu, L., *et al.* Perifosine inhibits mammalian target of rapamycin signaling through facilitating degradation of major components in the mTOR axis and induces autophagy. *Cancer Res* **69**, 8967-8976 (2009).
102. Chiarini, F., *et al.* The novel Akt inhibitor, perifosine, induces caspase-dependent apoptosis and downregulates P-glycoprotein expression in multidrug-resistant human T-acute leukemia cells by a JNK-dependent mechanism. *Leukemia* **22**, 1106-1116 (2008).
103. Papa, V., *et al.* Proapoptotic activity and chemosensitizing effect of the novel Akt inhibitor perifosine in acute myelogenous leukemia cells. *Leukemia* **22**, 147-160 (2008).
104. Tabellini, G., *et al.* Novel 2'-substituted, 3'-deoxy-phosphatidyl-myo-inositol analogues reduce drug resistance in human leukaemia cell lines with an activated phosphoinositide 3-kinase/Akt pathway. *Br J Haematol* **126**, 574-582 (2004).
105. de Frias, M., *et al.* Akt inhibitors induce apoptosis in chronic lymphocytic leukemia cells. *Haematologica* **94**, 1698-1707 (2009).
106. Evangelisti, C., *et al.* Preclinical testing of the Akt inhibitor triciribine in T-cell acute lymphoblastic leukemia. *J Cell Physiol* **226**, 822-831 (2011).
107. Hofbauer, S.W., *et al.* Modifying akt signaling in B-cell chronic lymphocytic leukemia cells. *Cancer Res* **70**, 7336-7344 (2010).
108. Yee, K.W., *et al.* Phase I/II study of the mammalian target of rapamycin inhibitor everolimus (RAD001) in patients with relapsed or refractory hematologic malignancies. *Clin Cancer Res* **12**, 5165-5173 (2006).
109. Decker, T., *et al.* A pilot trial of the mTOR (mammalian target of rapamycin) inhibitor RAD001 in patients with advanced B-CLL. *Ann Hematol* **88**, 221-227 (2009).
110. Choi, J., Chen, J., Schreiber, S.L. & Clardy, J. Structure of the FKBP12-rapamycin complex interacting with the binding domain of human FRAP. *Science* **273**, 239-242 (1996).
111. Teachey, D.T., *et al.* mTOR inhibitors are synergistic with methotrexate: an effective combination to treat acute lymphoblastic leukemia. *Blood* **112**, 2020-2023 (2008).
112. Recher, C., *et al.* Antileukemic activity of rapamycin in acute myeloid leukemia. *Blood* **105**, 2527-2534 (2005).
113. Rizzieri, D.A., *et al.* A phase 2 clinical trial of deforolimus (AP23573, MK-8669), a novel mammalian target of rapamycin inhibitor, in patients with relapsed or refractory hematologic malignancies. *Clin Cancer Res* **14**, 2756-2762 (2008).
114. Tamburini, J., *et al.* Mammalian target of rapamycin (mTOR) inhibition activates phosphatidylinositol 3-kinase/Akt by up-regulating insulin-like growth factor-1 receptor signaling in acute myeloid leukemia: rationale for therapeutic inhibition of both pathways. *Blood* **111**, 379-382 (2008).

115. Guo, W., *et al.* Suppression of leukemia development caused by PTEN loss. *Proc Natl Acad Sci U S A* **108**, 1409-1414 (2011).
116. Zent, C.S., *et al.* The treatment of recurrent/refractory chronic lymphocytic leukemia/small lymphocytic lymphoma (CLL) with everolimus results in clinical responses and mobilization of CLL cells into the circulation. *Cancer* **116**, 2201-2207 (2010).
117. Janes, M.R., *et al.* Effective and selective targeting of leukemia cells using a TORC1/2 kinase inhibitor. *Nat Med* **16**, 205-213 (2010).
118. Evangelisti, C., *et al.* Targeted inhibition of mTORC1 and mTORC2 by active-site mTOR inhibitors has cytotoxic effects in T-cell acute lymphoblastic leukemia. *Leukemia* **25**, 781-791 (2011).
119. Carayol, N., *et al.* Critical roles for mTORC2- and rapamycin-insensitive mTORC1-complexes in growth and survival of BCR-ABL-expressing leukemic cells. *Proc Natl Acad Sci U S A* **107**, 12469-12474 (2010).
120. Altman, J.K., *et al.* Dual mTORC2/mTORC1 targeting results in potent suppressive effects on acute myeloid leukemia (AML) progenitors. *Clin Cancer Res* **17**, 4378-4388 (2011).
121. Weisberg, E., *et al.* Potentiation of antileukemic therapies by the dual PI3K/PDK-1 inhibitor, BAG956: effects on BCR-ABL- and mutant FLT3-expressing cells. *Blood* **111**, 3723-3734 (2008).
122. Hahn, M., *et al.* Rapamycin and UCN-01 synergistically induce apoptosis in human leukemia cells through a process that is regulated by the Raf-1/MEK/ERK, Akt, and JNK signal transduction pathways. *Mol Cancer Ther* **4**, 457-470 (2005).
123. Maira, S.M., *et al.* Identification and characterization of NVP-BEZ235, a new orally available dual phosphatidylinositol 3-kinase/mammalian target of rapamycin inhibitor with potent in vivo antitumor activity. *Mol Cancer Ther* **7**, 1851-1863 (2008).
124. Chiarini, F., *et al.* Activity of the novel dual phosphatidylinositol 3-kinase/mammalian target of rapamycin inhibitor NVP-BEZ235 against T-cell acute lymphoblastic leukemia. *Cancer Res* **70**, 8097-8107 (2010).
125. Chapuis, N., *et al.* Dual inhibition of PI3K and mTORC1/2 signaling by NVP-BEZ235 as a new therapeutic strategy for acute myeloid leukemia. *Clin Cancer Res* **16**, 5424-5435 (2010).
126. Chiarini, F., *et al.* Dual inhibition of class IA phosphatidylinositol 3-kinase and mammalian target of rapamycin as a new therapeutic option for T-cell acute lymphoblastic leukemia. *Cancer Res* **69**, 3520-3528 (2009).
127. Park, S., *et al.* PI-103, a dual inhibitor of Class IA phosphatidylinositide 3-kinase and mTOR, has antileukemic activity in AML. *Leukemia* **22**, 1698-1706 (2008).
128. Zeng, Z., *et al.* Simultaneous inhibition of PDK1/AKT and Fms-like tyrosine kinase 3 signaling by a small-molecule KP372-1 induces mitochondrial dysfunction and apoptosis in acute myelogenous leukemia. *Cancer Res* **66**, 3737-3746 (2006).
129. Nishioka, C., Ikezoe, T., Yang, J., Koeffler, H.P. & Yokoyama, A. Blockade of mTOR signaling potentiates the ability of histone deacetylase inhibitor to induce growth arrest and differentiation of acute myelogenous leukemia cells. *Leukemia* **22**, 2159-2168 (2008).
130. Rahmani, M., *et al.* Coadministration of histone deacetylase inhibitors and perifosine synergistically induces apoptosis in human leukemia cells through Akt and ERK1/2 inactivation and the generation of ceramide and reactive oxygen species. *Cancer Res* **65**, 2422-2432 (2005).
131. Horton, T.M., *et al.* A phase 1 study of the proteasome inhibitor bortezomib in pediatric patients with refractory leukemia: a Children's Oncology Group study. *Clin Cancer Res* **13**, 1516-1522 (2007).

132. Saunders, P., Cisterne, A., Weiss, J., Bradstock, K.F. & Bendall, L.J. The mammalian target of rapamycin inhibitor RAD001 (everolimus) synergizes with chemotherapeutic agents, ionizing radiation and proteasome inhibitors in pre-B acute lymphocytic leukemia. *Haematologica* **96**, 69-77 (2011).
133. Gorre, M.E., *et al.* Clinical resistance to STI-571 cancer therapy caused by BCR-ABL gene mutation or amplification. *Science* **293**, 876-880 (2001).
134. Burchert, A., *et al.* Compensatory PI3-kinase/Akt/mTor activation regulates imatinib resistance development. *Leukemia* **19**, 1774-1782 (2005).
135. Okabe, S., Tauchi, T. & Ohyashiki, K. Characteristics of dasatinib- and imatinib-resistant chronic myelogenous leukemia cells. *Clin Cancer Res* **14**, 6181-6186 (2008).
136. Hui, R.C., *et al.* The forkhead transcription factor FOXO3a increases phosphoinositide-3 kinase/Akt activity in drug-resistant leukemic cells through induction of PIK3CA expression. *Mol Cell Biol* **28**, 5886-5898 (2008).
137. Joha, S., *et al.* GILZ inhibits the mTORC2/AKT pathway in BCR-ABL(+) cells. *Oncogene* **31**, 1419-1430 (2012).
138. Mancini, M., *et al.* mTOR inhibitor RAD001 (Everolimus) enhances the effects of imatinib in chronic myeloid leukemia by raising the nuclear expression of c-ABL protein. *Leuk Res* **34**, 641-648 (2010).
139. Parmar, S., *et al.* Differential regulation of the p70 S6 kinase pathway by interferon alpha (IFNalpha) and imatinib mesylate (STI571) in chronic myelogenous leukemia cells. *Blood* **106**, 2436-2443 (2005).
140. Tseng, P.H., *et al.* Synergistic interactions between imatinib mesylate and the novel phosphoinositide-dependent kinase-1 inhibitor OSU-03012 in overcoming imatinib mesylate resistance. *Blood* **105**, 4021-4027 (2005).
141. Klejman, A., Rushen, L., Morrione, A., Slupianek, A. & Skorski, T. Phosphatidylinositol-3 kinase inhibitors enhance the anti-leukemia effect of STI571. *Oncogene* **21**, 5868-5876 (2002).
142. Kharas, M.G., *et al.* Ablation of PI3K blocks BCR-ABL leukemogenesis in mice, and a dual PI3K/mTOR inhibitor prevents expansion of human BCR-ABL+ leukemia cells. *J Clin Invest* **118**, 3038-3050 (2008).
143. Burnett, A., Wetzler, M. & Lowenberg, B. Therapeutic advances in acute myeloid leukemia. *J Clin Oncol* **29**, 487-494 (2011).
144. Xu, Q., Thompson, J.E. & Carroll, M. mTOR regulates cell survival after etoposide treatment in primary AML cells. *Blood* **106**, 4261-4268 (2005).
145. Billottet, C., *et al.* A selective inhibitor of the p110delta isoform of PI 3-kinase inhibits AML cell proliferation and survival and increases the cytotoxic effects of VP16. *Oncogene* **25**, 6648-6659 (2006).
146. Sampath, D., *et al.* Pharmacodynamics of cytarabine alone and in combination with 7-hydroxystaurosporine (UCN-01) in AML blasts in vitro and during a clinical trial. *Blood* **107**, 2517-2524 (2006).
147. Wymann, M.P., *et al.* Wortmannin inactivates phosphoinositide 3-kinase by covalent modification of Lys-802, a residue involved in the phosphate transfer reaction. *Mol Cell Biol* **16**, 1722-1733 (1996).
148. Marley, S.B., Lewis, J.L., Schneider, H., Rudd, C.E. & Gordon, M.Y. Phosphatidylinositol-3 kinase inhibitors reproduce the selective antiproliferative effects of imatinib on chronic myeloid leukaemia progenitor cells. *Br J Haematol* **125**, 500-511 (2004).

149. Xu, Q., Simpson, S.E., Scialla, T.J., Bagg, A. & Carroll, M. Survival of acute myeloid leukemia cells requires PI3 kinase activation. *Blood* **102**, 972-980 (2003).
150. Zhao, S., *et al.* Inhibition of phosphatidylinositol 3-kinase dephosphorylates BAD and promotes apoptosis in myeloid leukemias. *Leukemia* **18**, 267-275 (2004).
151. Levy, D.S., Kahana, J.A. & Kumar, R. AKT inhibitor, GSK690693, induces growth inhibition and apoptosis in acute lymphoblastic leukemia cell lines. *Blood* **113**, 1723-1729 (2009).
152. Aleskog, A., *et al.* Rapamycin shows anticancer activity in primary chronic lymphocytic leukemia cells in vitro, as single agent and in drug combination. *Leuk Lymphoma* **49**, 2333-2343 (2008).
153. Hirase, C., Maeda, Y., Takai, S. & Kanamaru, A. Hypersensitivity of Ph-positive lymphoid cell lines to rapamycin: Possible clinical application of mTOR inhibitor. *Leuk Res* **33**, 450-459 (2009).
154. Sillaber, C., *et al.* Evaluation of antileukaemic effects of rapamycin in patients with imatinib-resistant chronic myeloid leukaemia. *Eur J Clin Invest* **38**, 43-52 (2008).
155. Mayerhofer, M., *et al.* Identification of mTOR as a novel bifunctional target in chronic myeloid leukemia: dissection of growth-inhibitory and VEGF-suppressive effects of rapamycin in leukemic cells. *FASEB J* **19**, 960-962 (2005).
156. Teachey, D.T., *et al.* The mTOR inhibitor CCI-779 induces apoptosis and inhibits growth in preclinical models of primary adult human ALL. *Blood* **107**, 1149-1155 (2006).
157. Hsieh, A.C., *et al.* Genetic dissection of the oncogenic mTOR pathway reveals druggable addiction to translational control via 4EBP-eIF4E. *Cancer Cell* **17**, 249-261 (2010).
158. Kojima, K., *et al.* The dual PI3 kinase/mTOR inhibitor PI-103 prevents p53 induction by Mdm2 inhibition but enhances p53-mediated mitochondrial apoptosis in p53 wild-type AML. *Leukemia* **22**, 1728-1736 (2008).
159. Neri, L.M., *et al.* The phosphoinositide 3-kinase/AKT1 pathway involvement in drug and all-trans-retinoic acid resistance of leukemia cells. *Mol Cancer Res* **1**, 234-246 (2003).
160. Cheong, J.W., *et al.* Inhibition of CK2{alpha} and PI3K/Akt synergistically induces apoptosis of CD34+CD38- leukaemia cells while sparing haematopoietic stem cells. *Anticancer Res* **30**, 4625-4634 (2010).
161. Redondo-Munoz, J., *et al.* Induction of B-chronic lymphocytic leukemia cell apoptosis by arsenic trioxide involves suppression of the phosphoinositide 3-kinase/Akt survival pathway via c-jun-NH2 terminal kinase activation and PTEN upregulation. *Clin Cancer Res* **16**, 4382-4391 (2010).
162. Cristobal, I., *et al.* PP2A impaired activity is a common event in acute myeloid leukemia and its activation by forskolin has a potent anti-leukemic effect. *Leukemia* **25**, 606-614 (2011).
163. Tazzari, P.L., *et al.* Synergistic proapoptotic activity of recombinant TRAIL plus the Akt inhibitor Perifosine in acute myelogenous leukemia cells. *Cancer Res* **68**, 9394-9403 (2008).
164. Akers, L.J., *et al.* Targeting glycolysis in leukemia: a novel inhibitor 3-BrOP in combination with rapamycin. *Leuk Res* **35**, 814-820 (2011).
165. Chan, S.M., Weng, A.P., Tibshirani, R., Aster, J.C. & Utz, P.J. Notch signals positively regulate activity of the mTOR pathway in T-cell acute lymphoblastic leukemia. *Blood* **110**, 278-286 (2007).
166. Boehrer, S., *et al.* Erlotinib antagonizes constitutive activation of SRC family kinases and mTOR in acute myeloid leukemia. *Cell Cycle* **10**, 3168-3175 (2011).
167. Hayun, R., *et al.* Rapamycin and curcumin induce apoptosis in primary resting B chronic lymphocytic leukemia cells. *Leuk Lymphoma* **50**, 625-632 (2009).

168. Gu, L., *et al.* Rapamycin sensitizes T-ALL cells to dexamethasone-induced apoptosis. *J Exp Clin Cancer Res* **29**, 150 (2010).
169. Bonapace, L., *et al.* Induction of autophagy-dependent necroptosis is required for childhood acute lymphoblastic leukemia cells to overcome glucocorticoid resistance. *J Clin Invest* **120**, 1310-1323 (2010).
170. Avellino, R., *et al.* Rapamycin stimulates apoptosis of childhood acute lymphoblastic leukemia cells. *Blood* **106**, 1400-1406 (2005).
171. Yang, X., *et al.* Antileukaemia effect of rapamycin alone or in combination with daunorubicin on Ph+ acute lymphoblastic leukaemia cell line. *Hematol Oncol* **30**, 123-130 (2012).
172. Nishioka, C., *et al.* Inhibition of mammalian target of rapamycin signaling potentiates the effects of all-trans retinoic acid to induce growth arrest and differentiation of human acute myelogenous leukemia cells. *Int J Cancer* **125**, 1710-1720 (2009).
173. Crazzolara, R., *et al.* Potentiating effects of RAD001 (Everolimus) on vincristine therapy in childhood acute lymphoblastic leukemia. *Blood* **113**, 3297-3306 (2009).
174. Hong, Z., *et al.* Arsenic disulfide synergizes with the phosphoinositide 3-kinase inhibitor PI-103 to eradicate acute myeloid leukemia stem cells by inducing differentiation. *Carcinogenesis* **32**, 1550-1558 (2011).

Chapter 3

Autophagy Inhibition as Targeted Therapy for ETV6-RUNX1 driven B-cell Precursor Acute Lymphoblastic Leukemia

R. Polak[1], M. B. Bierings[2], C. S. van der Leije[3], M. A. Sanders[3], O. Roovers[3], J. R. M. Marchante[1], J. M. Boer[1], J. J. Cornelissen[3], R. Pieters[4], M. L. den Boer[1]* & M. Buitenhuis[3]*

[1] *Dept. of Pediatric Oncology, Erasmus MC - Sophia Children's Hospital, Rotterdam, The Netherlands.*
[2] *Dept. of Pediatric Oncology, University Medical Center Utrecht, Utrecht, The Netherlands.*
[3] *Dept. of Hematology, Erasmus Medical Center, Rotterdam, The Netherlands.*
[4] *Princess Máxima Center for Pediatric Oncology, Utrecht, The Netherlands.*

Manuscript under consideration

ABSTRACT

Translocation t(12;21), resulting in the ETV6-RUNX1 (or TEL-AML1) fusion protein, is present in 25% of pediatric patients with B-cell precursor acute lymphoblastic leukemia (BCP-ALL) and is considered a first hit in leukemogenesis. A targeted therapy approach is not available for children with this subtype of leukemia. Here, we report an important role for autophagy in ETV6-RUNX1 positive BCP-ALL. To identify the molecular mechanisms underlying ETV6-RUNX1 driven leukemia, we performed gene expression profiling of healthy hematopoietic progenitors in which we ectopically expressed ETV6-RUNX1. We reveal an ETV6-RUNX1 driven transcriptional network that positively regulates proliferation, survival and cellular homeostasis. In addition, Vps34, an important regulator of autophagy, was found to be up-regulated in ETV6-RUNX1 positive BCP-ALL patient cells. We show that induction of Vps34 was transcriptionally regulated by ETV6-RUNX1 and correlated with high levels of autophagy. Knockdown of Vps34 in ETV6-RUNX1 positive cell lines severely reduced proliferation and survival. Inhibition of autophagy by hydroxychloroquine, a well-tolerated autophagy inhibitor, reduced cell viability in both BCP-ALL cell lines and primary patient-derived BCP-ALL cells and selectively sensitized primary ETV6-RUNX1 positive leukemic cells to L-asparaginase. These findings reveal a causal relationship between ETV6-RUNX1 and autophagy, and provide the first pre-clinical evidence for the efficacy of autophagy inhibitors in ETV6-RUNX1 driven leukemia.

INTRODUCTION

Acute lymphoblastic leukemia (ALL) is the most common pediatric malignancy. During the last decades, the overall survival rates of pediatric ALL have improved significantly[1]. This is primarily due to optimization of conventional chemotherapeutic drug regimens combined with risk-directed therapies[1]. However, to date, still 20% of pediatric ALL cases relapse because of resistance to therapy[2,3]. In addition, long-term treatment-induced side effects remain considerable[4,5]. New treatment regimens increasingly aim to target specific intrinsic characteristics of leukemia. This approach has, for example, led to the successful development of BCR-ABL1 inhibitors[6,7]. Regrettably, such a targeted approach is not available for the majority of children suffering from leukemia.

Translocation t(12;21)(p13;q22), resulting in the ETV6-RUNX1 fusion protein (also known as TEL-AML1), is present in 25% of pediatric patients with B-cell precursor acute lymphoblastic leukemia (BCP-ALL) and is therewith the most common fusion protein in childhood cancer[8-10]. The t(12;21)(p13;q22) rearrangement fuses the 5′ non-DNA binding region of the ETS family transcription factor ETV6 (TEL) to almost the entire RUNX1 (AML1) locus[11]. Despite the favorable prognosis associated with this cytogenetic type of BCP-ALL[9,12,13], resistance to chemotherapeutic drugs and relapse occur in 10-20% of these patients[13-18].

The ETV6-RUNX1 fusion protein induces a silent pre-leukemic clone that requires additional genetic hits for the transition to leukemia[15,16,19-22]. Although these pre-leukemic ETV6-RUNX1 positive hematopoietic stem cells (HSCs) still possess self-renewal properties and are capable of contributing to hematopoiesis, they fail to outcompete normal HSCs[20,21,23]. In ETV6-RUNX1 positive leukemia, this early genetic lesion is followed by a small number of 'driver' copy number alterations, which are predominantly directed to genes regulating normal B cell differentiation[24,25]. These alterations are acquired independently without preferential order, thereby generating a dynamic clonal architecture[24]. This genetic variation implies that targeted therapy in ETV6-RUNX1 driven ALL should be directed to targets of initial lesions that are present in all subclones. This concept is further supported by the observation that ETV6-RUNX1 positive cell lines are highly dependent on the expression of the fusion protein for their survival[26,27]. For the development of novel targeted therapies, it is important to identify the molecular pathways induced by expression of the ETV6-RUNX1 fusion protein. Previous reports revealed that enhanced levels of STAT3, heat-shock proteins, survivin, has-mir-125b-2, the erythropoietin receptor, and cytoskeleton regulatory genes and aberrant regulation of the TGFβ pathway are important for ETV6-RUNX1 positive BCP-ALL[26,28-35]. However, the complete molecular network underlying the persistence and maintenance of ETV6-RUNX1

BCP-ALL remains to be investigated. Additionally, to date, ETV6-RUNX1 positive cells cannot be selectively targeted or sensitized to conventional chemotherapy.

In this study, we elucidate the transcriptional network regulated by the ETV6-RUNX1 fusion protein and show that induction of autophagy is important for the survival and proliferation of ETV6-RUNX1 positive leukemic cells. Pharmacological inhibition of autophagy sensitized primary ETV6-RUNX1 positive cells to L-Asparaginase, one of the key chemotherapeutic drugs used in the treatment of childhood BCP-ALL. Herewith, we propose autophagy inhibition as a promising novel means to improve treatment for ETV6-RUNX1 positive ALL.

METHODS

Details are provided in the supplementary methods section.

Transduction and gene expression profiling of primary cells

CD34-positive hematopoietic progenitor cells (CB-CD34$^+$ cells) were derived from cord blood and transduced with retrovirus expressing *ETV6-RUNX1* and eGFP. DAPI$^-$ CD34$^+$ GFP$^+$ CB-CD34$^+$ cells were sorted using a BD ARIA II sorter. After sorting, cells were lysed and RNA was extracted and subsequently linearly amplified.

Bone marrow aspirates were obtained from children with newly diagnosed BCP-ALL prior to treatment. Leukemic blasts were collected and processed as previously described.

Affymetrix GeneChip HG-U133-Plus-2.0 microarrays were used for all samples. Microarray data of CB-CD34$^+$ cells are available in the ArrayExpress database under accession number E-MTAB-3466. Microarray data of BCP-ALL blasts are available in the Gene Expression Omnibus database.

Functional assays

For protein quantification, both western blot analysis as reverse phase protein arrays were used. Vps34 promoter activity was studied using a reporter construct consisting of a 1.4 kB region of the Vps34 promoter upstream of the Gaussia luciferase gene. Cell viability was quantified using MTT cytotoxicity assays or flow cytometry-based Annexin V - Propidium Iodide assays. Silencing of genes was achieved using transfection of specific siRNAs or a lentiviral knockdown approach using the pLKO.1 Mission vector containing a puromycin selection marker. Autophagy levels (number and volume of LC3B positive vesicles) were quantified using confocal scanning microscopy (Leica SP5).

Statistical analysis

Statistical analysis of microarray data of paired CB-CD34$^+$ cells was performed using a linear mixed model. Microarray data of primary cells from ALL patients were analyzed using LIMMA. Functional analysis of differential gene expression was performed using QIAGEN's Ingenuity Pathway Analysis. Both the Student's t-test and the Student's paired t-test were used as statistical test when applicable. Bar graphs represent the mean of biological replicates. Error bars represent standard error of the mean (S.E.M.).

RESULTS

Ectopic expression of ETV6-RUNX1 in healthy CD34$^+$ progenitors activates pro-proliferative and pro-survival transcriptional networks

In order to elucidate the molecular mechanisms underlying ETV6-RUNX1 driven BCP-ALL, we performed gene expression profiling on healthy, umbilical cord blood-derived, CD34-positive hematopoietic progenitors (CB-CD34$^+$) ectopically expressing the ETV6-RUNX1 fusion gene. To generate retrovirus, bicistronic retroviral DNA constructs were used co-expressing ETV6-RUNX1 and eGFP. CB-CD34$^+$ cells were retrovirally transduced with ETV6-RUNX1-eGFP or an eGFP expressing control vector. Forty hours after transduction, eGFP-positive cells were sorted from the non-transduced cells by fluorescent activated cell sorting (n = 5, Figure 1A). RT-PCR confirmed that the ETV6-RUNX1 fusion transcript was only expressed in the CB-CD34$^+$ cells transduced with ETV6-RUNX1 ($p \leq 0.001$; supplementary Figure 1C). Gene expression analysis revealed that 196 genes were differentially expressed in ETV6-RUNX1 transduced CB-CD34$^+$ cells in comparison to empty vector controls (2 – 40 fold; $p \leq 0.05$; Figure 1B). Ingenuity Pathway Analysis on these 196 genes predicted an interacting gene network of 36 genes with direct or indirect relationships (Figure 1C). One of these genes was *CDKN1A (p21)*, a previously described ETV6-RUNX1 target gene[36]. Other genes that were strongly upregulated are the transcription factors *GATA1*, *GATA2*, *HEY1* and *EGR1*, and the growth factors *IL8* and *CSF1* (Figure 1C). Analysis of gene ontology (GO) functional categories indicated that ETV6-RUNX1 induces a pro-survival and pro-proliferative phenotype (Figure 1D, E; supplementary Figure 2A, B). In addition, both an increase in cellular homeostasis (supplementary Figure 2B), and regulation of the cytoskeleton was predicted (data not shown). These data provide a better insight into the effects of the ETV6-RUNX1 fusion protein in healthy progenitors, and reveal a transcriptional network that activates proliferation and inhibits apoptosis.

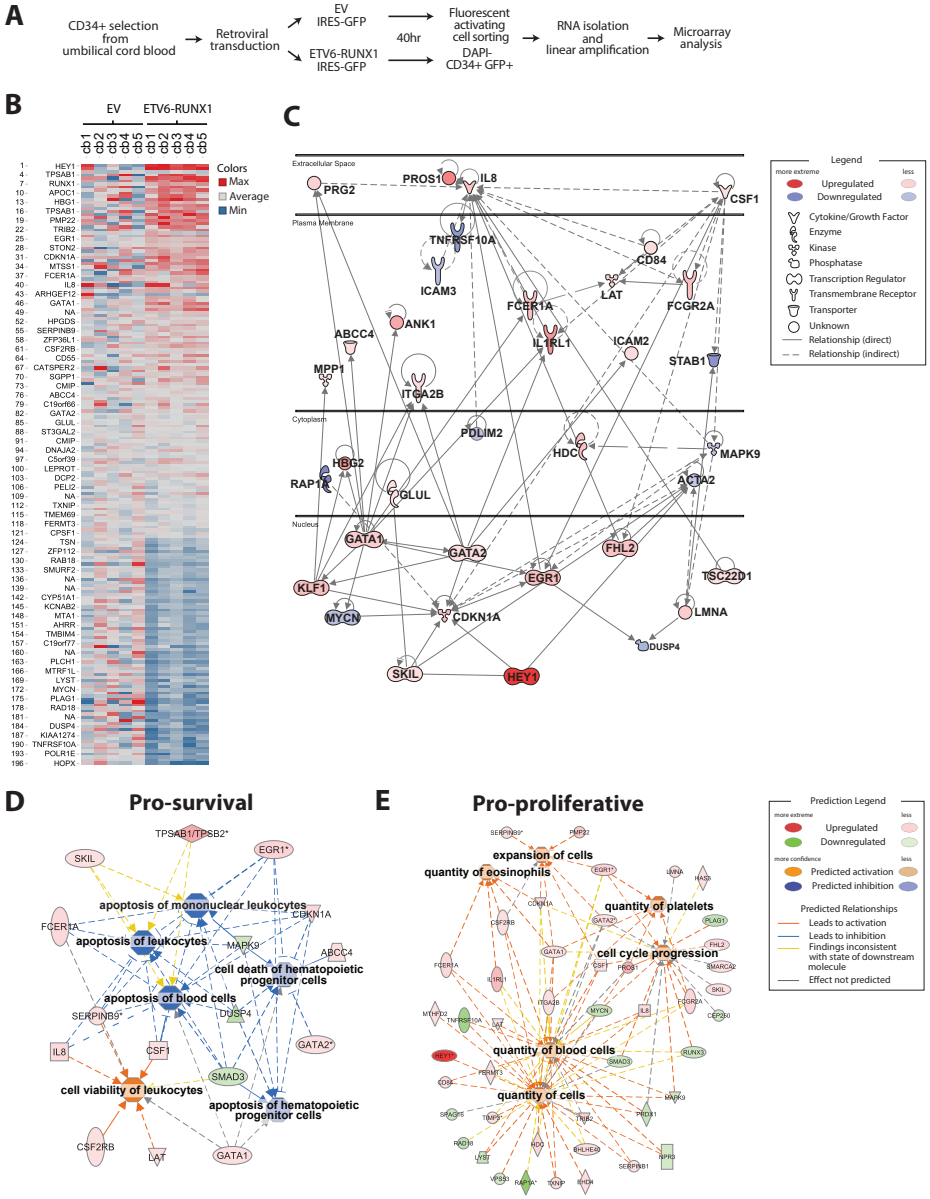

Figure 1. Ectopic expression of ETV6-RUNX1 in healthy CD34$^+$ progenitors activates pro-proliferative and pro-survival transcriptional networks.

CD34-positive hematopoietic progenitors (CB-CD34$^+$ cells) were isolated from cord blood, upon which cells were divided in two fractions. One fraction was transduced with ETV6-RUNX1-IRES-eGFP, while the other fraction was transduced with control EV-IRES-eGFP (n = 5 biological replicates). Forty hours after transduction, CD34$^+$ DAPI$^-$ eGFP$^+$ hematopoietic progenitors were sorted from non-transduced cells (for gating strategy see supplementary Figure 1). After sorting, RNA was extracted, checked for quality and linearly amplified. Gene expression analysis was subsequently performed using Affymetrix Genechip microarrays.

(A) Flowchart of the experimental approach.

Figure 1. Ectopic expression of ETV6-RUNX1 in healthy CD34$^+$ progenitors activates pro-proliferative and pro-survival transcriptional networks. (continued)
(B) Heat map displaying gene probe sets that were either over-expressed (in red) or under-expressed (in blue) in comparison to the mean expression of all probe sets. Forty hours after transduction, 196 gene probe sets were significantly ($p \leq 0.05$; FDR-adjusted) over-expressed or under-expressed in ETV6-RUNX1 positive CB-CD34$^+$ cells in comparison to control CB-CD34$^+$ cells. Data were analyzed using a linear mixed model. Genes were considered differentially expressed when $p \leq 0.05$ after multiple testing correction using false discovery rate (FDR). (C) Ingenuity pathway analysis of the differentially expressed genes was performed to elucidate the interconnected transcriptional network present within this gene set. The level of up- (red) and down-regulation (blue) of genes was visualized by the intensity of the colors. Direct relationships were marked with undotted arrows. Indirect relationships were marked with dotted arrows. (D/E) Ingenuity pathway analysis was used to analyze gene ontology (GO) functional categories and activation of disease/function annotation based on current literature. Functional categories inducing a pro-survival (D) or a pro-proliferative (E) state in ETV6-RUNX1 positive HPCs and the differentially regulated genes responsible for this prediction are shown.
See also supplementary Figure 1 and 2.

Vps34 is up-regulated in ETV6-RUNX1 positive BCP-ALL and is driven by the ETV6-RUNX1 fusion protein

To identify novel ETV6-RUNX1 target genes, the above-described ETV6-RUNX1 induced gene expression profiles in CB-CD34$^+$ cells were compared with gene expression profiles of primary ALL cells. For this analysis, we used data from cohorts in which ETV6-RUNX1 positive BCP-ALL patients were included[36-40] and data from an ETV6-RUNX1 knockdown study performed in a leukemic cell line[41] (Figure 2A). Pathway analysis on differentially expressed genes (top 500, see supplementary Table 1) in the largest patient cohort (Erasmus MC cohort, 654 ALL patients including 172 ETV6-RUNX1 positive BCP-ALL patients and 401 ETV6-RUNX1 negative BCP-ALL patients[42]) revealed a pro-survival and pro-proliferative phenotype in ETV6-RUNX1-positive patient cells, similar to the phenotype predicted in CB-CD34$^+$ cells ectopically expressing ETV6-RUNX1 (Figure 2F). The class III PI3-kinase Vps34 (PIK3C3) was found to be recurrently upregulated in ETV6-RUNX1 positive ALL patient cells (Figure 2A-C; 2.7-fold higher expression in Erasmus MC cohort, FDR-adjusted p = 7.24E-39).

To determine the direct effect of the ETV6-RUNX1 fusion protein on Vps34 expression, ETV6-RUNX1 was ectopically expressed in CB-CD34$^+$ cells. Forty hours after transduction, Vps34 mRNA expression was significantly up-regulated by 1.3-fold (Figure 2D; p = 0.03), confirming the induction of Vps34 by the ETV6-RUNX1 fusion protein. Reciprocal experiments were performed in ETV6-RUNX1 positive cells (REH cell line and ETV6-RUNX1 transduced CB-CD34$^+$ cells) using siRNAs directed to the ETV6-RUNX1 breakpoint. Although the ETV6-RUNX1 mRNA levels could only be reduced by 30-35% (supplementary Figure 3B; $p \leq 0.05$), this reduction was sufficient to significantly reduce the levels of Vps34 mRNA and protein both by approximately 40% (Figure 2E; $p \leq 0.05$).

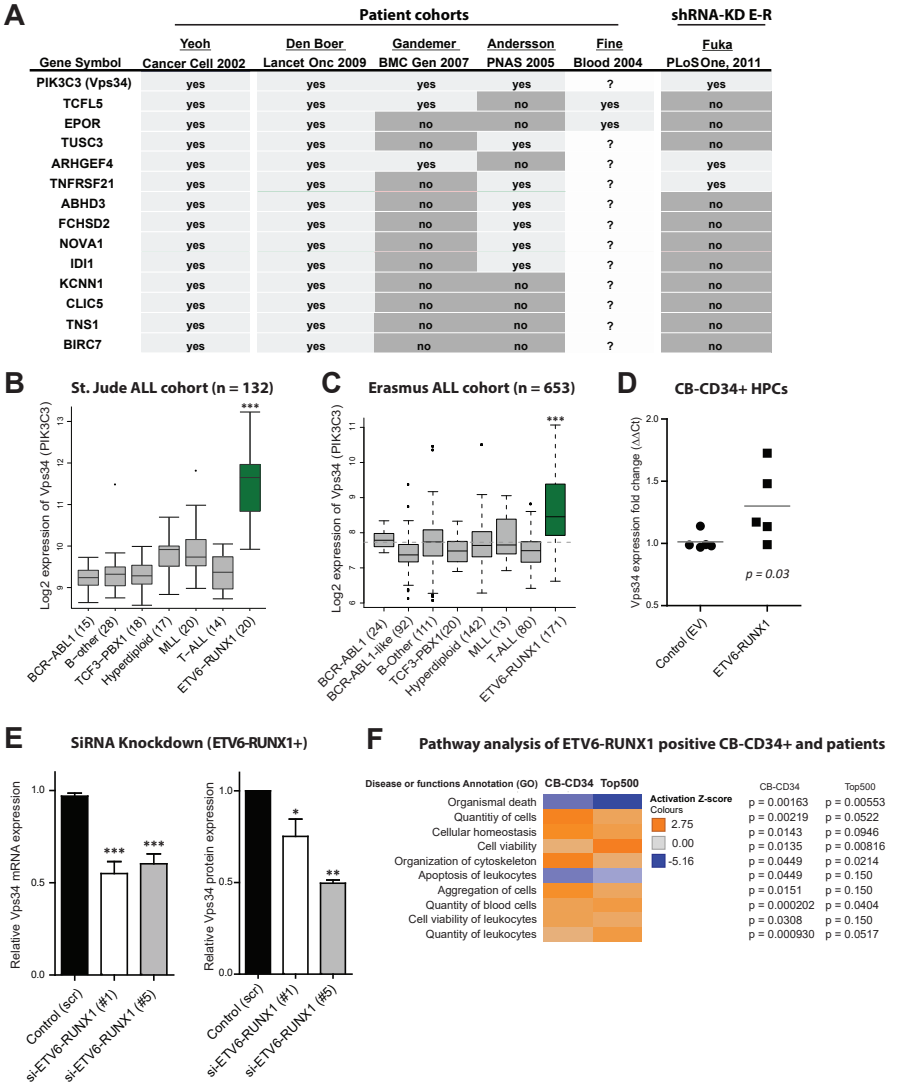

Figure 2. Vps34 is recurrently up-regulated in ETV6-RUNX1 positive BCP-ALL and is driven by the ETV6-RUNX1 fusion protein.

(A) We compared gene expression levels in ETV6-RUNX1 positive ALL cells with gene expression levels in ETV6-RUNX1 negative ALL cells. We used 5 cohorts in which ETV6-RUNX1 positive BCP-ALL patients were included and gene expression data were publically available. In addition, we analyzed differential gene expression in an ETV6-RUNX1 knockdown study performed in an ETV6-RUNX1 positive leukemic cell line. (B) 2log expression levels of the gene probe set mapped to Vps34 were analyzed in a cohort of 132 pediatric ALL patients published by Yeoh *et al.*[36]. Gene expression of ETV6-RUNX1 positive patients (green bar) was compared to gene expression of all other B-ALL patients (excluding T-ALL): *** FDR-adjusted $p = 3.45*10^{-15}$. (C) 2log expression levels of the gene probe set mapped to Vps34 were analyzed in a cohort of 653 pediatric ALL patients published by Van der Veer *et al.*[42]. Gene expression of ETV6-RUNX1 positive patients (green bar) was compared to gene expression of all other B-ALL patients (excluding T-ALL). Grey dashed line represents mean expression of all patients: *** FDR-adjusted $p = 7.24*10^{-39}$.

Figure 2. Vps34 is recurrently up-regulated in ETV6-RUNX1 positive BCP-ALL and is driven by the ETV6-RUNX1 fusion protein. (continued)
(D) CB-CD34$^+$ cells were transduced with ETV6-RUNX1-IRES-eGFP or with control EV-IRES-eGFP after which eGFP$^+$ cells were sorted and Vps34 mRNA levels were determined by Q-PCR and normalized to HPRT. Grey bars represent the mean of 5 biological replicates. Gene expression of Vps34 was compared between ETV6-RUNX1$^+$ CB-CD34$^+$ cells and EV-control CB-CD34$^+$ cells (n = 5; p = 0.03). (E) ETV6-RUNX1 positive cells were transfected with siRNAs directed to the ETV6-RUNX1 breakpoint or scrambled control siRNAs. Vps34 mRNA levels were determined in ETV6-RUNX1$^+$ cells (REH (n=2) and ETV6-RUNX1 transduced CB-CD34$^+$ cells (n=2)) by Q-PCR, normalized to HPRT, and compared to the average expression of cells transfected with scrambled control siRNAs (n = 3, p ≤ 0.001). Vps34 protein expression was quantified in REH cells by western blot and compared to protein expression of REH cells transfected with scrambled control siRNAs (n = 2, p ≤ 0.05 and p ≤ 0.01 for siRNA#1 and siRNA#5 respectively). Bars represent mean. Error bars represent S.E.M. (F) Ingenuity pathway analysis was used to analyze gene ontology (GO) functional categories and activation of disease/function annotation based on current literature. Table shows annotations that were similarly activated in ETV6-RUNX1 positive BCP-ALL patients and ETV6-RUNX1 positive CB-CD34$^+$ cells (40 hours after transduction). The top 500 differentially expressed genes between ETV6-RUNX1 positive and EVT6-RUNX1 negative patients in the Erasmus MC cohort were used for this analysis. See also supplementary Figure 3.

ETV6-RUNX1 and ETV6-RUNX1 target genes enhance Vps34 promoter activity

The up-regulation of Vps34 expression in ETV6-RUNX1 positive BCP-ALL patients and ETV6-RUNX1 transduced CB-CD34$^+$ cells, suggests that the Vps34 promoter is activated directly or indirectly by ETV6-RUNX1. Analysis of the Vps34 promoter, using publically available ChIP-seq data, revealed that transcription factors known to play an important role in regulation of hematopoiesis, including *GATA1, GATA2, EGR1* and *HEY1*[43-47], can interact with the Vps34 promoter (Figure 3A). Four of these transcription factors, namely *GATA1*, *GATA2*, *EGR1* and *HEY1*, were also found to be upregulated in ETV6-RUNX1 transduced CB-CD34$^+$ cells (Figure 1C, Figure 3B). The mRNA expression levels of these four genes were modestly increased in ETV6-RUNX1 transduced CB-CD34$^+$ cells 20 hours after transduction and significantly up-regulated after 40 hours: *GATA1, GATA2, EGR1,* and *HEY1* were up-regulated 3.8-fold (p = 0.046) 2.2-fold (p = 0.019), 5.0-fold (p = 0.004), and 24.9-fold (p = 0.015), respectively (Figure 3B).

To investigate the role of ETV6-RUNX1 and the transcription factors GATA1, GATA2, EGR1, and HEY1 in regulation of the activity of the Vps34 promoter, luciferase reporter assays were performed using a reporter construct consisting of the Gaussia luciferase gene downstream of a 1.4 kB region (-1383 to +58) of the Vps34 promoter (Figure 3C). Although RUNX1 expression alone was sufficient to induce Vps34 promoter activity (2.4-fold compared to control, p ≤ 0.01), co-expression of its cofactor CBFβ further enhanced Vps34 promoter activity (4.5-fold compared to control, p ≤ 0.05). Similarly, expression of ETV6-RUNX1 was sufficient to induce Vps34 promoter activity (4.2-fold compared to control, p ≤ 0.05), and luciferase expression was further enhanced by co-expression of CBFβ (13-fold compared to control, p ≤ 0.05). These results demonstrate that, although both RUNX1 and ETV6-

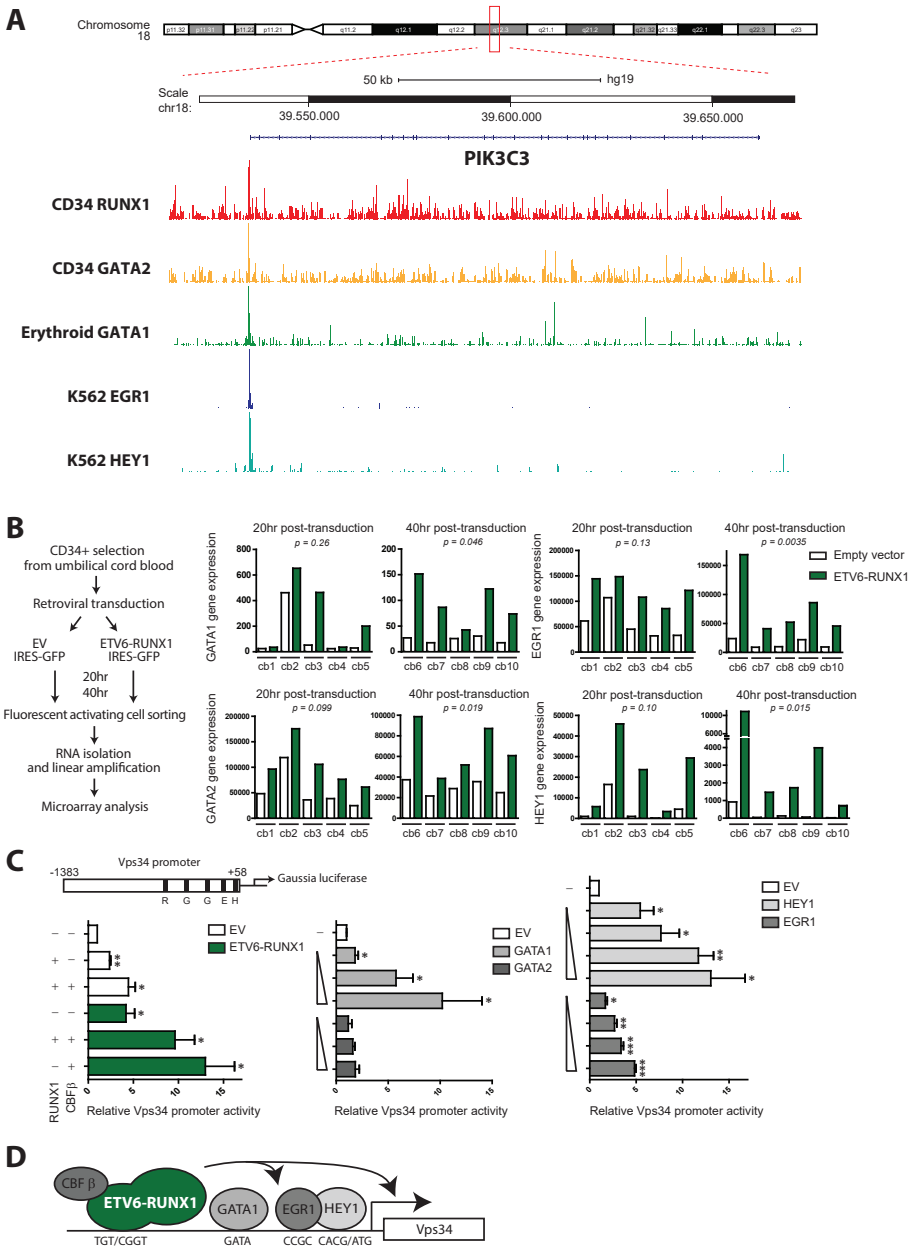

Figure 3. ETV6-RUNX1 and ETV6-RUNX1 target genes enhance Vps34 promoter activity.
(A) The UCSC genome browser (GRCh37/hg19) was used to analyze the transcription factors that bind to the Vps34 promoter. Several transcription factors known to play an important role in regulation of hematopoiesis were found to be interacting with this promoter region. Using publically available ChIP-seq data, the interaction of the transcription factors *RUNX1*, *GATA1*, *GATA2*, *EGR1* and *HEY1* with the Vps34 promoter is shown. (B) Umbilical cord blood-derived CD34^{+} cells were retrovirally transduced to ectopically express the ETV6-RUNX1 fusion protein. Gene expression analysis was performed 20 and 40 hours after transduction.

Figure 3. ETV6-RUNX1 and ETV6-RUNX1 target genes enhance Vps34 promoter activity. (continued)

For flow chart; see left panel. The gene expression levels of *GATA1*, *GATA2*, *EGR1* and *HEY1* are shown. P-values represent the differences between ETV6-RUNX1 positive (green bars) compared to ETV6-RUNX1 negative (white bars) CB-CD34^{+} cells (FDR-adjusted). (C) Upper panel: schematic representation of the -1383 to +58 region of the Vps34 promoter cloned upstream of the Gaussia luciferase gene. Bar graphs: HEK293T cells were co-transfected with a Vps34 promoter construct, RUNX1 and/or CBFβ (left panel), increasing concentrations of GATA1 and GATA2 (middle panel) or HEY1 and EGR1 (right panel) expression constructs. Luciferase activity was determined 48 hours after transfection. eGFP expression was quantified in each sample by flow cytometric analysis and used to normalize luciferase activity. Data were depicted as fold induction compared to empty vector controls. Error bars represent SEM. * $p \leq 0.05$, ** $p \leq 0.01$, *** $p \leq 0.001$. (D) Proposed model for activation of the Vps34 promoter by ETV6-RUNX1 and its downstream targets.

RUNX1 function as transcriptional activators of Vps34, ETV6-RUNX1 induces Vps34 promoter activity more efficiently (Figure 3C). In addition, these results demonstrate that CBFβ acts as a co-activator for both RUNX1 and ETV6-RUNX1 in inducing Vps34 promoter activity.

Additional luciferase reporter assays revealed that the ETV6-RUNX1 target genes *HEY1, EGR1* and *GATA1* induce Vps34 promoter activity in a dose-dependent manner. HEY1, EGR1, and GATA1 induced Vps34 promoter activity up to 13-fold ($p \leq 0.05$), 5.0-fold ($p \leq 0.001$), and 10-fold ($p \leq 0.05$), respectively (Figure 3C). GATA2 expression did not induce luciferase expression, which was in concordance with the absence of a GATA2 DNA binding domain in the -1338/+58 promoter region used for the reported assays (Figure 3A and 3C). Together, these results demonstrate that the Vps34 promoter is not only positively regulated by the ETV6-RUNX1 fusion protein itself, but also by its target genes *HEY1*, *EGR1* and *GATA1* (Figure 3D).

Autophagy levels are high in ETV6-RUNX1 positive BCP-ALL and regulated by ETV6-RUNX1 and Vps34

The class III PI3-kinase Vps34 is known to be a key player in regulation of autophagy [48-51]. We hypothesized that ETV6-RUNX1-mediated up-regulation of Vps34 induces autophagy in BCP-ALL cells. To investigate this, autophagy levels were determined in ALL cell lines and BCP-ALL primary patient cells by western blot analysis and Reverse Phase Protein Arrays (RPPA). Western blot analysis in a panel of ALL cell lines, revealed that Vps34 protein levels are the highest in the ETV6-RUNX1 positive cell line REH (Figure 4A). In comparison to ETV6-RUNX1 negative ALL cell lines, lower levels of p62 (SQSTM1) and LC3B, both specifically degraded by autophagy, were observed in REH cells. These results are in concordance with high levels of autophagy in REH cells (Figure 4A). RPPA on samples from a large cohort of newly diagnosed BCP-ALL patients revealed that the level of Vps34 was 9.6-fold higher in BCP-ALL cells compared to healthy bone marrow derived mononuclear cells (59 BCP-ALL patients versus 10 healthy controls, $p \leq 0.001$). Vps34 levels were also

significantly higher in ETV6-RUNX1 positive patient cells in comparison to ETV6-RUNX1 negative BCP-ALL (B-Other) patient cells (1.2-fold, $p \leq 0.05$). In line with this, lower p62 protein levels were observed in ETV6-RUNX1 positive in comparison to ETV6-RUNX1 negative BCP-ALL patient cells (1.4-fold, $p \leq 0.01$; Figure 4B). These RPPA data were confirmed by western blot in a smaller set of patients (supplementary Figure 4A, B)

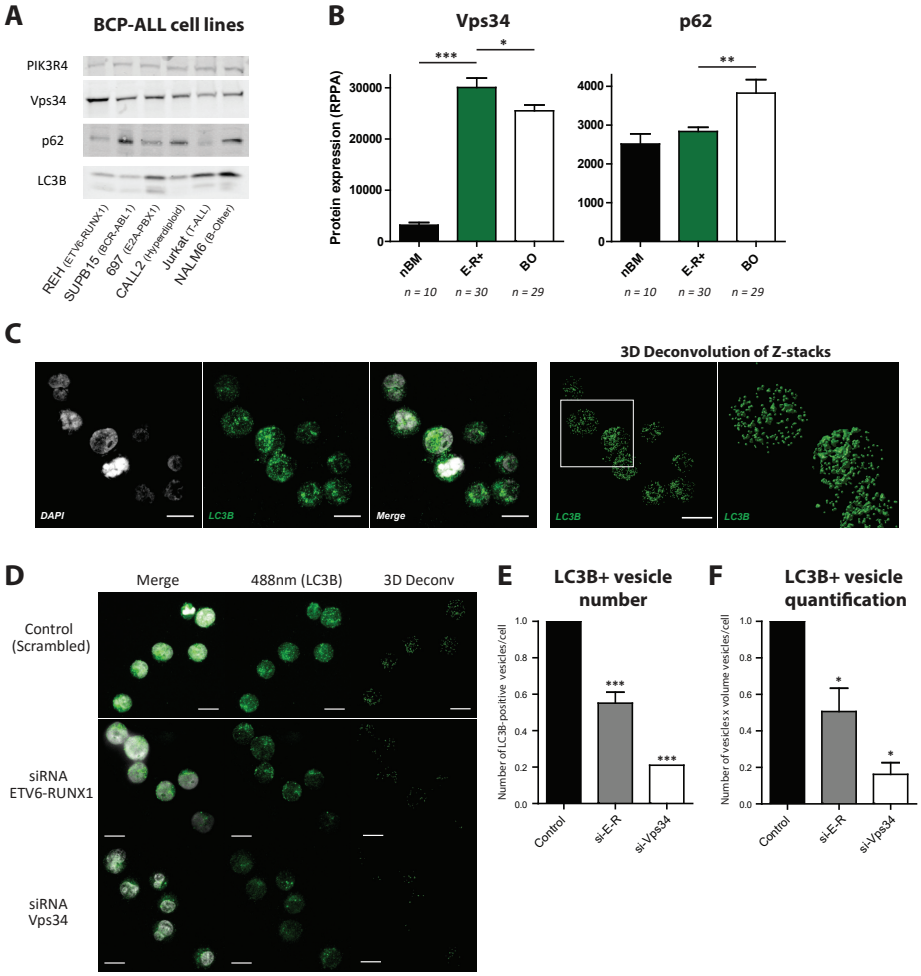

Figure 4. Autophagy levels are high in ETV6-RUNX1 positive BCP-ALL and regulated by ETV6-RUNX1 and Vps34.

(A) Western blot analysis was performed to determine the expression levels Vps34, p62 (sequestosome 1), and LC3B in ALL cell lines. PIK3R4 was used as a loading control.

Figure 4. Autophagy levels are high in ETV6-RUNX1 positive BCP-ALL and regulated by ETV6-RUNX1 and Vps34. (continued)
(B) Quantification of protein levels of Vps34 and p62 measured by reverse phase protein array (RPPA) in 10 normal bone marrow samples (nBM), 30 ETV6-RUNX1 positive primary BCP-ALL patient samples (ETV6-RUNX1+), and 29 B-Other primary BCP-ALL patient samples (BO). Data are means ± S.E.M.; * $p \leq 0.05$, ** $p \leq 0.01$, *** $p \leq 0.001$. (C) Representative confocal images of REH cells after permeabilization and staining with DAPI and LC3B antibody. Z-stacks were deconvolved using Huygens Professional software, after which number and volume of LC3B-positive vesicles could be quantified. (D) Representative confocal images showing LC3B-positive vesicles in ETV6-RUNX1 positive BCP-ALL cell line REH. Left panels show an overlay of LC3B expression and DAPI staining (nuclear staining). Middle panels show only LC3B expression. Right panel shows 3D representations after deconvolution of the 488nm signal representing the LC3B expression. For the quantification of number and volume of LC3B-positive vesicles, we excluded cells with atypical nuclei. Upper panels represent control conditions after transfection with scrambled siRNAs. Lower 6 panels represent conditions after transfection with siRNAs against ETV6-RUNX1 or Vps34. (E) Quantification of the number of LC3B-positive vesicles after 3D deconvolution of images (n = 3, *** $p \leq 0.001$). (F) Quantification of the number of LC3B-positive vesicles multiplied by the volume of these vesicles after 3D deconvolution of images (n = 3, * $p \leq 0.05$).
See also supplementary Figure 4.

An siRNA approach was used to investigate whether ETV6-RUNX1 regulates autophagy. To quantify the level of autophagy, the number and volume of LC3B-positive vesicles were calculated per cell with a 3D object analyzer using Huygens Professional software (Figure 4C). Knockdown of ETV6-RUNX1 resulted in a 45% reduction in the number of LC3B-positive vesicles and 50% reduction in the volume of LC3B-positive vesicles per cell ($p \leq 0.001$ and $p \leq 0.05$, respectively; Figure 4D-F). In addition, knockdown of Vps34 reduced the number of LC3B-positive vesicles and the volume of LC3B-positive vesicles with 79% ($p \leq 0.001$) and 84% ($p \leq 0.05$), respectively (Figure 4D-4F). These results show that autophagy levels are high in ETV6-RUNX1 positive BCP-ALL cells. In addition, both ETV6-RUNX1 and Vps34 are essential for maintaining high levels of autophagy in ETV6-RUNX1-positive leukemic cells.

Vps34 is essential for the survival of ETV6-RUNX1 positive leukemic cells

To determine the functional role of Vps34 in ETV6-RUNX1 positive leukemic cells, lentiviral knockdown studies were performed in two ETV6-RUNX1 positive cell lines (REH and REHS1). For these studies, four independent short hairpin RNAs were used. Short hairpins shVps34#1 and shVps34#2 were directed against the main Vps34 transcript variants, whereas shVps34#3 and shVps34#4 were directed against the two full length transcript variants only (Figure 5A and supplementary Figure 5A). Vps34 knockdown of at least 80% was achieved with all four individual shRNAs (Figure 5B, C and supplementary Figure 5B). Knockdown of only the full-length Vps34 transcript variants with shVps34#3 and shVps34#4 significantly reduced proliferation of the ETV6-RUNX1-positive cell lines REH and REHS1 ($p \leq 0.01$, supplementary Figure 5C, D). Knockdown of all main Vps34 transcript variants with shVps34#1 and shVps34#2 resulted in a complete growth arrest of these ETV6-RUNX1 positive

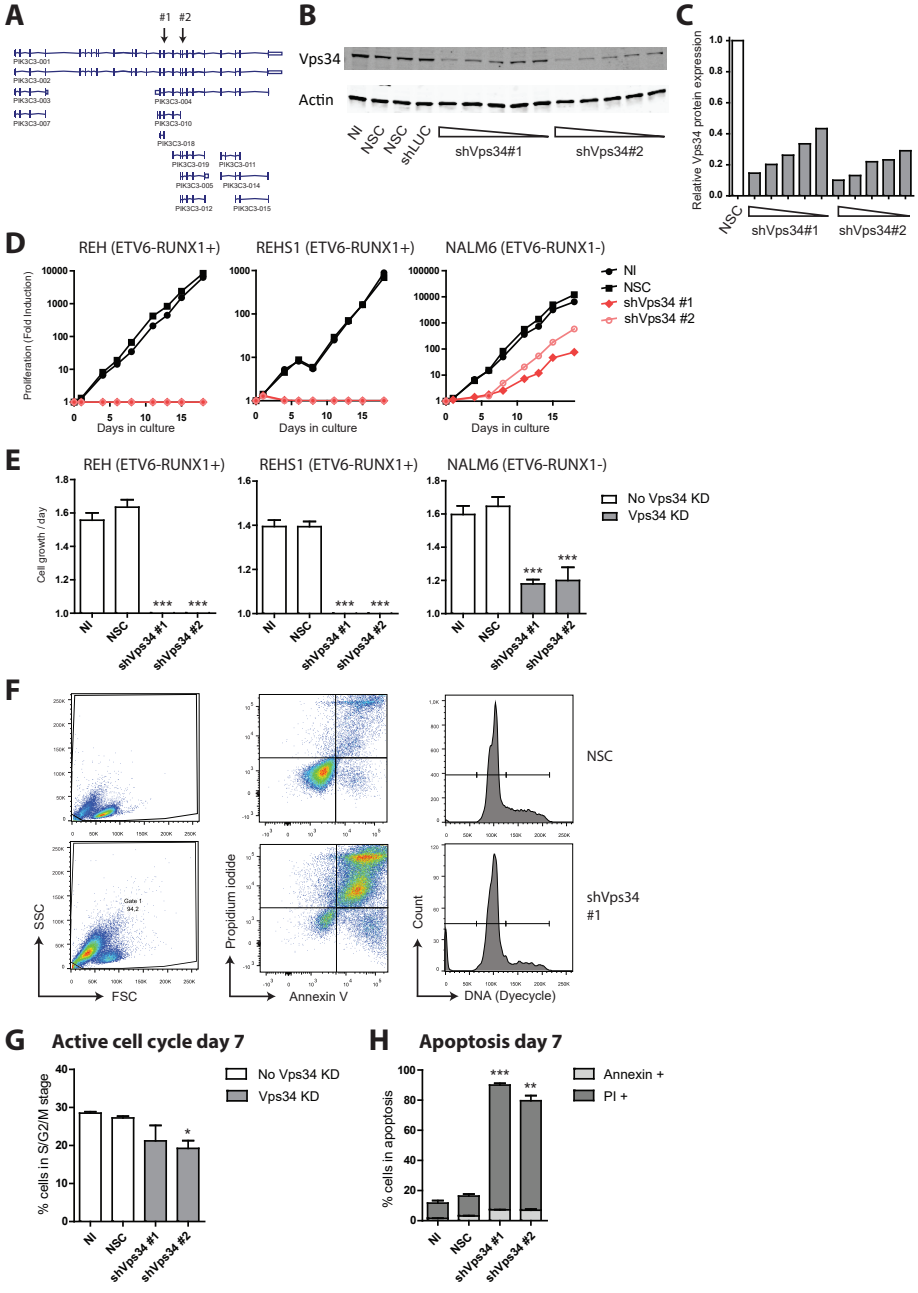

Figure 5. Vps34 is essential for the survival of ETV6-RUNX1 positive leukemic cells.
(A) Schematic representation of the known transcript variants of Vps34 (Ensembl Genome Browser; ENSG00000078142) and the shVps34#1 and shVps34#2 recognitions sites. (B) ETV6-RUNX1 positive (REH) BCP-ALL cells were lentivirally transduced with scrambled shRNA control, or two distinct shRNA constructs to silence Vps34 expression.

Figure 5. Vps34 is essential for the survival of ETV6-RUNX1 positive leukemic cells. (continued)
Western blot analysis was performed with an antibody against Vps34 or β-actin to visualize the knockdown of Vps34 in REH cells. A representative experiment is shown in which increasing concentrations of virus were used to emphasize the specificity of Vps34 knockdown. (C) Data were quantified and depicted as the relative Vps34 expression in comparison to the expression in cells transduced with scrambled (non-silencing) controls. (D-E) ETV6-RUNX1 positive (REH and REHS1) and ETV6-RUNX1 negative (NALM6) BCP-ALL cells were lentivirally transduced with scrambled shRNA control (NSC) or two distinct Vps34 shRNA constructs. NI represents non-infected cells. Cells were cultured for 18 days. To determine the effect on proliferation, cell counts were performed every 2-3 days. Representative graphs are shown in (D). The average increase in cell numbers per day is shown in (E). T-test was performed to compare control conditions (NSC) with Vps34 knockdown conditions (n = 3, ** $p \leq 0.01$, *** $p \leq 0.001$). Error bars represent S.E.M. (F-H) ETV6-RUNX1 positive (REH) BCP-ALL cells were lentivirally transduced with scrambled shRNA control (NSC) or two distinct shRNA constructs to silence Vps34 expression. After 7 days of culture, flow cytometrical analysis was performed to determine the effect of Vps34 knockdown on survival and cell cycle progression. Representative FACS plots are shown (n = 3). (G) The percentage of viable (AnnexinV positive, Propidium Iodide negative), actively cycling cells was determined using DyeCycle. Data were depicted as the percentage of cells in S, G2 M phase (n = 2, * $p \leq 0.05$). Error bars represent S.E.M. (H) The percentages of early apoptotic (AnnexinV positive, Propidium Iodide negative) and late apoptotic (Propidium Iodide positive) cells were determined 7 days after transduction (n = 2, ** $p \leq 0.01$, *** $p \leq 0.001$). Error bars represent S.E.M.
See also supplementary Figure 5.

cell lines ($p \leq 0.001$; Figure 5D, E). In contrast, knockdown of either all main Vps34 transcript variants or the full-length Vps34 transcripts in ETV6-RUNX1 negative NALM6 cells decreased proliferation to a lesser extent ($p \leq 0.001$; Figure 5D, E).

To investigate whether the observed growth arrest in ETV6-RUNX1 positive cells was due to a block in cell cycle progression or enhanced apoptosis, flow cytometric analysis was performed using DyeCycle and Annexin V. Cell cycle analysis revealed that knockdown of Vps34 modestly reduces the percentage of cycling ETV6-RUNX1 positive cells (Figure 5F, G and supplementary Figure 5E). In contrast, a remarkable reduction in survival was observed upon Vps34 knockdown. While shRNA mediated knockdown of the full length Vps34 transcript variants in ETV6-RUNX1 positive cells (shRNA#3 & shRNA#4) already resulted in 40-50% apoptotic cells (supplementary Figure 5F), targeting of all main Vps34 transcript variants resulted in even higher levels of apoptosis (80-90%, $p<0.01$; Figure 5F, H).

In conclusion, knockdown of Vps34 completely arrests cell growth of ETV6-RUNX1 positive cells by modestly reducing cell cycle progression and strongly inducing apoptosis. Although Vps34 knockdown also affects cell cycle progression and survival in ETV6-RUNX1 negative cells (data not shown), these cells were still able to proliferate.

ETV6-RUNX1 positive ALL cells are relatively sensitive to hydroxychloroquine

To date, no agents are clinically available that specifically inhibit Vps34 activity. However, the efficacy of autophagy inhibitors is currently examined in clinical cancer treatment trials. To investigate the effect of autophagy inhibition on ETV6-RUNX1 positive leukemia, we exposed leukemic cells to hydroxychloroquine (HCQ). This agent has favorable pharmacological properties and is safely used for decades in

the treatment of malaria and rheumatoid arthritis[42]. HCQ accumulates within and de-acidifies the lysosome, resulting in increased LC3B-II levels, which is indicative of impaired autophagy (Figure 6A). MTT assays were performed to determine the effect of HCQ on cell viability of ETV6-RUNX1 positive and ETV6-RUNX1 negative ALL cell lines (Figure 6B, C and supplementary Figure 6A, B). While treatment with 20 μg/ml HCQ resulted in 82% and 95% reduced cell viability of ETV6-RUNX1 positive

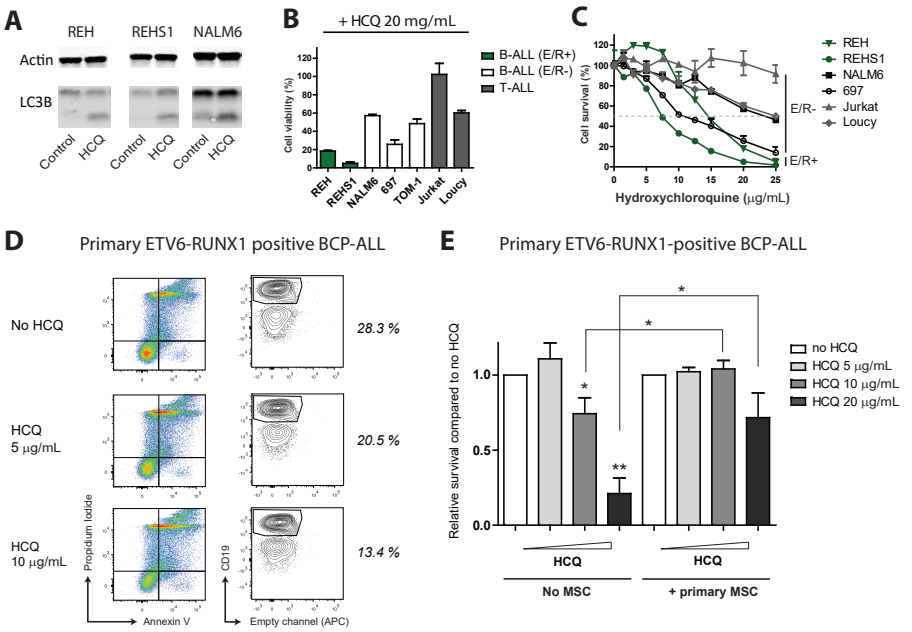

Figure 6. ETV6-RUNX1 positive ALL cells are relatively sensitive to treatment with hydroxychloroquine.

(A) ETV6-RUNX1 positive (REH and REHS1) and ETV6-RUNX1 negative (NALM6) BCP-ALL cells were cultured in absence or presence of HCQ (6.25 μg/ml) for 48 hours. Western blot analysis was performed using an antibody against LC3B to determine the effectivity of HCQ treatment. (B) ETV6-RUNX1 positive BCP-ALL, ETV6-RUNX1 negative BCP-ALL, and T-ALL cell lines were cultured in absence or presence of HCQ (20 μg/ml) for 4 days. An MTT assay was performed to determine the effect of HCQ treatment on the viability of the cells. Data were depicted as the percentage of viable cells compared to untreated control. Error bars represent S.E.M. (n=3). (C) ETV6-RUNX1 positive BCP-ALL, ETV6-RUNX1 negative BCP-ALL, and T-ALL cell lines were cultured in absence or presence of increasing concentrations of HCQ for 4 days. An MTT assay was performed to determine the effect of HCQ treatment on the viability of the cells. A representative experiment is shown in which data were depicted as the percentage of viable cells. (D) Primary ETV6-RUNX1 positive BCP-ALL cells were cultured in absence or presence of 5 or 10 μg/ml HCQ for 5 days. Flow cytometric analysis was performed to determine the percentage of non-apoptotic (Annexin V negative, Propidium Iodide negative, CD19 positive) cells. Representative FACS plots are shown (n = 5). (E) Co-culture experiments were performed with primary ETV6-RUNX1 positive BCP-ALL cells and mesenchymal stromal cells (MSCs). Cells were cultured in absence or presence of increasing concentrations of HCQ for 5 days. Flow cytometrical analysis was performed to determine the percentage of non-apoptotic (Annexin V negative, Propidium Iodide negative, CD19 positive) cells. Data were depicted as the relative reduction in survival compared to untreated cells (n = 6 for HCQ 5 μg/ml and HCQ 10 μg/ml; n = 4 for HCQ 20 μg/ml). Error bars represent S.E.M. * $p \leq 0.05$, ** $p \leq 0.01$.

See also supplementary Figure 6.

BCP-ALL cell lines (REH and REHS1), the viability of ETV6-RUNX1 negative cell lines was reduced to a lesser extent (NALM6: 43%, TOM1: 50%, Loucy: 40%, Jurkat: 0%; Figure 6B). The IC_{50} of HCQ was significantly lower in ETV6-RUNX1 positive ALL cell lines compared to ETV6-RUNX1 negative cell lines ($p \leq 0.001$; Figure 6C and supplementary Figure 6B). In addition, the effect of HCQ on the survival of primary BCP-ALL cells was determined. Primary BCP-ALL cells were cultured for 5 days upon which flow cytometric analysis was performed (for flow cytometric gating strategy see supplementary Figure 6C). Survival of primary ETV6-RUNX1 positive BCP-ALL cells was significantly reduced after treatment with 10 μg/ml HCQ (26%, $p \leq 0.05$; Figure 6D, E). In contrast, this treatment did not affect cell viability of primary ETV6-RUNX1 negative BCP-ALL cells (supplementary Figure 6D). The survival of primary ETV6-RUNX1 positive ALL cells was even further reduced after treatment with 20 μg/ml HCQ (79%, $p \leq 0.01$; Figure 6E). Co-culture of these ALL cells in the presence of primary bone marrow-derived mesenchymal stromal cells (MSCs) significantly rescued the HCQ-mediated induction of apoptosis in primary ETV6-RUNX1 positive ALL cells ($p \leq 0.05$; Figure 6E). These results demonstrate that although ETV6-RUNX1 positive BCP-ALL cells are relatively sensitive to HCQ treatment, this sensitivity is abrogated by primary MSCs.

Autophagy inhibition sensitizes ETV6-RUNX1 positive ALL cells to L-Asparaginase

As our results indicate that inhibition of autophagy reduces survival of ETV6-RUNX1 positive ALL cells, we investigated whether HCQ-mediated inhibition of autophagy could sensitize primary BCP-ALL cells to commonly used chemotherapeutics. To investigate the potential of HCQ treatment in sensitization to chemotherapeutics, the percentage of apoptotic cells was determined by flow cytometry after 5-days of culture either in absence or presence of IC_{50} values of the chemotherapeutic drug. Our results indicate that HCQ treatment (in clinically relevant concentrations[52,53]) selectively sensitizes ETV6-RUNX1 positive leukemic cells to L-Asparaginase treatment (Figure 7A, B and supplementary Figure 7A). Treatment of primary ETV6-RUNX1 positive ALL patient cells with 5 μg/mL or 10 μg/mL HCQ resulted in a 48% and 71% reduction in cell survival during L-Asparaginase exposure, respectively ($n = 5$, $p \leq 0.01$ and $p \leq 0.001$; Figure 7B), while ETV6-RUNX1 negative BCP-ALL cells were not sensitized to L-Asparaginase ($n = 3$; Figure 7B, supplementary Figure 7D). Co-culture of primary BCP-ALL cells with primary MSCs significantly reversed the HCQ-mediated sensitization to L-Asparaginase ($p \leq 0.01$, Figure 7C). To investigate whether these primary cells could still be sensitized, similar experiments were performed with a higher dose of HCQ (20 μg/mL). Inhibition of autophagy with 20 μg/mL HCQ was indeed sufficient to significantly sensitize primary ETV6-RUNX1 positive BCP-ALL

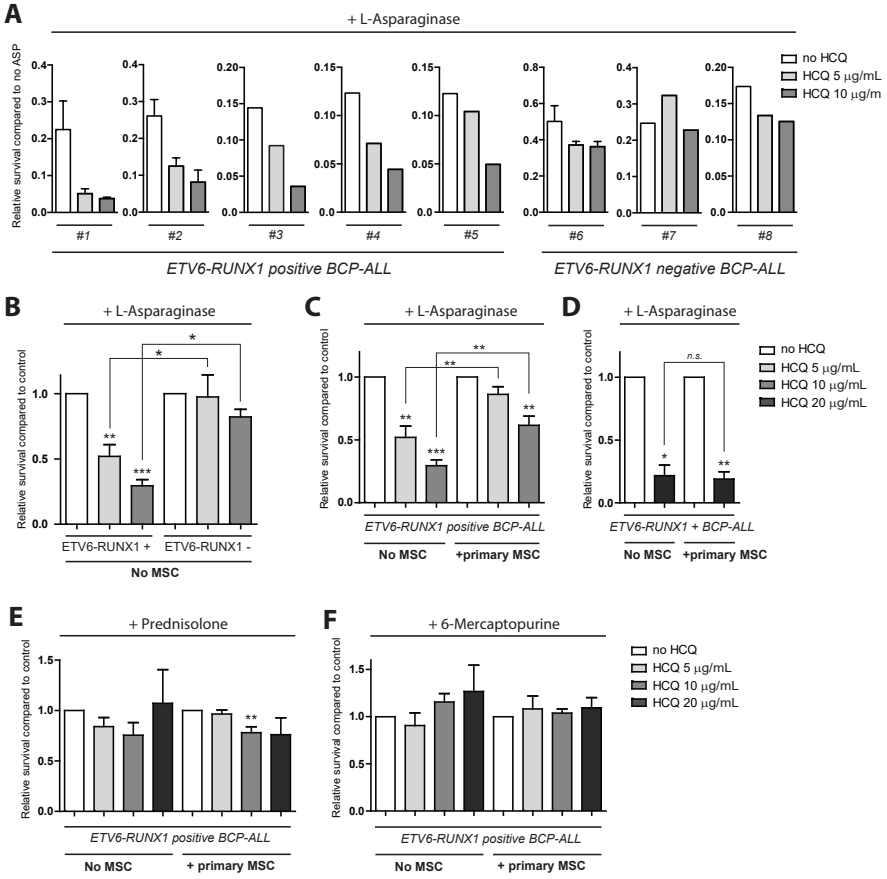

Figure 7. Autophagy inhibition sensitizes ETV6-RUNX1 positive ALL cells to L-Asparaginase.
(A) Primary ETV6-RUNX1 positive BCP-ALL cells were cultured in absence or presence of IC-50 concentrations of L-Asparaginase and increasing concentrations of HCQ. Flow cytometric analysis was performed to determine the percentage of non-apoptotic (Annexin V negative, Propidium Iodide negative, CD19 positive) cells (for gating strategy see supplementary Fig. 6C). The survival of primary leukemic blasts in presence of L-Asparaginase was compared to their survival in absence of L-Asparaginase. White bars represent the relative survival in absence of HCQ. Grey bars represent the relative survival in presence of HCQ (5 μg/ml HCQ (light grey) and 10 μg/ml HCQ (grey)). (B) Averages of data presented in (a), representing sensitization of primary leukemic blasts by HCQ to L-Asparaginase (n = 5 for ETV6-RUNX1 positive; n = 3 for ETV6-RUNX1 negative primary patient cells, * $p \leq 0.05$, ** $p \leq 0.01$). Error bars represent S.E.M. (C-D) Co-culture experiments were performed with primary ETV6-RUNX1 positive BCP-ALL cells and MSCs. Cells were cultured in presence or absence of L-Asparaginase and increasing concentrations of HCQ. Flow cytometric analysis was performed to determine the percentage of non-apoptotic (Annexin V negative, Propidium Iodide negative, CD19 positive) cells. First, the survival of primary leukemic blasts in presence of L-Asparaginase was compared to their survival in absence of L-Asparaginase. Next, data was depicted as fold reduction compared to HCQ-untreated controls (n = 5 for conditions in absence of MSCs, n = 7 for conditions in presence of MSCs for (C), n = 3 for conditions in absence of MSCs, n = 4 for conditions in presence of MSCs for (D)). Error bars represent S.E.M.

Figure 7. Autophagy inhibition sensitizes ETV6-RUNX1 positive ALL cells to L-Asparaginase. (continue)

(E-F) Co-culture experiments were performed with primary ETV6-RUNX1 positive BCP-ALL cells and MSCs. Cells were cultured in presence or absence of Prednisolone (E) or 6-Mercaptopurine (F) and increasing concentrations of HCQ. Flow cytometric analysis was performed to determine the percentage of non-apoptotic (Annexin V negative, Propidium Iodide negative, CD19 positive) cells. The survival of primary leukemic blasts in presence of Prednisolone (E) of 6-Mercaptopurine (F) was compared to their survival in absence of these drugs. Next, data was depicted as fold reduction compared to HCQ-untreated controls (n = 5 for conditions in absence of MSCs, n = 7 for conditions in presence of MSCs for (E), n = 4 for conditions in absence of MSCs, n = 4 for conditions in presence of MSCs for (F)). Error bars represent S.E.M.

cells to L-Asparaginase both in absence or presence of primary MSCs (80% reduced survival, $p \leq 0.05$ and $p \leq 0.01$ respectively; Figure 7D and supplementary Figure 7B, C). In contrast to L-Asparaginase, HCQ did not significantly induce apoptosis of primary BCP-ALL cells upon treatment with prednisolone or 6-mercaptopurine (Figure 7E, F).

These data show that HCQ-mediated inhibition of autophagy results in sensitization of ETV6-RUNX1 positive BCP-ALL cells, but not ETV6-RUNX1 negative BCP-ALL cells, to L-Asparaginase.

DISCUSSION

In this study, we show that the ETV6-RUNX1 fusion gene induces a transcriptional network regulating pre-leukemic features in hematopoietic progenitors. We show that this network facilitates the induction of autophagy by up-regulating Vps34 expression in ETV6-RUNX1 positive BCP-ALL (Figure 8). Additionally, our data show for the first time that inhibition of autophagy is a promising strategy for sensitization of ETV6-RUNX1 positive BCP-ALL cells to the important anti-leukemic agent L-Asparaginase.

The importance of the ETV6-RUNX1 fusion protein for modulation of proliferation, survival and cell cycle distribution has already been shown in cell lines[27,29,41] and mouse models[19,54]. Similarly, expression of the ETV6-RUNX1 fusion gene induces survival properties in human cord blood-derived progenitors transplanted in NOD/SCID mice or co-cultured in presence of murine MS-5 stromal cells[20,34,55]. However, to date, the downstream effectors of this pro-survival and pro-proliferative phenotype have not been elucidated. In this study, we uncovered the transcriptional network regulating these phenotypes in a human progenitor population by analyzing the gene expression profile after ectopic expression of ETV6-RUNX1. This approach allowed us to examine early effects of ETV6-RUNX1 expression in human hematopoietic progenitors. These data therefore provide a comprehensive and functional list of ETV6-RUNX1 target genes (supplementary

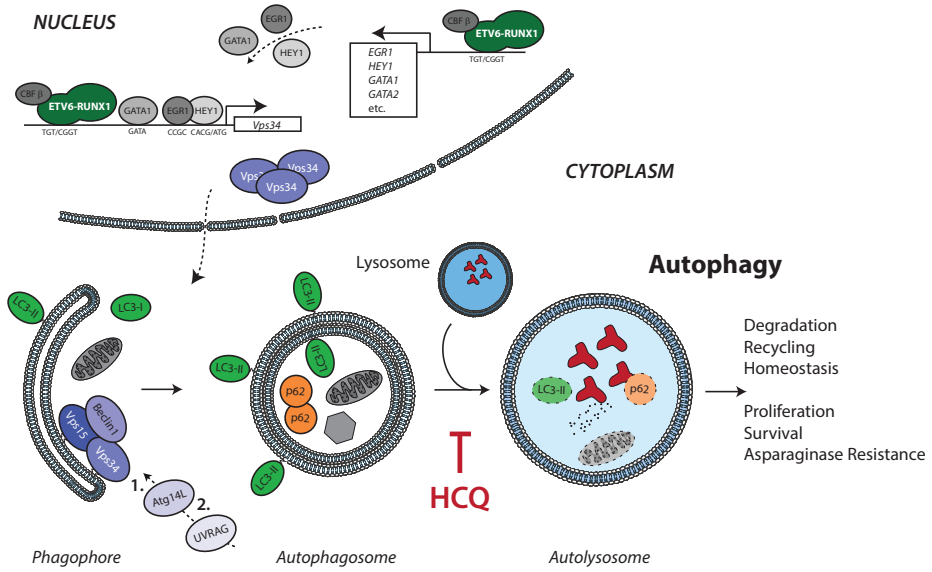

Figure 8. Proposed model for the induction of the Vps34-autophagy pathway in ETV6-RUNX1 positive BCP-ALL cells.

The ETV6-RUNX1 fusion protein can transcriptionally induce the expression of various transcription factors, including *GATA1*, *GATA2*, *HEY1*, and *EGR1*. ETV6-RUNX1 and its co-factor CBFβ, together with *GATA1*, *HEY1* and *EGR1* can activate the Vps34 promoter, resulting in enhanced Vps34 expression in ETV6-RUNX1 positive leukemic cells. Vps34, in turn, can initiate autophagy by forming a core autophagy-regulating complex with Beclin 1 and Vps15. This complex plays an important role in (1) the early initiation (in complex with Atg14L) and (2) the vesicle elongation phase (together with UVRAG) of autophagosome formation. Induction of autophagy allows ETV6-RUNX1 positive cells to maintain homeostasis by degrading and recycling damaged proteins and organelles. In addition, activation of the autophagy program in ETV6-RUNX1 positive cells results in enhanced proliferation, survival and drug resistance. Inhibition of autophagy in ETV6-RUNX1 positive cells, by treatment with hydroxychloroquine (HCQ) or knockdown of Vps34, is sufficient to reduce proliferation and survival of leukemic blasts and to induce sensitization to L-Asparaginase.

Table 2). In addition to a pro-survival and pro-proliferative phenotype, genes involved in cytoskeleton rearrangements and cellular homeostasis were found to be regulated by the ETV6-RUNX1 fusion protein (Figure 1). Furthermore, our results reveal that autophagy is induced in ETV6-RUNX1 positive cells because of transcriptional activation of *Vps34*, a member of the core (macro)autophagy-regulating complex[51] (Figure 2 – 4).

Autophagy is a cellular recycling system in which unwanted or damaged cellular components are degraded and recycled. All mammalian cells harbor low basal levels of autophagy that are used to maintain cellular homeostasis. These levels can be rapidly induced upon cellular stress. Autophagy is regulated by components of the core autophagy-regulating complex, including Vps34, Beclin-1, and Vps15 (reviewed in e.g.[51]). Although autophagy can sustain cell survival during stress conditions, it can also result in cell death because of progressive cellular consumption

(reviewed in e.g. [56,57]). Whether autophagy plays an initiating or suppressive role in cancer is still under debate and is most likely dependent on the oncogenic context (reviewed in e.g. [58-62]). This potential dual role of autophagy in cancer highlights the importance of studies on the context-specific role and the functional importance of autophagy in neoplastic processes before the start of autophagy-based therapeutic interventions. In the present study, we show that the oncogenic ETV6-RUNX1 fusion gene can directly up-regulate the level of autophagy in leukemic cells in absence of cellular stress. Our results demonstrate that these enhanced levels of autophagy are important to maintain proliferation and survival of ETV6-RUNX1 positive leukemic cells (Figure 5 - 7). Knockdown of Vps34 and inhibition of autophagy with HCQ reduced the proliferation and survival of ETV6-RUNX1 positive BCP-ALL cells, confirming the importance of induced autophagy in these cells (Figure 5, 6). Importantly, ETV6-RUNX1 negative primary BCP-ALL cells were not affected by autophagy inhibition.

Autophagy might play an important role in protecting leukemic cells during chemotherapeutic treatment with nutrient-modulating drugs like L-Asparaginase that actively inhibits protein biosynthesis by asparagine depletion, which leads to nutritional deprivation and effective killing of leukemic cells[63-65]. Here, we show that autophagy selectively protects ETV6-RUNX1 positive leukemic cells against L-Asparaginase treatment, whereas this effect is absent in ETV6-RUNX1 negative leukemic cells (Figure 7). HCQ-mediated inhibition of autophagy did not sensitize cells to prednisolone or 6-mercaptopurine, two other often used chemotherapeutics in treatment of BCP-ALL. These results highlight the importance of the cellular and molecular context in which autophagy inhibition is embedded and show that caution is warranted before the general introduction of autophagy inhibitors in the treatment of leukemia.

The leukemic microenvironment or niche has been shown to protect leukemic cells from elimination by immune responses and chemotherapeutic agents[66,67], and facilitates the development of drug resistance to classic and targeted chemotherapy[68]. Here, we show that MSCs can abrogate the effects of autophagy inhibition in ETV6-RUNX1 positive BCP-ALL cells. This highlights that the leukemic niche plays a crucial role in induction of resistance to chemotherapy, including autophagy inhibition. However, MSC-induced resistance of ETV6-RUNX1 positive cells could still be overcome when adequate concentrations of the autophagy inhibitor HCQ were used (Figure 7).

The efficacy of autophagy inhibitors during cancer treatment is currently examined in clinical trials (reviewed in e.g. [61,69]). Initial results indicate that HCQ treatment is safe and tolerated at high concentrations and might be effective in a subset of patients (e.g. [70-72]). In addition, autophagy-independent "off-target"

effects of chloroquines, resulting in enhanced response to chemotherapy have been reported[73,74]. This strengthens the point to use HCQ in clinical practice. However, more specific and potent autophagy inhibitors are currently developed and preclinical studies with these novel inhibitors (e.g. Lys05) show promising results[75]. In addition, the recent determination of the crystal structure of Vps34[50] enables the development of clinically available Vps34 inhibitors in the near future[76-78]. Our observation that the ETV6-RUNX1 fusion protein induces Vps34 expression and subsequently autophagy, strongly indicates that Vps34/autophagy inhibitors should be considered in future protocols of ETV6-RUNX1 positive BCP-ALL.

Acknowledgements
we thank all members of the research laboratory Pediatric Oncology of the Erasmus MC for their help in processing leukemic and mesenchymal stromal cell samples, in particular R.E.S van den Dungen. E. Bindels and B. de Rooij for scientific input and critical discussions; The Erasmus Optical Imaging Centre for providing support of CLSM; The Department of Hematology of the Erasmus MC for providing the use of CLSM and Flow Cytometers; The Vlietland Ziekenhuis for collecting and providing cord blood. The work described in this paper was funded by the KiKa Foundation (Stichting Kinderen Kankervrij – Kika-39), the Dutch Cancer Society (UVA 2008; 4265, EMCR 2010; 4687), the Netherlands Organization for Scientific Research (NWO – VICI M.L. den Boer) and the Pediatric Oncology Foundation Rotterdam.

Author contributions
RPo designed the study, performed the experiments, collected and analyzed all data, and wrote the paper. MLDB, MB, and MBB designed the study, analyzed data, and wrote the paper. CSL performed experiments and analyzed data. MAS and JRMM analyzed gene expression data. JMB normalized and curated gene expression data. OR provided support of CSLM. JJC and RPi discussed data and wrote the paper. All authors discussed the results and approved the submitted manuscript.

Conflict of interest disclosure
none of the authors have a competing financial interest.

REFERENCES

1. Pui, C.H. & Evans, W.E. Drug therapy - Treatment of acute lymphoblastic leukemia. *New England Journal of Medicine* **354**, 166-178 (2006).
2. Pui, C.H., Carroll, W.L., Meshinchi, S. & Arceci, R.J. Biology, risk stratification, and therapy of pediatric acute leukemias: an update. *J Clin Oncol* **29**, 551-565 (2011).
3. Nguyen, K., *et al.* Factors influencing survival after relapse from acute lymphoblastic leukemia: a Children's Oncology Group study. *Leukemia* **22**, 2142-2150 (2008).
4. Robison, L.L. Late effects of acute lymphoblastic leukemia therapy in patients diagnosed at 0-20 years of age. *Hematology Am Soc Hematol Educ Program* **2011**, 238-242 (2011).
5. Oeffinger, K.C., Nathan, P.C. & Kremer, L.C. Challenges after curative treatment for childhood cancer and long-term follow up of survivors. *Hematol Oncol Clin North Am* **24**, 129-149 (2010).
6. Goldman, J.M. & Melo, J.V. Chronic myeloid leukemia--advances in biology and new approaches to treatment. *N Engl J Med* **349**, 1451-1464 (2003).
7. Bhojwani, D. & Pui, C.H. Relapsed childhood acute lymphoblastic leukaemia. *Lancet Oncol* **14**, e205-217 (2013).
8. Romana, S.P., *et al.* The t(12;21) of acute lymphoblastic leukemia results in a tel-AML1 gene fusion. *Blood* **85**, 3662-3670 (1995).
9. Shurtleff, S.A., *et al.* TEL/AML1 fusion resulting from a cryptic t(12;21) is the most common genetic lesion in pediatric ALL and defines a subgroup of patients with an excellent prognosis. *Leukemia* **9**, 1985-1989 (1995).
10. Golub, T.R., *et al.* Fusion of the TEL gene on 12p13 to the AML1 gene on 21q22 in acute lymphoblastic leukemia. *Proc Natl Acad Sci U S A* **92**, 4917-4921 (1995).
11. Zelent, A., Greaves, M. & Enver, T. Role of the TEL-AML1 fusion gene in the molecular pathogenesis of childhood acute lymphoblastic leukaemia. *Oncogene* **23**, 4275-4283 (2004).
12. McLean, T.W., *et al.* TEL/AML-1 dimerizes and is associated with a favorable outcome in childhood acute lymphoblastic leukemia. *Blood* **88**, 4252-4258 (1996).
13. Loh, M.L., *et al.* Prospective analysis of TEL/AML1-positive patients treated on Dana-Farber Cancer Institute Consortium Protocol 95-01. *Blood* **107**, 4508-4513 (2006).
14. Seeger, K., *et al.* TEL-AML1 fusion in relapsed childhood acute lymphoblastic leukemia. *Blood* **94**, 374-376 (1999).
15. Ford, A.M., *et al.* Origins of "late" relapse in childhood acute lymphoblastic leukemia with TEL-AML1 fusion genes. *Blood* **98**, 558-564 (2001).
16. Kuster, L., *et al.* ETV6/RUNX1-positive relapses evolve from an ancestral clone and frequently acquire deletions of genes implicated in glucocorticoid signaling. *Blood* **117**, 2658-2667 (2011).
17. van Delft, F.W., *et al.* Clonal origins of relapse in ETV6-RUNX1 acute lymphoblastic leukemia. *Blood* **117**, 6247-6254 (2011).
18. Stams, W.A., *et al.* Incidence of additional genetic changes in the TEL and AML1 genes in DCOG and COALL-treated t(12;21)-positive pediatric ALL, and their relation with drug sensitivity and clinical outcome. *Leukemia* **20**, 410-416 (2006).
19. Tsuzuki, S., Seto, M., Greaves, M. & Enver, T. Modeling first-hit functions of the t(12;21) TEL-AML1 translocation in mice. *Proc Natl Acad Sci U S A* **101**, 8443-8448 (2004).
20. Hong, D., *et al.* Initiating and cancer-propagating cells in TEL-AML1-associated childhood leukemia. *Science* **319**, 336-339 (2008).

21. Schindler, J.W., *et al.* TEL-AML1 corrupts hematopoietic stem cells to persist in the bone marrow and initiate leukemia. *Cell Stem Cell* **5**, 43-53 (2009).
22. van der Weyden, L., *et al.* Modeling the evolution of ETV6-RUNX1-induced B-cell precursor acute lymphoblastic leukemia in mice. *Blood* **118**, 1041-1051 (2011).
23. Castor, A., *et al.* Distinct patterns of hematopoietic stem cell involvement in acute lymphoblastic leukemia. *Nat Med* **11**, 630-637 (2005).
24. Anderson, K., *et al.* Genetic variegation of clonal architecture and propagating cells in leukaemia. *Nature* **469**, 356-361 (2011).
25. Mullighan, C.G., *et al.* Genome-wide analysis of genetic alterations in acute lymphoblastic leukaemia. *Nature* **446**, 758-764 (2007).
26. Diakos, C., *et al.* RNAi-mediated silencing of TEL/AML1 reveals a heat-shock protein- and survivin-dependent mechanism for survival. *Blood* **109**, 2607-2610 (2007).
27. Fuka, G., *et al.* Silencing of ETV6/RUNX1 abrogates PI3K/AKT/mTOR signaling and impairs reconstitution of leukemia in xenografts. *Leukemia* **26**, 927-933 (2012).
28. Mangolini, M., *et al.* STAT3 mediates oncogenic addiction to TEL-AML1 in t(12;21) acute lymphoblastic leukemia. *Blood* **122**, 542-549 (2013).
29. Torrano, V., Procter, J., Cardus, P., Greaves, M. & Ford, A.M. ETV6-RUNX1 promotes survival of early B lineage progenitor cells via a dysregulated erythropoietin receptor. *Blood* **118**, 4910-4918 (2011).
30. Diakos, C., *et al.* TEL-AML1 regulation of survivin and apoptosis via miRNA-494 and miRNA-320a. *Blood* **116**, 4885-4893 (2010).
31. Roudaia, L., *et al.* CBFbeta is critical for AML1-ETO and TEL-AML1 activity. *Blood* **113**, 3070-3079 (2009).
32. Gefen, N., *et al.* Hsa-mir-125b-2 is highly expressed in childhood ETV6/RUNX1 (TEL/AML1) leukemias and confers survival advantage to growth inhibitory signals independent of p53. *Leukemia* **24**, 89-96 (2010).
33. Palmi, C., *et al.* Cytoskeletal Regulatory Gene Expression and Migratory Properties of B Cell Progenitors are Affected by the ETV6-RUNX1 Rearrangement. *Mol Cancer Res* (2014).
34. Ford, A.M., *et al.* The TEL-AML1 leukemia fusion gene dysregulates the TGF-beta pathway in early B lineage progenitor cells. *J Clin Invest* **119**, 826-836 (2009).
35. Inthal, A., *et al.* Role of the erythropoietin receptor in ETV6/RUNX1-positive acute lymphoblastic leukemia. *Clin Cancer Res* **14**, 7196-7204 (2008).
36. Yeoh, E.J., *et al.* Classification, subtype discovery, and prediction of outcome in pediatric acute lymphoblastic leukemia by gene expression profiling. *Cancer Cell* **1**, 133-143 (2002).
37. Den Boer, M.L., *et al.* A subtype of childhood acute lymphoblastic leukaemia with poor treatment outcome: a genome-wide classification study. *Lancet Oncol* **10**, 125-134 (2009).
38. Gandemer, V., *et al.* Five distinct biological processes and 14 differentially expressed genes characterize TEL/AML1-positive leukemia. *BMC Genomics* **8**, 385 (2007).
39. Andersson, A., *et al.* Molecular signatures in childhood acute leukemia and their correlations to expression patterns in normal hematopoietic subpopulations. *Proc Natl Acad Sci U S A* **102**, 19069-19074 (2005).
40. Fine, B.M., *et al.* Gene expression patterns associated with recurrent chromosomal translocations in acute lymphoblastic leukemia. *Blood* **103**, 1043-1049 (2004).
41. Fuka, G., Kauer, M., Kofler, R., Haas, O.A. & Panzer-Grumayer, R. The leukemia-specific fusion gene ETV6/RUNX1 perturbs distinct key biological functions primarily by gene repression. *PLoS One* **6**, e26348 (2011).

42. van der Veer, A., *et al.* Independent prognostic value of BCR-ABL1-like signature and IKZF1 deletion, but not high CRLF2 expression, in children with B-cell precursor ALL. *Blood* **122**, 2622-2629 (2013).
43. Min, I.M., *et al.* The transcription factor EGR1 controls both the proliferation and localization of hematopoietic stem cells. *Cell Stem Cell* **2**, 380-391 (2008).
44. Laurenti, E., *et al.* The transcriptional architecture of early human hematopoiesis identifies multilevel control of lymphoid commitment. *Nat Immunol* **14**, 756-763 (2013).
45. Vicente, C., Conchillo, A., Garcia-Sanchez, M.A. & Odero, M.D. The role of the GATA2 transcription factor in normal and malignant hematopoiesis. *Crit Rev Oncol Hematol* **82**, 1-17 (2012).
46. Gupta, P., *et al.* PU.1: An ETS family transcription factor that regulates leukemogenesis besides normal hematopoiesis. *Stem Cells Dev* **15**, 609-617 (2006).
47. Crispino, J.D. GATA1 in normal and malignant hematopoiesis. *Semin Cell Dev Biol* **16**, 137-147 (2005).
48. Jaber, N., *et al.* Class III PI3K Vps34 plays an essential role in autophagy and in heart and liver function. *Proc Natl Acad Sci U S A* **109**, 2003-2008 (2012).
49. Kihara, A., Noda, T., Ishihara, N. & Ohsumi, Y. Two distinct Vps34 phosphatidylinositol 3-kinase complexes function in autophagy and carboxypeptidase Y sorting in Saccharomyces cerevisiae. *J Cell Biol* **152**, 519-530 (2001).
50. Miller, S., *et al.* Shaping development of autophagy inhibitors with the structure of the lipid kinase Vps34. *Science* **327**, 1638-1642 (2010).
51. Funderburk, S.F., Wang, Q.J. & Yue, Z. The Beclin 1-VPS34 complex--at the crossroads of autophagy and beyond. *Trends Cell Biol* **20**, 355-362 (2010).
52. Munster, T., *et al.* Hydroxychloroquine concentration-response relationships in patients with rheumatoid arthritis. *Arthritis Rheum* **46**, 1460-1469 (2002).
53. Rangwala, R., *et al.* Phase I trial of hydroxychloroquine with dose-intense temozolomide in patients with advanced solid tumors and melanoma. *Autophagy* **10**, 1369-1379 (2014).
54. Bernardin, F., *et al.* TEL-AML1, expressed from t(12;21) in human acute lymphocytic leukemia, induces acute leukemia in mice. *Cancer Res* **62**, 3904-3908 (2002).
55. Fan, D., *et al.* Stem cell programs are retained in human leukemic lymphoblasts. *Oncogene* (2014).
56. Levine, B. & Klionsky, D.J. Development by self-digestion: molecular mechanisms and biological functions of autophagy. *Dev Cell* **6**, 463-477 (2004).
57. Mizushima, N. & Komatsu, M. Autophagy: renovation of cells and tissues. *Cell* **147**, 728-741 (2011).
58. Guo, J.Y., Xia, B. & White, E. Autophagy-mediated tumor promotion. *Cell* **155**, 1216-1219 (2013).
59. Mathew, R., Karantza-Wadsworth, V. & White, E. Role of autophagy in cancer. *Nat Rev Cancer* **7**, 961-967 (2007).
60. Levine, B. & Kroemer, G. Autophagy in the pathogenesis of disease. *Cell* **132**, 27-42 (2008).
61. White, E. Deconvoluting the context-dependent role for autophagy in cancer. *Nat Rev Cancer* **12**, 401-410 (2012).
62. Gump, J.M., *et al.* Autophagy variation within a cell population determines cell fate through selective degradation of Fap-1. *Nat Cell Biol* **16**, 47-54 (2014).
63. Avramis, V.I. Asparaginases: biochemical pharmacology and modes of drug resistance. *Anticancer Res* **32**, 2423-2437 (2012).

64. Willems, L., *et al.* Inhibiting glutamine uptake represents an attractive new strategy for treating acute myeloid leukemia. *Blood* **122**, 3521-3532 (2013).
65. Pieters, R., *et al.* L-asparaginase treatment in acute lymphoblastic leukemia: a focus on Erwinia asparaginase. *Cancer* **117**, 238-249 (2011).
66. Fujisaki, J., *et al.* In vivo imaging of Treg cells providing immune privilege to the haematopoietic stem-cell niche. *Nature* **474**, 216-219 (2011).
67. Arai, F., *et al.* Tie2/angiopoietin-1 signaling regulates hematopoietic stem cell quiescence in the bone marrow niche. *Cell* **118**, 149-161 (2004).
68. McMillin, D.W., Negri, J.M. & Mitsiades, C.S. The role of tumour-stromal interactions in modifying drug response: challenges and opportunities. *Nat Rev Drug Discov* **12**, 217-228 (2013).
69. Amaravadi, R.K., *et al.* Principles and current strategies for targeting autophagy for cancer treatment. *Clin Cancer Res* **17**, 654-666 (2011).
70. Rosenfeld, M.R., *et al.* A phase I/II trial of hydroxychloroquine in conjunction with radiation therapy and concurrent and adjuvant temozolomide in patients with newly diagnosed glioblastoma multiforme. *Autophagy* **10**, 1359-1368 (2014).
71. Rangwala, R., *et al.* Combined MTOR and autophagy inhibition: Phase I trial of hydroxychloroquine and temsirolimus in patients with advanced solid tumors and melanoma. *Autophagy* **10**, 1391-1402 (2014).
72. Vogl, D.T., *et al.* Combined autophagy and proteasome inhibition: A phase 1 trial of hydroxychloroquine and bortezomib in patients with relapsed/refractory myeloma. *Autophagy* **10**, 1380-1390 (2014).
73. Maes, H., *et al.* Tumor Vessel Normalization by Chloroquine Independent of Autophagy. *Cancer Cell* **26**, 190-206 (2014).
74. Eng, C.H., *et al.* Macroautophagy is dispensable for growth of KRAS mutant tumors and chloroquine efficacy. *Proc Natl Acad Sci U S A* **113**, 182-187 (2016).
75. McAfee, Q., *et al.* Autophagy inhibitor Lys05 has single-agent antitumor activity and reproduces the phenotype of a genetic autophagy deficiency. *Proc Natl Acad Sci U S A* **109**, 8253-8258 (2012).
76. Bago, R., *et al.* Characterization of VPS34-IN1, a selective inhibitor of Vps34, reveals that the phosphatidylinositol 3-phosphate-binding SGK3 protein kinase is a downstream target of class III phosphoinositide 3-kinase. *Biochem J* **463**, 413-427 (2014).
77. Ronan, B., *et al.* A highly potent and selective Vps34 inhibitor alters vesicle trafficking and autophagy. *Nat Chem Biol* **10**, 1013-1019 (2014).
78. Dowdle, W.E., *et al.* Selective VPS34 inhibitor blocks autophagy and uncovers a role for NCOA4 in ferritin degradation and iron homeostasis in vivo. *Nat Cell Biol* **16**, 1069-1079 (2014).

SUPPLEMENTARY DATA

SUPPLEMENTARY METHODS

Cell lines

B-cell precursor acute lymphoblastic leukemia (BCP-ALL) cell lines NALM6 (B-Other), REH (ETV6-RUNX1), and 697 (TCF3-PBX1), T-ALL cell lines JURKAT (hypotetraploid) and LOUCY (del(5); t(16;20)) and human embryonic kidney cell line HEK293T were obtained from DSMZ (Braunschweig, Germany) and used only at low passages. REHS1 (REH subclone #1; ETV6-RUNX1) is a ETV6-RUNX1 positive cell line with identical genetic background as REH, but with different phenotypic characteristics (proliferation and drug resistance profiles). DNA fingerprinting was performed routinely on these cell lines to verify their genetic status. ALL cell lines were cultured in RPMI-1640 medium (Gibco, Life Technologies, Bleiswijk, the Netherlands) supplemented with 10% fetal calf serum (FCS) and 1% penicillin-streptomycin at 37 °C and 5% CO_2. HEK293T cells were cultured in high glucose Dulbecco's Modified Eagle's Medium with Glutamax (Gibco) supplemented with 10% FCS and 1% penicillin-streptomycin at 37 °C and 5% CO_2.

Isolation of CD34-positive hematopoietic cells from cord blood

Mononuclear cells were isolated from umbilical cord blood (UCB) using Lymphoprep sucrose-gradient centrifugation (1.077 g/ml, Nycomed Pharma, Oslo, Norway). Immunomagnetic cell separation, using magnetic beads coated with CD34 antibodies (Miltenyi Biotec, Gladbach, Germany), was performed to isolate CD34-positive hematopoietic progenitor cells (CB-$CD34^+$ cells). Cells were cultured in Iscove's Modified Dulbecco's Medium (Gibco) supplemented with 10% FCS, 50μM β-mercaptoethanol, 1% penicillin-streptomycin, 2mM glutamine, stem cell factor (SCF; 50ng/mL; Peprotech) and fms-like tyrosine kinase-3 ligand (Flt3L; 50 ng/mL; Peprotech) at 37°C and 5% CO2. UCB was obtained after informed consent was provided according to the Declaration of Helsinki. Protocols were approved by the ethics committee of the Erasmus University Medical Centre in Rotterdam.

Isolation of primary BCP-ALL leukemic blasts from patients

Bone marrow aspirates were obtained from children with newly diagnosed BCP-ALL prior to treatment. Immunophenotype and genetic subtype were determined by local hospital procedures and monitored by the central diagnostic laboratory of the Dutch Childhood Oncology Group (DCOG) in The Hague. Primary BCP-ALL cells were subsequently isolated as previously described[1]. We included 654 ALL patients

including 172 ETV6-RUNX1 positive BCP-ALL patients and 401 ETV6-RUNX1 negative BCP-ALL patients. In short, mononuclear cells were collected using Lymphoprep sucrose-gradient centrifugation (1.077 g/ml, Nycomed Pharma, Oslo, Norway). To determine the percentage of leukemic cells in the mononuclear cell fraction, May-Grünwald-Giemsa staining was performed on cytospin preparations. If necessary, the samples were further enriched, to obtain at least 95% leukemic blasts, by depletion of normal hematopoietic cells using anti-CD lineage marker coated magnetic beads (Dynal, Oslo, Norway). Cells were cultured in RPMI Dutch-modified medium (Gibco) supplemented with 20% FCS, Insulin transferrin sodium selenite (ITS), glutamin and gentamycin at 37 °C and 5% CO_2. Bone marrow aspirates were obtained after informed consent was provided according to the Declaration of Helsinki. Protocols were approved by the ethics committee of the Erasmus University Medical Centre in Rotterdam.

Isolation and characterization of primary MSCs

Mesenchymal stromal cells (MSCs) were isolated, as previously described[2], from bone marrow aspirates collected during diagnostic procedures. In short, colony-forming MSCs were selected by culturing bone marrow aspirates in low glucose DMEM (Gibco) supplemented with 15% FCS, 1% penicillin-streptomycin, vitamin C, and fibroblast growth factor (FGF) at 37°C and 5% CO_2. A panel of positive (CD44/ CD90/ CD105/ CD54/ CD73/ CD146/ CD166/ STRO-1) and negative surface markers (CD19/ CD45/ CD34) was used to characterize primary MSCs. Flow cytometric analysis was performed using the human mesenchymal stem cell marker antibody panel (R&D Systems, Minneapolis, MN, USA) and the monoclonal antibodies CD54-PE, CD73-PE, CD34-PE, and IgG1-PE (BD Biosciences, San Jose, CA, USA). The multilineage potential of the selected MSCs was confirmed by allowing the cells to differentiate towards adipocytes (Oil Red O staining), osteocytes (*Alizarin Red* S staining), and chondrocytes (Col2a/Thionine/Alcian Blue staining).

Production of bicistronic retrovirus and retroviral transduction of CB-CD34+ cells

To generate retrovirus, bicistronic retroviral DNA constructs were used expressing the *ETV6-RUNX1* fusion gene and enhanced Green Fluorescent Protein (eGFP). As a control, a construct expressing only eGFP was used. Both vectors consisted of a pMSCV promoter region, an internal ribosomal entry site and an ampicillin resistance cassette. HEK293T cells were co-transfected with these constructs and second-generation retroviral packaging vectors using XtremeGENE 9 tranfection reagents (Roche, Basel, Switzerland). Viral particles were collected in IMDM 48 hours after transfection. $CD34^+$ hematopoietic progenitors were pre-cultured overnight as

described above, upon which cells were divided in two fractions. One fraction was transduced with ETV6-RUNX1-IRES-eGFP, while the other fraction was transduced with control EV-IRES-eGFP. Transductions were performed with fresh retrovirus in retronectin (Takara, Otsu, Japan) coated wells.

Fluorescence activated cell sorting of transduced CB-CD34$^+$ cells

Transduced CB-CD34$^+$ cells were sorted using a BD ARIA II sorter (BD Biosciences) after staining with DAPI (Sigma) and PeCy7-conjugated CD34 antibody (BD Biosciences). The DAPI negative, CD34 positive and GFP positive population (see Fig. S6C for gating strategy) was used for further experiments. The purity of the sorts, as determined by flowcytometric analysis of the sorted cells, was in all cases at least 95% (see Fig. S1B for a representative post-sort analysis of purity).

Linear RNA amplification and gene expression profiling of CB-CD34$^+$ cells

After sorting, DAPI$^-$ CD34$^+$ GFP$^+$ CB-CD34$^+$ cells were lysed and RNA was extracted using Nucleospin RNA XS extraction columns according to manufacturer's protocol (Macherey-Nagel, Düren, Germany). Quality of RNA was determined by on-chip-electrophoresis using a RNA Pico Chip according to manufacturer's protocol (Agilent Technologies, Santa Clara, CA, USA). RNA Integrity scores (RIN) were higher than 8 for all samples. RNA was subsequently linearly amplified using the Nugen WT-Amplification™ pico system (Nugen, San Carlos, CA, USA). This system is based on RNA-dependent DNA polymerase activity and was previously reported to be most suitable for amplification and gene expression of picograms of input RNA[3]. Samples were run on Affymetrix GeneChip Human Genome U133 Plus 2.0 microarrays (Santa Clara, CA, USA). Data were normalized using vsnRMA[4] and analyzed using a linear mixed model[5]. The model was fitted to ETV6-RUNX1, RUNX1-RUNX1T1 and EV data derived for each respective umbilical cord blood donor. Data derived from the RUNX1-RUNX1T1 transduced umbilical cord blood donors were omitted for further analyses in this manuscript and singularly used for estimating the within umbilical cord blood variance. Genes were considered differentially expressed when $p \leq 0.05$ after multiple testing correction using false discovery rate (FDR). Differential gene expression was visualized using TIBCO Spotfire software (Perkin Elmer, Waltham, MA, USA). Microarray data are available in the ArrayExpress database (http://www.ebi.ac.uk/arrayexpress) under accession number E-MTAB-3466.

Gene expression profiling of primary BCP-ALL leukemic blasts from patients

Sample preparation and gene expression profiling of leukemic blasts derived from bone marrow aspirates was performed as earlier described[6]. In short, DNA and total RNA were isolated using TRIzol reagents (Invitrogen Life Technologies,

Breda, the Netherlands) or using the QIAamp DNA Blood mini kit (Qiagen, Venlo, the Netherlands) in accordance with the manufacturer's protocol and subsequently RNA quality was determined using a Bioanalyzer 2100 (Agilent, Amstelveen, the Netherlands). Only samples with an RNA integrity value >7 were processed further. cDNA and cRNA were synthesized using an in vitro transcription one-cycle kit (Affymetrix, Santa Clara, CA). Affymetrix U133 plus 2.0 gene-expression microarrays were processed, and data were extracted, as described previously[1]. Microarray data are available in the Gene Expression Omnibus database (http://www.ncbi.nlm.nih.gov/geo/).

Ingenuity Pathway Analysis

Gene networks were generated and functional analysis of differential gene expression was performed using QIAGEN's Ingenuity Pathway Analysis (IPA, QIAGEN, Redwood City, USA). The expected increase or decrease of biological functions, based on the observed change in gene expression, was defined as a regulation Z score and was considered significant when larger than 2 or smaller than -2. P-values represent results of a right-tailed Fisher's Exact Test after Benjamini-Hochberg multiple testing correction.

Western blot

For protein analysis, cells were lysed using a cold lysis buffer containing 25 mM Tris pH 7.4, 150 mM NaCl, 5mM EDTA pH 8.0, 1% Triton X-100, 10% Glycerol, 10 mM Sodium-pyrophosphate, 1 mM Sodium-orthovanadate, 10 mM Glycerolphosphate, Dithiothreitol, Phenylmethylsulfonyl Fluoride, Aprotinin and Sodium-Fluoride. Equal amounts of protein were separated on a 10% acrylamide gel and subsequently blotted on a nitrocellulose membrane using the Trans-Blot Turbo Transfer System (Bio-rad, Hercules, CA, USA). Primary antibodies used were: β-actin (ab6276, Abcam, Cambridge, UK), LC3B (#2775, Cell Signaling, Danvers, MA, USA), SQSTM1/p62 (#8025, Cell Signaling), Vps34 (#3358, Cell Signaling) and Vps34 (#4263, Cell Signaling). Fluorescently labeled secondary IRDye antibodies were purchased from LI-COR Biosciences (Lincoln, NE, USA) and blots were scanned using an Odyssey Infrared Imaging System (LI-COR Biosciences).

Reverse Phase Protein Array

Reverse phase protein arrays were performed in collaboration with prof. dr. E. Petricoin (George Mason University, Manassas, VA, USA) as previously described [7]. In short, normal bone-marrow samples and pediatric BCP-ALL patient cells were lysed in Tissue Protein extraction reagent (T-PER; Pierce, Thermo Scientific, Waltham, MA, USA), containing 300mM NaCl, 1 mM orthovanadate and protease

inhibitors. Lysates were spotted twice in triplicate on glass-backed nitrocellulose-coated array slides. Reverse-phase protein arrays were performed according to manufacturer's protocol. Data were normalized for total protein levels and was corrected for background staining. Primary antibodies used were: Vps34 (#3358 and #4263, Cell Signaling), and SQSTM1/p62 (#8025, Cell Signaling).

siRNA knockdown

Silencing of ETV6-RUNX1 and Vps34 in REH cells or ETV6-RUNX1 transduced CB-CD34$^+$ cells was achieved by transfection of siRNAs with Dharmafect 4 (Thermo Scientific). 72 hours after transfection, cells were transfected again. Twenty-four hours after the second hit, cells were analyzed.

siRNAs used to silence ETV6-RUNX1 have been described previously[8]. siETV6-RUNX1 #1: CCAUUGGGAGAAUAGCAGAAUGCAU; siETV6-RUNX1 #5: UGGGAGAAUAGCAGAAUGCAUACUU. Vps34 targeting siRNAs were purchased from Origene (Rockville, MD, USA).

Real-time PCR

RNA was extracted using Nucleospin RNA XS extraction columns according to manufacturer's protocol (Macherey-Nagel, Düren, Germany), upon which cDNA was synthesized. mRNA levels were quantified by incorporation of SYBR green (Thermo Scientific) during quantitative real-time PCR (Applied Biosystems 7900HT). Primers for *ETV6-RUNX1* were 5′-TCGGGAAGACCTGGCTTACA-3′ (forward) and 5′-TGGCATCGTGGACGTCTCTA-3′ (reverse). Primers for *PIK3C3* (Vps34) were 5′-CCTGGAAGACCCAATGTTGAAG-3′ (forward) and 5′-CGGGACCATACACATCCCAT-3′ (reverse) or 5′-AGTTCCCGGTGTAGGTGGTA-3′ (forward) and 5′-ACATTGGGTCTTCCAGGACA-3′ (reverse). To normalize data, *HPRT* or *RPS20* were used as reference genes. Primers used were: *HPRT* 5′-TGACACTGGCAAAACAATGCA-3′ (forward) and 5′-GGTCCTTTTCACCAGCAAGCT (reverse); *RPS20*: 5′-AAGGGCTGAGGATTTTTG-3′ (forward) and 5′-CGTTGCGGCTTGTTAG-3′ (reverse).

Luciferase reporter assays

To study Vps34 promoter activity, a pEZX reporter construct consisting of a 1.4 kB region (-1383 to +58) of the Vps34 promoter upstream of the Gaussia luciferase gene (Genecopoeia, Rockville, MD, USA; HPRM12127) was used. The reporter construct was transfected in HEK293T cells together with the constructs of interest. In all experimental conditions, the amount of transfected DNA was equalized per backbone. At the end of the experiment, GFP expression was quantified in each sample by flow cytometric analysis and used to normalize luciferase activity. Constructs used were:

pCMV5-RUNX1 (Addgene; plasmid 12426[9]); pCMV5-CBFβ (Addgene; plasmid 12427[9]), pMSCV-ETV6-RUNX1 (a kind gift from Dr. Owen Williams, London, UK) , pCMV6-XL5-HEY1 (Origene; plasmid SC115467), pcDNA3-EGR1 (Addgene; plasmid 11729[10]), pMT2-GATA1 (Addgene; plasmid 13626[11]), pFLAG-CMV2-GATA2 (Addgene; plasmid 1418[12]).

MTT cytotoxicity assay

The sensitivity of ALL cell lines to hydroxychloroquine was analyzed using 3-(4,5-dimethylthiazol-2-yl)-2,5-diphenyltetrazolium bromide (MTT) assay as described before[1,13]. Cell survival was determined after 4 days of hydroxychloroquine exposure. Background signal was subtracted and experimental conditions are depicted as the percentage of signal compared to the untreated control.

Lentiviral knockdown of Vps34

Lentivirus was produced by transfecting HEK293T cells with second generation lentiviral helper vectors pPax2 (Addgene plasmid 12260) and VSV-G envelope (pMD2G; Addgene plasmid 12259) together with pLKO.1 Mission vector (Sigma) targeting *PIK3C3* (Vps34). Transfection was performed using XtremeGENE transfection reagent according to manufacturer's protocol (Promega, Madison, WI, USA). Target sequences used to silence PIK3C3 were: GCTGCACAACAGACATTTGTA (shVps34#1; TRCN0000037798); GAGGCAAATATCCAGTTATAT (shVps34#2; TRCN0000196290); CCACGAGAGATCAGTTAAATA (shVps34#3; TRCN0000037794); GAGATGTACTTGAACGTAATG (shVps34#4; TRCN0000196840). Target sequence for used non-mammalian shRNA control vector was CAACAAGATGAAGAGCACCAA (NSC; SHC002). Virus was collected and concentrated by ultracentrifugation. For every experiment and every cell line, virus was titrated to obtain a transduction efficiency of 90%. This condition was equal to an MOI of 2.5. Cell lines were transduced using a spin-infection protocol. Cells were subsequently selected using the puromycin selection marker. A MACSQuant Analyzer (Miltenyi Biotec, Germany) was used to determine the number of viable, Propidium Iodide negative, cells.

Confocal laser scanning microscopy

Autophagy levels were visualized by the number and volume of LC3B positive vesicles. To quantify autophagy levels, confocal scanning microscopy was performed. REH cells were allowed to attach to a glass slide coated with 10 μg/mL fibronectin (Sigma) for 30 minutes. Cells were subsequently fixated using 3% formaldehyde in PBS for 10 minutes at room temperature. After fixation, slides were blocked with 10% FCS and 0.2% goat serum in PBS and subsequently incubated overnight at 4°C

with LC3B antibody (#2775, Cell Signaling). Slides were subsequently washed twice with PBS and stained with goat-anti-rabbit-Alexa 488 secondary antibody for 1 hour. After three PBS washes, slides were stained with DAPI (Sigma) for 5 minutes and mounted with ProLong Gold antifade reagent (Life Technologies). Images were acquired using a confocal laser scanning microscope (Leica SP5). Sequential scanning of different channels was performed at a resolution of 1024 x 1024 pixels in the *x y* plane and 0.15 μm steps in z-direction.

The system was equipped with a 63× plan-apochromat oil 1.4 NA DIC objective. The pinhole diameter was set to 1 airy unit (95.5 μm). DAPI and LC3B-anti-rabbit-Alexa 488 were excited with a 488-nm Argon laser and a 405-nm Diode-Pumped Solid-State laser, respectively. Fiji software was used for imaging processing. Brightness and contrast were optimized and applied to the entire image. Z-project using all slides and maximum intensity projection was used to show the number of LC3B-positive vesicles in Figure 4. For quantification of LC3B-positive vesicles, Z-stacks of images were deconvolved and processed using Huygens Professional software. Both the number and the average volume of vesicles were analyzed. For the quantification of number and volume of LC3B-positive vesicles, we excluded cells with atypical nuclei. For each experiment, LC3B-positive vesicles were quantified in at least 6 cells. 3D-deconvolved images shown in Fig. 4 were created using the same software.

Cell viability assays

Primary patient cells (1 x 10^6 cells) were co-cultured with or without primary mesenchymal stromal cells (5 x 10^4) for five days in a 24-well plate at 37 °C and 5% CO_2. Stromal cells were allowed to attach prior to the start of the experiment. Before the start of each experiment, leukemic cells were screened for CD19 positivity (Brilliant Violet 421 anti-human CD19 antibody). After five days of culture the percentage of viable leukemic cells was determined by flow cytometic analysis after staining with Brilliant Violet 421 anti-human CD19 antibody (Biolegend), FITC Annexin V (Biolegend), and Propidium Iodide (PI; Sigma) Primary leukemic cells were exposed to L-Asparaginase, Prednisolone or 6-Mercaptopurine in a concentration that was lethal to 50% of the patient derived leukemic cells (IC_{50}) as determined upfront by a 4-day MTT assay[1].

Statistical analysis

Statistical analysis of microarray data of paired (EV-eGFP$^+$ versus ETV6-RUNX1-eGFP$^+$) CB-CD34$^+$ was performed using a linear mixed model in which multiple testing correction was applied by FDR (see also Material and Methods section on linear RNA amplification and gene expression profiling of CB-CD34$^+$ cells).

Microarray data of primary cells from ALL patients was normalized using vsnrma[4], batch effects were removed using the empirical Bayes method[14], and data were analyzed using LIMMA[15] and FDR multiple testing correction.

Both the Student's t-test and the Student's paired t-test were used as statistical test when applicable. Bar graphs represent the mean of biological replicates. Error bars represent standard error of the mean (S.E.M.).

REFERENCES

1. Den Boer ML, Harms DO, Pieters R, et al. Patient stratification based on prednisolone-vincristine-asparaginase resistance profiles in children with acute lymphoblastic leukemia. *J Clin Oncol*. 2003;21(17):3262-3268.
2. van den Berk LC, van der Veer A, Willemse ME, et al. Disturbed CXCR4/CXCL12 axis in paediatric precursor B-cell acute lymphoblastic leukaemia. *Br J Haematol*. 2014;166(2):240-249.
3. Clement-Ziza M, Gentien D, Lyonnet S, Thiery JP, Besmond C, Decraene C. Evaluation of methods for amplification of picogram amounts of total RNA for whole genome expression profiling. *BMC Genomics*. 2009;10:246.
4. Huber W, von Heydebreck A, Sultmann H, Poustka A, Vingron M. Variance stabilization applied to microarray data calibration and to the quantification of differential expression. *Bioinformatics*. 2002;18 Suppl 1:S96-104.
5. Bates D, Mächler M, Bolker B, Walker S. Fitting linear mixed-effects models using lme4. *arXiv preprint arXiv:14065823*. 2014.
6. van der Veer A, Waanders E, Pieters R, et al. Independent prognostic value of BCR-ABL1-like signature and IKZF1 deletion, but not high CRLF2 expression, in children with B-cell precursor ALL. *Blood*. 2013;122(15):2622-2629.
7. Petricoin EF, 3rd, Espina V, Araujo RP, et al. Phosphoprotein pathway mapping: Akt/mammalian target of rapamycin activation is negatively associated with childhood rhabdomyosarcoma survival. *Cancer Res*. 2007;67(7):3431-3440.
8. Zaliova M, Madzo J, Cario G, Trka J. Revealing the role of TEL/AML1 for leukemic cell survival by RNAi-mediated silencing. *Leukemia*. 2011;25(2):313-320.
9. Meyers S, Lenny N, Hiebert SW. The t(8;21) fusion protein interferes with AML-1B-dependent transcriptional activation. *Mol Cell Biol*. 1995;15(4):1974-1982.
10. Yu J, de Belle I, Liang H, Adamson ED. Coactivating factors p300 and CBP are transcriptionally crossregulated by Egr1 in prostate cells, leading to divergent responses. *Mol Cell*. 2004;15(1):83-94.
11. Monticelli S, Solymar DC, Rao A. Role of NFAT proteins in IL13 gene transcription in mast cells. *J Biol Chem*. 2004;279(35):36210-36218.
12. Tong Q, Tsai J, Tan G, Dalgin G, Hotamisligil GS. Interaction between GATA and the C/EBP family of transcription factors is critical in GATA-mediated suppression of adipocyte differentiation. *Mol Cell Biol*. 2005;25(2):706-715.
13. Pieters R, Loonen AH, Huismans DR, et al. In vitro drug sensitivity of cells from children with leukemia using the MTT assay with improved culture conditions. *Blood*. 1990;76(11):2327-2336.
14. Johnson WE, Li C, Rabinovic A. Adjusting batch effects in microarray expression data using empirical Bayes methods. *Biostatistics*. 2007;8(1):118-127.
15. Smyth G. Bioinformatics and Computational Biology Solutions using R and Bioconductor. New York: Springer; 2005.

SUPPLEMENTARY FIGURES

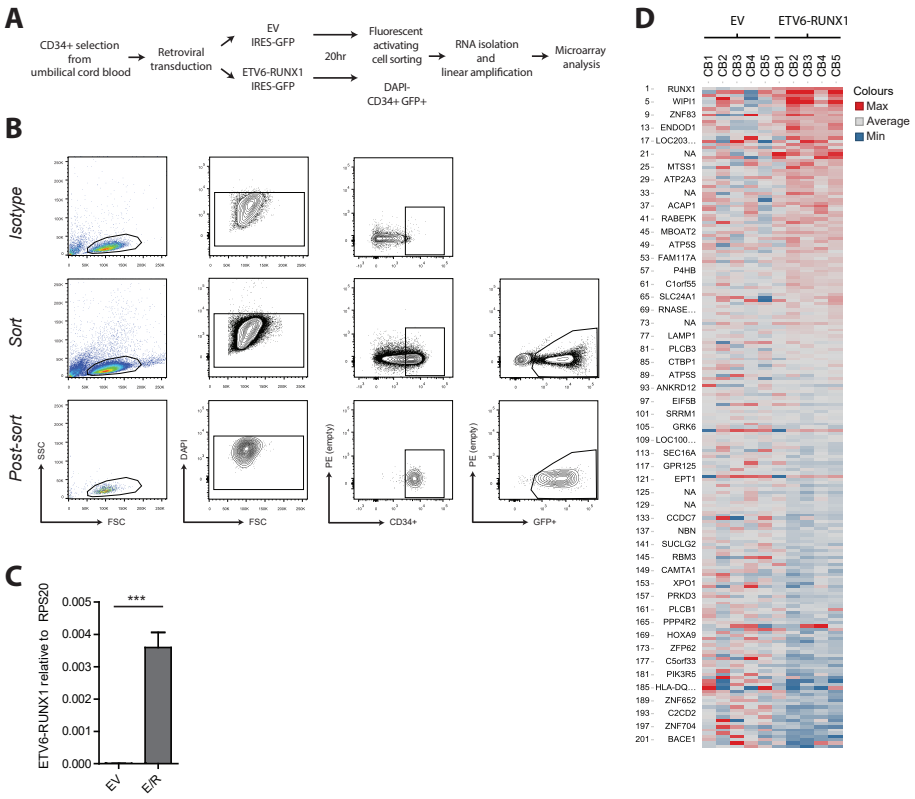

Supplementary Figure 1. Early effects of ETV6-RUNX1 expression in CB-CD34+ cells.
(A) Flow chart used to study the early effects of ETV6-RUNX1 fusion protein expression in cord blood-derived CD34-positive hematopoietic progenitors (CB-CD34+ cells). CB-CD34+ cells were isolated from cord blood. Per cord blood donor, cells were divided in two fractions of which one was transduced with ETV6-RUNX1-IRES-GFP and the other fraction with control EV-IRES-GFP. Viable transduced HPCs were sorted after 20 hours based on DAPI negativity and CD34 and GFP positivity. RNA was extracted from sorted CB-CD34+ cells, controlled for quality and linearly amplified after which gene expression analysis was performed with Affymetrix GeneChip Human Genome U133 Plus 2.0 microarrays.
(B) Graphs showing the gating strategy used to sort alive, CD34-positive, transduced cord blood cells. First living cells were gated based on FSC, SSC and the absence of DAPI incorporation. CD34-positive cells were selected based on the positive expression compared to an isotype control. Finally, CD34-positive transduced cells were sorted based on eGFP expression. Post-sort purity was more than 95%. (C) Graph showing gene expression levels of *ETV6-RUNX1* relative to housekeeping gene RPS20 quantified with Q-PCR (n = 5). EV represents levels in CB-CD34+ cells transduced with the empty vector control. ETV6-RUNX1 represents levels in CB-CD34+ cells transduced with the ETV6-RUNX1 vector. Data are means ± SEM; *** $p \leq 0.001$. (D) Heat map showing which gene probe sets are relatively over-expressed (in red) and which gene probe sets are relatively under-expressed (in blue) compared to the mean expression of all differentially regulated gene probe sets. 203 gene probe sets were significantly ($p \leq 0.05$; FDR-adjusted) over-expressed or under-expressed when ETV6-RUNX1 positive HPCs were compared to control HPCs 20 hours after transduction.

A

Diseases or Functions Annotation	p-Value	Activation z-score
survival of organism	3,93E-02	3,221
production of reactive oxygen species	4,49E-02	2,979
organization of cytoplasm	4,49E-02	2,612
expansion of cells	4,49E-02	2,578
quantity of cells	2,19E-03	2,554
differentiation of bone marrow cells	2,56E-02	2,412
degranulation of phagocytes	3,05E-03	2,355
cellular homeostasis	1,43E-02	2,297
aggregation of cells	1,51E-02	2,206
differentiation of HPCs	2,42E-02	2,187
quantity of blood platelets	4,49E-02	2,169
quantity of eosinophils	2,92E-02	2,125
binding of cells	9,47E-03	2,118
cell cycle progression	3,73E-02	2,042
engulfment of cells	2,19E-02	2,024
recruitment of leukocytes	2,44E-03	2,021
response of granulocytes	2,19E-02	2,000
fibrosis	4,49E-02	-2,126
apoptosis of hematopoietic progenitor cells	4,49E-02	-2,183
cell death of hematopoietic progenitor cells	1,70E-02	-2,211
inflammation of liver	1,51E-02	-2,236
apoptosis of blood cells	3,69E-02	-2,349
apoptosis of leukocytes	4,49E-02	-2,369
apoptosis of mononuclear leukocytes	4,49E-02	-2,401
hypertrophy of heart	4,49E-02	-2,425
organismal death	1,63E-03	-2,601

Activation Z-score
Colors
3,22
0.00
-2,60

B

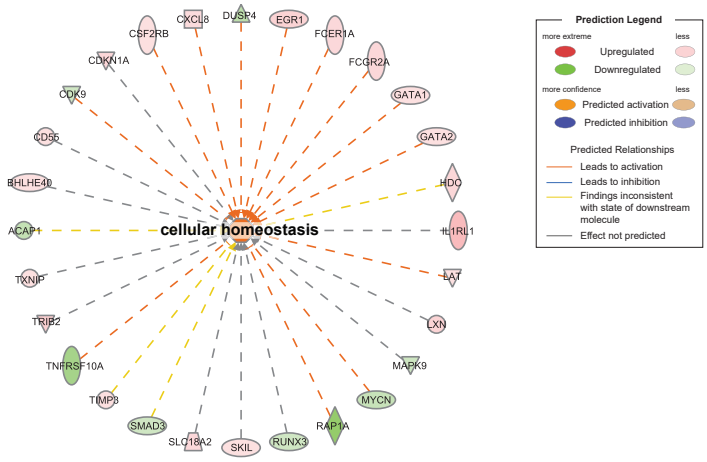

Supplementary Figure 2. Pathway analysis of ETV6-RUNX1 positive CB-CD34+ cells.
(A) Ingenuity pathway analysis was used to analyze gene ontology (GO) functional categories and activation of disease/ function annotation based on current literature. Significantly regulated functional categories are listed with their p-value (right-tailed Fisher Exact Test after Benjamini-Hochberg multiple testing correction) and regulation Z-score. This analysis reflect the pathways induced in CB-CD34+ cells by ETV6-RUNX1 40 hours after transduction. (B) Schematic representation of differentially regulated genes predicted to induce cellular homeostasis.

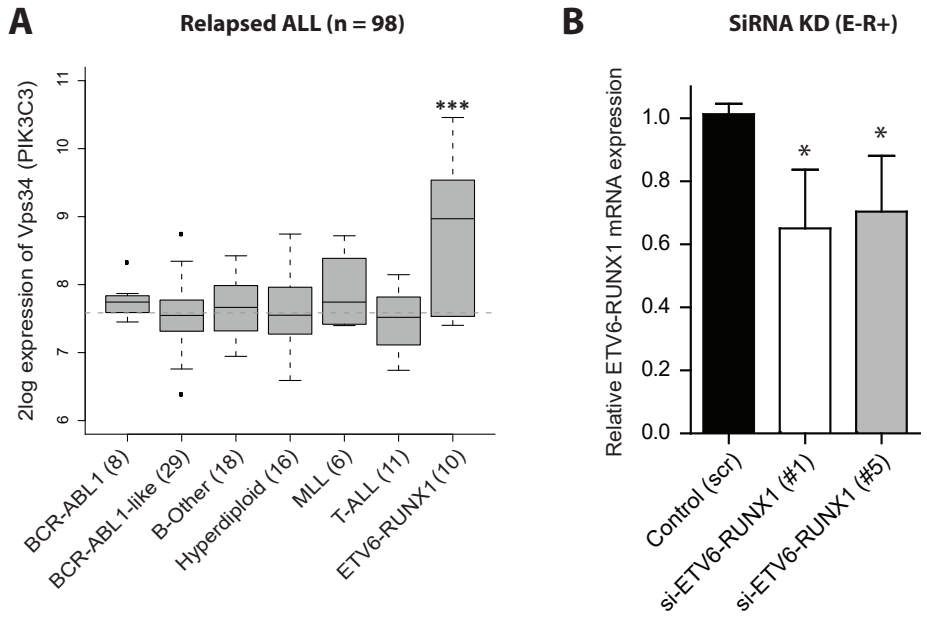

Supplementary Figure 3. Vps34 expression in ETV6-RUNX1 positive cells.
(A) Graph showing the 2log expression (at initial diagnosis) of the gene probe set mapped to Vps34 in a cohort of 98 pediatric ALL patients that eventually relapsed after treatment (relapsed patients in the Erasmus MC cohort). Grey dashed line represents mean expression of all patients. Gene expression of ETV6-RUNX1 positive patients was compared to gene expression of all other B-ALL patients (excluding T-ALL): *** FDR-adjusted $p = 5.11*10^{-6}$. (B) Graph showing gene expression of ETV6-RUNX1 after knockdown of the ETV6-RUNX1 fusion protein. mRNA levels were determined in REH (n=2) and ETV6-RUNX1 transduced CB-CD34+ cells (n=1) by Q-PCR, normalized to HPRT, and compared to the average expression of cells transfected with scrambled control siRNAs ($n = 3$, $p \leq 0.05$).

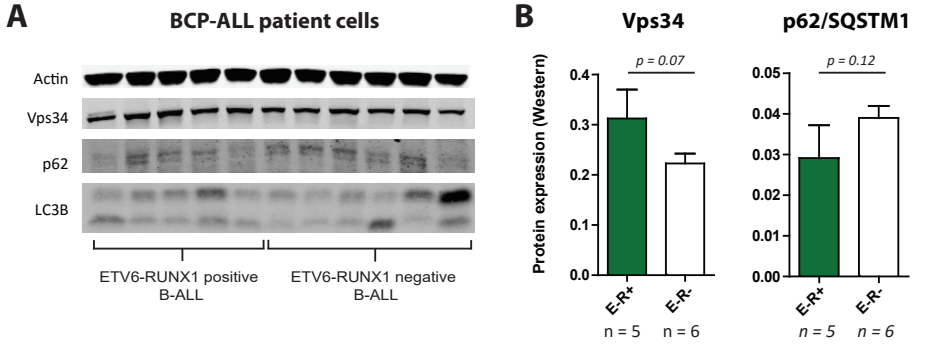

Supplementary Figure 4. Autophagy levels are high in ETV6-RUNX1 positive BCP-ALL cells.
(A) Western blot analysis of proteins important in the autophagy pathway, namely Vps34, p62 (sequestosome 1), and LC3B in primary patient BCP-ALL cells (n=5 for ETV6-RUNX1 positive BCP-ALL patients; n=6 for ETV6-RUNX1 negative BCP-ALL patients). (B) Quantification of experiment performed in (a). Protein expression of Vps34 and p62 is relative to actin expression.

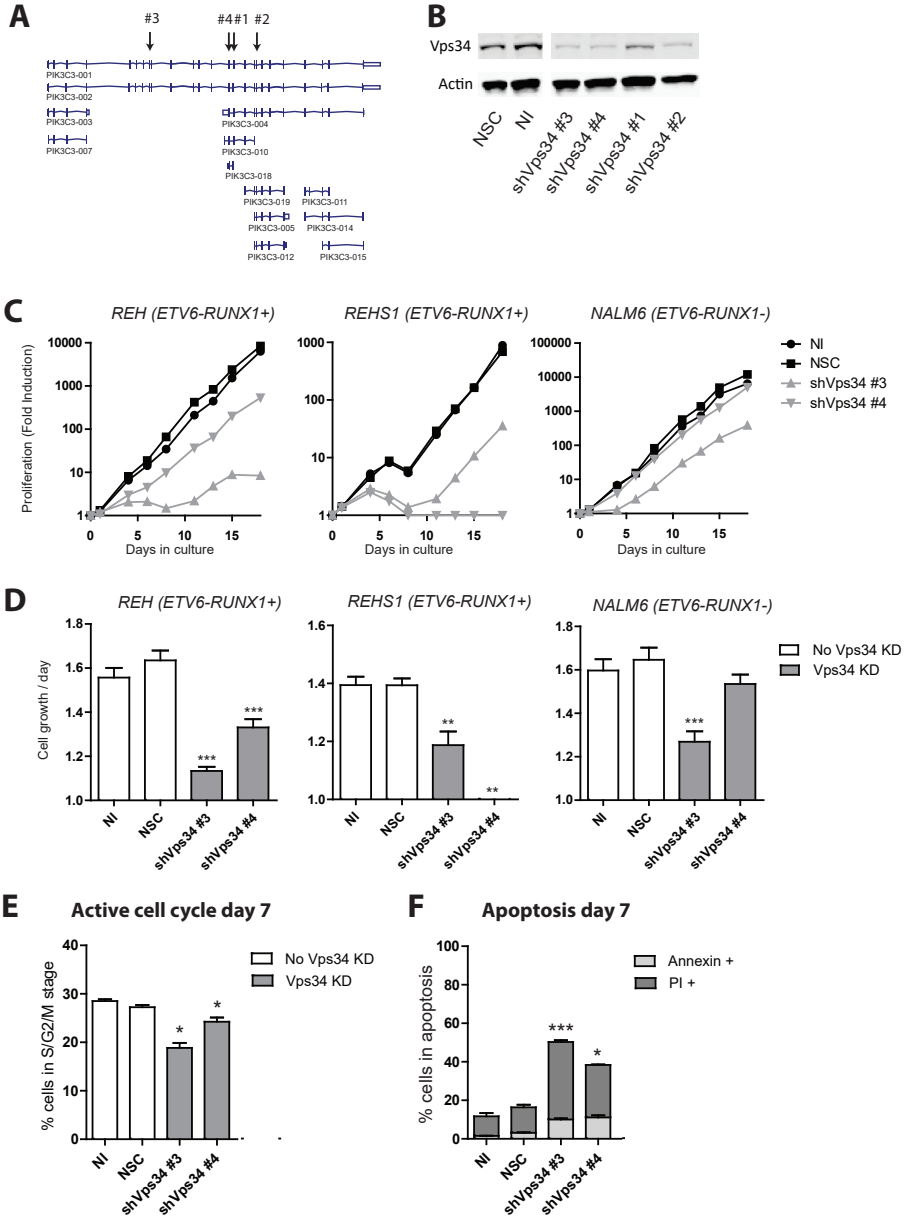

Supplementary Figure 5. Vps34 is essential for the survival of ETV6-RUNX1 positive leukemic cells.

(A) Schematic representation of the different transcript variants of Vps34, based on currently available literature (Ensembl Genome Browser; ENSG00000078142) and the binding locations of shVps34#1-shVps34#4. (B) Representative western blot showing the knockdown of Vps34 in REH cells.

Supplementary Figure 5. Vps34 is essential for the survival of ETV6-RUNX1 positive leukemic cells. (continued)

(C-D) ETV6-RUNX1 positive (REH and REHS1) and ETV6-RUNX1 negative (NALM6) BCP-ALL cells were lentivirally transduced with scrambled shRNA control (NSC, black) or two distinct Vps34 shRNA constructs (grey; shVps34 #3 and shVps34#4). NI represents non-infected cells. Cells were cultured for 18 days. To determine the effect on proliferation, cell counts were performed every 2-3 days. Representative graphs are shown in (C). Representative average increase in cell numbers per day is shown in (D). White bars represent control conditions (NI and NSC). Grey bars represent conditions in which Vps34 was knocked down. T-test was performed to compare control conditions (NSC) with Vps34 knockdown conditions ($n = 3$, ** $p \leq 0.01$, *** $p \leq 0.001$). Error bars represent S.E.M.

(E-F) ETV6-RUNX1 positive (REH) BCP-ALL cells were lentivirally transduced with scrambled shRNA control (NSC) or two distinct shRNA constructs to silence Vps34 expression. After 7 days of culture, flow cytometrical analysis was performed to determine the effect of Vps34 knockdown on survival and cell cycle progression. (E) The percentage of viable (AnnexinV positive, Propidium Iodide negative), actively cycling cells was determined using DyeCycle. Data were depicted as the percentage of cells in active cell cycle (S, G2, M stage) at day 7 after transduction ($n = 2$, * $p \leq 0.05$). Error bars represent S.E.M. **(**F) The percentages of early apoptotic (AnnexinV positive, Propidium Iodide negative) and late apoptotic (Propidium Iodide positive) cells were determined 7 days after transduction ($n = 2$, * $p \leq 0.05$, *** $p \leq 0.001$). Error bars represent S.E.M.

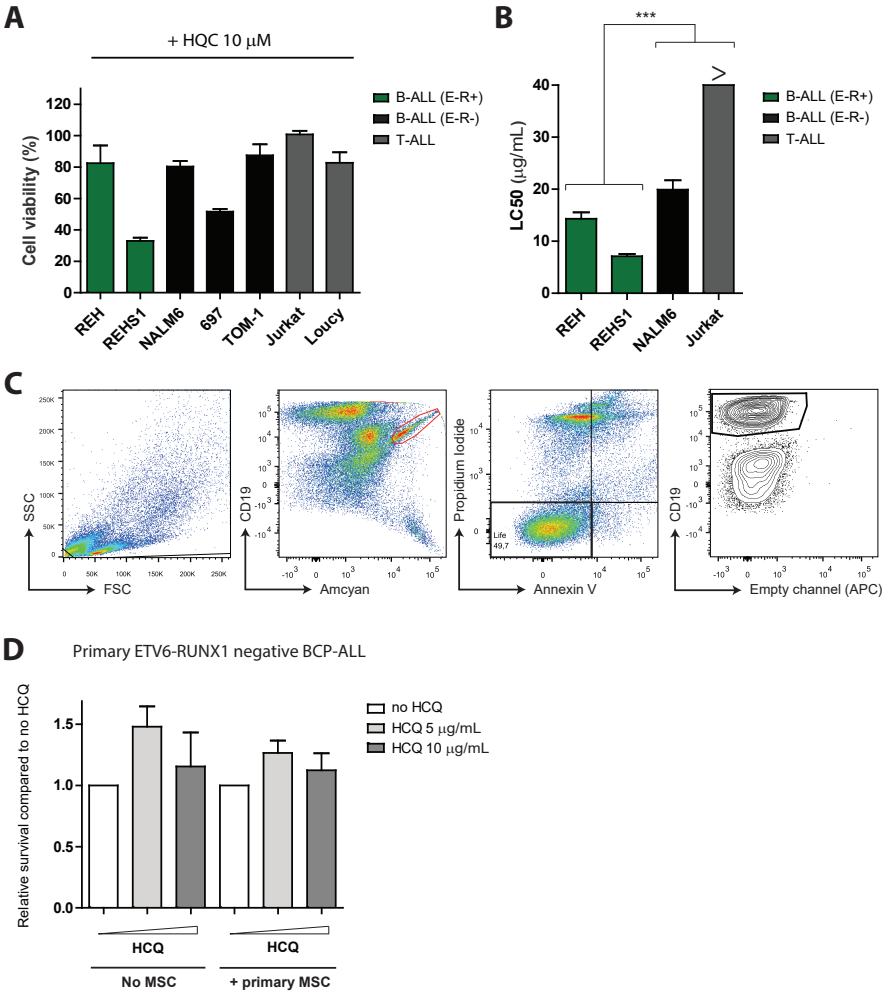

Supplementary Figure 6. ETV6-RUNX1 negative ALL cells are not sensitive to treatment with hydroxychloroquine.

(A) Bar graph showing the cell viability of HCQ-treated conditions (10 μg/ml) compared to HCQ-untreated conditions after 4 days (MTT). Green bars represent ETV6-RUNX1 positive BCP-ALL cell lines. Black bars represent ETV6-RUNX1 negative BCP-ALL cell lines. Dark grey bars represent T-ALL cell lines. (B) Calculation of IC_{50} concentrations of two ETV6-RUNX1 positive ALL cell lines (green), and two ETV6-RUNX1 negative ALL cell lines (black and gray). n = 4, *** $p \leq 0.001$. IC_{50} values for Jurkat cells were not reached during treatment with 40 μg/ml HCQ (the highest concentration used in this assay). (C) Flow cytometrical gating strategy used to analyze survival after HCQ treatment of primary BCP-ALL patient samples in co-culture. First, forward and sideward scatter were used to gate living and apoptotic events. Second, primary mesenchymal stromal cells (MSCs) were gated out based on CD19-expression and autofluorescence in the Amcyan channel (events in red gate were excluded from analysis). Then, viable cells were gated based on Annexin-V and Propidium Iodide staining and subsequently based on CD19-expression. Percentage of living cells was calculated by dividing the number of AnnexinV negative, PI negative, CD19 positive events by the number of events after gating out the MSCs. (D) Graph showing relative survival of primary ETV6-RUNX1 negative BCP-ALL cells after treatment with increasing concentrations of HCQ compared to untreated controls. Light grey bars represent treatment with 5 μg/ml HCQ. Grey bars represent treatment with 10 μg/ml HCQ. Experiment was performed in absence and presence of primary MSCs (n=3 for conditions in absence of MSCs, n = 5 for conditions in presence of MSCs).

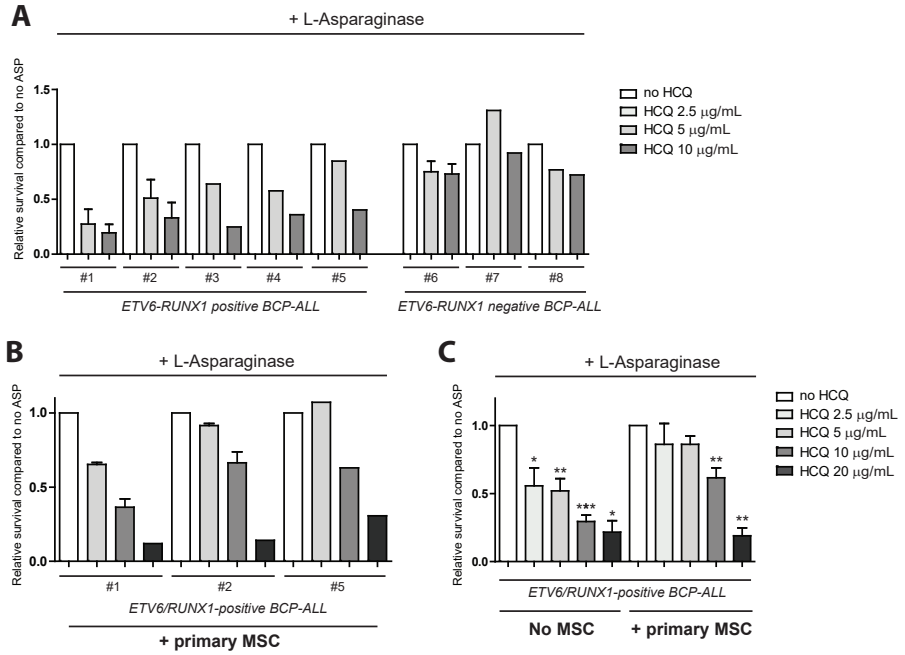

Supplementary Figure 7. Autophagy inhibition sensitizes ETV6-RUNX1 positive BCP-ALL.
(A) Primary ETV6-RUNX1 positive BCP-ALL cells were cultured in absence or presence of IC-50 concentrations of L-Asparaginase and increasing concentrations of HCQ. Flow cytometric analysis was performed to determine the percentage of non-apoptotic (Annexin V negative, Propidium Iodide negative, CD19 positive) cells (for gating strategy see supplementary Figure 6d). First, the survival of primary leukemic blasts in presence of L-Asparaginase was compared to their survival in absence of L-Asparaginase (see Figure 7A for the effect of asparaginase in the absence of treatment with other effectors). Next, data was depicted as fold reduction compared to HCQ-untreated controls. (B) Primary ETV6-RUNX1 positive BCP-ALL cells were co-cultured with primary MSCs in absence or presence of IC-50 concentrations of L-Asparaginase and increasing concentrations of HCQ. Flow cytometric analysis was performed to determine the percentage of non-apoptotic cells. The survival of primary leukemic blasts in presence of L-Asparaginase was compared to their survival in absence of L-Asparaginase. Next, data from individual patients was depicted as fold reduction compared to HCQ-untreated controls. Light grey bars represent treatment with 5 μg/ml HCQ. Grey bars represent treatment with 10 μg/ml HCQ. Dark grey bars represent treatment with 20 μg/ml HCQ. Experiment was performed twice with cells of patients #1 and #2. (C) Co-culture experiments were performed with primary ETV6-RUNX1 positive BCP-ALL cells and MSCs. Cells were cultured in presence or absence of L-Asparaginase and increasing concentrations of HCQ. Flow cytometric analysis was performed to determine the percentage of non-apoptotic cells. The survival of primary leukemic blasts in presence of L-Asparaginase was compared to their survival in absence of L-Asparaginase. Next, data from individual patients was depicted as fold reduction compared to HCQ-untreated controls. Data were depicted as fold reduction compared to HCQ-untreated controls (n=4 for HCQ 2.5 μg/ml; n = 5 for HCQ 5 μg/ml and 10 μg/ml; n=3 for HCQ 20 μg/ml). Error bars represent S.E.M.

SUPPLEMENTARY TABLES

Due to space restrictions, supplementary tables are not included in the print version of this thesis. On request, tables are readily available.

Chapter 4

Small molecule inhibition of LARG/RhoA signaling blocks migration of ETV6-RUNX1 positive B-cell Precursor Acute Lymphoblastic Leukemia

Roel Polak[1], Marc B. Bierings[2]*, Rosanna E.S. van den Dungen[1]*, Bob de Rooij[1], Rob Pieters[3], Miranda Buitenhuis[4]* & Monique L. den Boer[1]*

[1] *Dept. of Pediatric Oncology, Erasmus MC, Sophia Children's Hospital, Rotterdam, The Netherlands.*
[2] *Dept. of Pediatric Oncology, University Medical Center Utrecht, Utrecht, The Netherlands.*
[3] *Princess Máxima Center for Pediatric Oncology, Utrecht, The Netherlands.*
[4] *Dept. of Hematology, Erasmus MC, Wytemaweg 80, 3015 CN Rotterdam, The Netherlands.*

* These authors contributed equally to this work and the study

Manuscript under consideration

ABSTRACT

Leukemic cells reside in the bone marrow microenvironment, where they are nurtured and protected against chemotherapy. In this study, we aimed to find novel ways to disrupt the leukemic niche by targeting intracellular signaling pathways that are essential for migration of leukemic cells. We focused on pediatric B-cell precursor acute lymphoblastic leukemia harboring t(12;21)(p13;q22), resulting in the ETV6-RUNX1 (or TEL-AML1) fusion protein.

We show that Leukemia Associated Rho Guanine nucleotide exchange factor (LARG or ARHGEF12) is selectively up-regulated in ETV6-RUNX1 positive leukemic cells, and induced by ectopic expression of ETV6-RUNX1 in healthy hematopoietic progenitors. LARG is a RhoA-selective RhoGEF, switching RhoA to an active state. Pharmacological small molecule inhibition of LARG/RhoA significantly inhibited the migration of ETV6-RUNX1 positive cell lines and primary cells toward mesenchymal stromal cells (MSCs) and CXCL12. This reduction was not caused by toxicity, since proliferation and drug resistance were unaffected. In contrast, migration of ETV6-RUNX1 negative cells was not altered by LARG/RhoA inhibition. These data suggest that enhanced LARG/RhoA signaling is important for migration of ETV6-RUNX1 positive leukemic cells toward their microenvironment. The specificity of this process for ETV6-RUNX1 positive leukemic cells might enable selective targeting of the leukemic niche with small molecule inhibitors.

INTRODUCTION

The bone marrow microenvironment is shown to be essential in facilitating and initiating leukemogenesis[1-4]. This leukemic niche protects leukemic and pre-leukemic cells from elimination by immune responses and chemotherapeutic agents, and can facilitate the development of drug resistance[5-8]. Since close proximity to the niche is essential for this protection, disruption of the leukemic niche is an important consideration for new therapeutic strategies[9-13]. Several studies have used G-CSF or small molecule inhibitors targeting the CXCR4/CXCL12 axis to inhibit migration of leukemic cells toward the niche and show promising pre-clinical results, mainly in patients with acute myeloid leukemia[11-21]. Another approach to disrupt the leukemic niche is to target intracellular signaling pathways that are intrinsically important for migration of leukemic cells. This approach may lead to a more specific inhibition of the leukemic niche, without interfering with healthy hematopoietic niches. However, the molecular mechanisms driving leukemic migration are largely unknown.

This study intends to find the molecular drivers of migration in pediatric B-cell precursor acute lymphoblastic leukemia harboring t(12;21)(p13;q22). This rearrangement fuses the 5′ non-DNA binding region of the ETS family transcription factor ETV6 (TEL) to almost the entire RUNX1 (AML1) locus[22], resulting in the ETV6-RUNX1 fusion protein (also known as TEL-AML1). ETV6-RUNX1 is present in 25% of pediatric patients with B-cell precursor acute lymphoblastic leukemia (BCP-ALL) and is therewith the most common fusion gene in childhood cancer[23,24]. Despite the favorable prognosis associated with this cytogenetic subtype of BCP-ALL[24-26], resistance to chemotherapeutic drugs and occurrence of relapse occurs in ~10% of these patients[25-29]. In this study, we show that ETV6-RUNX1 drives the expression of genes regulating cytoskeleton organization and migration, including the G-protein-regulated Rho Guanine Exchange Factor 12 (ARHGEF12), otherwise known as Leukemia Associated Rho GEF (LARG). LARG is a RhoA-selective RhoGEF, switching RhoA from a GDP-bound/inactive to a GTP-bound/active state[30-32]. Activation of LARG/RhoA signaling has been implicated in transformation to leukemia, regulation of migration, and regulation of cell division[32-39]. With the development of small molecule inhibitors of LARG and RhoA[40-42], it becomes feasible to target these processes. In the present paper, we demonstrate that ETV6-RUNX1 positive cells are sensitive for small molecule inhibitors of LARG/RhoA.

METHODS

Details are provided in the supplementary methods section.

Transduction and gene expression profiling of primary cells

CD34-positive hematopoietic progenitor cells (CB-CD34$^+$ cells) were derived from human cord blood and transduced with retrovirus expressing *ETV6-RUNX1* and eGFP. DAPI$^-$ CD34$^+$ GFP$^+$ CB-CD34$^+$ cells were sorted using a BD ARIA II sorter. After sorting, cells were lysed and RNA was extracted and subsequently linearly amplified.

Bone marrow aspirates were obtained from children with newly diagnosed BCP-ALL prior to treatment. Leukemic blasts were collected and processed as previously described.

Affymetrix GeneChip HG-U133-Plus-2.0 microarrays were used for all samples. Microarray data of CB-CD34$^+$ cells are available in the ArrayExpress database under accession number E-MTAB-3466. Microarray data of BCP-ALL blasts are available in the Gene Expression Omnibus database.

Functional assays

Migration and chemotaxis was quantified using a 6.5 mm diameter transwell system (Corning, NY, USA) with a pore size of 5 μm. Prior to the start of the experiment, we cultured 5 x 10^4 primary MSCs in the lower compartment of a transwell system for 48 hours (bottom compartment) and leukemic cells in absence or presence of LARG inhibitors (Y16+G04) or AMD3100 for 16 hours. Next, leukemic cells were added to the upper compartment and allowed to migrate for 6 hours. At the end of experiment, all cells in the bottom compartment were harvested and stained with DAPI (Life Technologies) and antibodies against human CD19 (Brilliant Violet 421 anti-human CD19 antibody, Biolegend, San Diego, CA, USA). A MACSQuant analyzer (Miltenyi Biotec, Gladbach, Germany) was used to determine the number/percentage of migrated DAPI$^-$/CD19$^+$ cells. Silencing of genes was achieved using a lentiviral knockdown approach using the pLKO.1 Mission vector containing a puromycin selection marker. Protein phosphorylation was analyzed using a multiplex cell signaling assay according to manufacturer's protocol (MILLIPLEX MAP Multi-pathway Magnetic Bead 9-Plex; Merck Millipore). Cell viability of primary leukemic cells was quantified using flow cytometry-based Annexin V - Propidium Iodide assays in presence or in absence of the small molecules G04 and Y16.

Statistical analysis

Statistical analysis of microarray data of paired CB-CD34^{+} cells was performed using a linear mixed model. Microarray data of primary cells from ALL patients were analyzed using LIMMA. Functional analysis of differential gene expression was performed using QIAGEN's Ingenuity Pathway Analysis. Both the Student's t-test and the Student's paired t-test were used as statistical test when applicable. Bar graphs represent the mean of biological replicates. Error bars represent standard error of the mean (S.E.M.).

RESULTS

Stromal support induces survival and drug resistance of BCP-ALL cells

In order to visualize the beneficial effects of the stromal microenvironment on BCP-ALL cell survival, we co-cultured BCP-ALL cells from 10 different patients with or without primary MSCs. We observed a consistent increase in BCP-ALL cell survival in co-culture conditions (average 2 fold induction compared to mono-culture, $p \geq 0.001$, Figure 1A). In addition, we performed similar experiments in absence or presence of prednisolone or l-asparaginase, two spearhead drugs in ALL treatment. MSCs significantly induced prednisolone and l-asparaginase resistance (84% vs 17% and 81% vs 30% reduced viability during prednisolone and l-asparaginase treatment, respectively; $p \geq 0.001$; Figure 1B and 1C). In correspondence with this finding, we previously showed that drug resistance is induced due to direct binding of leukemic cells to MSCs via so-called tunneling nanotubes[8]. These data underline the importance of hampering leukemic cell migration toward the leukemic niche.

ETV6-RUNX1 drives a pro-migratory signature in CD34^{+} progenitors and BCP-ALL

In order to elucidate the molecular mechanisms driven by the ETV6-RUNX1 fusion protein, we performed gene expression profiling on healthy, umbilical cord blood-derived, CD34 positive hematopoietic progenitors (CB-CD34^{+}) ectopically expressing the ETV6-RUNX1 fusion gene and compared their gene expression to CB-CD34^{+} cells expressing a control vector. Ingenuity pathway analysis on the 196 differentially expressed genes showed significant enrichment of genes involved in regulation of cellular movement, migration of cells, and cell morphology ($p = 3.92E^{-06}$, $p = 2.44E^{-04}$, and $p = 1.14E^{-06}$ respectively; Figure 1D). These genes were predicted to activate the recruitment of leukocytes, leukocyte migration, and cellular movement of leukocytes, and to affect morphology of blood cells and activation of leukocytes (supplementary Figure 1A). Furthermore, we observed differential regulation of

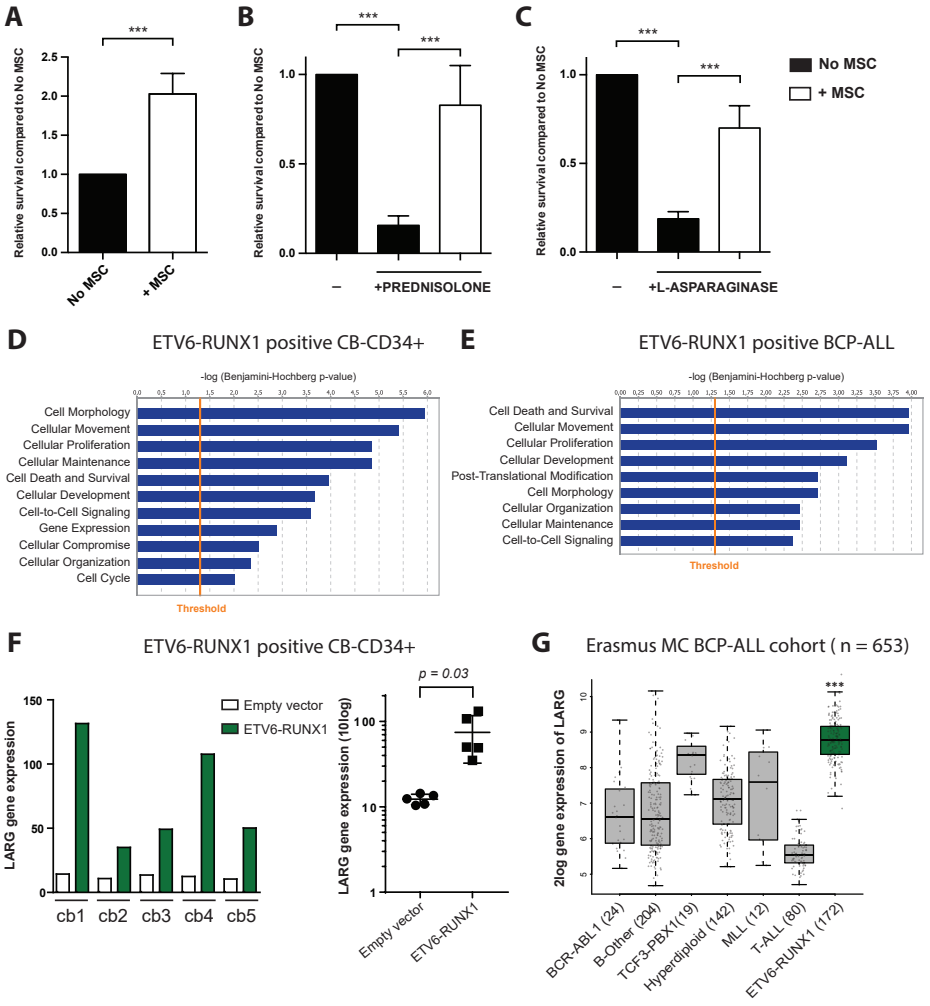

Figure 1. ETV6-RUNX1 induces a pro-migration gene expression signature including LARG.
(A) Primary blasts were isolated from 10 pediatric BCP-ALL patients and subsequently cultured for 5 days in absence or presence of primary bone marrow-derived MSCs. Black bars represent the percentage of CD19-positive, annexin-PI-negative cells in mono-culture. White bars represent the percentage of CD19-positive, annexin-PI-negative cells in co-culture with MSCs. Error bars represent SEM (n = 10). *** $p < 0.001$. (B-C) Primary blasts were isolated from 10 pediatric BCP-ALL patients and subsequently cultured for 5 days in absence or presence of primary MSCs during exposure to prednisolone (B**)** or l-asparaginase (C). Black bars represent the percentage of CD19-positive, annexin-PI-negative cells in mono-culture. White bars represent the percentage of CD19-positive, annexin-PI-negative cells in co-culture with MSCs. (D) Gene expression profiling was performed on healthy, umbilical cord blood-derived, CD34-positive hematopoietic progenitors (CB-CD34$^+$) ectopically expressing the ETV6-RUNX1 fusion gene and CB-CD34$^+$ cells expressing a control vector. Ingenuity pathway analysis of the differentially expressed genes (n = 196) was performed to analyze gene ontology (GO) functional categories that are predicted to be affected by the ectopic expression of ETV6-RUNX1 in CB-CD34$^+$ cells. A right-tailed Fisher's Exact Test after Benjamini-Hochberg multiple testing correction was used in all analyses to identify significantly regulated functional categories (>-log2 are depicted). (E**)** Gene expression profiles of ETV6-RUNX1 positive BCP-ALL (n = 172) and ETV6-RUNX1 negative BCP-ALL patients (n = 401; excluding T-ALL) were compared.

Figure 1. ETV6-RUNX1 induces a pro-migration gene expression signature including LARG. (Continued)
The top 500 most differentially regulated genes were subsequently used for pathway analysis. Ingenuity pathway analysis of the differentially expressed genes was used to analyze gene ontology (GO) functional categories that are predicted to be affected by this differential gene expression. (F) CB-CD34$^+$ cells were isolated from umbilical cord blood upon which the cells were divided in two fractions. One fraction was transduced with ETV6-RUNX1-IRES-eGFP, while the other fraction was transduced with control EV-IRES-eGFP. Forty hours after transduction, CD34$^+$eGFP$^+$ cells were sorted after which gene expression profiling was performed using Affymetrix GeneChip Human Genome U133 Plus 2.0 microarrays. Left panel represents the gene expression (linear) of *LARG* (*ARHGEF12*) in 5 different cord blood donors. Right panel represents mean and SD of *LARG* expression (^{10}log) in all donors (n = 5, p = 0.03) (G) Gene expression of *LARG* in ETV6-RUNX1 positive patients was compared to *LARG* expression in ETV6-RUNX1 negative patients. Graph shows the 2log expression of the gene probe set mapped to *LARG* (201334_s_at).
See also Supplementary Figure 1.

genes important in regulation of cytoskeletal organization (supplementary Figure 1C). Similar pathways were found to be enriched in leukemic cells of ETV6-RUNX1 positive BCP-ALL patients. We performed pathway analysis on differential gene expression between ETV6-RUNX1 positive (n = 172) and ETV6-RUNX1 negative (n = 481) patient-derived BCP-ALL cells. ETV6-RUNX1 positive BCP-ALL cells showed significant enrichment of genes involved in regulation of cellular movement and cell morphology (p = 1.10E^{-04} and p = 1.96E^{-03} respectively; Figure 1E).

LARG is up-regulated in ETV6-RUNX1 positive CB-CD34+ cells and ETV6-RUNX1 positive BCP-ALL

To identify ETV6-RUNX1 target genes that are responsible for the observed pro-migratory gene expression signature, we compared and ranked differentially expressed genes in ETV6-RUNX1 positive CB-CD34$^+$ cells and ETV6-RUNX1 positive BCP-ALL cells. In this analysis, *LARG* (*ARHGEF12*) showed to be significantly induced in both cell types (rank 1 for combined differential expression, supplementary Figure 1B). *LARG* was 5.4-fold up-regulated in CB-CD34$^+$ cells expressing ETV6-RUNX1 (p = 0.03; Figure 1F). In addition, *LARG* was 5.7-fold higher expressed in ETV6-RUNX1 positive primary ALL cells in comparison to ETV6-RUNX1 negative BCP-ALL cells (p = 1.02E^{-61}; Figure 1G).

Small molecule inhibition of LARG blocks chemotaxis and migration of ETV6-RUNX1 positive BCP-ALL cells

Since LARG and RhoA play an important role in regulation of cytoskeletal rearrangement and migration, we hypothesized that the induction of the LARG/RhoA signaling pathway contributes to the ETV6-RUNX1 induced migratory phenotype. Recently, Shang *et al.*[40,41] identified and validated two specific small molecules inhibiting the LARG/RhoA pathway: Y16, a specific LARG inhibitor, and G04 (Rhosin), a specific RhoA inhibitor. Combined, these small molecules exhibited

optimal functional inhibition[41]. To evaluate the effect of disruption of the LARG/RhoA axis on migration of BCP-ALL cells, we performed migration assays with ETV6-RUNX1 positive (REH and REHS1) and ETV6-RUNX1 negative cell lines (NALM6 and 697). Leukemic cells were allowed to migrate for 5 hours toward CXCL12 (SDF1) or primary mesenchymal stromal cells (MSCs) of three different donors, either in absence or presence of LARG/RhoA inhibitors. Blocking CXCR4 activity with AMD3100 (Plerixafor) resulted in 80-95% reduction in migration toward CXCL12 in all BCP-ALL cell lines, irrespective of the cytogenetic subtype (supplementary Figure 2A). In contrast, LARG/RhoA inhibition reduced migration of ETV6-RUNX1 positive cell lines toward CXCL12 by 75-80%, but did not affect chemotaxis of ETV6-RUNX1 negative BCP-ALL cell lines ($p \leq 0.05$; supplementary Figure 2B). In correspondence, migration of ETV6-RUNX1 positive BCP-ALL cell lines toward primary bone marrow derived MSCs was reduced by 75-90% after treatment with LARG/RhoA inhibitors ($p \leq 0.01$; Figure 2A). In contrast, migration of ETV6-RUNX1 negative BCP-ALL cells toward MSCs was either not affected or even induced by LARG/RhoA inhibition ($p \leq 0.05$; Figure 2B). Additionally, migration of ETV6-RUNX1 positive REH cells toward conditioned MSC medium was 70% reduced upon inhibition of LARG/RhoA ($p \leq 0.001$; Figure 2C). Next, we used bone marrow-derived primary leukemic cells of ETV6-RUNX1 positive BCP-ALL patients to confirm these findings. LARG/RhoA inhibition significantly reduced migration of primary ETV6-RUNX1 positive BCP-ALL cells toward CXCL12 by 25-45% ($n = 2$, $p \leq 0.05$; Figure 2D). Blocking CXCR4 activity with AMD3100 was more effective in inhibiting migration toward CXCL12 ($n = 2$, 65-70%, $p \leq 0.01$; Figure 2D) compared to LARG/RhoA inhibition, however combined inhibition of CXCR4 and LARG/RhoA almost completely abrogated migration of cells from patient #1 toward CXCL12 (95% reduction, $p \leq 0.001$; Figure 2E). Migration of cells from patient #2 was also significantly reduced by combined inhibition (80% reduction, $p \leq 0.001$; Figure 2E).

The above described experiments were also performed with solely small molecule inhibition of LARG (Y16), since we found LARG to be upregulated in ETV6-RUNX1 positive cells. A similar significant reduction in migration of ETV6-RUNX1 positive cell line and primary cells during LARG inhibition was observed (supplementary Figure 2C -2F).

LARG inhibition does not affect survival and drug resistance of primary BCP-ALL cells

Since RhoA activation has been implicated in regulation of cell division and the induction of drug resistance[43], we studied whether the observed reduced migration capacity was not caused by toxicity of the inhibitors. To investigate this, we performed survival analysis in an *ex vivo* co-culture model using primary BCP-ALL blasts and

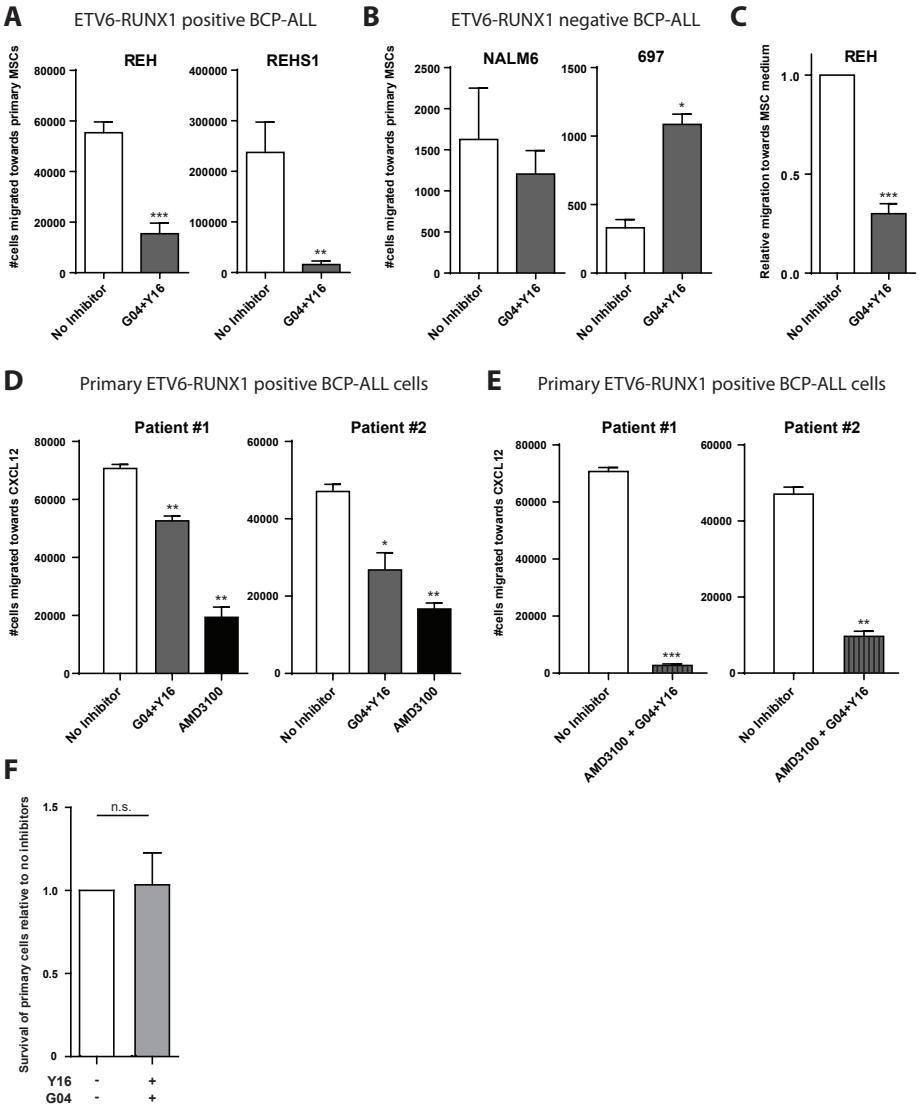

Figure 2. Small molecule inhibition of LARG / RhoA reduces migration of ETV6-RUNX1 positive BCP-ALL cells.

(A-B) Transwell migration assays were performed to analyze the effects of small molecule inhibition of LARG/RhoA on the migration of ETV6-RUNX1 positive (A) or ETV6-RUNX1 negative (B) BCP-ALL cells toward bone marrow-derived MSCs of three distinct donors. BCP-ALL cells were treated overnight with LARG and RhoA inhibitors (Y16 + G04) to inhibit the LARG/RhoA axis. Graphs represent the number of BCP-ALL cells that migrated toward primary MSCs (n = 4 for REH/REHS1/NALM6, n = 2 for 697; * $p \leq 0.05$, ** $p \leq 0.01$, *** $p \leq 0.001$). Error bars represent SEM. (C) REH cells were allowed to migrate toward conditioned medium of primary MSCs in a transwell migration assay in absence of presence of LARG/RhoA inhibitors. REH cells were treated overnight with Y16 and G04 (n = 7, *** $p < 0.001$).

Figure 2. Small molecule inhibition of LARG / RhoA reduces migration of ETV6-RUNX1 positive BCP-ALL cells. (continued)

(D-E) Primary leukemic cells of two patients with ETV6-RUNX1 positive BCP-ALL (Patient #1 and Patient #2) were allowed to migrate toward CXCL12 in a transwell migration assay in absence of presence of LARG/RhoA inhibitors and/or CXCR4 antagonist AMD3100/Plerixafor. BCP-ALL cells were treated overnight with LARG (Y16) and RhoA inhibitors (G04). AMD3100 was added 2 hours before the start of the experiment. (D) Bars represent number of migrated primary leukemic cells in presence of Y16 and G04 (dark grey bars), or in presence of AMD3100 (black bars). Error bars represent SEM of technical duplicates. * $p \leq 0.05$, ** $p \leq 0.01$. (E) Bars represent number of migrated primary leukemic cells in presence of Y16, G04 and AMD3100 (dark grey/black striped bars). Error bars represent SEM of technical duplicates. ** $p \leq 0.01$, *** $p \leq 0.001$. (F) Primary ETV6-RUNX1 positive BCP-ALL cells were co-cultured together with primary MSCs for 5 days in absence or presence of the LARG inhibitor Y16 and the RhoA inhibitor G04. Graph shows the relative survival (Annexin$^-$, Propidium Iodide$^-$, CD19$^+$ cells) of treated ETV6-RUNX1 positive BCP-ALL cells compared to the untreated control cells (n = 4). Error bars represent SEM. See also Supplementary Figure 2 - 5.

primary bone-marrow derived MSCs (supplementary Figure 3). Inhibition of LARG/RhoA signaling did not affect cell survival of primary ETV6-RUNX1 positive BCP-ALL cells in co-culture (Figure 2F). Similar results were obtained in experiments using only LARG inhibitor Y16 (supplementary Figure 2G).

Additionally, the effect of complete disruption of LARG/RhoA signaling on the proliferation and survival of BCP-ALL cell lines was investigated by silencing *LARG* expression using lentiviral short hairpin RNAs (supplementary Figure 4A). Knockdown of LARG mildly affected the proliferation of the ETV6-RUNX1 positive cell lines REH and REHS1 and the ETV6-RUNX1 negative cell line NALM6 ($p<0.05$; supplementary Figure 4B). However, all cell lines were still able to proliferate exponentially. The reduced proliferation was due to a moderate induction of apoptosis, but not to altered cell cycle progression (REH; supplementary Figure 4C and 4D). Also, phosphorylation of key signaling proteins in the PI3K/PKB/mTOR pathway (PKB/Akt and P70S6K), the MAPK/ERK pathway (ERK and p38), the SAPK/JNK pathway (JNK), NFκB signaling (NFκB) or JAK/STAT signaling (STAT3 and STAT5A/B) were not affected by LARG knockdown (supplementary Figure 5). Only the level of phosphorylated CREB (S133) was significantly reduced in LARG-knockdown BCP-ALL cells ($p < 0.05$; supplementary Figure 4E). This suggests a causal interaction between the activation of the LARG/RhoA axis and the activation of CREB, which is in line with earlier findings[44,45].

These results show that the strong inhibitory effect of LARG/RhoA inhibitors on the migratory phenotype of ETV6-RUNX1 positive leukemic cells cannot be attributed to reduced proliferation and/or apoptosis.

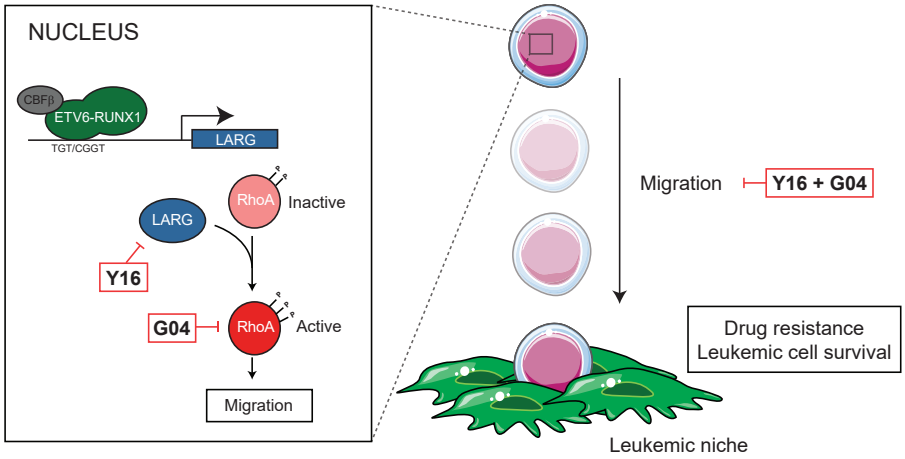

Figure 3. Proposed model for the induction of migration by LARG in ETV6-RUNX1 positive BCP-ALL cells.

ETV6-RUNX1 induces a pro-migration gene expression signature by inducing gene expression of LARG. The RhoA-sekective RhoGEF LARG subsequently switches RhoA from a GDP-bound/inactive to a GTP-bound/active state. This switch induces the migratory phenotype of the leukemic cells. Small molecule inhibition of LARG (Y16) and RhoA (G04) signaling selectively reduces migration of ETV6-RUNX1 positive leukemic cells. This observed reduction was not caused by toxicity of the inhibitors. Due to LARG/RhoA inhibition, ETV6-RUNX1 positive cells stop migrating toward the leukemic niche. Consequently, the leukemic niche, that normally facilitates leukemic cell survival and induces drug resistance, is disrupted. Hence, LARG/RhoA signaling may be a promising new approach to optimize treatment of ETV6-RUNX1 positive leukemia.

DISCUSSION

Disruption of the interaction between leukemic cells and their microenvironment remains a major challenge in leukemia treatment. Since CXCR4/CXCL12 signalling represents the most important chemokine axis regulating migration of hematopoietic stem cells[46,47] and lymphocytes[48], several studies have used growth factors disrupting the CXCR4/CXCL12 axis (e.g. G-CSF)[21,49] or small molecule inhibitors targeting the CXCR4/CXCL12 axis to inhibit migration of leukemic cells toward the niche. The promising pre-clinical results in these studies were mainly found in models representing acute myeloid leukemia[11-21]. In addition, phase 1/2 clinical trials have shown the feasibility of using CXCR4 antagonists during chemotherapeutic treatment of AML patients[19,50-52]. However, growth factor priming (with G-CSF/GM-CSF) of AML in more than 4000 AML patients has not resulted in an improved overall survival[53]. Moreover, recent data argues that leukemia stem cells are not mobilized by CXCR4 inhibition[54], suggesting that CXCR4 inhibition is not sufficient to completely disrupt leukemic niches. Furthermore, CXCR4 inhibition does not only interrupt the leukemic, but also the healthy hematopoietic niche[46,47].

Here, we show that the ETV6-RUNX1 fusion protein drives a pro-migratory gene expression signature in both healthy $CD34^+$ hematopoietic progenitors and leukemic cells. These findings are in concordance with a recent study showing that ETV6-RUNX1 induces expression of genes involved in cytoskeletal regulation and enhances the migratory capacity of mouse B cells[55], and with gene expression studies in ETV6-RUNX1 positive BCP-ALL cells showing significant enrichment of genes involved in the regulation of migration[56,57]. This study aimed to find the molecular drivers of migration in ETV6-RUNX1 positive leukemic cells. The discovery of the importance of the LARG/RhoA signaling pathway in migration of ETV6-RUNX1 positive leukemic cells makes selective inhibition of migration possible. Since our data indicate that migration of ETV6-RUNX1 positive ALL cells was significantly reduced by LARG/RhoA inhibitors, while migration of ETV6-RUNX1 negative cells was unaffected, we speculate that healthy hematopoietic niches are not affected by inhibiting LARG/RhoA signaling. In addition, our data suggest that LARG/RhoA inhibitors can work synergistically with CXCR4 antagonists, possibly boosting the potential of such agents in ETV6-RUNX1 positive BCP-ALL. For future clinical application of these findings, it is important to study the effects of small molecule inhibition of LARG/RhoA on both the healthy niche and the ETV6-RUNX1 positive leukemic niche *in vivo*. In addition, these experiments may reveal whether inhibiting migration of ETV6-RUNX1 positive cells is sufficient to enhance treatment efficiency.

In conclusion, we demonstrate that ETV6-RUNX1 induces a pro-migration gene expression signature and identify LARG as an important regulator of this phenotype. Small molecule inhibition of LARG/RhoA signaling selectively reduced migration of ETV6-RUNX1 positive leukemic cells. The observed reduced migration capacity was not caused by toxicity of the inhibitors. Therefore, small molecule inhibition of LARG/RhoA signaling may be a promising new approach to disrupt the ETV6-RUNX1 positive leukemic niche.

Author contributions

rPo designed the study, performed the experiments, collected and analyzed all data, and wrote the paper. MLDB, MB, and MBB designed the study, analyzed data, and wrote the paper. RESD performed experiments and analyzed data. BdR performed experiments, analyzed data, and wrote the paper. RPi discussed data and wrote the paper. All authors discussed the results and approved the submitted manuscript.

Acknowledgements

we thank all members of the research laboratory Pediatric Oncology of the Erasmus MC for their help in processing leukemic and mesenchymal stromal cell samples; The Department of Hematology of the Erasmus MC for providing the use of Flow

Cytometers; The Vlietland Ziekenhuis for collecting and providing cord blood. The work described in this paper was funded by the KiKa Foundation (Stichting Kinderen Kankervrij – Kika-39), the Dutch Cancer Society (UVA 2008; 4265, EMCR 2010; 4687), the Netherlands Organization for Scientific Research (NWO – VICI M.L. den Boer) and the Pediatric Oncology Foundation Rotterdam.

REFERENCES

1. Walkley, C.R., *et al.* A microenvironment-induced myeloproliferative syndrome caused by retinoic acid receptor gamma deficiency. *Cell* **129**, 1097-1110 (2007).
2. Raaijmakers, M.H., *et al.* Bone progenitor dysfunction induces myelodysplasia and secondary leukaemia. *Nature* **464**, 852-857 (2010).
3. Flynn, C.M. & Kaufman, D.S. Donor cell leukemia: insight into cancer stem cells and the stem cell niche. *Blood* **109**, 2688-2692 (2007).
4. Hanahan, D. & Weinberg, R.A. Hallmarks of cancer: the next generation. *Cell* **144**, 646-674 (2011).
5. Fujisaki, J., *et al.* In vivo imaging of Treg cells providing immune privilege to the haematopoietic stem-cell niche. *Nature* **474**, 216-219 (2011).
6. Nakasone, E.S., *et al.* Imaging tumor-stroma interactions during chemotherapy reveals contributions of the microenvironment to resistance. *Cancer Cell* **21**, 488-503 (2012).
7. McMillin, D.W., *et al.* Tumor cell-specific bioluminescence platform to identify stroma-induced changes to anticancer drug activity. *Nat Med* **16**, 483-489 (2010).
8. Polak, R., de Rooij, B., Pieters, R. & den Boer, M.L. B-cell precursor acute lymphoblastic leukemia cells use tunneling nanotubes to orchestrate their microenvironment. *Blood* **126**, 2404-2414 (2015).
9. Sipkins, D.A., *et al.* In vivo imaging of specialized bone marrow endothelial microdomains for tumour engraftment. *Nature* **435**, 969-973 (2005).
10. Matsunaga, T., *et al.* Interaction between leukemic-cell VLA-4 and stromal fibronectin is a decisive factor for minimal residual disease of acute myelogenous leukemia. *Nat Med* **9**, 1158-1165 (2003).
11. Burger, J.A. & Peled, A. CXCR4 antagonists: targeting the microenvironment in leukemia and other cancers. *Leukemia* **23**, 43-52 (2009).
12. Tavor, S., *et al.* CXCR4 regulates migration and development of human acute myelogenous leukemia stem cells in transplanted NOD/SCID mice. *Cancer Res* **64**, 2817-2824 (2004).
13. Nervi, B., *et al.* Chemosensitization of acute myeloid leukemia (AML) following mobilization by the CXCR4 antagonist AMD3100. *Blood* **113**, 6206-6214 (2009).
14. Burger, M., *et al.* Small peptide inhibitors of the CXCR4 chemokine receptor (CD184) antagonize the activation, migration, and antiapoptotic responses of CXCL12 in chronic lymphocytic leukemia B cells. *Blood* **106**, 1824-1830 (2005).
15. Juarez, J., *et al.* CXCR4 antagonists mobilize childhood acute lymphoblastic leukemia cells into the peripheral blood and inhibit engraftment. *Leukemia* **21**, 1249-1257 (2007).
16. Tavor, S., *et al.* The CXCR4 antagonist AMD3100 impairs survival of human AML cells and induces their differentiation. *Leukemia* **22**, 2151-5158 (2008).
17. Parameswaran, R., Yu, M., Lim, M., Groffen, J. & Heisterkamp, N. Combination of drug therapy in acute lymphoblastic leukemia with a CXCR4 antagonist. *Leukemia* **25**, 1314-1323 (2011).
18. O'Callaghan, K., *et al.* Targeting CXCR4 with cell-penetrating pepducins in lymphoma and lymphocytic leukemia. *Blood* **119**, 1717-1725 (2012).
19. Fierro, F.A., *et al.* Combining SDF-1/CXCR4 antagonism and chemotherapy in relapsed acute myeloid leukemia. *Leukemia* **23**, 393-396 (2009).

20. Zeng, Z., *et al.* Targeting the leukemia microenvironment by CXCR4 inhibition overcomes resistance to kinase inhibitors and chemotherapy in AML. *Blood* **113**, 6215-6224 (2009).
21. Lowenberg, B., *et al.* Effect of priming with granulocyte colony-stimulating factor on the outcome of chemotherapy for acute myeloid leukemia. *N Engl J Med* **349**, 743-752 (2003).
22. Zelent, A., Greaves, M. & Enver, T. Role of the TEL-AML1 fusion gene in the molecular pathogenesis of childhood acute lymphoblastic leukaemia. *Oncogene* **23**, 4275-4283 (2004).
23. Golub, T.R., *et al.* Fusion of the TEL gene on 12p13 to the AML1 gene on 21q22 in acute lymphoblastic leukemia. *Proc Natl Acad Sci U S A* **92**, 4917-4921 (1995).
24. Shurtleff, S.A., *et al.* TEL/AML1 fusion resulting from a cryptic t(12;21) is the most common genetic lesion in pediatric ALL and defines a subgroup of patients with an excellent prognosis. *Leukemia* **9**, 1985-1989 (1995).
25. Loh, M.L., *et al.* Prospective analysis of TEL/AML1-positive patients treated on Dana-Farber Cancer Institute Consortium Protocol 95-01. *Blood* **107**, 4508-4513 (2006).
26. Pieters, R., *et al.* Successful Therapy Reduction and Intensification for Childhood Acute Lymphoblastic Leukemia Based on Minimal Residual Disease Monitoring: Study ALL10 From the Dutch Childhood Oncology Group. *J Clin Oncol* **34**, 2591-2601 (2016).
27. Stams, W.A., *et al.* Incidence of additional genetic changes in the TEL and AML1 genes in DCOG and COALL-treated t(12;21)-positive pediatric ALL, and their relation with drug sensitivity and clinical outcome. *Leukemia* **20**, 410-416 (2006).
28. Seeger, K., *et al.* TEL-AML1 fusion in relapsed childhood acute lymphoblastic leukemia. *Blood* **94**, 374-376 (1999).
29. van Delft, F.W., *et al.* Clonal origins of relapse in ETV6-RUNX1 acute lymphoblastic leukemia. *Blood* **117**, 6247-6254 (2011).
30. Booden, M.A., Siderovski, D.P. & Der, C.J. Leukemia-associated Rho guanine nucleotide exchange factor promotes G alpha q-coupled activation of RhoA. *Mol Cell Biol* **22**, 4053-4061 (2002).
31. Fukuhara, S., Chikumi, H. & Gutkind, J.S. RGS-containing RhoGEFs: the missing link between transforming G proteins and Rho? *Oncogene* **20**, 1661-1668 (2001).
32. Reuther, G.W., *et al.* Leukemia-associated Rho guanine nucleotide exchange factor, a Dbl family protein found mutated in leukemia, causes transformation by activation of RhoA. *J Biol Chem* **276**, 27145-27151 (2001).
33. Shi, Y., *et al.* The mDial formin is required for neutrophil polarization, migration, and activation of the LARG/RhoA/ROCK signaling axis during chemotaxis. *J Immunol* **182**, 3837-3845 (2009).
34. Guilluy, C., *et al.* The Rho GEFs LARG and GEF-H1 regulate the mechanical response to force on integrins. *Nat Cell Biol* **13**, 722-727 (2011).
35. Saci, A. & Carpenter, C.L. RhoA GTPase regulates B cell receptor signaling. *Mol Cell* **17**, 205-214 (2005).
36. Goulimari, P., Knieling, H., Engel, U. & Grosse, R. LARG and mDia1 link Galpha12/13 to cell polarity and microtubule dynamics. *Mol Biol Cell* **19**, 30-40 (2008).
37. Kourlas, P.J., *et al.* Identification of a gene at 11q23 encoding a guanine nucleotide exchange factor: evidence for its fusion with MLL in acute myeloid leukemia. *Proc Natl Acad Sci U S A* **97**, 2145-2150 (2000).
38. Lessey-Morillon, E.C., *et al.* The RhoA guanine nucleotide exchange factor, LARG, mediates ICAM-1-dependent mechanotransduction in endothelial cells to stimulate transendothelial migration. *J Immunol* **192**, 3390-3398 (2014).

39. Kitzing, T.M., *et al.* Positive feedback between Dia1, LARG, and RhoA regulates cell morphology and invasion. *Genes Dev* **21**, 1478-1483 (2007).
40. Shang, X., *et al.* Rational design of small molecule inhibitors targeting RhoA subfamily Rho GTPases. *Chem Biol* **19**, 699-710 (2012).
41. Shang, X., *et al.* Small-molecule inhibitors targeting G-protein-coupled Rho guanine nucleotide exchange factors. *Proc Natl Acad Sci U S A* **110**, 3155-3160 (2013).
42. Vigil, D., Cherfils, J., Rossman, K.L. & Der, C.J. Ras superfamily GEFs and GAPs: validated and tractable targets for cancer therapy? *Nat Rev Cancer* **10**, 842-857 (2010).
43. Doublier, S., *et al.* RhoA silencing reverts the resistance to doxorubicin in human colon cancer cells. *Mol Cancer Res* **6**, 1607-1620 (2008).
44. Ha, J.H., Ward, J.D., Varadarajalu, L., Kim, S.G. & Dhanasekaran, D.N. The gep proto-oncogene Galpha12 mediates LPA-stimulated activation of CREB in ovarian cancer cells. *Cell Signal* **26**, 122-132 (2014).
45. Sordella, R., *et al.* Modulation of CREB activity by the Rho GTPase regulates cell and organism size during mouse embryonic development. *Dev Cell* **2**, 553-565 (2002).
46. Aiuti, A., Webb, I.J., Bleul, C., Springer, T. & Gutierrez-Ramos, J.C. The chemokine SDF-1 is a chemoattractant for human CD34+ hematopoietic progenitor cells and provides a new mechanism to explain the mobilization of CD34+ progenitors to peripheral blood. *The Journal of experimental medicine* **185**, 111-120 (1997).
47. Peled, A., *et al.* Dependence of human stem cell engraftment and repopulation of NOD/SCID mice on CXCR4. *Science* **283**, 845-848 (1999).
48. Bleul, C.C., Fuhlbrigge, R.C., Casasnovas, J.M., Aiuti, A. & Springer, T.A. A highly efficacious lymphocyte chemoattractant, stromal cell-derived factor 1 (SDF-1). *The Journal of experimental medicine* **184**, 1101-1109 (1996).
49. Petit, I., *et al.* G-CSF induces stem cell mobilization by decreasing bone marrow SDF-1 and up-regulating CXCR4. *Nat Immunol* **3**, 687-694 (2002).
50. Uy, G.L., *et al.* A phase 1/2 study of chemosensitization with the CXCR4 antagonist plerixafor in relapsed or refractory acute myeloid leukemia. *Blood* **119**, 3917-3924 (2012).
51. Borthakur, G. BL-8040, a Peptidic CXCR4 Antagonist, Induces Leukemia Cell Death and Specific Leukemia Cell Mobilization in Relapsed/Refractory Acute Myeloid Leukemia Patients in an Ongoing Phase IIa Clinical Trial. *ASH Abstract 950* (2014).
52. Becker, P.S. Targeting the CXCR4 Pathway: Safety, Tolerability and Clinical Activity of Ulocuplumab (BMS-936564), an Anti-CXCR4 Antibody, in Relapsed/Refractory Acute Myeloid Leukemia. *ASH Abstract 386* (2014).
53. Ottmann, O.G., Bug, G. & Krauter, J. Current status of growth factors in the treatment of acute myeloid and lymphoblastic leukemia. *Semin Hematol* **44**, 183-192 (2007).
54. Heuser, M., *et al.* Priming reloaded? *Blood* **114**, 925-926; author reply 926-927 (2009).
55. Palmi, C., *et al.* Cytoskeletal Regulatory Gene Expression and Migratory Properties of B Cell Progenitors are Affected by the ETV6-RUNX1 Rearrangement. *Mol Cancer Res* (2014).
56. Linka, Y., *et al.* The impact of TEL-AML1 (ETV6-RUNX1) expression in precursor B cells and implications for leukaemia using three different genome-wide screening methods. *Blood Cancer J* **3**, e151 (2013).
57. Gandemer, V., *et al.* Five distinct biological processes and 14 differentially expressed genes characterize TEL/AML1-positive leukemia. *BMC Genomics* **8**, 385 (2007).

SUPPLEMENTARY DATA

SUPPLEMENTARY METHODS

Cell lines and reagents

BCP-ALL cell lines NALM6 (B-Other), REH (ETV6-RUNX1), 697 (TCF3-PBX1), and human embryonic kidney cell line HEK293T were obtained from DSMZ (Braunschweig, Germany) and used only at low passages. REHS1 (REH subclone #1; ETV6-RUNX1) is an ETV6-RUNX1 positive cell line with an identical genetic background as REH, but with different phenotypic characteristics (proliferation and drug resistance profiles). DNA fingerprinting was performed routinely to verify authenticity of cell lines. ALL cell lines were cultured in RPMI-1640 medium (Gibco, Life Technologies, Bleiswijk, the Netherlands) supplemented with 10% fetal calf serum (FCS) and 1% penicillin-streptomycin at 37 °C and 5% CO_2. HEK293T cells were cultured in high glucose Dulbecco's Modified Eagle's Medium with Glutamax (Gibco) supplemented with 10% FCS and 1% penicillin-streptomycin at 37 °C and 5% CO_2. LARG inhibitor Y16, and RhoA inhibitor G04 were obtained from Calbiochem (Calbiochem, Merck Millipore, Billerica, MA, USA). AMD3100 was obtained from Sigma (Sigma-Aldrich, St. Louis, MO, USA).

Isolation of CD34 positive hematopoietic cells from cord blood

Mononuclear cells were isolated from human umbilical cord blood (UCB) using Lymphoprep sucrose-gradient centrifugation (1.077 g/ml, Nycomed Pharma, Oslo, Norway). Immunomagnetic cell separation, using magnetic beads coated with CD34 antibodies (Miltenyi Biotec, Gladbach, Germany), was performed to isolate CD34 positive hematopoietic progenitor cells (CB-$CD34^+$ cells). Cells were cultured in Iscove's Modified Dulbecco's Medium (Gibco) supplemented with 10% FCS, 50μM β-mercaptoethanol, 1% penicillin-streptomycin, 2mM glutamine, stem cell factor (SCF; 50ng/mL; Peprotech) and fms-like tyrosine kinase-3 ligand (Flt3L; 50 ng/mL; Peprotech) at 37°C and 5% CO2. UCB was obtained after informed consent was provided according to the Declaration of Helsinki. Protocols were approved by the ethics committee of the Erasmus University Medical Centre in Rotterdam.

Isolation of primary BCP-ALL leukemic blasts from patients

Bone marrow aspirates were obtained from children with newly diagnosed BCP-ALL prior to treatment. Immunophenotype and genetic subtype were determined according to local hospital procedures and monitored by the central diagnostic laboratory of the Dutch Childhood Oncology Group (DCOG) in The Hague. Primary

BCP-ALL cells were isolated as described previously[1]. Primary ALL samples used in this study contained more than 95% leukemic cells. Cells were cultured in RPMI Dutch-modified medium (Gibco) supplemented with 20% FCS, Insulin transferrin sodium selenite (ITS), glutamin and gentamycin at 37 °C and 5% CO_2. Bone marrow aspirates were obtained after informed consent of patients and/or parents/guardians was provided according to the Declaration of Helsinki. Protocols were approved by the ethics committee of the Erasmus University Medical Centre in Rotterdam.

Isolation and characterization of primary MSCs

Mesenchymal stromal cells (MSCs) were isolated, as described previously[2], from bone marrow aspirates collected during diagnostic procedures. A panel of positive (CD44/ CD90/ CD105/ CD54/ CD73/ CD146/ CD166/ STRO-1) and negative surface markers (CD19/ CD45/ CD34) was used to characterize the MSCs (the human mesenchymal stem cell marker antibody panel, R&D Systems, Minneapolis, MN, USA, and the monoclonal antibodies CD54-PE, CD73-PE, CD34-PE, and IgG1-PE, BD Biosciences, San Jose, CA, USA). The multilineage potential of the selected MSCs was confirmed by allowing the cells to differentiate toward adipocytes (Oil Red O staining), osteocytes (Alizarin Red S staining), and chondrocytes (Col2a/Thionine/ Alcian Blue staining).

Retroviral transduction of CB-CD34$^+$ cells, cell sorting and gene expression profiling.

Retroviral transduction, cell sorting and gene expression profiling was performed. In short, to generate retrovirus, bicistronic retroviral DNA constructs were used co-expressing the ETV6-RUNX1 fusion gene and enhanced Green Fluorescent Protein (eGFP). As a control, a construct expressing eGFP alone was used. HEK293T cells were co-transfected with these constructs and second-generation retroviral packaging vectors using XtremeGENE 9 transfection reagents (Roche, Basel, Switzerland). Viral particles were filtered and collected in IMDM. CD34$^+$ hematopoietic progenitors, pre-cultured overnight as described above, were subsequently transduced with fresh retrovirus in retronectin (Takara, Otsu, Japan) coated wells. Transduced CB-CD34$^+$ cells were sorted using a BD ARIA II sorter (BD Biosciences) after staining with DAPI (Sigma) and incubation with a PeCy7-conjugated CD34 antibody (BD Biosciences). The DAPI negative, CD34 positive and eGFP positive population was used for further experiments. After lysis, RNA was extracted using Nucleospin RNA XS extraction columns according to manufacturer's protocol (Macherey-Nagel, Düren, Germany). Quality of RNA was determined by on-chip-electrophoresis using a RNA Pico Chip according to manufacturer's protocol (Agilent Technologies, Santa Clara, CA, USA). RNA Integrity scores (RIN) were higher than 8 for all samples. RNA was

subsequently amplified in a linear manner using the Nugen WT-Amplification™ pico system (Nugen, San Carlos, CA, USA). Samples were run on Affymetrix gene expression arrays (Santa Clara, CA, USA). Data was normalized using vsnRMA and analyzed using a linear mixed model[3]. Genes were considered differentially expressed when $p \leq 0.05$ after multiple testing using FDR.

Ingenuity Pathway Analysis

Network and functional analyses of differential gene expression were generated by QIAGEN's Ingenuity Pathway Analysis (IPA, QIAGEN, Redwood City, USA). The expected change in biological functions, based on the observed change in gene expression, was tested using right-tailed Fisher's Exact Test after Benjamini-Hochberg multiple testing correction.

BCP-ALL chemotaxis and migration assays

All experiments were performed using RPMI without FCS at 37°C and 5% CO_2. 5 x 10^4 primary MSCs cells were cultured in the lower compartment of a transwell in a volume of 750 μL for 48 hours prior to the start of the experiment (bottom compartment). Leukemic cells were cultured overnight in absence or presence of LARG inhibitors (Y16, or Y16+G04) or AMD3100 in RPMI without FCS. At the start of experiment, 5 x 10^5 cells, in a volume of 250 μL, were added to the upper compartment of a 6.5 mm diameter transwell system (Corning, NY, USA) with a pore size of 5 μm. Cells were allowed to migrate for 6 hours. At the end of experiment, all cells in the bottom compartment were harvested and stained with DAPI (Life Technologies) and antibodies against human CD19 (Brilliant Violet 421 anti-human CD19 antibody, Biolegend, San Diego, CA, USA). A MACSQuant analyzer (Miltenyi Biotec, Gladbach, Germany) was used to determine the number/percentage of migrated $DAPI^-/CD19^+$ cells.

Lentiviral knockdown of LARG

Lentivirus was produced by transfecting HEK293T cells with second generation lentiviral helper vectors pPax2 (Addgene plasmid 12260) and VSV-G envelope (pMD2G; Addgene plasmid 12259) together with pLKO.1 Mission vector (Sigma) targeting *LARG* (*ARHGEF12*). Transfection was performed using XtremeGENE transfection reagent according to manufacturer's protocol (Promega, Madison, WI, USA). Target sequences used to silence *LARG* were: GCGTTGCGTAATCATCCAGAA (LARG#1; TRCN0000047480); CGTCGCATCTTCCTTGAGTTT (LARG#2; TRCN0000047478); CCAGAAGTTCAAAGGCACTTA (LARG#3; TRCN0000047481); GCGAGTATCCAGAGAAGGAAT (LARG#4; TRCN0000047482); CCACTCAAATGCAAAGGCTTA (LARG #5; TRCN0000047479). Efficient reduction

of LARG protein levels was achieved using constructs LARG#1, LARG#4, and LARG#5. However, LARG#4 was predicted to partially bind three other human RNAs (LYRM1, DHRS7C, and LOC101927461). Therefore, only LARG#1 and LARG#5 were used for further experiments. Target sequence used for non-mammalian shRNA control vector was CAACAAGATGAAGAGCACCAA (NSC; SHC002). Virus was collected and concentrated by ultracentrifugation for 2 hours at 13.000 rpm. For each experiment and cell line, virus was titrated to obtain a transduction efficiency of ~90%. This condition was equal to a MOI of 2.5. Cell lines were transduced using a spin-infection protocol. Cells were subsequently selected using the puromycin selection marker. A MACSQuant Analyzer (Miltenyi Biotec, Germany) was used to determine the number of viable, Propidium Iodide negative, cells.

Analysis of protein phosphorylation.

To analyze protein phosphorylation, we used a multiplex cell signaling assay according to manufacturer's protocol (MILLIPLEX MAP Multi-pathway Magnetic Bead 9-Plex; Merck Millipore). In short, equal amount of cells were lysed with MILLIPLEX MAP Lysis Buffer containing freshly prepared protease inhibitors. Next, we added β-tubulin control beads as a loading control and performed protein expression quantification using the Luminex system (Luminex Corp., Austin, TX, USA). This assay was used to quantify the level of phosphorylation of the following proteins: CREB (pS133), ERK (pT185/pY187), NFκB (pS536), JNK (pT183/pY185), p38 (pT180/pY182), p70 S6K (pT412), STAT3 (pS727), STAT5A/B (pY694/699), PKB/Akt (pS473).

Cell viability assays on primary patient cells

Primary patient cells (1×10^6 cells) were co-cultured in absence or presence of primary MSCs (5×10^4) for five days in a 24-well plate at 37 °C and 5% CO_2 in presence or in absence of the small molecules G04 and/or Y16. Stromal cells were allowed to attach prior to the start of the experiment. Before the start of each experiment, leukemic cells were screened for CD19 positivity (anti-human CD19 Brilliant Violet 421 antibody). After five days of culture the percentage of viable leukemic cells was determined by flow cytometric analysis after staining with anti-human CD19 Brilliant Violet 421 antibody (Biolegend), Annexin V FITC (Biolegend), and Propidium Iodide (PI; Sigma). Primary leukemic cells were exposed to L-Asparaginase, Prednisolone or 6-Mercaptopurine in a concentration that was lethal to 50% of the patient derived leukemic cells (LC50) as determined upfront by a 4-day MTT assay[1].

Statistical analysis

Statistical analysis of microarray data of paired (EV-eGFP$^+$ versus ETV6-RUNX1-eGFP$^+$) CB-CD34$^+$ was performed using a linear mixed model in which multiple testing correction was applied by FDR. Microarray data of primary cells from ALL patients were analyzed using ANOVA and FDR multiple testing.

Both the Student's t-test and the Student's paired t-test were used as statistical test when applicable (indicated in figure legends). Bar graphs represent the mean of biological replicates. Error bars represent standard error of the mean (SEM).

REFERENCES

1. Den Boer ML, Harms DO, Pieters R, Kazemier KM, Gobel U, Korholz D, *et al.* Patient stratification based on prednisolone-vincristine-asparaginase resistance profiles in children with acute lymphoblastic leukemia. *J Clin Oncol* 2003 Sep 1; **21**(17)**:** 3262-3268.
2. van den Berk LC, van der Veer A, Willemse ME, Theeuwes MJ, Luijendijk MW, Tong WH, *et al.* Disturbed CXCR4/CXCL12 axis in paediatric precursor B-cell acute lymphoblastic leukaemia. *Br J Haematol* 2014 Jul; **166**(2)**:** 240-249.
3. Bates D, Mächler M, Bolker B, Walker S. Fitting linear mixed-effects models using lme4. *arXiv preprint arXiv:14065823* 2014.

SUPPLEMENTARY FIGURES

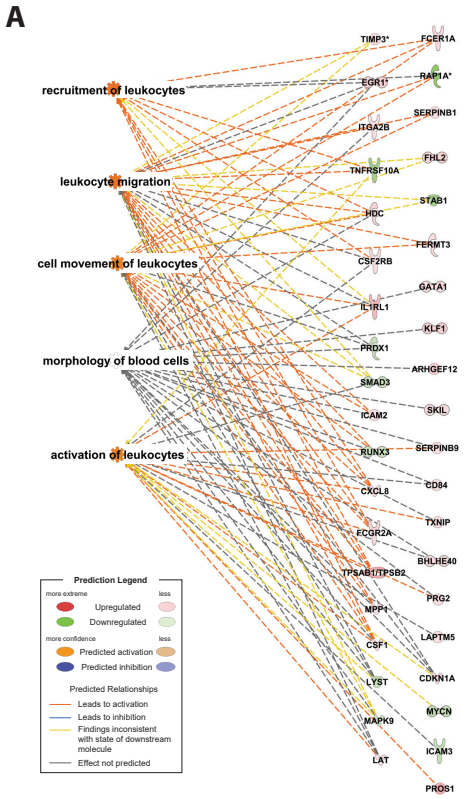

B

	BCP-ALL		CB-CD34+		
Gene name	p-value	Fold Change	p-value	Fold Change	*Rank*
LARG	1.02E-61	5.75	0.0298	5.38	*1*
HOPX	2.24E-16	2.77	0.0464	7.37	*2*
FAM171A1	6.14E-17	2.47	0.0108	7.087	*3*
KCNK6	4.08E-11	1.23	0.0350	9.427	*4*
SPINK2	1.78E-19	2.26	0.0317	4.537	*5*
TIMP3	3.10E-16	1.37	0.0415	3.84	*6*
TRIB2	2.00E-11	1.59	0.0328	5.72	*7*
LMO4	1.31E-23	1.35	0.00148	2.95	*8*
CDKN1A	8.24E-12	1.92	0.0355	4.74	*9*
GATA2	2.16E-21	1.23	0.0449	2.61	*10*
STXBP5	1.34E-13	1.52	0.0240	3.76	*11*
DLC1	5.83E-11	1.57	0.0383	4.46	*12*
RUNX1	0.0177	1.25	0.00764	9.36	*13*
DLC1	0.000414	1.11	0.0367	3.83	*14*
PLAG1	5.56E-34	1.83	0.00230	2.12	*15*
CATSPER2	1.15E-15	1.29	0.0222	2.62	*16*
AP1S1	3.06E-11	1.32	0.0244	2.85	*17*
KIAA1274	1.24E-13	1.41	0.0289	2.77	*18*
NHEDC2	4.28E-22	1.59	0.00638	2.18	*19*
CMIP	1.04E-07	1.27	0.0320	2.61	*20*
MTSS1	0.00103	1.22	0.0317	4.67	*21*
PROS1	3.60E-05	1.11	0.0317	9.64	*22*
TNFRSF10A	5.24E-08	1.19	0.0355	3.41	*23*
CMIP	4.37E-13	1.25	0.0317	2.49	*24*
BHLHE40	1.96E-08	1.97	0.00350	3.07	*25*

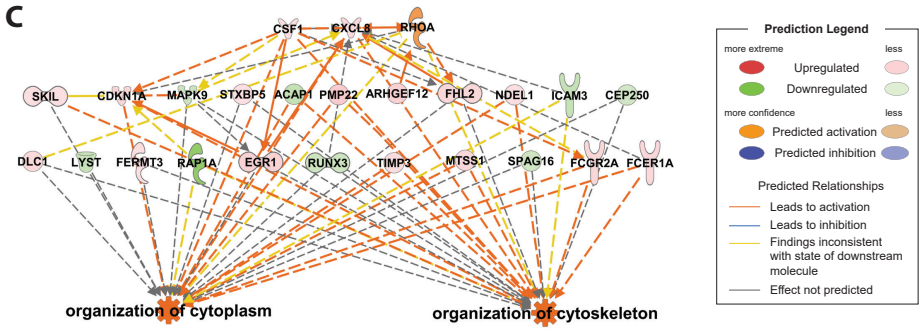

Supplementary Figure 1. ETV6-RUNX1 drives a pro-migratory signature in hematopoietic progenitors.

(A) Ingenuity pathway analysis was used to visualize genes inducing the migratory phenotype of ETV6-RUNX1 positive cells. This overview shows the predicted effect of differentially expressed genes in ETV6-RUNX1 positive CB-CD34^{+} cells on cellular processes involved in cell morphology and cellular movement (recruitment of leukocytes, leukocyte migration, cell movement of leukocytes, morphology of blood cells, and activation of leukocytes). Dashed lines indicate indirect regulation. Solid lines indicate direct regulation.

Supplementary Figure 1. ETV6-RUNX1 drives a pro-migratory signature in hematopoietic progenitors. (Continued)

(B) Differentially expressed genes in ETV6-RUNX1 positive CB-CD34$^+$ cells and ETV6-RUNX1 positive BCP-ALL cells were ranked (the top 500 most differentially regulated genes in BCP-ALL by p-value, and the differentially regulated genes in CB-CD34$^+$ cells by fold change of expression). The sum of ranks was calculated and genes were ordered based on the lowest sum of ranks, which correlated with the highest differential expression in this combined analyses. This table provides a toplist of this analysis. (C) Ingenuity pathway analysis was used to visualize genes important for the predicted change in cytoskeletal regulation. This overview shows the predicted effect of differentially expressed genes in ETV6-RUNX1 positive CB-CD34$^+$ cells on cellular processes involved in organization of cytoskeleton and cytoplasm. Dashed lines indicate indirect regulation. Solid lines indicate direct regulation.

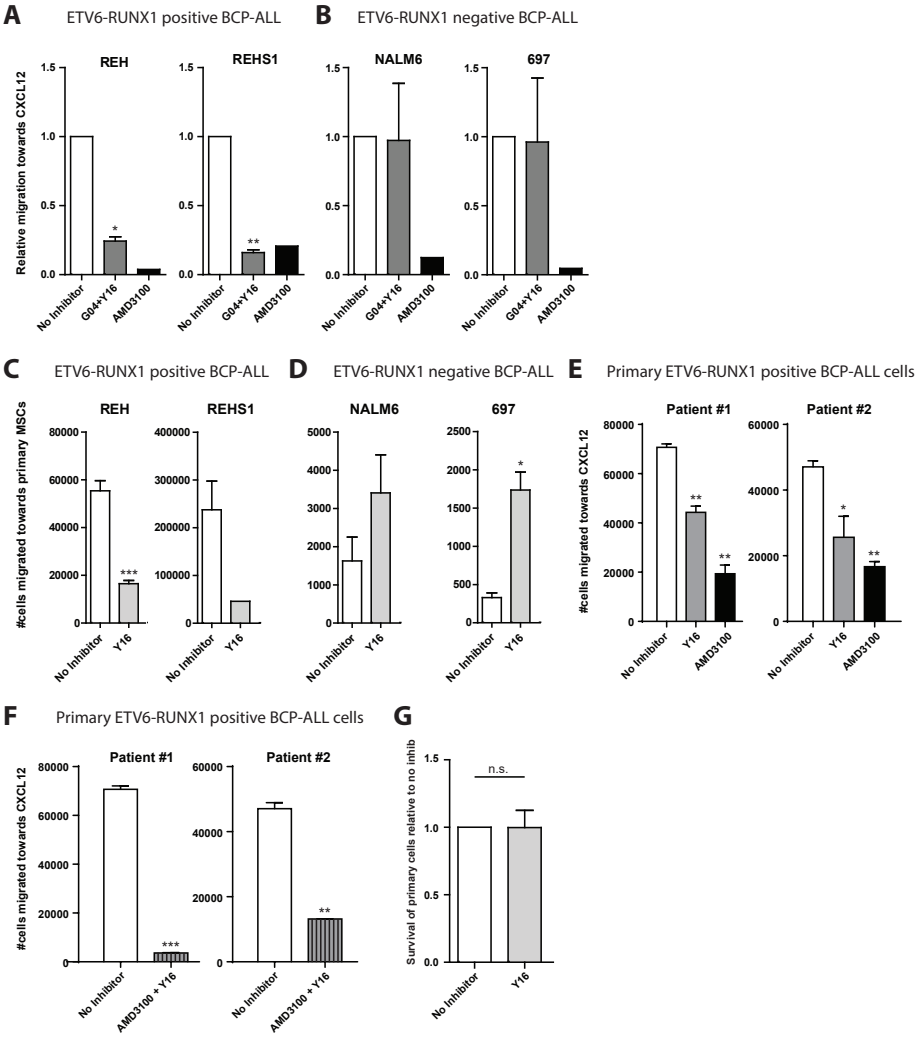

Supplementary Figure 2. Small molecule inhibition of LARG reduces migration of ETV6-RUNX1 positive BCP-ALL.

Supplementary Figure 2. Small molecule inhibition of LARG reduces migration of ETV6-RUNX1 positive BCP-ALL. (Continued)

(A-B) Transwell migration assays were performed to analyze the effects of small molecule inhibition of LARG/RhoA on the migration of BCP-ALL cells toward CXCL12. (A) shows the relative migration of the ETV6-RUNX1 positive cell lines REH and REHS1 toward CXCL12 in absence or presence of inhibitors. (B) shows the relative migration of ETV6-RUNX1 negative cell lines NALM6 and 697 toward CXCL12 in absence of presence of inhibitors. We used Y16 (LARG inhibitor) and G04 (RhoA inhibitor) to disrupt the LARG/RhoA signaling axis (n = 2, * $p < 0.05$; ** $p < 0.01$). As a positive control we used AMD3100, a CXCR4 antagonist (n = 1). BCP-ALL cells were treated overnight with Y16 and G04. AMD3100 was added 2 hours before the start of the experiment. (C-D) Transwell migration assays were performed to analyze the effects of small molecule inhibition of LARG on the migration of ETV6-RUNX1 positive (C) or ETV6-RUNX1 negative (D) BCP-ALL cells toward bone marrow-derived MSCs of three distinct donors. BCP-ALL cells were treated overnight with LARG inhibitors. Graphs represent the number of BCP-ALL cells that migrated toward primary MSCs (n = 4 for REH /NALM6, n = 2 for 697, n = 1 for REHS1). Error bars represent SEM. *** $p \leq 0.001$. (E-F) Primary leukemic cells of two patients with ETV6-RUNX1 positive BCP-ALL (Patient #1 and Patient #2) were allowed to migrate toward CXCL12 in a transwell migration assay in absence of presence of LARG inhibitors and/or CXCR4 antagonist AMD3100. BCP-ALL cells were treated overnight with LARG (Y16). AMD3100 was added 2 hours before the start of the experiment. (E) Bars represent number of migrated primary leukemic cells in presence of Y16 (grey bars), or in presence of AMD3100 (black bars). Error bars represent SEM of technical duplicates. * $p \leq 0.05$, ** $p \leq 0.01$. (F) Bars represent number of migrated primary leukemic cells in presence of Y16 and AMD3100 (grey/black striped bars). Error bars represent SEM of technical duplicates. ** $p \leq 0.01$, *** $p \leq 0.001$. (G) Primary ETV6-RUNX1 BCP-ALL cells were cultured for 5 days in absence of presence of the LARG inhibitor Y16. Graph shows the relative survival (Annexin$^-$, Propidium Iodide$^-$, CD19$^+$ cells) of treated ETV6-RUNX1 BCP-ALL cells compared to the untreated control cells (n = 4).

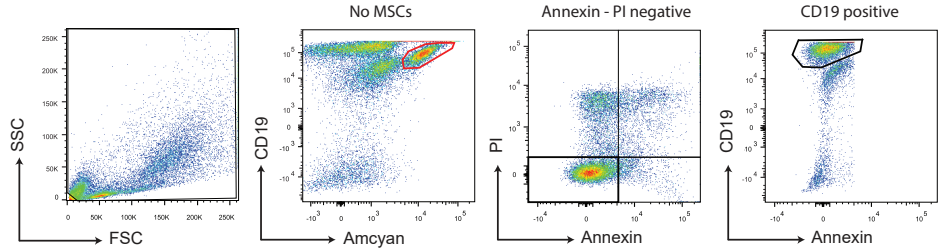

Supplementary Figure 3. Gating strategy used to quantify the number of living primary BCP-ALL cells in co-culture.

Primary ETV6-RUNX1 BCP-ALL cells were co-cultured together with primary MSCs for 5 days after which we analyzed survival using Annexin V, Propidium Iodide and CD19. Flow cytometrical analysis was performed as depicted here. The red gate in the second panel shows the mesenchymal stromal cells. MSCs were excluded in further survival analyses.

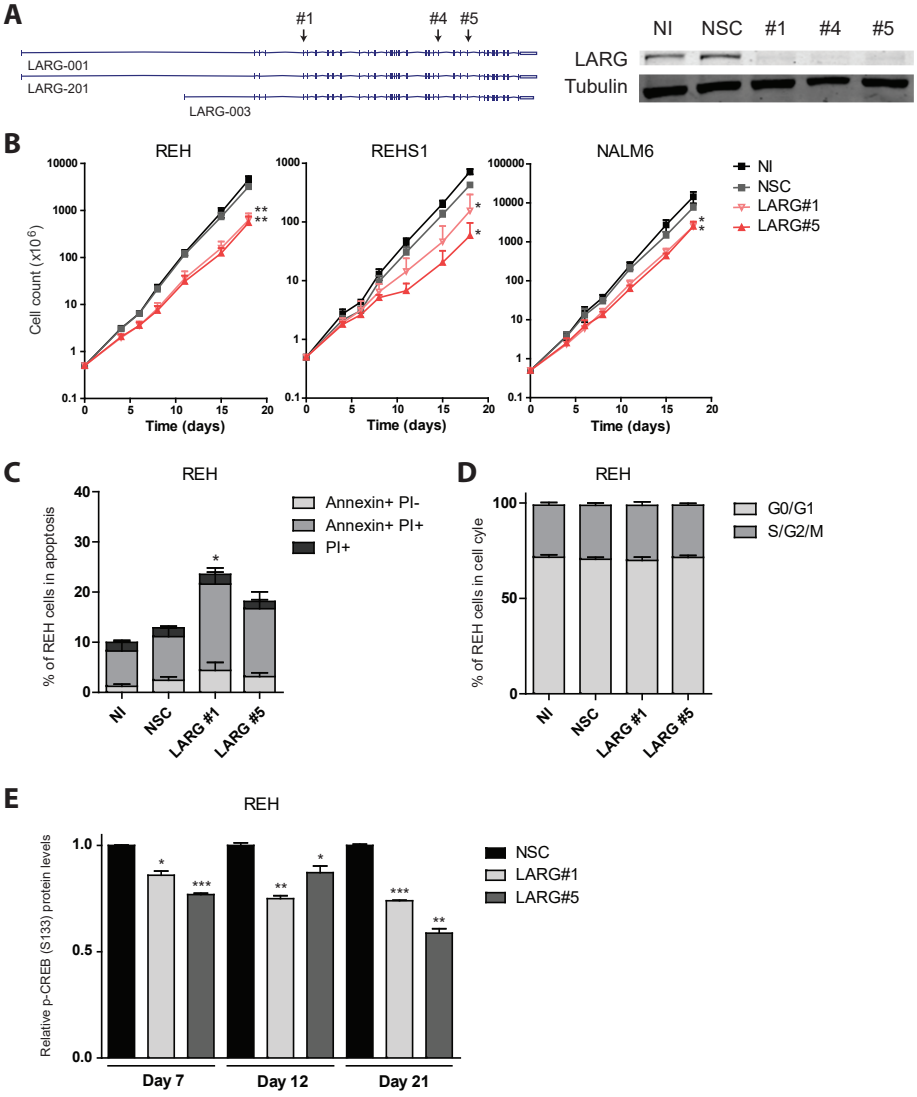

Supplementary Figure 4. LARG knockdown reduces cell proliferation by a modest induction of apoptosis.

(A) To analyze the long-term effect of abrogation of the LARG/RhoA axis in BCP-ALL cells, we performed lentiviral RNA knockdown studies with short hairpins targeting LARG. Left panel shows a schematic representation of the known transcript variants of LARG and the LARG#1, LARG#4 and LARG#5 recognition sites. LARG knockdown was visualized by western blot analysis using antibodies against LARG or β-Tubulin (right panel). A representative experiment is shown (n = 4). Efficient reduction of LARG protein levels was achieved using constructs LARG#1, LARG#4, and LARG#5. Since LARG#4 was predicted to partially bind three other human RNAs (LYRM1, DHRS7C, and LOC101927461) we performed functional experiments with LARG#1 and LARG#5 only. (B) ETV6-RUNX1 positive (REH and REHS1) and ETV6-RUNX1 negative (NALM6) cells were lentivirally transduced with scrambled shRNA control (NSC) or two distinct LARG shRNA constructs (LARG#1 and LARG#5). Cells were cultured for 18 days. To determine the effect on proliferation, cells were counted every 2-3 days using a MAQSQuant Analyzer. Proliferation of leukemic cells transduced with a shRNA targeting LARG was compared to leukemic cells transduced with a NSC control vector (n = ≥ 3 ; * $p \leq 0.05$; ** $p \leq 0.01$).

Supplementary Figure 4. LARG knockdown reduces cell proliferation by a modest induction of apoptosis. (continued)

(C-D) ETV6-RUNX1 positive REH cells were lentivirally transduced with scrambled shRNA control or two distinct LARG shRNA constructs. After seven days of culture, flow cytometrical analysis was performed to determine the effect of LARG knockdown on survival and cell cycle progression. The percentage of apoptotic cells (Annexin V and/or Propidium Iodide positive; C) and actively cycling cells (determined using DyeCycle; D) is depicted (n = 3; * $p \leq 0.05$). (E) To quantify protein phosphorylation after LARG knockdown in REH cells, we used a multiplex cell signaling assay quantifying phosphorylation of the following proteins: CREB (pS133), ERK (pT185/pY187), NFκB (pS536), JNK (pT183/pY185), p38 (pT180/pY182), p70 S6K (pT412), STAT3 (pS727), STAT5A/B (pY694/699), PKB/Akt (pS473). Protein levels of phospho-CREB were first normalized to β-tubulin protein levels. Graph shows the relative levels of phosphorylated CREB in REH cells transduced with two distinct LARG shRNA constructs compared to REH cells transduced with scrambled shRNA control construct. Data of the other tested proteins can be found in Supplementary Figure 5. Experiment was performed at three different time points post-transduction. * $p \leq 0.05$, ** $p \leq 0.01$, *** $p \leq 0.001$.

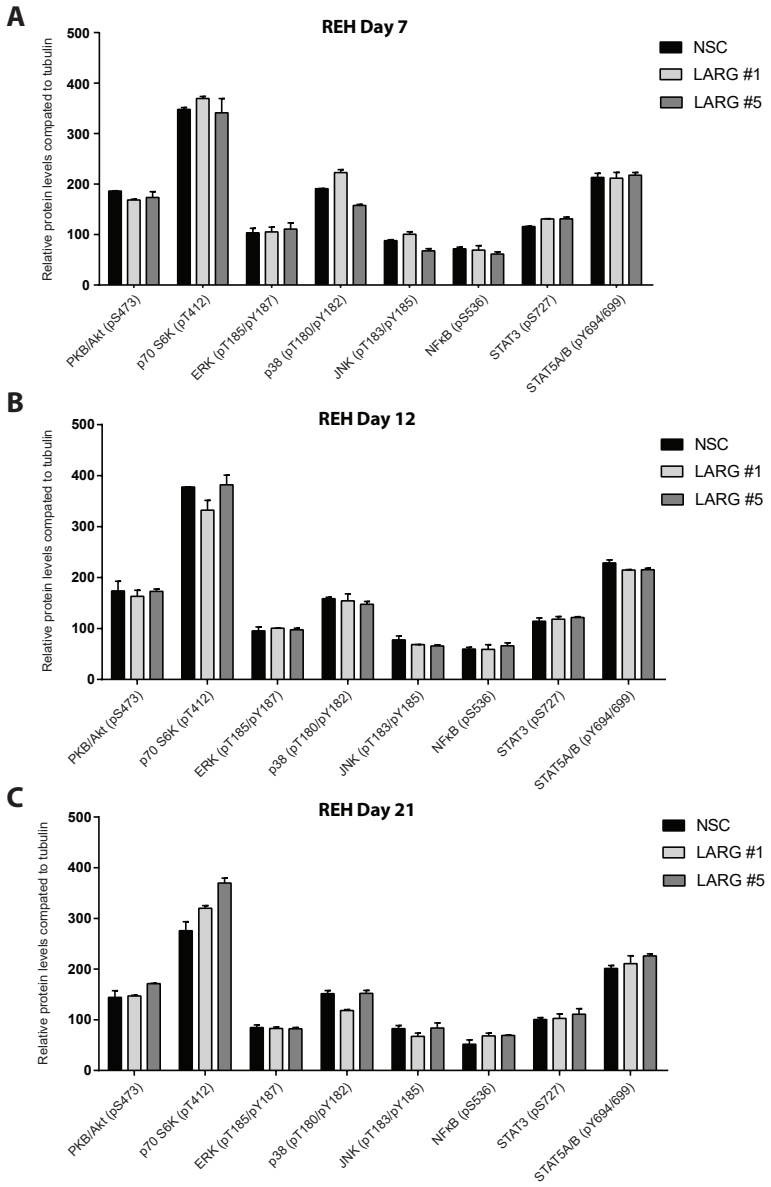

Supplementary Figure 5. Analysis of protein expression after LARG knockdown in REH cells.
(A-C) To quantify protein phosphorylation after LARG knockdown in REH cells, we used a multiplex cell signaling assay in which we quantified phosphorylation of the following proteins: ERK (pT185/pY187), NFκB (pS536), JNK (pT183/pY185), p38 (pT180/pY182), p70 S6K (pT412), STAT3 (pS727), STAT5A/B (pY694/699), PKB/Akt (pS473). Graph shows the relative levels of phosphorylated protein in REH cells compared to the protein level of tubulin. Bars represent REH cells transduced with two distinct LARG shRNA constructs or a scrambled shRNA control construct. Experiment was performed at day 7 (A), day 12 (B), and day 21 (C) post-transduction. Error bars represent SEM of technical duplicates. Phosphorylation of key signaling proteins in the PI3K/PKB/mTOR pathway (PKB/Akt and P70S6K), the MAPK/ERK pathway (ERK and p38), the SAPK/JNK pathway (JNK), NFκB signaling (NFκB) or JAK/STAT signaling (STAT3 and STAT5A/B) were not affected by LARG knockdown.

Chapter 5

B-cell precursor acute lymphoblastic leukemia cells use tunneling nanotubes to orchestrate their microenvironment

Roel Polak[1]*, Bob de Rooij[1]*, Rob Pieters[1,2] & Monique L. den Boer[1]

[1] *Dept. of Pediatric Oncology, Erasmus MC, Sophia Children's Hospital, Rotterdam, The Netherlands.*
[2] *Princess Máxima Center for Pediatric Oncology, Utrecht, The Netherlands.*

* These authors contributed equally to this work and the study

Blood. 2015 Nov 19;126(21): 2404-14

ABSTRACT

Acute lymphoblastic leukemia (ALL) cells reside in the bone marrow microenvironment which nurtures and protects cells from chemotherapeutic drugs. The disruption of cell-cell communication within the leukemic niche may offer an important new therapeutic strategy. Tunneling nanotubes (TNTs) have been described as a novel mode of intercellular communication, but their presence and importance in the leukemic niche are currently unknown. Here, we show for the first time that primary B-cell precursor ALL cells use TNTs to signal to primary mesenchymal stromal cells (MSCs). This signaling results in secretion of pro-survival cytokines, such as IP10/CXCL10, IL8 and MCP-1/CCL2. A combination of TNT disrupting conditions allows us to analyze the functional importance of TNTs in an *ex vivo* model. Our results indicate that TNT signaling is important for the viability of patient-derived B-cell precursor ALL cells and induces stroma-mediated prednisolone resistance. Disruption of TNTs significantly inhibits these leukemogenic processes and re-sensitizes B-cell precursor ALL cells to prednisolone. Our findings establish TNTs as a novel communication mechanism by which ALL cells modulate their bone marrow microenvironment. The identification of TNT signaling in ALL-MSC communication gives insight into the pathobiology of ALL and opens new avenues to develop more effective therapies that interfere with the leukemic niche.

INTRODUCTION

Acute lymphoblastic leukemia (ALL) cells reside in the local microenvironment of the bone marrow and are able to disrupt normal hematopoietic stem cell niches[1]. The disrupted, so called leukemic, niche is essential in initiating and facilitating leukemogenesis[2-6]. In addition, the leukemic niche protects leukemic cells from elimination by immune responses and chemotherapeutic agents, and can facilitate the development of drug resistance of leukemic cells[7-10]. Therefore, the disruption of the ALL-leukemic niche interaction offers a promising new therapeutic strategy[11-16]. However, it is still largely unclear how crosstalk occurs within the leukemic niche, and how this drives leukemic cell survival and chemotherapy resistance.

Recently, tunneling nanotubes (TNTs), or membrane nanotubes, have been described as a novel mode of communication between eukaryotic cells[17-21]. TNTs are thin membrane protrusions consisting of F-actin, that connect cells and facilitate the transport of several types of cargo, including organelles, pathogens, calcium fluxes, death signals, and membrane bound proteins[19,20,22-24]. These intercellular membrane conduits have been observed in several cell types, like cancer cells, complex tissues and organisms[20,21,24-29]. The pathophysiological importance of TNTs has become evident by studies showing that prions and HIV-1 particles use TNTs to promote disease spread[21,30]. However, the presence of TNTs within the leukemic niche and hence their role in communication between leukemic cells and the bone marrow microenvironment has not yet been addressed. Here, we study the role of TNT signaling in communication between primary B-cell precursor ALL (BCP-ALL) cells and MSCs and the contribution of TNT signaling to mesenchymal-mediated survival and resistance to the chemotherapeutic drug prednisolone.

METHODS

Cell lines

BCP-ALL cell lines, NALM6 (B-Other) and REH (TEL-AML1), were obtained from DSMZ (Braunschweig, Germany). Only low cell passages were used, and the identity of cell lines was routinely verified by DNA fingerprinting. Immortalized hTERT-MSCs were a kind gift from Prof. Dr. D. Campana, St. Jude Children's Hospital, Memphis, TN, USA.

Primary patient-derived material

Bone marrow aspirates were obtained from children with newly diagnosed BCP-ALL prior to treatment. Mononuclear leukemic cells were collected and processed

as previously described[31]. All samples used in this study contained ≥97% leukemic blasts (supplementary Figure 7). Mesenchymal stromal cells (MSCs) were isolated from bone-marrow aspirates obtained from newly diagnosed BCP-ALL patients (before treatment) and healthy controls. MSCs were processed as described previously[32]. Primary MSCs were characterized using positive (CD44/ CD90/ CD105/ CD54/ CD73/ CD146/ CD166/ STRO-1) and negative surface markers (CD19/ CD45/ CD34) (supplementary Figure 6). Multilineage potential of MSCs was confirmed for adipocyte (Oil Red O staining), osteocyte (Alizarin Red S staining), and chondrocyte (Col2a/ Thionine/ Alcian Blue staining) differentiation.

Dye transfer experiments

Cells were stained with 1,1'-dioctadecyl-3,3,3'3'-tetramethylindocarbocyanine perchlorate (DiI; yellow), 3,3'-dioctadecyloxacarbocyanine (DiO; green), 1,1'-dioctadecyl-3,3,3'3'-tetramethylindodicarbocyanine perchlorate (DiD; red), or Calcein red-orange AM (all from Life Technologies) according to the manufacturer's protocol. Target populations were analyzed before and after co-culture with flow cytometry (BD Bioscience, San Jose, CA, USA) or confocal microscopy (see below).

Confocal laser scanning microscopy

For high resolution images, differentially stained cells were cultured on a glass slide coated with 10 μg/mL fibronectin (Sigma) at 37 °C and 5% CO_2. Cells were fixated as previously described[33]. Confocal images were acquired with sequential scanning of different channels at a resolution of 1024 x 1024 pixels in the x ^{x} y plane and 0.15 μm steps in z-direction (Leica SP5). For time-lapse confocal imaging, cultures were maintained at 37°C on a heated stage at 5% CO_2 and images were acquired with sequential scanning of different channels at a resolution of 512 x 512 pixels in the x ^{x} y plane and 0.5 μm steps in z-direction. 3D image stacks were acquired by optical sectioning using the LAS software provided with the instrument. The system was equipped with a 63× plan-apochromat oil 1.4 NA DIC objective. The pinhole diameter was set to 1 airy unit (95.5 μm). DiO and DiI were excited with a 488-nm Argon laser and a 561-nm Diode-Pumped Solid-State laser, respectively. Phalloidin-FITC (Sigma) was excited with the 488-nm Argon laser. Image processing was done with Fiji software[34].

TNT inhibition

TNTs were inhibited using actin inhibition by latrunculin B (125 – 500 nM; Sigma) or cytochalasin D (250 nM – 1 μM; Sigma)[20], by mechanical disruption via gentle shaking of cell cultures (250 rpm)[21,35], or by physical separation of leukemic cells (cultured in

a 3.0 μm pore-sized insert) and MSCs (cultured in the bottom compartment of a transwell system; Corning, NY, USA)[21,36].

Cell viability assays

Primary patient cells (1 x 10^6 cells) were co-cultured with or without primary MSCs (5 x 10^4) for five days in a 24-well plate at 37 °C and 5% CO_2. The percentage of viable leukemic cells was determined by staining with Brilliant Violet 421 anti-human CD19 or CD45 antibody (Biolegend), FITC Annexin V (Biolegend), and Propidium Iodide (PI; Sigma), after which the percentage of $AnnexinV^{neg}/PI^{neg}/CD19^{pos}/CD45^{pos}$ cells within the MSC negative fraction (see Figure 6A for gating strategy) was determined by flow cytometry (BD Biosciences). In supplementary Figure 10, viable leukemic cells were counted ($PI^{neg}/CD19^{pos}$) using a MACSQuant analyzer (Miltenyi Biotec, Gladbach, Germany).

Multiplexed fluorescent bead-based immunoassay (Luminex)

Primary leukemic cells and leukemic cell lines were co-cultured with primary MSCs with or without TNT inhibition (shaking or transwell condition) for indicated time points at 37 °C and 5% CO_2. Next, the supernatant was collected and cell viability of leukemic cells was assessed as described above. The concentration of 64 cytokines/chemokines in supernatants of ALL-MSC co-cultures was analyzed using a fluorescent bead-based immunoassay (Luminex Human Cytokine/Chemokine Panel I and II; Merck Millipore) according to the manufacturer's protocol.

Statistical analysis

Student's t-test was used as a statistical test and a Student's paired t-test was used when applicable (indicated in figure legends). Bar graphs represent the mean of biological replicates. Error bars show as standard error of the mean (SEM).

For more details see supplementary methods.

RESULTS

BCP-ALL cells use TNTs to effectively signal to MSCs

TNT formation within the hematopoietic niche was studied by confocal microscopy and flow cytometry. TNTs are thin membrane tethers and can be visualized using lipophilic carbocyanine dyes[20,21]. These dyes stain lipophilic structures in the entire cell, and exhibit very low cell toxicity, while passive transfer of these dyes is negligible. Therefore, these dyes are widely used in live cell tracking experiments[1,37]. Interestingly, it has been shown that organelles and membrane components stained

by these dyes can be actively transported via TNTs[20]. Therefore, these dyes were used to visualize intercellular communication via TNTs within the leukemic niche.

Differential staining of NALM6 BCP-ALL cells (stained with DiI-yellow) and mesenchymal stromal cells (hTERT-MSCs; stained with DiO-green) revealed that TNTs were formed within 3 hours of co-culture (Figure 1A, supplementary Figure 1M-P). 3D reconstruction of these images shows that nanotubular structures *between cells* do not connect with the substratum (i.e. the fibronectin-coated glass slide; see supplementary Video 1A-B and supplementary Video 2). As expected, staining with Phalloidin-FITC shows the presence of F-Actin filaments in these nanotubular structures (see supplementary Figure 1Q-R). Importantly, bidirectional transfer of lipophilic dyes was observed, indicating active crosstalk within the leukemic niche (Figure 1A). Besides formation of TNTs between leukemic cells and MSCs, TNT networks and transfer of lipophilic dye was also observed in mono-cultures of BCP-ALL cells and MSCs (supplementary Figure 1A-L and supplementary Figure 2).

In order to quantify active crosstalk via TNTs we used flow cytometrical analysis of dye transfer from labeled donor cells to unlabeled recipient cells. CD19-positive BCP-ALL cell lines (NALM6 and REH) were stained with lipophilic dye DiI and co-cultured with unstained CD19-negative hTERT-MSCs (supplementary Figure 3A-C for gating strategy). After 6 hours of culture, more than 50% of the MSCs were positive for DiI. This number increased to >85% after 24 hours, highlighting the efficient dye transfer from leukemic cells to MSCs (Figure 1B and supplementary Figure 3D). In reciprocal experiments we also observed dye transfer from MSCs to BCP-ALL cells, but the magnitude of dye transfer was strikingly less than from ALL cells towards MSCs (175-fold, p-value ≤ 0.001) (Figure 1C-D).

Transfer of lipophilic dyes can be mediated by several processes including TNT signaling and signaling via extracellular vesicles (ECV). To evaluate the contribution of TNT signaling to the observed lipophilic dye transfer between leukemic cells and MSCs, we inhibited TNTs using three independent experimental setups: 1) reducing TNT formation through actin inhibition[20], 2) mechanical disruption of TNT connections through gentle shaking of cell cultures[21,35], and 3) prevention of TNT formation by physically separating leukemic cells (cultured in a 3.0 μm pore-sized insert) and MSCs (cultured in the bottom compartment of a transwell system)[21,36].

For inhibition of the polymerized F-actin of which TNTs are composed[20], we used two classes of F-actin polymerization inhibitors: cytochalasin D and latrunculin B. In addition to F-actin elements, TNTs need prolonged cell contact to signal efficiently. Gentle shaking of ALL-MSC co-cultures reduces the lifespan of TNTs, while direct contact between BCP-ALL cells and MSCs is still possible. However, it is well established in literature that flow-derived shear forces (gentle shaking) induce integrin-mediated signaling[38,39]. Therefore, we also physically separate ALL cells and

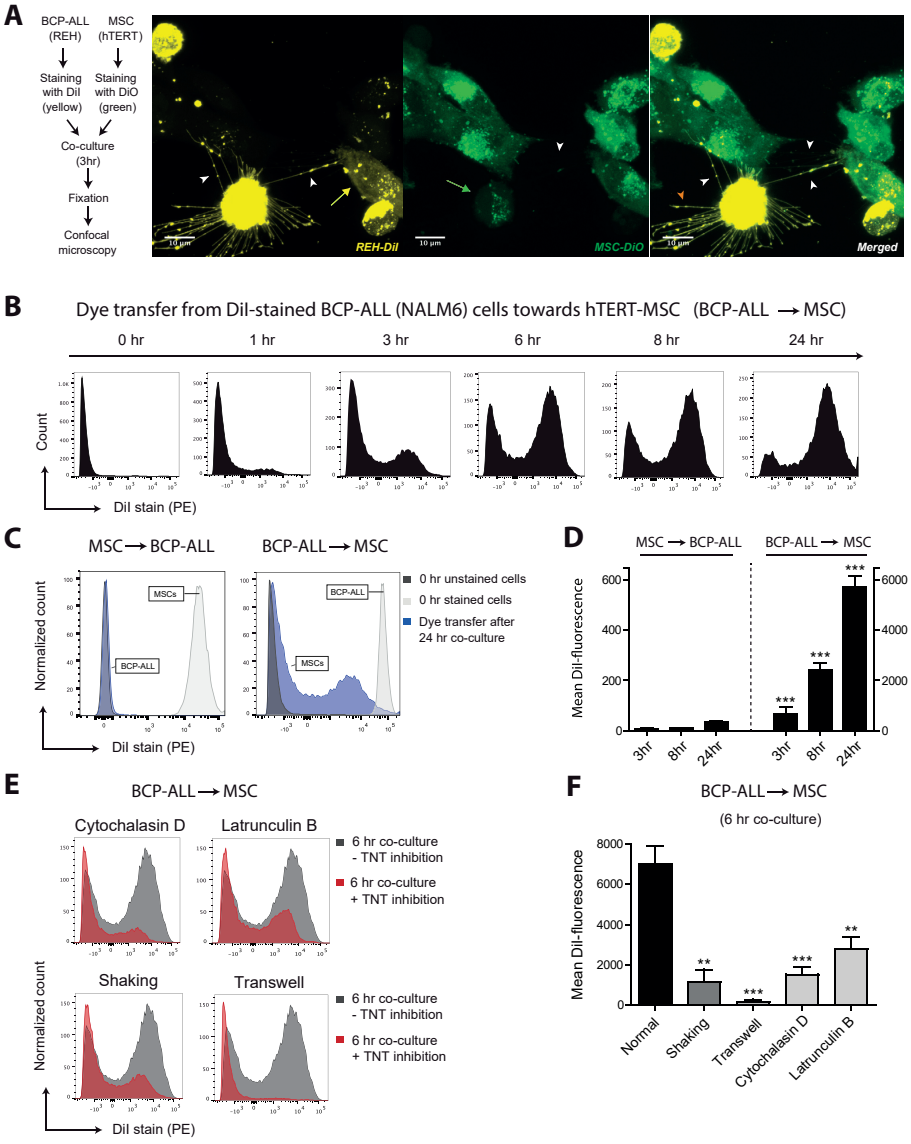

Figure 1. TNT signaling between BCP-ALL cells and MSCs.
(A) Representative confocal images (Z-stack) showing TNT networks (white arrowheads) between BCP-ALL cell line REH (DiI, yellow) and hTERT-immortalized MSCs (DiO, green) after co-culture for 3 hours. Bidirectional exchange of lipophilic dye via TNTs was observed (green arrow for MSC to ALL, yellow arrow for ALL to MSC). Leukemic cells also formed TNT-like structures towards the fibronectin-coated substratum (orange arrowhead). (B) Graph showing quantification of dye transfer from DiI-stained NALM6 cells towards unstained hTERT-MSCs (cultured in 4:1 ratio) in time. Figure shows representative experiment (n = 3).

Figure 1. TNT signaling between BCP-ALL cells and MSCs. (continued)
(C) Graph showing quantification of dye transfer after 24 hours of co-culture (cultured in 1:1 ratio). Left panel shows dye transfer from DiI-stained hTERT-MSCs towards unstained NALM6 cells. Right panel shows the reciprocal experiment (also performed in a 1:1 ratio). White and grey histograms represent staining intensity at the start of each experiment. (D) Quantification of dye transfer in time of experiment as exemplified in (C), performed with two different BCP-ALL cell lines (REH and NALM6). Dye transfer from MSCs towards ALL was compared to dye transfer from ALL towards MSCs (n = 4; two-tailed t-test, unpaired). (E) Graph showing quantification of dye transfer from DiI-stained NALM6 cells towards unstained hTERT-MSCs with (red histograms) or without (grey histograms) TNT inhibition. Cells were co-cultured in 4:1 ratio for 6 hours. Three independent TNT inhibiting conditions were used: actin inhibition by cytochalasin D or latrunculin B, physical disruption by gentle shaking, or culture in a 3.0 μm transwell system. (F) Quantification of dye transfer experiment exemplified in (E), performed with two different BCP-ALL cell lines (REH and NALM6) (n = 4; one-tailed t-test, unpaired).
Data are means ± SEM; ** $p \leq 0.01$, *** $p \leq 0.001$. See also supplementary Figures 1 and 3, and supplementary Videos 1A-B and 2.

MSCs using a transwell system, to exclude the effects of increased integrin signaling. We used a 3.0 μm transwell system to investigate the contribution of extracellular vesicle signaling to lipophilic dye transfer. In this transwell system leukemic cells are physically separated from MSCs, while exchange of extracellular vesicles (30-1000 nm) is still possible.

Cytochalasin D and latrunculin B both caused a dose-dependent reduction of dye transfer after 6 hours of co-culture ($p \leq 0.01$; Figure 1E-F and supplementary Figure 3E-F). Due to the short half-time of these actin inhibitors[40,41], TNT formation was restored within 24 hours (supplementary Figure 3E-F). Disruption of TNT structures by gentle shaking reduced dye transfer by more than 5-fold ($p \leq 0.01$; Figure 1E-F and supplementary Figure 3G). Importantly, dye transfer from BCP-ALL cell lines to MSCs was nearly absent in transwell experiments ($p \leq 0.001$), which indicates that dye transfer occurs mainly via TNTs and not via extracellular vesicles (Figure 1E-F and supplementary Figure 3H).

The TNT forming capacity was also evaluated in an *ex vivo* niche model using leukemic cells and MSCs that were both freshly obtained from patients with newly diagnosed BCP-ALL (Figure 2A, supplementary Figure 4A-J, supplementary Figure 5A-D, supplementary Figure 6 and supplementary Figure 7). *Ex vivo* co-cultures revealed that TNTs rapidly (< 3 hours) form between primary BCP-ALL cells and primary MSCs, and efficiently transfer lipophilic dye (Figure 2B, supplementary Figure 4G-J, supplementary Figure 5). The source of MSC did not affect the efficacy of TNT signaling. Dye transfer was similarly efficient from ALL cells towards 10 different primary MSCs (n = 5 healthy and n = 5 leukemic primary patient-derived MSCs; Figure 2C-D and supplementary Figure 8A-C).

The dynamics of TNT formation between BCP-ALL cells and MSCs were investigated using time-lapse confocal microscopy. Leukemic cells initiated formation of TNTs and transferred lipophilic dye towards MSCs within minutes (Figure 3A; supplementary Videos 3 and 4A). Leukemic cells were able to form multiple TNTs

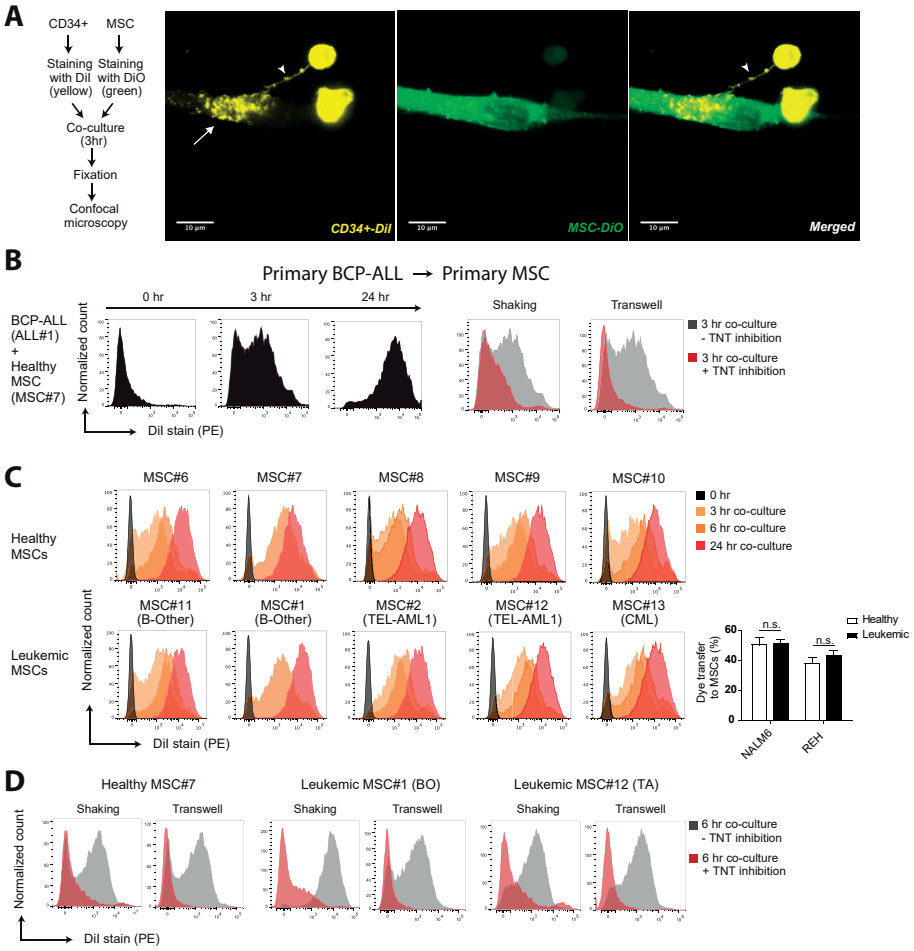

Figure 2. Primary BCP-ALL cells signal to MSCs via TNTs.
(A) Representative confocal images (Z-stack) showing TNT formation (white arrowhead) between a primary CD34-positive cell (DiI, yellow) and a hTERT-immortalized MSC (DiO, green) after co-culture for 3 hours. White arrow indicates transfer of dye to recipient cell. (B) Graphs showing quantification of dye transfer in co-cultures of BCP-ALL patient cells with primary MSCs (cultured in 4:1 ratio). Inhibition of TNTs was performed by gentle shaking of co-cultures, or co-culture in a 3.0 μm transwell system (red histograms). (C) Graphs showing quantification of dye transfer from DiI-stained NALM6 cells towards 10 different unstained primary MSCs (cultured in 4:1 ratio) obtained from leukemia patients (n = 5) and healthy controls (n = 5). (D) Graphs showing quantification of dye transfer from DiI-stained NALM6 cells towards 3 different primary MSCs with (red histograms) or without (grey histograms) TNT inhibition.
See also supplementary Figures 4-8.

and signal to several MSCs simultaneously (Figure 3B; and supplementary Videos 3 and 4A-B). TNTs formed between MSCs and leukemic cells were stable for multiple hours and could reach several cell diameters in length (Figure 3C, supplementary

Videos 3 and 4A). After 10 hours, the majority of MSCs became DiI-positive (supplementary Videos 3 and 4B), as confirmed by flow cytometry (Figure 1B).

TNTs are important players in signaling from BCP-ALL cells to MSCs

The above-mentioned findings suggest that TNT signaling is a highly effective communication mechanism between ALL cells and MSCs. This was further illustrated by comparing TNT signaling to other intercellular communication mechanisms, including gap junctions, integrins and ECV (Figure 4A). Dye transfer from leukemic cells towards MSCs was minimal using a 3.0 μm transwell system, in which ECV signaling is possible (> 500 fold lower compared to normal co-culture after 24 hours; $p \leq 0.001$; Figure 4B-C). Transfer experiments with the gap junction-specific dye Calcein revealed that signaling from leukemic cells towards primary MSCs via gap junctions is highly ineffective compared to signaling via TNTs (> 90 fold lower after 24 hours; $p \leq 0.001$; Figure 4D-E). Integrin signaling has been implicated in the induction of TNTs[42], raising the question whether TNTs function autonomously or in an integrin-dependent manner. To inhibit integrin signaling between BCP-ALL cells and MSCs, we used RGDS-peptides, reported to prevent the binding of integrins to membranes[43]. RGDS negatively affected the efficiency of lipophilic dye transfer via TNTs whereas the transfer in the presence of negative control peptides (GRADSP) remained unaffected (Figure 4F). The reduction in lipophilic dye transfer was limited to a maximum of 30% ($p \leq 0.01$). Taken together, these data reveal that TNT signaling acts independently of other important intercellular communication mechanisms, i.e. signaling via extracellular vesicles, gap junctions, and integrins.

BCP-ALL cells use TNTs to drive cytokine release within the microenvironment

The question remains how TNT signaling from leukemic cells affect their microenvironment. Since cytokines and chemokines can greatly affect the survival of leukemic cells[44,45], we considered that the microenvironment responds to TNT signaling by secreting supportive soluble factors. Therefore we investigated the secreted levels of 64 known cytokines/chemokines in co-cultures of primary leukemic cells of two BCP-ALL patients with different sources of primary MSCs. Co-culture of these cells induced the secretion of several cytokines. The cytokine signature produced within co-cultures suggested that this secretion was leukemia-driven and independent of the MSC source (Figure 5). IP10/CXCL10 levels increased more than 1000-fold when patient ALL#7 cells were co-cultured with MSCs, but were undetectable in co-cultures from patient ALL#9 cells (Figure 5A and 5E). Likewise, MDC/CCL22 and TARC/CCL17, both undetectable in patient ALL#7 co-cultures, were induced 6-18 fold when patient ALL#9 cells were co-cultured with MSCs (Figure 5C-D and 5G-H). Interleukin-8 (IL8) levels were induced (2-7 fold)

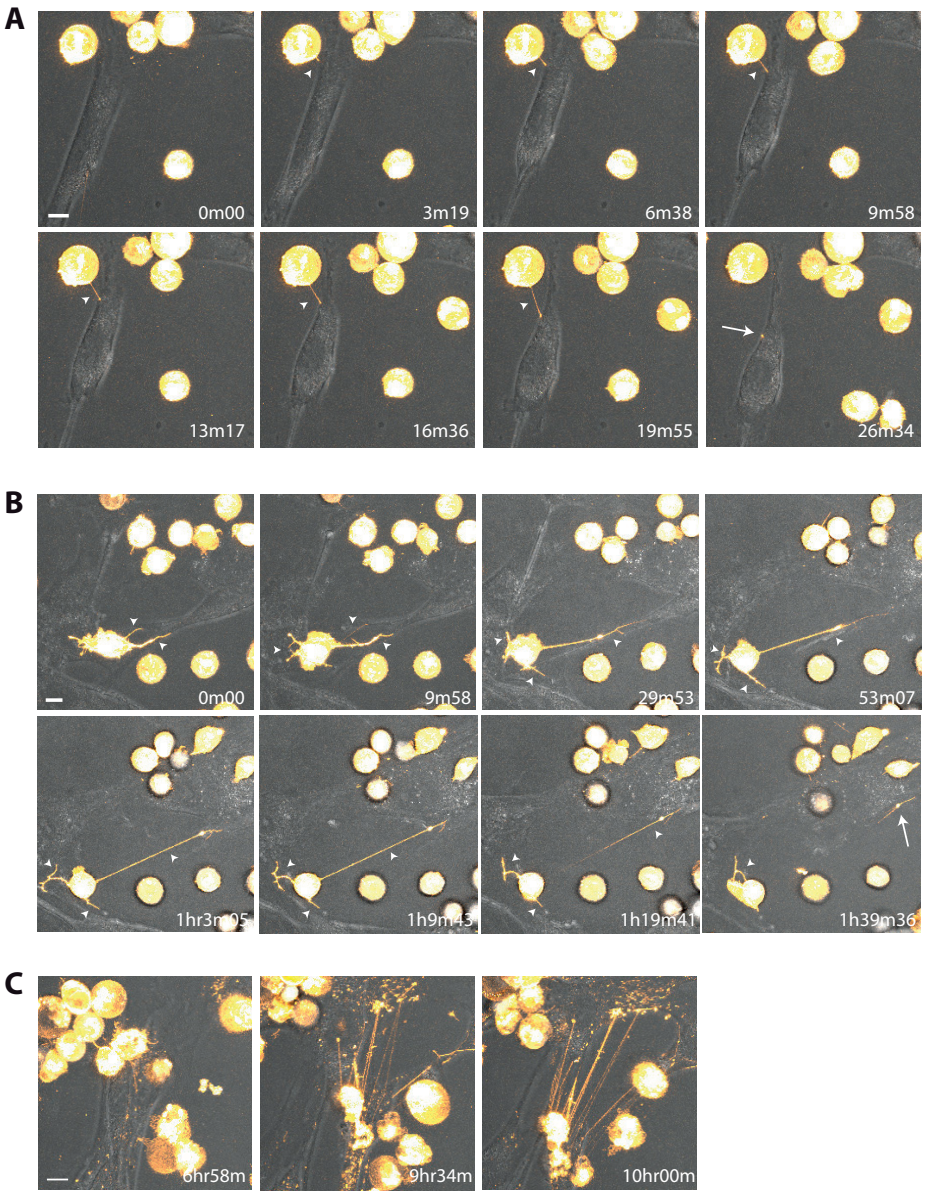

Figure 3. Dynamic nature of TNT formation between BCP-ALL cells and MSCs.
(A-C) Time-lapse confocal images (3D image stacks) showing TNT formation (white arrowhead) between NALM6 cells (DiI, yellow) and primary MSCs at multiple time points. White arrow indicates transfer of dye to recipient cell. Time indicated in the right lower corner is the duration from start of the experiment. Orange Hot look-up table (LUT) and transmission overlays were used to illustrate dye transfer towards MSCs. Scale bars represent 10 μm. (A and C) Depicted images are close-ups of the upper left corner of supplementary Video 3. (B) Depicted images are close-ups of supplementary Video 4A.
Data is representative of three independent experiments. See also supplementary Figure 5 and supplementary Videos 3 and 4A-B.

by primary ALL cells from both patients (Figure 5B and 5F). Cytokines that were induced less than 2 fold in co-culture are shown in supplementary Figure 9. Only a limited number of cytokines/chemokines were found to be significantly upregulated in patients' ALL-MSC co-cultures compared to mono-cultures of both cell types. Also in a proliferative setting (using the BCP-ALL cell line NALM6), a limited number of known cytokines were upregulated in co-culture with two different primary MSCs:

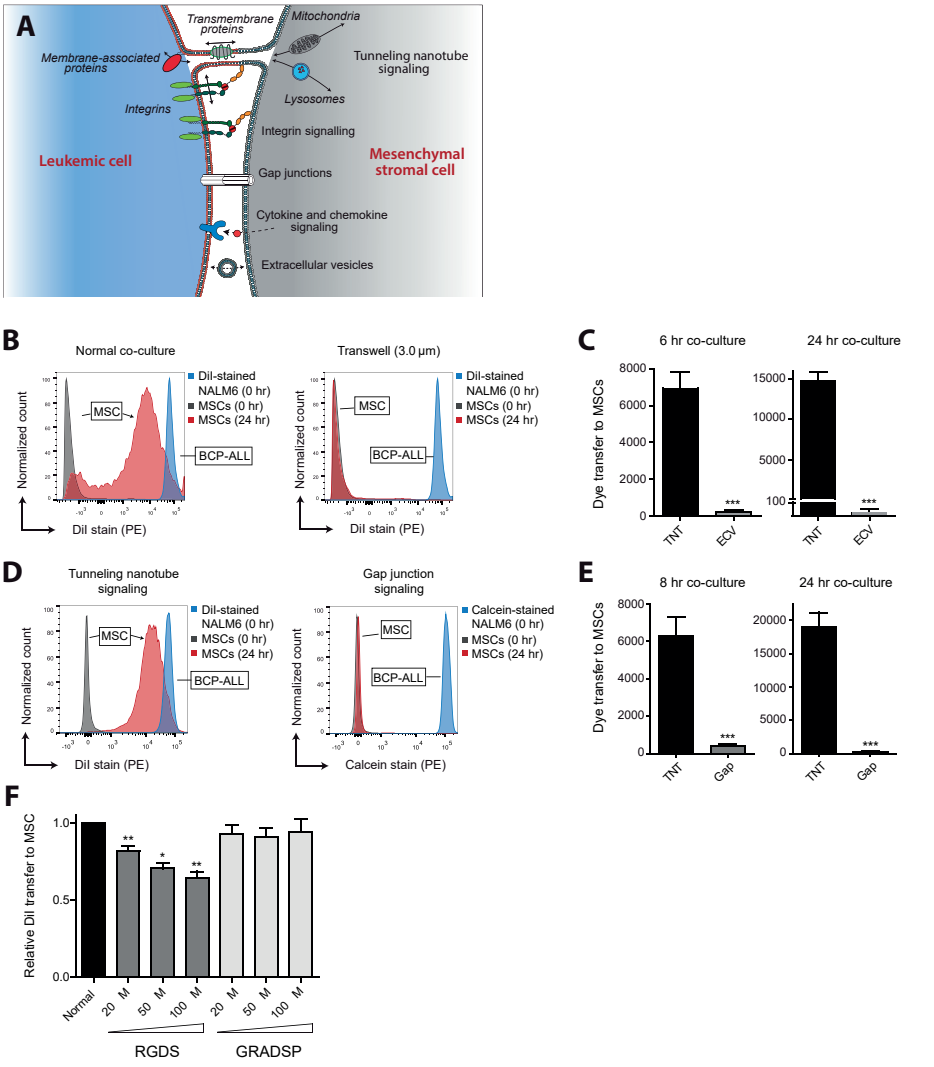

Figure 4. TNTs are important players in signaling from BCP-ALL cells to MSCs.
(A) Model of crosstalk between leukemic cells and MSCs in the hematopoietic niche. (B) Graphs showing quantification of dye transfer from DiI-stained NALM6 cells towards unstained hTERT-MSCs. Blue and grey histograms represent staining intensity at the start of each experiment. Red histogram represents signaling efficiency via TNTs (normal co-culture; left panel) and via extracellular vesicles (ECV) (3.0 µm transwell; right panel).

Figure 4. TNTs are important players in signaling from BCP-ALL cells to MSCs. (continued)
(C) Bar graphs of experiment shown in (B) after 6 hours (left panel) and 24 hours (right panel) of co-culture (n = 4; two-tailed t-test, unpaired). (D) Graphs showing quantification of dye transfer from BCP-ALL cell line NALM6, stained with either DiI or calcein, towards primary MSCs after 24 hours of co-culture. Blue and grey histograms represent staining intensity at the start of each experiment. Red histogram shows signaling efficiency via TNTs (left panel) and via gap junctions (right panel). (E) Bar graphs of experiment shown in (D) after 8 hours (n = 6; left panel) and 24 hours (n = 4; right panel) of co-culture (two-tailed t-test, unpaired). (F) Bar graphs representing dye transfer from DiI-stained REH cells towards unstained primary MSCs with and without integrin blocking. Integrin signaling was blocked by addition of RGDS peptide, and compared to addition of the integrin non-binding peptide GRADSP (n = 5; one-tailed t-test, paired).
Data are means ± SEM; * $p \leq 0.05$, ** $p \leq 0.01$, *** $p \leq 0.001$.

IL8 and VEGF levels were on average induced 2 and 3 fold respectively (n=3, $p \leq 0.01$, Supplementary Figure 9E-H). These MSC-independent and leukemia-consistent cytokine signatures suggest that leukemic cells, and not MSCs, are responsible for the active modulation of the tumor microenvironment.

Induction of the observed cytokines was dependent on TNT signaling, as TNT inhibition significantly lowered the secreted levels of these factors (Figure 5A-H, Supplementary Figure 9E-H). However, TNT inhibition only partly reversed the induction of cytokine levels in ALL-MSC co-cultures, suggesting that, next to TNT signaling, other intercellular signaling routes contribute to the induction of these secretomes.

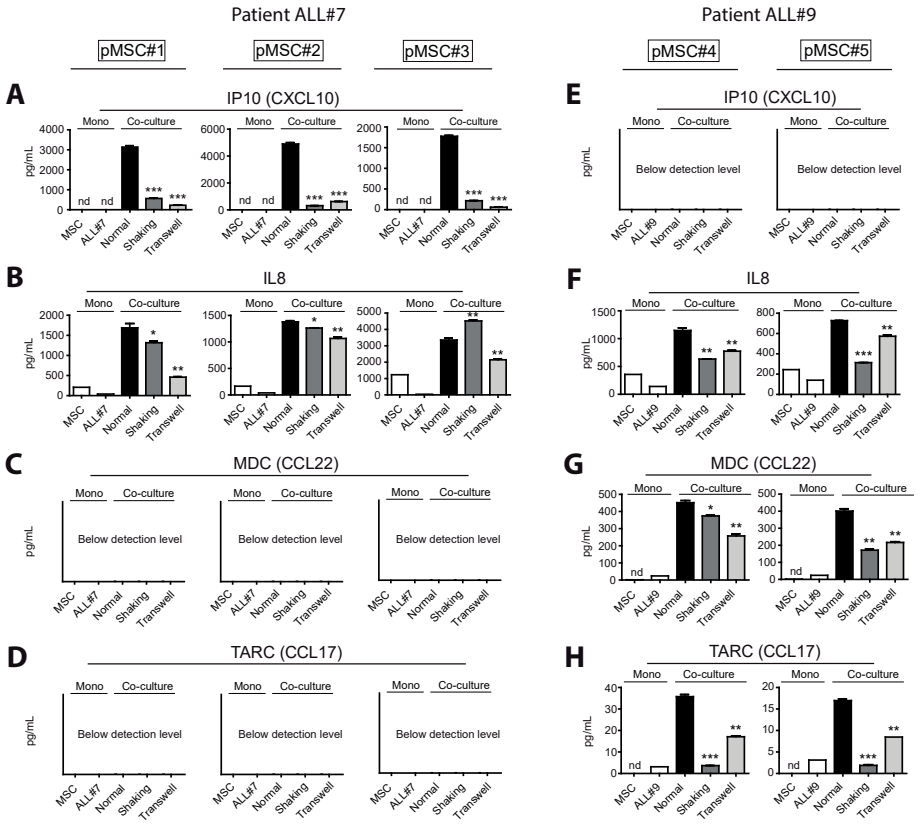

Figure 5. BCP-ALL cells use TNTs to drive cytokine release within the microenvironment.
(A) IP10/CXCL10 supernatant levels in co-culture of primary leukemic patient ALL#7 cells with primary MSC#1 (left panel), MSC#2 (middle panel), or MSC#3 (right panel). TNT signaling was inhibited by gentle shaking or culture in a transwell system (one-tailed t-test, unpaired). (B) Same as (A) for IL8 levels. (C) Same as (A) for MDC (CCL22) levels. (D) Same as (A) for TARC (CCL17) levels. (E) IP10/CXCL10 supernatant levels in co-culture of primary leukemic patient ALL#9 cells with primary MSC#4 (left panel), or MSC#5 (right panel). (F) Same as (E) for IL8 levels. (G) Same as (E) for MDC (CCL22) levels. (H) Same as (E) for TARC (CCL17) levels.
Data are means ± SEM; * $p \leq 0.05$, ** $p \leq 0.01$. nd = not detectable (below detection level).
See also supplementary Figure 9.

TNT signaling is important for the survival of primary BCP-ALL cells

Several studies have shown the importance of the microenvironment for the survival of malignant cells, but without elucidating how[46]. In order to study the effect of TNT signaling on leukemic cell viability, we used *ex vivo* co-cultures of primary BCP-ALL cells and primary MSCs (see table S1 for BCP-ALL subtype information, Figure 6A for gating strategy). Primary BCP-ALL cell survival significantly increased in 5-day co-cultures with primary MSCs compared to mono-cultures. When TNT formation was prevented by shaking of co-cultures or by transwell conditions, this increase

significantly reduced 3.5- and 3.6-fold, respectively (n = 7, p ≤ 0.001; Figure 6B-D). The effect of TNT inhibition was consistent across leukemic cells from multiple cytogenetic BCP-ALL subgroups (TEL-AML1, BCR-ABL1-like, and B-Other).

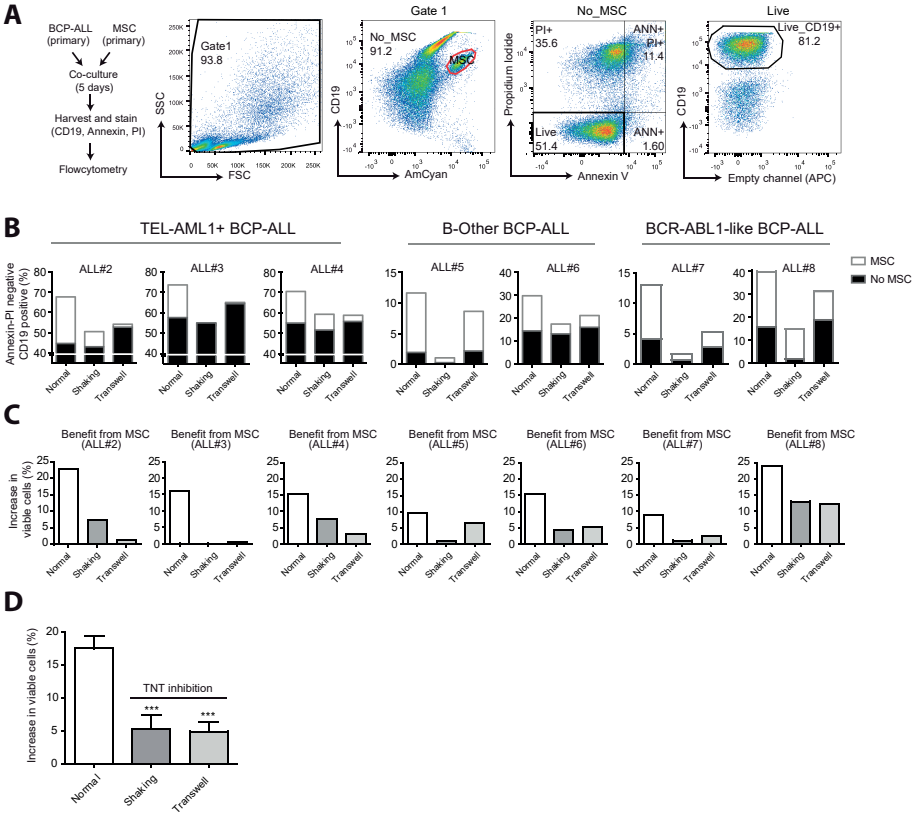

Figure 6. TNT signaling is important for the survival of primary BCP-ALL cells.
(A) Flow chart and flow cytometrical gating strategy used to study the effect of TNTs on BCP-ALL cell survival. Co-cultures of $CD19^{positive}$ leukemic cells and $CD19^{negative}$ MSCs were stained with Brilliant Violet 421™ anti-human CD19 antibody, FITC Annexin V, and Propidium Iodide (PI). MSCs were excluded (red gate), and the percentage of viable BCP-ALL blasts ($AnnexinV^{neg}/PI^{neg}/CD19^{pos}$ cells) was determined within the MSC-negative fraction. (B) Percentage of viable primary leukemic patient cells (n = 3 TEL-AML1, n = 2 B-Other, n = 2 BCR-ABL1-like) in mono-culture (black bars) or co-culture with patient MSCs (white bars) after 5-day co-culture. (C) The survival benefit for primary leukemic patient cells (n = 3 TEL-AML1, n = 2 B-Other, n = 2 BCR-ABL1-like) in co-culture with patient MSCs. (D) The mean survival benefit for primary leukemic patient cells in co-culture with patient MSCs (n = 7; one-tailed t-test, paired).
Data are means ± SEM; *** p ≤ 0.001.

Inhibition of TNTs sensitizes BCP-ALL cells to prednisolone

We investigated whether inhibition of TNT signaling also affects the response of leukemic cells to chemotherapeutic drugs. BCP-ALL patient cells were treated with

the ALL spearhead drug prednisolone for 5 days. Prednisolone was less effective in inducing apoptosis of primary BCP-ALL cells in the presence of primary MSCs compared to mono-cultures of primary BCP-ALL cells (70% vs 5% reduced viability; $p \geq 0.001$; Figure 7A), underlining the importance of MSCs in the induction of prednisolone resistance (Figure 7A). The protective effect of MSCs was significantly reduced by 2-3 fold ($n = 4$, $p \leq 0.001$; Figure 7A) when TNT signaling was inhibited. TNT inhibition alone was not sufficient to abrogate all microenvironment-induced drug resistance. In shaking and transwell conditions, which allow signaling via integrins, soluble factors or ECVs, microenvironment-induced resistance to prednisolone was still present ($p \geq 0.01$). Since *ex vivo* cultured leukemic patient cells lose their propensity to proliferate, we also addressed the effect of TNT signaling on drug resistance in a proliferative setting using the BCP-ALL cell line NALM6. Similar to primary BCP-ALL cells, co-culture with MSCs induced prednisolone resistance of NALM6 cells (Figure 7B). Inhibition of TNT formation by shaking of co-cultures or transwell conditions significantly reduced this effect 4.5- and 8.5- fold, respectively ($p \leq 0.01$; Figure 7B and supplementary Figure 10A-B). These data show that inhibition of TNT signaling in co-cultures sensitizes BCP-ALL cells to the anti-leukemic effects of prednisolone in both a primary non-proliferative and a proliferative setting.

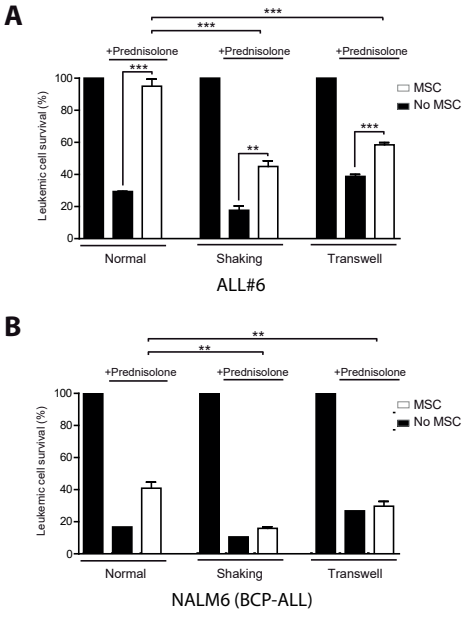

Figure 7. Inhibition of TNTs sensitizes BCP-ALL cells to prednisolone.

(A) Leukemic cell survival of patient ALL#6 cells cultured with or without MSCs after 5 days of prednisolone exposure (0.3 μg/mL). All graphs show percentage compared to untreated control. TNT signaling was inhibited by shaking or transwell conditions (one-tailed t-test, unpaired). Quadruplicates represent four different sources of MSCs (MSC#1, MSC#2, MSC#6, MSC#7). (B) Leukemic cell survival of BCP-ALL cell line NALM6 cultured with or without MSCs after 5 days of prednisolone exposure. All graphs show percentage compared to untreated control. TNT signaling was inhibited by shaking or transwell conditions (one-tailed t-test, unpaired). Triplicates represent three different sources of MSCs (hTERT, MSC#1, and MSC#2).

Data are means ± SEM; * $p \leq 0.05$, ** $p \leq 0.01$. See also supplementary Figure 10.

DISCUSSION

The presented study identifies TNT formation as a novel regulator of interaction between BCP-ALL cells and their bone marrow niche, which facilitates signaling from leukemic cells towards MSCs and affects the release of cytokines and chemokines in the microenvironment. Disruption of TNTs inhibits this release, decreases the survival benefit that MSCs provide to primary BCP-ALL cells, and sensitizes BCP-ALL cells to the important anti-leukemic drug prednisolone (Figure 8).

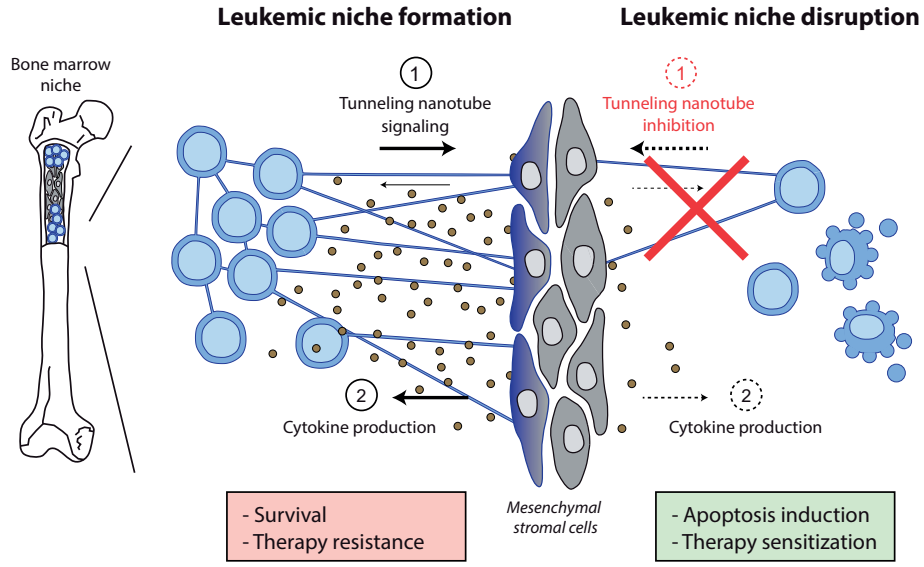

Figure 8. Model of the TNT-driven leukemic niche.
Model depicting the role of TNT signaling in leukemic niche formation. Leukemic cells use TNTs to modulate their microenvironment by directing non-malignant stromal cells to produce pro-survival cytokines and chemokines. This leukemic niche promotes cell survival and drug resistance and can be disrupted by inhibiting TNT signaling.

Relapse of leukemia is caused by a small number of leukemic cells that are able to withstand chemotherapy and can cause the complete reconstitution of the tumor. Leukemogenic mouse models show the importance of signaling between leukemic cells and their bone marrow microenvironment and emphasize the pathophysiological relevance of cytokines within the leukemic niche[1,47-49]. However, a major shortcoming in our knowledge about the leukemic niche is the lack of insight into the functional mechanism mediating crosstalk between leukemic cells and their local niche. Our data adds significant insight into this process and provides an opportunity to inhibit the leukemic niche. Importantly, primary BCP-ALL cells use

TNTs to modulate their microenvironment, identifying the leukemic cell, and not MSCs, as the driver of niche modulation.

Although less pronounced as seen between ALL cells and MSCs, TNTs are also used for communication between leukemic cells. This discovery may reveal a new aspect of tumor heterogeneity. In many cancer types, clonal evolution has been observed[50]. A recent study in T-ALL by Blackburn et al. shows that leukemia subclones acquire mutations, that can mediate chemotherapy resistance even without prior drug exposure[51]. Leukemic cells might exploit TNTs, which can transfer a broad spectrum of molecules and organelles like membrane-associated signaling molecules (e.g. H-Ras[19]), to transfer mutant proteins and subsequently chemotherapy resistance between subclones.

Several studies report that the leukemic niche can induce drug resistance for both classical chemotherapeutic agents and newly developed targeted therapies[9,44-46,52-54]. The seminal papers by Strausmann et al, and Wilson et al. revealed the widespread potential for growth-factor-driven resistance to kinase inhibitors in several tumor types. A recent study by Manshouri et al., showed the induction of resistance against JAK2 inhibitors by bone marrow stroma-secreted cytokines in JAK2-mutated primary hematopoietic cells. BCP-ALL cells use TNTs to induce a pro-inflammatory cytokine signature within their microenvironment[55]. These cytokines have been reported to be involved in leukemia survival and resistance to therapy, like IP10/CXCL10[54], IL-8[56], and MCP-1/CCL2[57]. When TNTs were inhibited, this signature was partly reversed and simultaneously leukemic cell survival was decreased. Since these cytokines also have a chemoattractive function, it is likely that migration towards the stromal compartments of the niche and subsequent induction of contact-dependent signaling modules, like integrins and gap junctions, also play a role in this process. Further, we observed TNT signaling from MSCs towards leukemic cells, which might also influence drug resistance of leukemic cells. For example, TNTs have been shown to transport drug-efflux pumps such as P-glycoproteins[24], and to transport mitochondria preferentially towards cancer cells[28].

Interestingly, we observed leukemia-specific cytokine patterns in MSC-ALL co-cultures that were affected by abrogation of TNT signaling. This observation opens the discussion how TNT signaling can lead to the upregulation of different soluble factors. The broad spectrum of signaling molecules that are transported by TNTs potentially allows the ALL to convey specific messages to MSCs in order to differentially regulate the secretion of soluble factors by its microenvironment. In addition, leukemia is a highly heterogeneous disease consisting of different (cyto) genetic subtypes that also have individual heterogeneity with regards to their

transcriptome and proteome[58]. These factors are all likely to contribute to leukemia-unique demands for microenvironmental support.

Targeting TNT-directed communication between leukemic cells and their supportive niche may be a promising new approach to kill leukemic cells and prevent drug resistance in clinical practice. As of yet, no agents are available that induce specific inhibition of TNT signaling, but our data point to the importance to develop such agents. TNT signaling can be disrupted through shear stress, applying a physical distance between the cells, actin inhibition, and in some cases tubulin inhibition. In additional experiments, we observed that tubulin inhibition did not inhibit TNT signaling between BCP-ALL cells and MSCs (data not shown). The common building block for all TNTs reported in literature is F-actin, making it an obvious target for TNT disruption. Actin inhibitors are derived from fungi, plants and sponges, which developed these toxins as a defense mechanism. Consequently, these compounds inhibit TNT formation (Figure 1E-F) and induce cell death (data not shown). Therefore, it is important to develop more specific and less-toxic small molecule inhibitors that target elements of the actin cytoskeleton important for TNT formation. We propose our primary patient-derived *ex vivo* model system as a highly suitable platform to identify such inhibitors. Once identified, these TNT-specific agents will allow us to investigate TNT signaling also *in vivo*.

In conclusion, the discovery of TNT signaling between BCP-ALL cells and mesenchymal stromal cells adds significant insight into the mechanisms of communication in the leukemic niche. BCP-ALL cells use TNT networks to modify their healthy microenvironment and hereby create a leukemic niche that induces survival and drug resistance. Current chemotherapeutic regimens are primarily focused on combating tumor intrinsic properties. Our data provide a new concept to develop alternative therapeutic strategies that include targeting of the leukemic niche in B-cell acute lymphoblastic leukemia.

Acknowledgements
We thank all members of the research laboratory Pediatric Oncology of the Erasmus MC for their help in processing leukemic and mesenchymal stromal cell samples, in particular L.C.J. van den Berk, C. van de Ven, and F. Meijers-Stalpers; M. Buitenhuis and M. Bierings for critical discussions and reading of the manuscript; D. Geerts for scientific input and critical discussions; The Erasmus Optical Imaging Centre for providing support of CLSM; The Department of Hematology of the Erasmus MC for providing the use of CLSM and Flow Cytometers; The Vlietland Ziekenhuis for collecting and providing cord blood. The work described in this paper was funded by the KiKa Foundation (Stichting Kinderen Kankervrij – Kika-39), the Dutch

Cancer Society (UVA 2008; 4265, EMCR 2010; 4687), the Netherlands Organization for Scientific Research (NWO – VICI M.L. den Boer) and the Pediatric Oncology Foundation Rotterdam.

Author contributions

Co-first authors R. Polak and B. de Rooij contributed equally to the study and are listed alphabetically. R. Polak and B. de Rooij designed the study, performed the experiments, collected and analyzed all data, and wrote the paper. M.L. den Boer designed the study, analyzed data, and wrote the paper. R. Pieters analyzed data and wrote the paper. All authors discussed the results and approved the submitted manuscript.

Conflict of interest disclosure

the authors declare no competing financial interests.

REFERENCES

1. Colmone, A., *et al.* Leukemic cells create bone marrow niches that disrupt the behavior of normal hematopoietic progenitor cells. *Science* **322**, 1861-1865 (2008).
2. Flynn, C.M. & Kaufman, D.S. Donor cell leukemia: insight into cancer stem cells and the stem cell niche. *Blood* **109**, 2688-2692 (2007).
3. Raaijmakers, M.H., *et al.* Bone progenitor dysfunction induces myelodysplasia and secondary leukaemia. *Nature* **464**, 852-857 (2010).
4. Walkley, C.R., *et al.* A microenvironment-induced myeloproliferative syndrome caused by retinoic acid receptor gamma deficiency. *Cell* **129**, 1097-1110 (2007).
5. Walkley, C.R., Shea, J.M., Sims, N.A., Purton, L.E. & Orkin, S.H. Rb regulates interactions between hematopoietic stem cells and their bone marrow microenvironment. *Cell* **129**, 1081-1095 (2007).
6. Yilmaz, O.H., *et al.* Pten dependence distinguishes haematopoietic stem cells from leukaemia-initiating cells. *Nature* **441**, 475-482 (2006).
7. Arai, F., *et al.* Tie2/angiopoietin-1 signaling regulates hematopoietic stem cell quiescence in the bone marrow niche. *Cell* **118**, 149-161 (2004).
8. Fujisaki, J., *et al.* In vivo imaging of Treg cells providing immune privilege to the haematopoietic stem-cell niche. *Nature* **474**, 216-219 (2011).
9. McMillin, D.W., *et al.* Tumor cell-specific bioluminescence platform to identify stroma-induced changes to anticancer drug activity. *Nat Med* **16**, 483-489 (2010).
10. Nakasone, E.S., *et al.* Imaging tumor-stroma interactions during chemotherapy reveals contributions of the microenvironment to resistance. *Cancer Cell* **21**, 488-503 (2012).
11. Jin, L., Hope, K.J., Zhai, Q., Smadja-Joffe, F. & Dick, J.E. Targeting of CD44 eradicates human acute myeloid leukemic stem cells. *Nat Med* **12**, 1167-1174 (2006).
12. Matsunaga, T., *et al.* Interaction between leukemic-cell VLA-4 and stromal fibronectin is a decisive factor for minimal residual disease of acute myelogenous leukemia. *Nat Med* **9**, 1158-1165 (2003).
13. Nervi, B., *et al.* Chemosensitization of acute myeloid leukemia (AML) following mobilization by the CXCR4 antagonist AMD3100. *Blood* **113**, 6206-6214 (2009).
14. Sipkins, D.A., *et al.* In vivo imaging of specialized bone marrow endothelial microdomains for tumour engraftment. *Nature* **435**, 969-973 (2005).
15. Tavor, S., *et al.* CXCR4 regulates migration and development of human acute myelogenous leukemia stem cells in transplanted NOD/SCID mice. *Cancer Res* **64**, 2817-2824 (2004).
16. Zeng, Z., *et al.* Targeting the leukemia microenvironment by CXCR4 inhibition overcomes resistance to kinase inhibitors and chemotherapy in AML. *Blood* **113**, 6215-6224 (2009).
17. Chauveau, A., Aucher, A., Eissmann, P., Vivier, E. & Davis, D.M. Membrane nanotubes facilitate long-distance interactions between natural killer cells and target cells. *Proc Natl Acad Sci U S A* **107**, 5545-5550 (2010).
18. Onfelt, B., Nedvetzki, S., Yanagi, K. & Davis, D.M. Cutting edge: Membrane nanotubes connect immune cells. *J Immunol* **173**, 1511-1513 (2004).
19. Rainy, N., *et al.* H-Ras transfers from B to T cells via tunneling nanotubes. *Cell Death Dis* **4**, e726 (2013).
20. Rustom, A., Saffrich, R., Markovic, I., Walther, P. & Gerdes, H.H. Nanotubular highways for intercellular organelle transport. *Science* **303**, 1007-1010 (2004).

21. Sowinski, S., *et al.* Membrane nanotubes physically connect T cells over long distances presenting a novel route for HIV-1 transmission. *Nat Cell Biol* **10**, 211-219 (2008).
22. Watkins, S.C. & Salter, R.D. Functional connectivity between immune cells mediated by tunneling nanotubules. *Immunity* **23**, 309-318 (2005).
23. Arkwright, P.D., *et al.* Fas stimulation of T lymphocytes promotes rapid intercellular exchange of death signals via membrane nanotubes. *Cell Res* **20**, 72-88 (2010).
24. Pasquier, J., *et al.* Different modalities of intercellular membrane exchanges mediate cell-to-cell p-glycoprotein transfers in MCF-7 breast cancer cells. *J Biol Chem* **287**, 7374-7387 (2012).
25. Chinnery, H.R., Pearlman, E. & McMenamin, P.G. Cutting edge: Membrane nanotubes in vivo: a feature of MHC class II+ cells in the mouse cornea. *J Immunol* **180**, 5779-5783 (2008).
26. Marzo, L., Gousset, K. & Zurzolo, C. Multifaceted roles of tunneling nanotubes in intercellular communication. *Front Physiol* **3**, 72 (2012).
27. Seyed-Razavi, Y., Hickey, M.J., Kuffova, L., McMenamin, P.G. & Chinnery, H.R. Membrane nanotubes in myeloid cells in the adult mouse cornea represent a novel mode of immune cell interaction. *Immunol Cell Biol* **91**, 89-95 (2013).
28. Pasquier, J., *et al.* Preferential transfer of mitochondria from endothelial to cancer cells through tunneling nanotubes modulates chemoresistance. *J Transl Med* **11**, 94 (2013).
29. Lou, E., *et al.* Tunneling nanotubes provide a unique conduit for intercellular transfer of cellular contents in human malignant pleural mesothelioma. *PLoS One* **7**, e33093 (2012).
30. Gousset, K., *et al.* Prions hijack tunnelling nanotubes for intercellular spread. *Nat Cell Biol* **11**, 328-336 (2009).
31. Den Boer, M.L., *et al.* Patient stratification based on prednisolone-vincristine-asparaginase resistance profiles in children with acute lymphoblastic leukemia. *J Clin Oncol* **21**, 3262-3268 (2003).
32. van den Berk, L.C., *et al.* Disturbed CXCR4/CXCL12 axis in paediatric precursor B-cell acute lymphoblastic leukaemia. *Br J Haematol* **166**, 240-249 (2014).
33. Sowinski, S., Alakoskela, J.M., Jolly, C. & Davis, D.M. Optimized methods for imaging membrane nanotubes between T cells and trafficking of HIV-1. *Methods* **53**, 27-33 (2011).
34. Schindelin, J., *et al.* Fiji: an open-source platform for biological-image analysis. *Nat Methods* **9**, 676-682 (2012).
35. Sourisseau, M., Sol-Foulon, N., Porrot, F., Blanchet, F. & Schwartz, O. Inefficient human immunodeficiency virus replication in mobile lymphocytes. *J Virol* **81**, 1000-1012 (2007).
36. Gyorgy, B., *et al.* Membrane vesicles, current state-of-the-art: emerging role of extracellular vesicles. *Cellular and molecular life sciences : CMLS* **68**, 2667-2688 (2011).
37. Lo Celso, C., *et al.* Live-animal tracking of individual haematopoietic stem/progenitor cells in their niche. *Nature* **457**, 92-96 (2009).
38. Alon, R. & Dustin, M.L. Force as a facilitator of integrin conformational changes during leukocyte arrest on blood vessels and antigen-presenting cells. *Immunity* **26**, 17-27 (2007).
39. Alon, R. & Ley, K. Cells on the run: shear-regulated integrin activation in leukocyte rolling and arrest on endothelial cells. *Curr Opin Cell Biol* **20**, 525-532 (2008).
40. Huang, F.Y., *et al.* The antitumour activities induced by pegylated liposomal cytochalasin D in murine models. *Eur J Cancer* **48**, 2260-2269 (2012).
41. Salu, K.J., *et al.* Effects of cytochalasin D-eluting stents on intimal hyperplasia in a porcine coronary artery model. *Cardiovasc Res* **69**, 536-544 (2006).
42. Obermajer, N., *et al.* Cathepsin X-mediated beta2 integrin activation results in nanotube outgrowth. *Cellular and molecular life sciences : CMLS* **66**, 1126-1134 (2009).

43. Ruoslahti, E. & Pierschbacher, M.D. New perspectives in cell adhesion: RGD and integrins. *Science* **238**, 491-497 (1987).
44. Straussman, R., *et al.* Tumour micro-environment elicits innate resistance to RAF inhibitors through HGF secretion. *Nature* **487**, 500-504 (2012).
45. Wilson, T.R., *et al.* Widespread potential for growth-factor-driven resistance to anticancer kinase inhibitors. *Nature* **487**, 505-509 (2012).
46. McMillin, D.W., Negri, J.M. & Mitsiades, C.S. The role of tumour-stromal interactions in modifying drug response: challenges and opportunities. *Nat Rev Drug Discov* **12**, 217-228 (2013).
47. Medyouf, H., *et al.* Myelodysplastic Cells in Patients Reprogram Mesenchymal Stromal Cells to Establish a Transplantable Stem Cell Niche Disease Unit. *Cell Stem Cell* (2014).
48. Schepers, K., *et al.* Myeloproliferative neoplasia remodels the endosteal bone marrow niche into a self-reinforcing leukemic niche. *Cell Stem Cell* **13**, 285-299 (2013).
49. Zhang, B., *et al.* Altered microenvironmental regulation of leukemic and normal stem cells in chronic myelogenous leukemia. *Cancer Cell* **21**, 577-592 (2012).
50. Greaves, M. & Maley, C.C. Clonal evolution in cancer. *Nature* **481**, 306-313 (2012).
51. Blackburn, J.S., *et al.* Clonal Evolution Enhances Leukemia-Propagating Cell Frequency in T Cell Acute Lymphoblastic Leukemia through Akt/mTORC1 Pathway Activation. *Cancer Cell* (2014).
52. Konopleva, M.Y. & Jordan, C.T. Leukemia stem cells and microenvironment: biology and therapeutic targeting. *J Clin Oncol* **29**, 591-599 (2011).
53. Pallasch, C.P., *et al.* Sensitizing protective tumor microenvironments to antibody-mediated therapy. *Cell* **156**, 590-602 (2014).
54. Manshouri, T., *et al.* Bone marrow stroma-secreted cytokines protect JAK2(V617F)-mutated cells from the effects of a JAK2 inhibitor. *Cancer Res* **71**, 3831-3840 (2011).
55. Bernardo, M.E. & Fibbe, W.E. Mesenchymal stromal cells: sensors and switchers of inflammation. *Cell Stem Cell* **13**, 392-402 (2013).
56. Francia di Celle, P., *et al.* Interleukin-8 induces the accumulation of B-cell chronic lymphocytic leukemia cells by prolonging survival in an autocrine fashion. *Blood* **87**, 4382-4389 (1996).
57. Burgess, M., *et al.* CCL2 and CXCL2 enhance survival of primary chronic lymphocytic leukemia cells in vitro. *Leuk Lymphoma* **53**, 1988-1998 (2012).
58. Roberts, K.G. & Mullighan, C.G. Genomics in acute lymphoblastic leukaemia: insights and treatment implications. *Nat Rev Clin Oncol* **12**, 344-357 (2015).

SUPPLEMENTARY DATA

SUPPLEMENTARY METHODS

Cell lines and reagents

B-cell precursor ALL (BCP-ALL) cell lines, NALM6 (B-Other) and REH (TEL-AML1), are obtained from DSMZ (Braunschweig, Germany), are used only at low cell passages, and are routinely verified by DNA fingerprinting. Cell lines were cultured in RPMI-1640 medium (Invitrogen, Life Technologies, Breda, the Netherlands) containing 10% fetal calf serum (FCS; Integro, Zaandam, The Netherlands), 1% penicillin-streptomycin at 37 °C and 5% CO_2. Immortalized hTERT-MSCs (a kind gift from Prof. Dr. D. Campana, St. Jude Children's Hospital, Memphis, TN, USA) were cultured in Dulbecco's modified Eagle medium (DMEM) low glucose medium (Invitrogen), containing 15% FCS, 1% penicillin-streptomycin, 100 μM ascorbic acid (Sigma, St Louis, MO, USA) and 1 ng/mL basic fibroblast growth factor (bFGF; Serotec, Kidlington, UK) at 37°C and 5% CO_2.

Isolation of primary BCP-ALL leukemic blasts from patients

Bone marrow aspirates were obtained from children with newly diagnosed B-cell precursor (BCP) ALL prior to treatment. Immunophenotype and genetic subtype were determined by local hospital procedures and monitored by the central diagnostic laboratory of the Dutch Childhood Oncology Group (DCOG) in The Hague. Mononuclear cells were collected using Lymphoprep sucrose-gradient centrifugation (1.077 g/mL; Nycomed Pharma, Oslo, Norway). The percentage of processed leukemic cells was determined using May-Grünwald-Giemsa staining of cytospin preparations. All samples used in this study contained ≥97% leukemic blasts. CD19-expression of leukemic blasts was determined for all samples with flow cytometry or fluorescence microscopy. Brilliant Violet 421 anti-human CD19 antibody (Biolegend, San Diego, CA, USA) was used to stain patient cells after which flow cytometry was performed. For fluorescence microscopy cells were allowed to attach on fibronectin-coated glass slides, fixated with 2% paraformaldehyde and stained with monoclonal mouse anti-human CD19 antibody (IQ Products, Groningen, The Netherlands) and DyLight-488 goat anti-mouse IgG (Biolegend). The cytogenetic subtype was determined by the central diagnostic laboratory and is summarized in table S1. Cells were cultured in RPMI Dutch-modified medium (Invitrogen) containing 20% FCS, Insulin transferrin sodium selenite (ITS), glutamin, and gentamycin at 37 °C and 5% CO_2. Bone marrow aspirates were obtained after informed consent was signed according to the Declaration of Helsinki. Protocols

were approved by the ethics committee of the Erasmus University Medical Center in Rotterdam.

Isolation and characterization of healthy and leukemic primary MSCs

Mesenchymal stromal cells (MSCs) were isolated from bone marrow aspirates taken during diagnostic procedures as indicated above. Colony-forming MSCs were selected by culturing in DMEM medium modified as above at 37 °C and 5% CO_2. Primary MSCs were characterized using positive (CD44/ CD90/ CD105/ CD54/ CD73/ CD146/ CD166/ STRO-1) and negative surface markers (CD19/ CD45/ CD34). Expression of surface markers was measured with flow cytometry using the human mesenchymal stem cell marker antibody panel (R&D Systems, Minneapolis, MN, USA) and CD54-PE, CD73-PE, CD34-PE, IgG1-PE monoclonal antibodies (BD Biosciences, San Jose, CA, USA). Multilineage potential of MSCs was confirmed for adipocyte (Oil Red O staining), osteocyte (*Alizarin Red* S staining), and chondrocyte (Col2a/ Thionine/ Alcian Blue staining) differentiation.

Confocal laser scanning microscopy

To assess the formation of TNTs we used confocal scanning microscopy of fixated co-cultures as well as time-lapse imaging of co-cultures. In all experiments BCP-ALL cell lines (REH and NALM6) or primary leukemic cells were co-cultured with primary or hTERT-immortalized MSCs in a 4:1 ratio. These conditions represent 50-60% MSC confluence and normal leukemic cell culture conditions (200.000 cells/ mL). For high resolution images, differentially stained cells were cultured on a glass slide coated with 10 μg/mL fibronectin (Sigma) at 37 °C and 5% CO_2. Cells were fixated after 3 or 24 hours using 1.5% glutaraldehyde, 2% formaldehyde in PBS for 10 minutes at room temperature, as previously described[56]. After fixation, slides were mounted with ProLong Gold antifade reagent (Life Technologies) and imaged using a confocal laser scanning microscopy (Leica SP5). Images were acquired with sequential scanning of different channels at a resolution of 1024 x 1024 pixels in the x ^{x} y plane and 0.15 μm steps in z-direction. For time-lapse imaging, DiO-stained MSCs were allowed to attach to a glass slide before start of the experiment. At start of experiment, DiI-stained leukemic cells were added and imaged using a confocal laser scanning microscope (Leica SP5). Cultures were maintained at 37°C on a heated stage and at 5% CO_2 and imaged starting roughly 5 minutes after the start of the co-culture. Images were acquired every 3.3 minutes for a total duration of 10 hours with sequential scanning of different channels at a resolution of 512 x 512 pixels in the x ^{x} y plane and 0.5 μm steps in z-direction.

3D image stacks were acquired by optical sectioning using the LAS software provided with the instrument. The system was equipped with a 63× plan-

apochromatic oil 1.4 NA DIC objective. The pinhole diameter was set to 1 airy unit (95.5 μm). DiO and DiI were excited with a 488-nm Argon laser and a 561-nm Diode-Pumped Solid-State laser, respectively. Phalloidin-FITC was excited with the 488-nm Argon laser. Transmission images were obtained using the 488-nm Argon laser.

Image processing was done with Fiji software. Brightness and contrast were optimized and applied to the entire image. Z-project using all sides and maximum intensity projection was used to analyze 3D image stacks. For 3D projections, standard settings with brightest point projection were used.

Flow cytometry

Leukemic cells were co-cultured with MSCs. To quantify TNT signaling from leukemic cells to MSCs, leukemic cells were stained with DiI (5 μL per 10^6 cells, 5 minutes at 37 °C) and thereafter co-cultured with unstained MSCs for the indicated time periods. In dye transfer experiments presented in Figure 1A and 1E-F, Figure 2B-D, Figure 4B-F, supplementary Figure 3, and supplementary Figure 8, leukemic cells were co-cultured with MSCs in a 4:1 ratio. To allow a fair comparison between dye transfer from leukemic cells to MSCs versus dye transfer from MSCs towards leukemic cells, leukemic cells were co-cultured with MSCs in a 1:1 ratio for experiments shown in Figure 1C-D. Signaling via gap junctions from leukemic cells towards MSCs was quantified in a similar fashion using BCP-ALL cell lines stained with Calcein Red-Orange AM (2 μM, 30 minutes at room temperature). DiI-stained MSCs were co-cultured with unstained leukemic cells to quantify TNT signaling from MSCs towards leukemic cells. After co-cultures, cells were stained with Brilliant Violet 421 anti-human CD19 antibody (Biolegend). Dye transfer towards the unstained fraction was assessed at different time points using flow cytometry (BD Bioscience).

To quantify interleukemic TNT formation, BCP-ALL cell lines (REH and NALM6) were stained with DiO and mixed with an equal amount of cells stained with DiD (5 μL per 10^6 cells, 5 minutes at 37 °C). Double positive cells (DiO^{pos}/DiD^{pos}) were quantified after 24 hours as a measure of interleukemic TNT signaling by flow cytometry.

We used three independent experimental setups to inhibit TNT formation: 1) Inhibition of the actin cytoskeleton with 250 nM – 1 μM cytochalasin D (Sigma) or 125 - 500 nM latrunculin B (Sigma). 2) Mechanical disruption of TNTs through gentle shaking (250 rpm) of cell cultures. 3) Prevention of TNT formation by applying a physical distance between leukemic cells and the MSCs using a 3.0 μm transwell system (Corning, NY, USA). To assess the contribution of integrins to TNT signaling, we used 20 - 100 μM Arg-Gly-Asp-Ser (RGDS) -peptide (Sigma) to inhibit integrins receptor binding. As a negative control, equal concentrations of the non-RGD containing peptide Gly-Arg-Ala-Asp-Ser-Pro (GRADSP;

Sigma, St Louis, USA) were used. All flow cytometry data was analyzed using FlowJo V10 software (Treestar Inc., Ashland, USA).

Cell viability assays

Primary patient cells (1 x 10^6 cells) were co-cultured with or without primary mesenchymal stromal cells (5 x 10^4) for five days in a 24-well plate at 37 °C and 5% CO_2. Stromal cells were allowed to attach prior to the start of an experiment. Cells were cultured either static, with gentle shaking or in a 3.0 μm transwell system (leukemic cells in upper compartment, MSCs in bottom compartment). Before the start of each experiment, leukemic cells were screened for CD19 positivity (Brilliant Violet 421 anti-human CD19 antibody) and CD45 positivity (Brilliant Violet 421 anti-human CD45 antibody; Biolegend), which was used to discriminate leukemic cells from $CD19^{neg}/CD45^{neg}$ MSCs. The percentage of viable leukemic cells was determined after 5 days of culture by staining with Brilliant Violet 421 anti-human CD19 or CD45 antibody (Biolegend), FITC Annexin V (Biolegend), and Propidium Iodide (PI; Sigma), after which the percentage of $AnnexinV^{neg}/PI^{neg}/CD19^{pos}/CD45^{pos}$ cells within the MSC negative fraction (see Figure 6A for gating strategy) was determined by flow cytometry (BD Biosciences).

To establish the effect of TNTs on cellular responsiveness to drugs, primary leukemic cells were exposed to prednisolone in a concentration which was lethal to 50% of the patient derived leukemic cells (LC50 in μg/mL) or which inhibited proliferation of NALM6 cell lines by 50% (GI50 in μg/mL) as determined upfront by a 4-day MTT assay[41]. Viable leukemic cells were counted ($PI^{neg}/CD19^{pos}$) using a MACSQuant analyzer (Miltenyi Biotec, Gladbach, Germany).

Multiplexed fluorescent bead-based immunoassay (Luminex)

Primary leukemic cells or cell lines were co-cultured with different sources of primary MSCs with or without TNT inhibition (shaking or transwell condition) for 5 days (3 days for cell lines) at 37 °C and 5% CO_2. Next, supernatant was collected and cell viability of leukemic cells was assessed as described above. The concentration of 64 known cytokines/chemokines in these supernatants was analyzed using fluorescent bead-based immunoassay (Luminex Human Cytokine/Chemokine Panel I and II; Merck Millipore) according to the manufacturer's protocol.

SUPPLEMENTARY TABLES

Supplementary Table 1. Characteristics of primary BCP-ALL cells.

Name	Subtype	Remarks
ALL#1	BCR-ABL1	-
ALL#2	TEL-AML1	-
ALL#3	TEL-AML1	-
ALL#4	TEL-AML1	-
ALL#5	B-Other	E2A-rearranged subclone (21%)
ALL#6	B-Other	-
ALL#7	BCR-ABL1-like	-
ALL#8	BCR-ABL1-like	Down syndrome
ALL#9	BCR-ABL1-like	-
ALL#10	B-Other	ETV6 loss

Supplementary Table 2. Characteristics of primary MSCs.

Name	Subtype	Remarks
MSC#1	B-Other	-
MSC#2	TEL-AML1	-
MSC#3	B-Other	-
MSC#4	Remission	1 year after treatment
MSC#5	AML	-
MSC#6	Healthy	-
MSC#7	Healthy	-
MSC#8	Healthy	-
MSC#9	Healthy	-
MSC#10	Healthy	-
MSC#11	B-Other	-
MSC#12	TEL-AML1	-
MSC#13	CML	-

Supplementary Table 3. Cytokine secretion in mono and co-cultures of ALL and MSCs.

Cytokine	MSCs	ALL	Co-culture*	Cytokine	MSCs	ALL	Co-culture*
6Ckine				IL33			
BCA-1				IL4			
CTACK				IL5			
EGF	x	x		IL6	x		
ENA-78				IL7			
Eotaxin		x		IL8	x	x	x
Eotaxin-2				IL9			
Eotaxin-3	x			IP10			x
FGF-2	x			LIF			
Flt3 Ligand				MCP-1	x	x	
Fractalkine				MCP-2			
G-CSF				MCP-3			
GM-CSF	x			MCP-4			
GRO	x			MDC		x	
I-309				MIP-1alpha		x	
IFNalpha2				MIP-1beta		x	
IFNgamma				MIP-1delta			
IL10				PDGF-AA	x	x	
IL12				PDGF-BB		x	
p70				RANTES			
IL13				sCD40L			
IL15				SCF	x		
IL16				SDF1-alpha/beta	x		
IL17A				TARC			x
IL1alpha				TGFalpha			
IL1beta				TNFalpha		x	
IL1-ra				TNFbeta			
IL2				TPO			
IL20				TRAIL			
IL21				TSLP			
IL23				VEGF	x	x	x
IL28a							
IL3							

*Crosses indicate upregulation of this cytokine in co-culture compared to monocultures.

SUPPLEMENTARY FIGURES

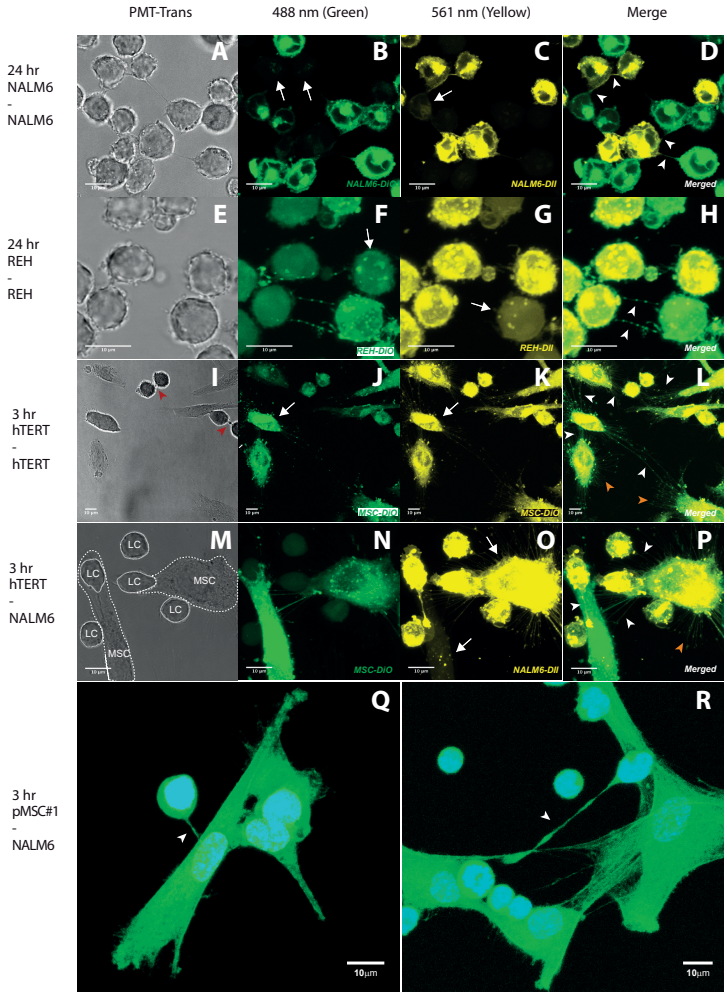

Supplementary Figure 1. TNTs between BCP-ALL cells and MSCs.
(A-H) Interleukemic TNT networks (exemplified by white arrowheads) and exchange of lipophilic dye (exemplified by arrows) between NALM6 (A-D) or REH (E-H) cells (DiI, yellow; DiO, green) were observed after 24 hours of co-culture. White arrows indicate transfer of dye to recipient cell. (I-L) TNT networks were formed and dye transfer was present between hTERT-immortalized MSCs (DiI, yellow; DiO, green). TNT-like structures also attached to the fibronectin-coated substratum (exemplified by orange arrowheads; right panel). Red arrowheads (left panel) represent 'midbodies'. These midbodies look similar to TNTs, but are a short-lasting remainder of cell division. (M-P) Co-cultures of hTERT-immortalized MSCs (indicated by MSC) and BCP-ALL cell line NALM6 (indicated by LC) showed elaborate TNT networks and dye transfer after 3 hours of co-culture. (Q-R) Phalloidin-FITC staining of F-actin, shows the presence of F-Actin in TNTs between BCP-ALL cells (NALM6) and MSCs (primary MSC#1). White arrowheads indicate TNTs. DAPI-staining (blue) was used to stain nuclei.
Images M-P are 3D image stacks. Scale bars represent 10 µm.

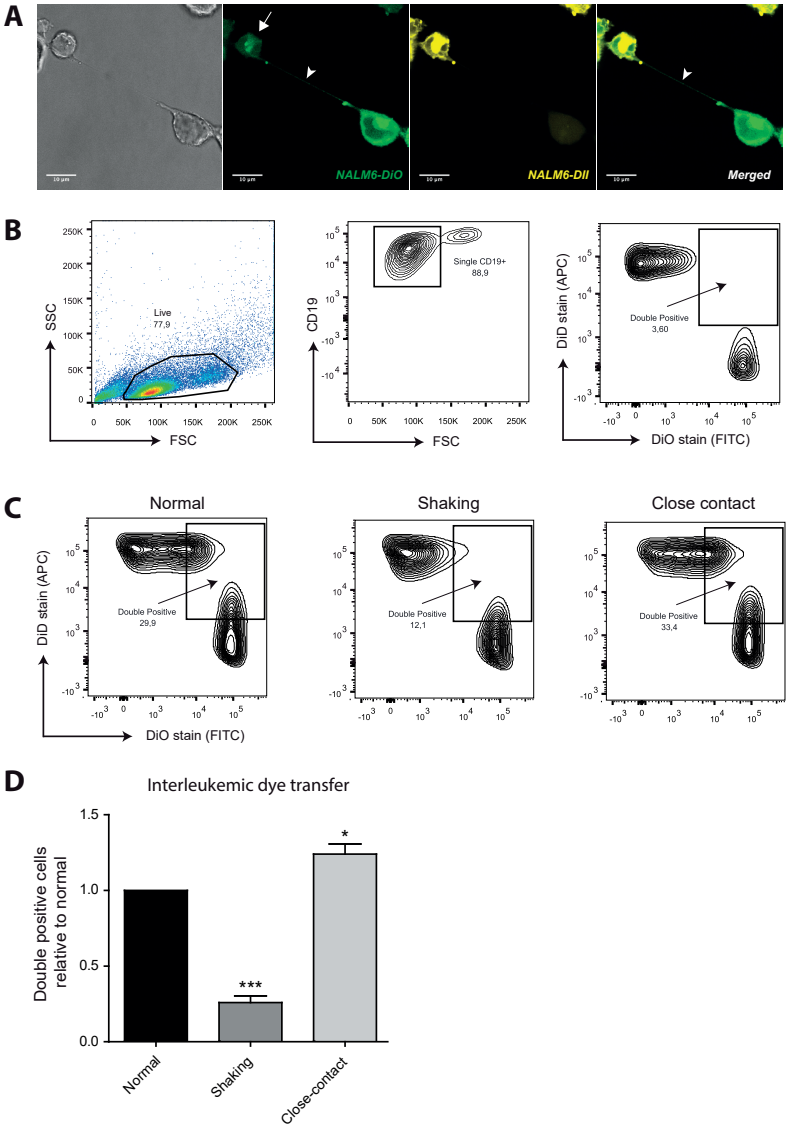

Supplementary Figure 2. TNT signaling between BCP-ALL cells.

(A) Representative confocal images showing TNT formation (white arrowhead) between two NALM6 cells (DiI, yellow; DiO, green) after co-culture for 24 hours. White arrow indicates transfer of dye to recipient cell. (B) DiD-stained BCP-ALL NALM6 cells were cultured in a 1:1 ratio with DiO-stained BCP-ALL NALM6 cells for 24 hours. Double positive cells (DiD+/DiO+) were quantified and used as a measure of interleukemic signaling. Right panel represents the start of the experiment. (C) Graphs showing quantification of interleukemic dye transfer between NALM6 cells. Gentle shaking reduced interleukemic TNT signaling whereas culture in a 3.0 μm transwell system – in which leukemic cells reside in close contact - increased interleukemic TNT signaling. (D) Bar graphs representing interleukemic dye transfer in TNT-inhibiting and TNT-inducing conditions, exemplified in (C), compared to dye transfer in normal co-culture (n = 4; one-tailed t-test, paired).

Data are means ± SEM; * $p \leq 0.05$, ** $p \leq 0.01$, *** $p \leq 0.001$.

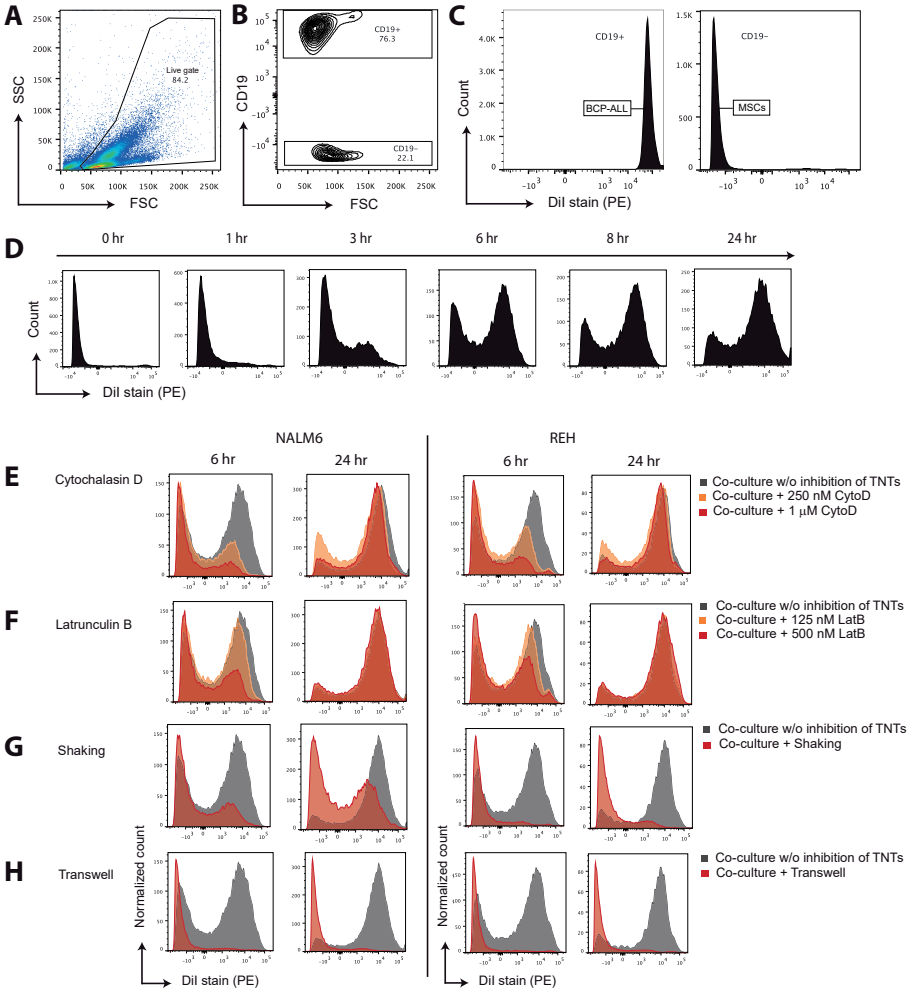

Supplementary Figure 3. Lipophilic dye transfer is caused by TNT signaling.
DiI-stained CD19^{pos} BCP-ALL cells (NALM6 and REH) were co-cultured with unstained CD19^{neg} hTERT-MSCs and transfer of DiI staining to hTERT-MSCs was analyzed by flow cytometry at the indicated time points.
(A-C) Gating strategy for analysis of dye transfer from leukemic cells towards MSCs. Panel C represents the start of the experiment. (D) Quantification of dye transfer showing efficient transfer from DiI-stained REH cells towards unstained hTERT-MSCs in time (cultured in 4:1 ratio). Data is representative of three independent experiments. (E-H) After 6 hours of co-culture, dye transfer from DiI –stained NALM6 cells towards unstained hTERT-MSCs was decreased using three independent TNT inhibiting conditions: actin inhibition (E: cytochalasin D, F: latrunculin B), physical disruption by gentle shaking (G), or culture in a 3.0 μm transwell system (H). TNT inhibition by gentle shaking, or culture in a 3.0 μm transwell system was continuous, while the inhibition of TNT signaling with actin inhibitors (observed after 6 hours of co-culture) was reversed after 24 hours, due to the short half-life of these inhibitors. Data is representative of three independent experiments.

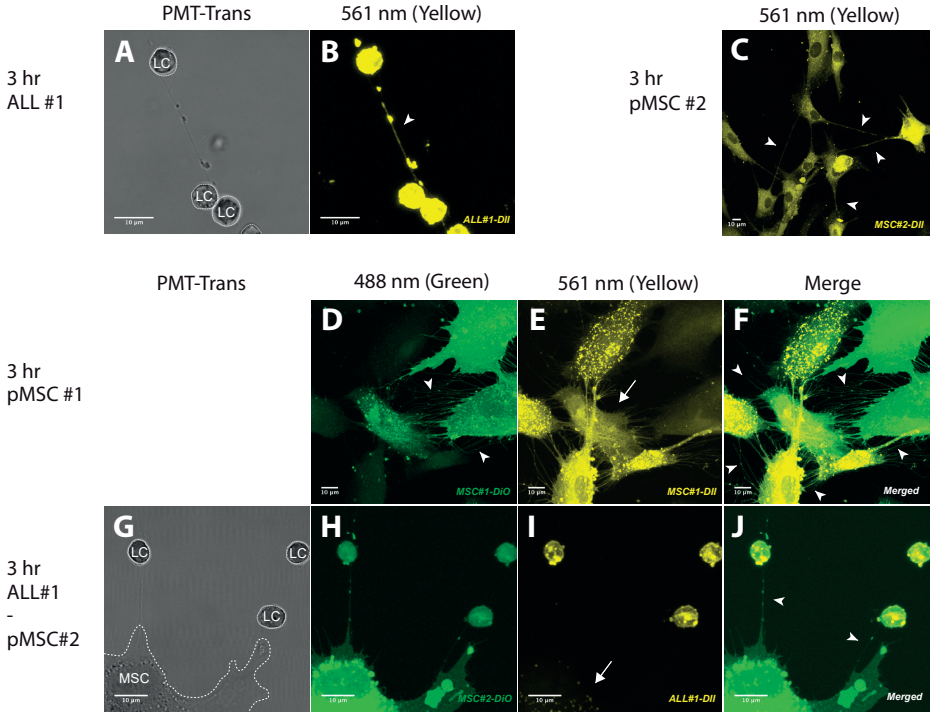

Supplementary Figure 4. TNT networks between primary cells.
(A-B) Culture of BCP-ALL patient cells showed interleukemic TNT formation (arrowhead) after 3 hours. (C-F) Culture of BCP-ALL patient MSCs (c: MSC#1, d-f: MSC#2) showed the formation of intermesenchymal TNT networks (arrowheads) which have transferred dye (arrow) after 3 hours. (G-J) TNT signaling between primary BCP-ALL cells (DiI; yellow) and primary MSCs (DiO; green) after co-culture for 3 hours showed bidirectional exchange of lipophilic dye (arrows) via TNTs (white arrowheads).
Images are 3D image stacks. Data is representative of at least 3 experiments. Scale bars represent 10 μm.

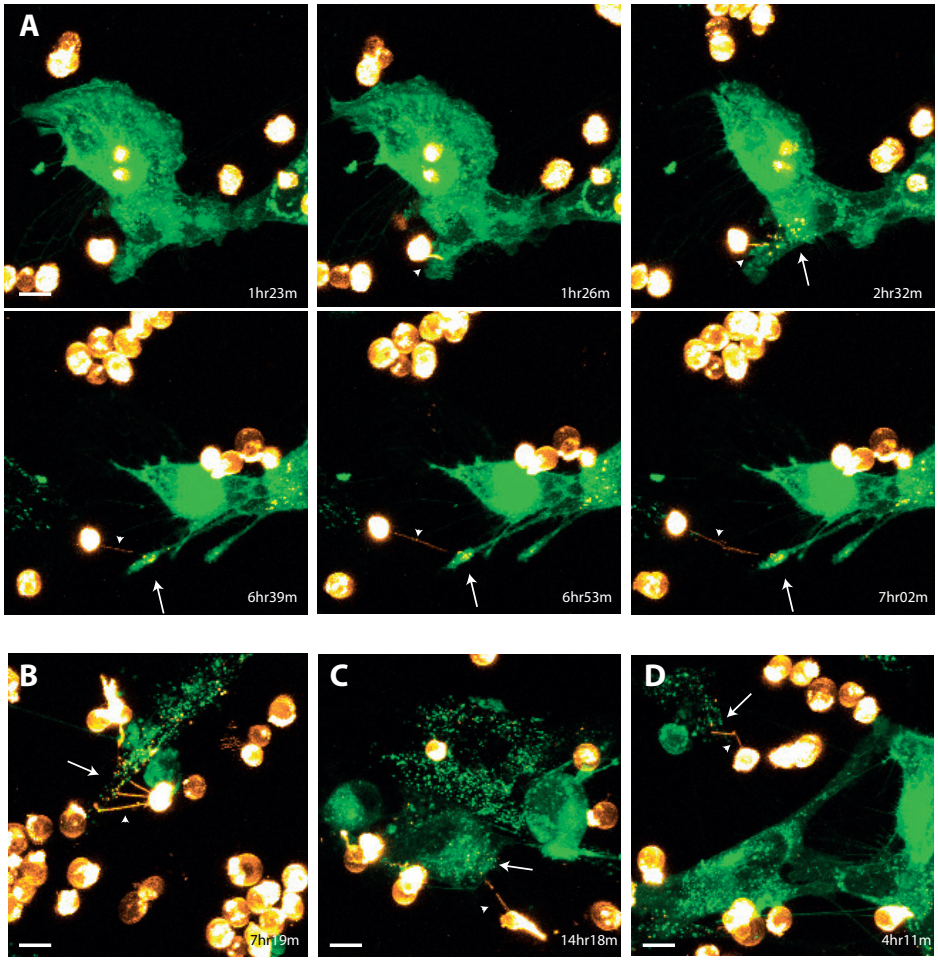

Supplementary Figure 5. Dynamics of TNT formation between primary cells.
(A) Time-lapse confocal images (3D image stacks) showing TNT formation (white arrowhead) between primary BCP-ALL cells (ALL#10; DiI, yellow) and primary MSCs (pMSC#1; DiO, green) at multiple time points. White arrow indicates transfer of dye to recipient cell. Time indicated in the right lower corner is the duration from start of the experiment. Orange Hot look-up table (LUT) was used to visualize DiI. Scale bars represent 10 μm. (B-D) Single frames of time-lapse confocal microscopy experiments (3D image stacks) showing TNT formation and signaling from primary BCP-ALL cells (ALL#10; DiI, yellow) and primary MSCs (pMSC#1; DiO, green).

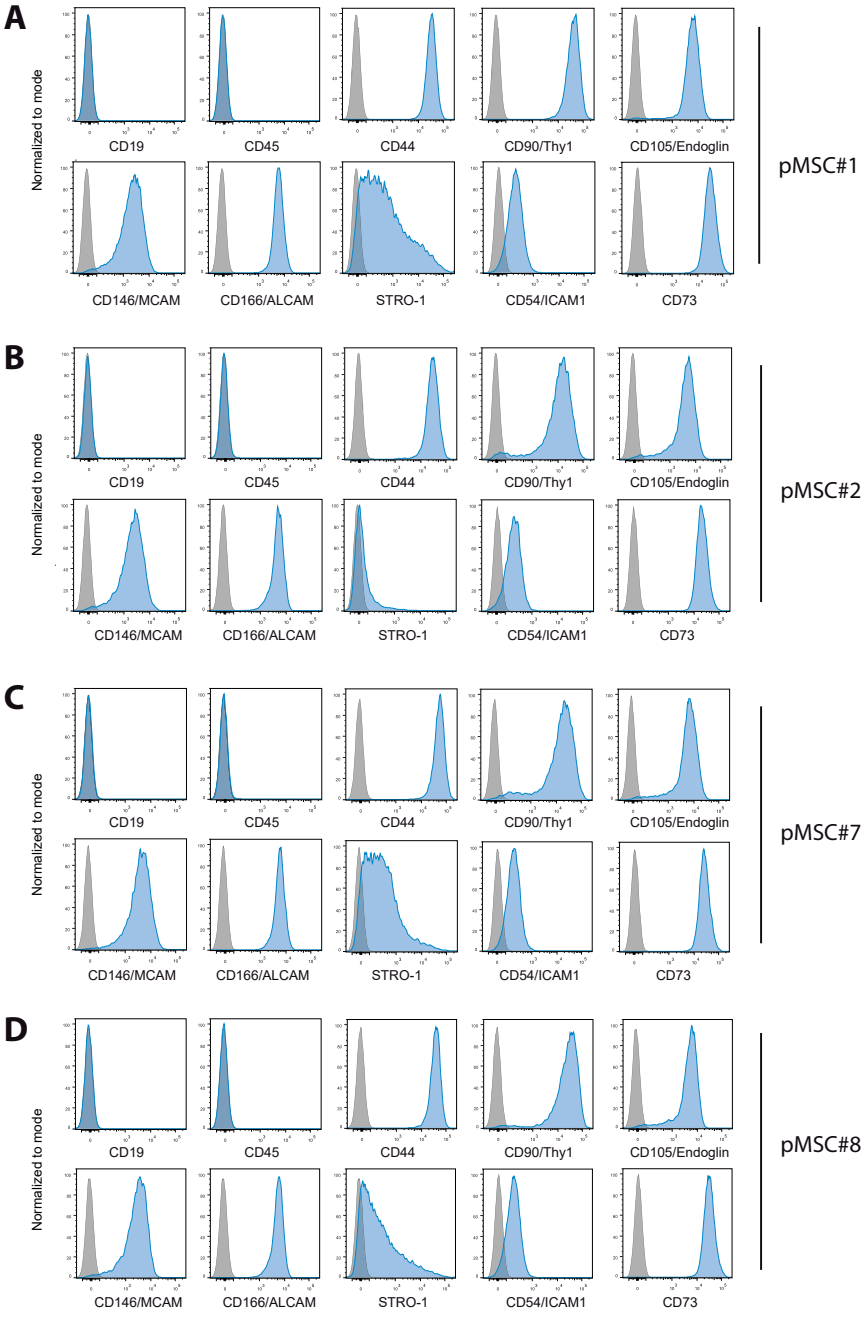

Supplementary Figure 6. Surface marker expression of primary human MSCs.
All primary human MSCs were characterized using positive (CD44/ CD90/ CD105/ CD54/ CD73/ CD146/ CD166/ STRO-1) and negative surface markers (CD19/ CD45/ CD34). (A-D) Representative graphs showing the expression of surface markers on 4 primary MSCs. Blue graphs represent surface marker expression. Gray graphs represent expression of isotype controls.

A

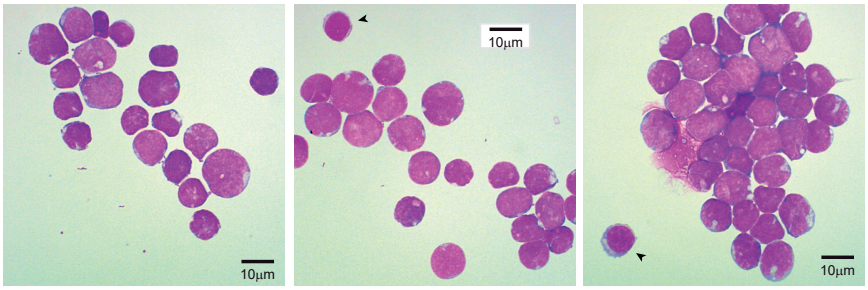

B

	Subgroup	Blasts	Lympho	Mono	Neutro	Me/My
ALL#1	*TA*	98%	-	-	-	2%
ALL#2	*TA*	99%	1%	-	-	-
ALL#3	*TA*	97%	3%	-	-	-
ALL#4	*TA*	98%	1%	-	-	1%
ALL#5	*BO*	98%	1%	1%	-	-
ALL#6	*BO*	97%	3%	-	-	-
ALL#7	*BAL*	99%	1%	-	-	-
ALL#8	*BAL*	97%	1%	-	1%	1%

C

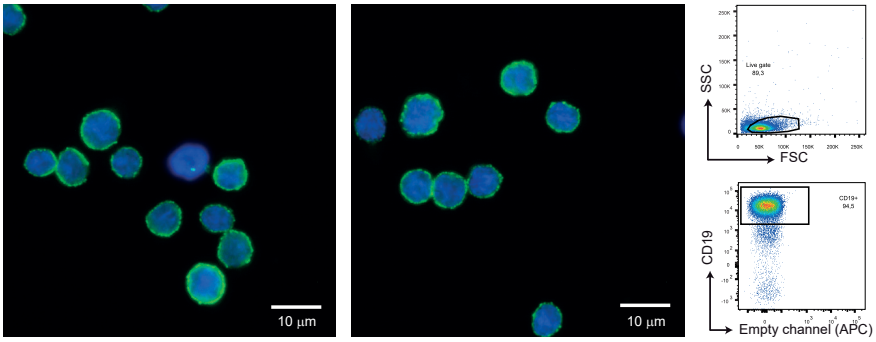

Supplementary Figure 7. Characterization of primary leukemic blasts.
(A) The percentage of processed leukemic cells was determined using May-Grünwald-Giemsa staining of cytospin preparations. Images show representative cytospin preparation of leukemic blasts of patient ALL#3. Black arrowheads indicate lymphocytes. All other cells are scored as leukemic blasts. (B) Table containing blast percentages of primary BCP-ALL samples obtained by scoring at least 200 cells per sample. (C) CD19-expression of leukemic blasts was determined for all samples with flow cytometry or fluorescence microscopy. Images are representative and show CD19 surface marker expression of leukemic blasts of patient ALL#3. Dot plots show CD19 surface marker expression of leukemic blasts of patient ALL#3 using flow cytometry.

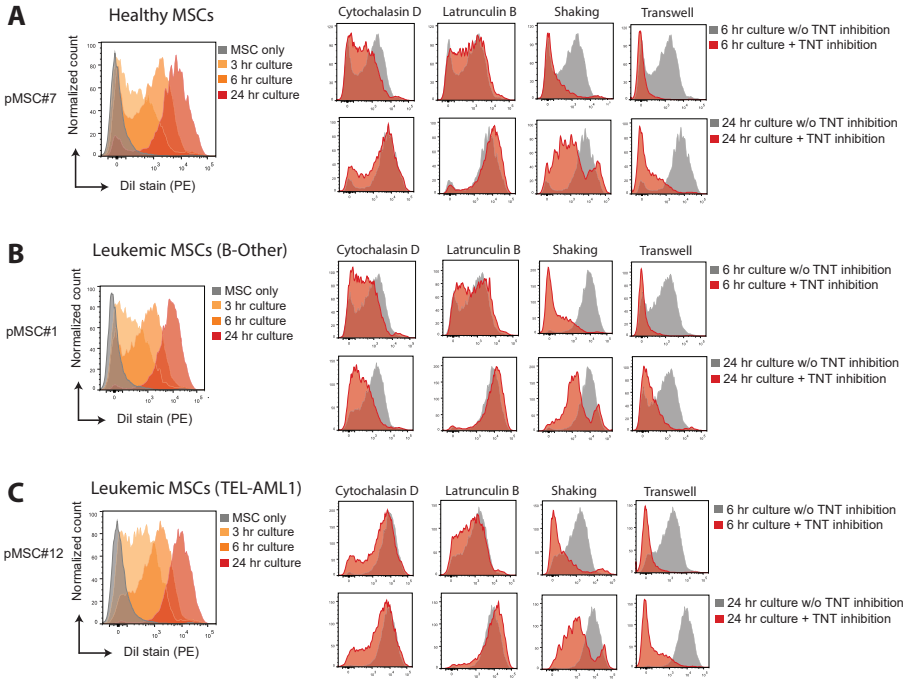

Supplementary Figure 8. TNT signaling to healthy and leukemic MSCs is similarly efficient.
Quantification of dye transfer indicating similarly efficient transfer from DiI-stained REH cells towards unstained primary healthy and primary leukemic MSCs (cultured in 4:1 ratio) in time.
(A) Dye transfer from DiI –stained NALM6 cells towards unstained primary MSCs of a healthy donor. Three independent TNT inhibiting conditions (actin inhibition (cytochalasin D; 1μM, latrunculin B; 500 nM), physical disruption by gentle shaking, or culture in a 3.0 μm transwell system) decreased dye transfer from leukemic cells towards primary MSCs. (B) Same as (A) for transfer towards unstained primary MSCs of a BCP-ALL patient (B-Other). (C) Same as (A) for transfer towards unstained primary MSCs of a BCP-ALL patient (TEL-AML1).

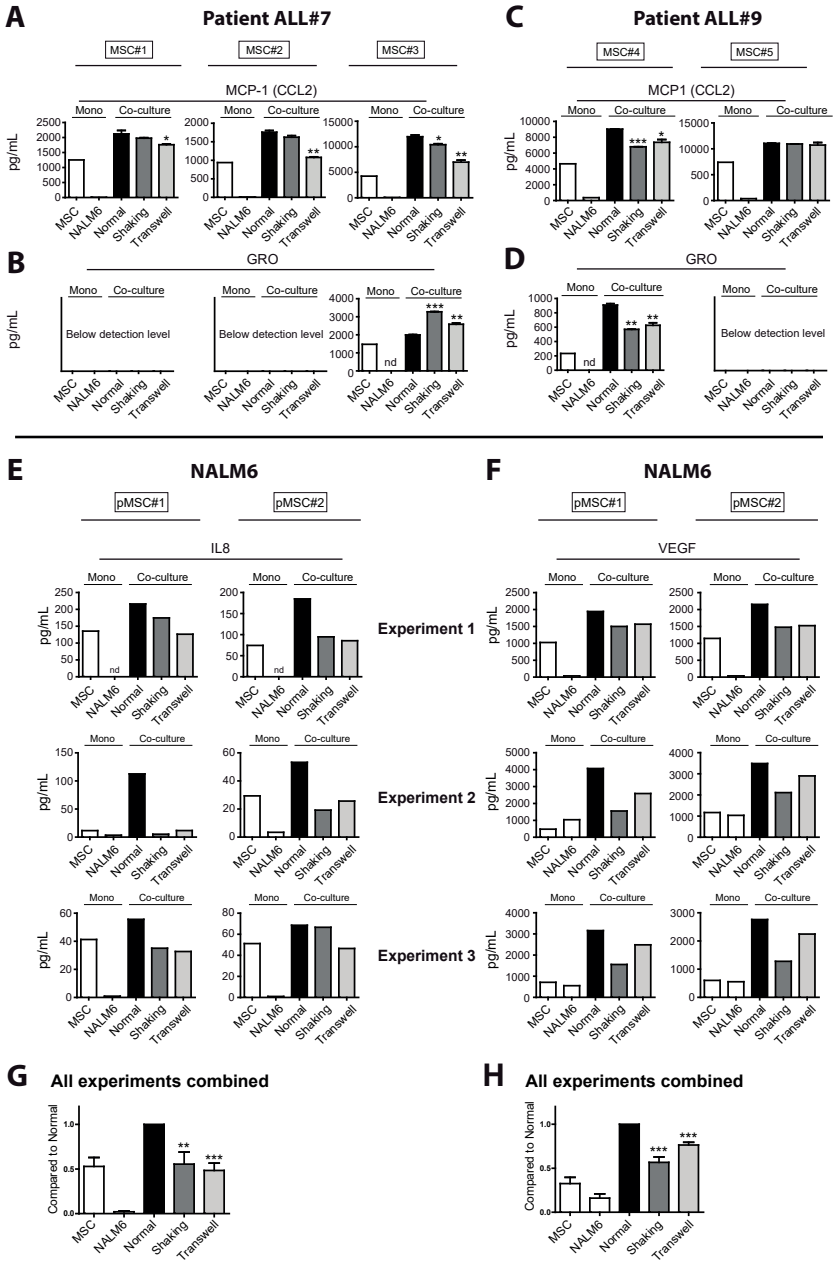

Supplementary Figure 9. Secretion of cytokines induced by primary BCP-ALL cells.
(A) MCP-1 (CCL2) supernatant levels in co-culture of primary leukemic patient ALL#7 cells with primary MSC#1 (left panel), MSC#2 (middle panel), or MSC#3 (right panel). TNT signaling was inhibited by gentle shaking or culture in a transwell system. *p<0.05, **p<0.01 (one-tailed t-test, unpaired). (B) Same as (A) for GRO levels. (C) MCP-1 (CCL2) supernatant levels in co-culture of primary leukemic patient ALL#9 cells with primary MSC#4 (left panel), or MSC#5 (right panel).

Supplementary Figure 9. Secretion of cytokines induced by primary BCP-ALL cells. (continued)
(D) Same as (C) for GRO levels. (E) IL8 supernatant levels in co-culture of BCP-ALL cells (NALM6) with primary MSC#1 (left panel) or MSC#2 (right panel). TNT signaling was inhibited by gentle shaking or culture in a transwell system. (F) VEGF supernatant levels in co-culture of BCP-ALL cells (NALM6) with primary MSC#1 (left panel) or MSC#2 (right panel). (G) IL8 measurements as seen in (F) relative to the 'Normal' condition (one-tailed t-test, paired) (H) VEGF measurements as seen in (C) relative to the 'Normal' condition (one-tailed t-test, paired)
Data are means ± SEM. * $p \leq 0.05$, ** $p \leq 0.01$, *** $p \leq 0.001$ (one-tailed t-test, unpaired). nd = not detectable (below detection level).

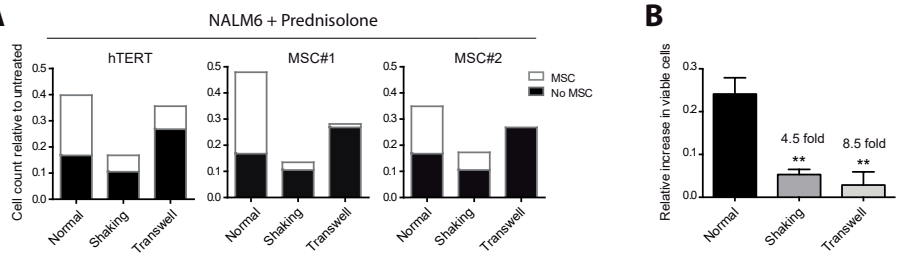

Supplementary Figure 10. TNTs contribute to drug resistance.
These data represent the same experiment as shown in Figure 7B.
(A) BCP-ALL cell line NALM6 was cultured with (white bars) or without (black bars) MSCs (of three different sources) and cultures were exposed to prednisolone. Bars represent the cell count relative to an untreated control. (B) The relative survival benefit for NALM6 cells in co-culture with MSCs. Inhibition of TNT signaling (by gentle shaking or culture in a 3.0 μm transwell system) re-sensitized to prednisolone (n = 3; one-tailed t-test, unpaired). Data are means ± SD. ** $p \leq 0.01$ (one-tailed t-test, unpaired).

SUPPLEMENTARY VIDEOS

Video 1. TNT formation between BCP-ALL cells and MSCs.
TNTs are thin membrane tethers containing F-Actin that do not contact the substratum. These videos show that membrane tethers between BCP-ALL cells and MSCs do not touch the substratum.
(A) Video showing all z-stacks of images shown in Figure 1A-D. Video starts at the highest Z-stack and moves towards the fibronectin-coated glass slide. (B) Video showing 3D projections of all z-stacks of images in Figure 1A-D.

Video 2. TNT connecting a BCP-ALL cell and a MSC.
Video showing a thin membrane tether between a BCP-ALL cell (NALM6; DiI; in red) and a MSC (hTERT-MSC; in green) that does not touch the substratum. Dye transfer from the BCP-ALL cell to the MSC is illustrated by the presence of red dye in the MSC.

Video 3. Time lapse analysis of TNT formation between BCP-ALL cells and MSCs.
Time-lapse confocal imaging showing TNT formation from NALM6 cells (DiI; yellow) towards primary MSCs (DiO; green) in time (red arrows). NALM6 cells were labeled with the fluorescent lipophilic dye DiI, and primary MSCs were labeled with the fluorescent lipophilic dye DiO.
Frames were collected every 3 minutes and 19 seconds and the video runs at 3 frames/second, except between 0:09 and 0:15 seconds, where the playback speed is increased 1.5 times. All frames are 3D image stacks as described in Figure 3 and Supplementary Methods. 3D projections of start and end of experiment are included to show the amount of dye transfer and are confocal signals of 561-nm laser overlaid to bright field images.

Video 4. Time lapse analysis of TNT formation between BCP-ALL cells and MSCs.
(A) Time-lapse confocal imaging showing TNT formation from NALM6 cells (DiI; yellow) towards primary MSCs (DiO; green) in time (red arrows). Blue arrow indicates a TNT formed by MSCs. NALM6 cells were labeled with the fluorescent lipophilic dye DiI, and primary MSCs were labeled with the fluorescent lipophilic dye DiO. Frames were collected every 3 minutes and 19 seconds and the video runs at 3 frames/second. (B) 3D projections of start (0 hr) and end (10 hr) of experiment to illustrate the amount of dye transfer. Confocal signals of 561-nm laser are overlaid to bright field images.

These supplementary videos are available online: www.bloodjournal.org/content/126/21/2404.

Chapter 6

Acute lymphoblastic leukemia cells create a leukemic niche without affecting the CXCR4/CXCL12 axis

Bob de Rooij[1]*, Roel Polak[1]*, Lieke C.J. van den Berk[1], Femke Stalpers[1], Rob Pieters[2] & Monique L. den Boer[1]

[1] *Dept. of Pediatric Oncology, Erasmus MC, Sophia Children's Hospital, Rotterdam, The Netherlands.*
[2] *Princess Máxima Center for Pediatric Oncology, Utrecht, The Netherlands.*

* *These authors contributed equally to this work and the study.*

Adapted to letter format for publishing.

Haematologica 2017 Oct;102(10):e389-e393

ABSTRACT

Acute leukemia cells disrupt the healthy bone marrow microenvironment to create a leukemic niche. Several studies have tried to target this leukemic niche by inhibiting CXCR4/CXCL12 signaling. Here, we show that B-cell precursor acute lymphoblastic leukemia (BCP-ALL) cells modify their niche without affecting the CXCR4/CXCL12 axis. We used a patient-derived co-culture model in which the leukemic niche was represented by BCP-ALL cells and mesenchymal stromal cells (MSCs). Leukemic co-cultures significantly induced migration of leukemic counterparts, while inhibiting migration of healthy $CD34^+$ hematopoietic cells and MSCs. This induction of leukemic cell migration was not affected by CXCR4 blockade. Moreover, CXCL12 levels were unaltered in co-cultures of primary BCP-ALL cells and primary MSCs. Instead, we found the induction of patient-unique secretion patterns affecting alternative chemokine pathways, including CCR4, CXCR1/2, and CXCR3 ligands. Also in serum of bone marrow aspirates from BCP-ALL patients, we found a significant and recurrent increase of CCR4 and CXCR1/2 ligands compared to matched bone marrow of the same patients in remission and to healthy controls. These data show that BCP-ALL cells modify the migration properties of their niche without altering the CXCR4/CXCL12 axis, and identify CCR4 and CXCR1/2 signaling as candidate factors for leukemic niche disruption.

INTRODUCTION

Acute lymphoblastic leukemia (ALL) is characterized by an outgrowth of malignant lymphoblasts that occupy the bone marrow microenvironment, where they reside with mesenchymal stromal cells (MSCs)[1]. Leukemic cells are able to disrupt the healthy microenvironment and create a leukemic niche that shelters malignant cells from elimination through cytostatic treatment and immune responses[2-7]. Disrupting intercellular communication in this malignant microenvironment sensitizes leukemic cells to chemotherapeutic drugs[8].

Homing of ALL cells toward the bone marrow microenvironment is thought to be similar to that of hematopoietic stem cells (HSCs)[9,10]. Human $CD34^+$ hematopoietic cells are attracted by stromal cell-derived factor 1 (SDF-1/CXCL12), a chemoattractant actively produced by MSCs in the bone marrow[9-11]. CXCL12 binds to the CXCR4 receptor, which is highly expressed on HSCs. Disturbance of the CXCR4/CXCL12 axis, by treatment with cytokines and/or CXCR4 antagonists, mobilizes HSCs to the peripheral blood and is used to harvest HSCs for stem cell transplantation[12]. Like HSCs, ALL cells have high CXCR4 surface expression and disruption of CXCR4/CXCL12 interaction reduces ALL engraftment in animal models[13,14]. However, in mice suffering from ALL, CXCR4/CXCL12 inhibition as mono-treatment did not reduce the leukemic cell number in the bone marrow[13,15]. This suggests that ALL cells use additional mechanisms to retain a protective microenvironment. In this study, we used an *ex vivo* co-culture model in which we cultured B-cell precursor ALL (BCP-ALL) cells with MSCs obtained from patients. Our data reveal that BCP-ALL cells create a self-reinforcing leukemic microenvironment that significantly attracts malignant cells and repels healthy hematopoietic cells independent of CXCR4/CXCL12 signaling. This study highlights the need for specific inhibitors other than CXCR4 antagonists for the disruption of the leukemic niche in ALL.

METHODS

Cell lines and reagents

B-cell precursor ALL (BCP-ALL) cell lines, NALM6 (B-Other) and REH (TEL-AML1), were obtained from DSMZ (Braunschweig, Germany), used at low cell passages, and routinely verified by DNA fingerprinting. Cell lines were cultured in RPMI-1640 medium containing 10% fetal calf serum (FCS), 1% penicillin-streptomycin at 37 °C and 5% CO_2.

Isolation of primary BCP-ALL leukemic blasts from patients

Primary BCP-ALL leukemic blasts were isolated from patients as described earlier[8]. In short, mononuclear leukemic cells were collected from bone marrow aspirates obtained from children with newly diagnosed BCP-ALL prior to treatment. All samples used in this study contained > 95% leukemic blasts.

Isolation and characterization of primary MSCs

Primary MSCs were isolated and characterized using positive (CD44/ CD90/ CD105/ CD54/ CD73/ CD146/ CD166/ STRO-1) and negative surface markers (CD19/ CD45/ CD34)[8]. In addition multilineage potential was confirmed as described earlier[8].

Isolation of $CD34^+$ cells

$CD34^+$ cells were obtained from umbilical cord blood using the Direct CD34 Progenitor Cell Isolation kit, human (Miltenyi Biotec, Gladback, Germany). $CD34^+$ cells were positively selected by magnetic microbeads using the MACS LS column (Miltenyi Biotec) in combination with a MACS separator (Miltenyi Biotec). The purity of the isolated cells was confirmed by flow cytometry using the CD34-PE fluorescent antibody (BD Pharmingen, San Diego, USA).

Collection of bone marrow aspirates

Serum samples of bone marrow aspirates were collected from children with ALL at initial diagnosis and after completion of two courses of chemotherapy according to the ALL-10 protocol of the Dutch Childhood Oncology Group (day 79 after start of treatment) as previously described[11]. This study was approved by the Institutional Review Board and informed consent was obtained from parents or guardians.

Cell viability assays

Cell viability assays of primary material was performed as earlier described[8]. In short, primary patient cells (1×10^6 cells) were co-cultured with or without primary stromal cells (5×10^4) for five days in a 24-well plate at 37 °C and 5% CO_2. Stromal cells were allowed to attach prior to the start of an experiment. Before the start of each experiment, leukemic cells were screened for CD19 positivity (Brilliant Violet 421 anti-human CD19 antibody), which was used to discriminate leukemic cells from $CD19^{neg}$ MSCs. The percentage of viable leukemic cells was determined after 5 days of culture by staining with Brilliant Violet 421 anti-human CD19 (Biolegend), FITC Annexin V (Biolegend), and Propidium Iodide (PI; Sigma), after which the percentage of $AnnexinV^{neg}/PI^{neg}/CD19^{pos}$ cells within the MSC negative fraction was determined by flow cytometry (BD Biosciences).

Multiplexed fluorescent bead-based immunoassay (Luminex)

Primary leukemic cells were co-cultured with different sources of primary MSCs for 5 days at 37°C and 5% CO_2. Supernatant was collected upon which the viability of leukemic cells was assessed as described above. The concentration of 64 known cytokines/chemokines in these supernatants was analyzed using fluorescent bead-based immunoassay (Luminex Human Cytokine/Chemokine Panel I and II; Merck Millipore) according to the manufacturer's protocol.

Serum of bone marrow aspirates of leukemia patients or healthy controls were used to determine the concentration of 64 known cytokines/chemokines using the same fluorescent bead-based immunoassay (Luminex Human Cytokine/Chemokine Panel I and II; Merck Millipore) according to the manufacturer's protocol

BCP-ALL migration assay

BCP-ALL migration experiments were performed using RPMI 10% FCS at 37°C and 5% CO_2. 5 x 10^4 primary MSCs and 2 x 10^5 BCP-ALL cells were cultured either separate or in co-culture in the lower compartment of a transwell in a volume of 750 μL for 24 hours prior to the start of the experiment. At the start of experiment, 4 x 10^5 NALM6-GFP cells in a volume of 250 μL were added to the upper compartment of a 6.5 mm diameter transwell system (Corning, NY, USA) with a pore size of 3.0 μm. Cells were allowed to migrate for 48 hours. At the end of experiment, transwells were removed and cells in the bottom compartment were harvested and stained with DAPI (Life Technologies). $DAPI^-/GFP^+$ cells were used as a measure for cell migration and quantified by flow cytometry using a MACSQuant analyzer (Miltenyi Biotec, Gladbach, Germany).

$CD34^+$ migration assay

Experiments were performed using either RPMI Dutch Modified 15%FCS or Iscove modified Dulbecco medium (Gibco) containing 10% FCS, 50μM β-mercaptoethanol, 1% penicillin-streptomycin, 2mM glutamine, stem cell factor (SCF; 50ng/mL; Peprotech) and fms-like tyrosine kinase-3 ligand (Flt3L; 50 ng/mL; Peprotech) at 37°C and 5% CO_2. Primary MSCs (5 x 10^4) and NALM6-GFP cells (2 x 10^5) were cultured either separate or in co-culture in a volume of 750 μL for 24 hours prior to start of experiment (bottom compartment). At the start of experiment, 5 x 10^5 $CD34^+$ cells in a volume of 250 μL were added to the top chamber of a 3.0 μm transwell system (Corning, NY, USA) and allowed to migrate for 48 hours at 37°C and 5% CO_2. At the end of experiment, transwell inserts were removed upon which the cells in the bottom compartment were harvested and stained with Propidium Iodide (PI; Sigma) and Brilliant Violet 421 anti-human CD45 antibody (Biolegend). $PI^-/GFP^-/CD45^+$ cells were quantified by flow cytometry using a MACSQuant analyzer (Miltenyi Biotec, Gladbach, Germany).

MSC migration assay

Experiments were performed using DMEM medium containing 5% FCS, 1% penicillin-streptomycin at 37°C and 5% CO_2. REH cells (0.1 – 1.6 x 10^6) and primary MSCs (5 x 10^4) were cultured either separate or in co-culture in a volume of 750 µL for 48 hours prior to start of experiment. At the start of experiment, 5 x 10^4 MSCs were added to the top chamber of a 8.0 µm transwell system (Corning) and allowed to migrate through the membrane overnight (12-16 hours). Non-migrated cells were removed from the upper side of the transwell insert using a cotton swab. Cells that migrated through the membrane insert were fixed using 10% Formalin (Sigma) for 10 minutes, washed with PBS and stained for 30 minutes with Crystal violet at room temperature. Images were captured using a Leica DM IL microscope mounted with a Leica DFC430C camera (Leica, Germany). Next, Crystal violet contained by MSCs was dissolved in 150 µL methanol, quantified by spectrophotometer using 540-570 nm wavelength settings (Versamax, San Francisco) and used as a measure of migration.

Statistical analysis

We used the R2 Genomics Analysis and Visualization Platform (http://r2.amc.nl) to visualize gene expression data in Figure 4 and performed one way analysis of variance (ANOVA). For other statistics, Student's t-test was used and a Student's paired t-test was used when applicable. Bar graphs represent the mean of biological replicates. Error bars show standard error of the mean (SEM).

RESULTS

ALL-MSC co-cultures induce leukemic cell migration without affecting the CXCR4/CXCL12 axis

Several studies have shown that ALL cells home toward the bone marrow microenvironment in a CXCR4/CXCL12 dependent manner[1,13,14,16]. We confirmed these findings by assessing the migration of GFP-positive BCP-ALL cells (NALM6) toward patient-derived MSCs, using a transwell system. MSCs induced migration of BCP-ALL cells by 5-16 fold compared to medium controls ($p < 0.05$; Figure 1A and supplementary Figure 1A-B). The induction of migration correlated with the level of CXCL12 produced by the primary MSCs: MSC#3 and MSC#4 secreted lower levels of CXCL12, and hence were less effective in attracting leukemic cells compared to MSC#1 and MSC#2 (Figure 1B). Inhibition of the CXCR4/CXCL12 axis with AMD3100 significantly impaired migration of BCP-ALL cells toward MSCs (4.5-fold reduction, $p < 0.01$; Figure 1C).

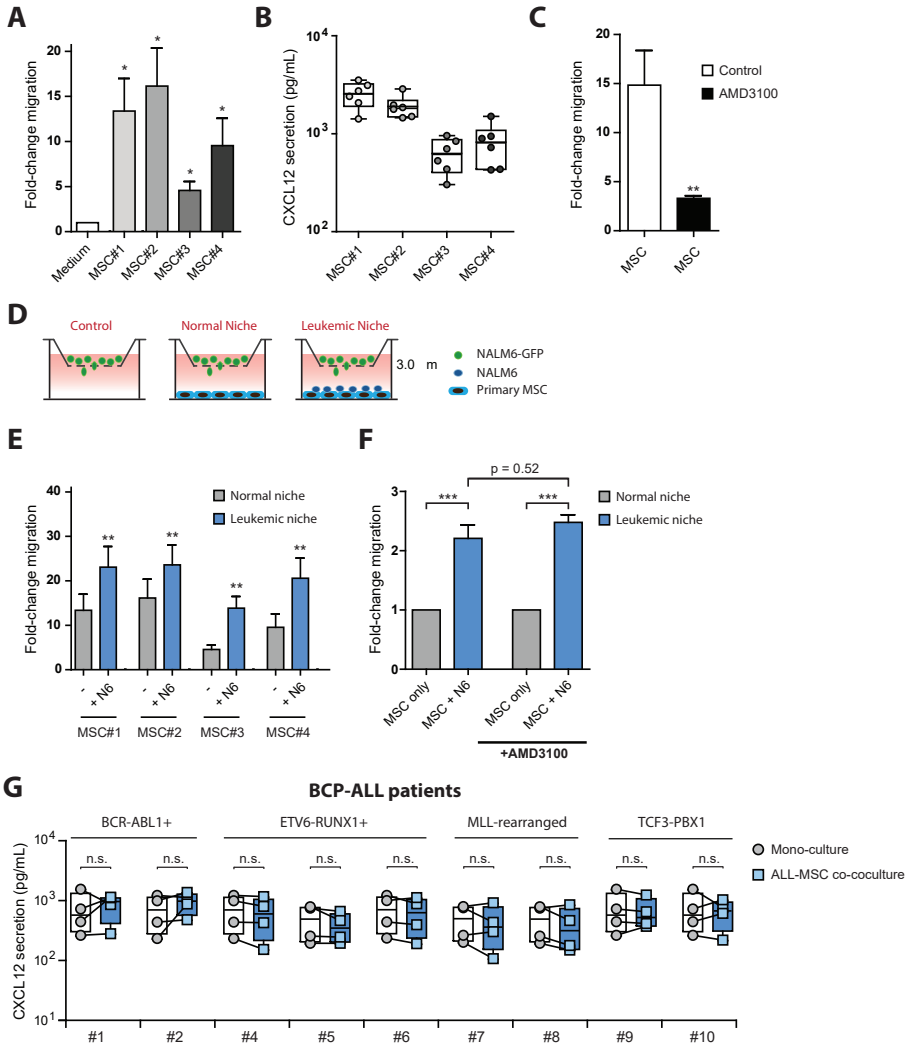

Figure 1. ALL-MSC co-cultures induce leukemic cell migration without affecting the CXCR4/CXCL12 axis.

(A) Graph showing the fold-change in migration of GFP-positive BCP-ALL cells (NALM6) toward four distinct primary bone marrow-derived MSCs compared to background migration toward culture medium after 48 hours in a 3.0 μm transwell system (n = 5 for each MSC; one-tailed t-test, unpaired). Migration towards culture medium was used to calculate the fold-change migration. (B) Graph showing the secretion of CXCL12 by primary MSCs as determined using a fluorescent bead-based immunoassay (n = 6 for each MSC). (C) Graph showing the effect of CXCR4 blockade with AMD3100 (10μM) on the migration of NALM6 cells toward primary MSCs after 48 hours in a 3.0 μm transwell system (n = 4; one-tailed t-test, paired). Migration towards culture medium was used to calculate the fold-change migration. For this experiment we combined the data of four distinct primary MSCs (MSC#1-4). (D) Schematic overview of the experimental conditions used for experiments shown in Figure 1E-F. The migration of GFP-positive NALM6 cells is measured toward: culture medium (Control), primary MSCs (Normal Niche) or GFP-negative ALL-MSC co-cultures (Leukemic Niche). (E) Graph showing the migration of NALM6 cells toward MSCs in mono-culture (normal niche, grey bars) or toward ALL-MSC co-cultures (leukemic niche, blue bars), after 48 hours in a 3.0 μm transwell system (n = 5 for each MSC; one-tailed t-test, paired).

Figure 1. ALL-MSC co-cultures induce leukemic cell migration without affecting the CXCR4/CXCL12 axis. (continued)
Migration towards culture medium was used to calculate the fold-change migration. Experiments were performed with MSCs from four different donors. (F) Graph showing that the leukemic niche affects the migration of BCP-ALL cells independent of CXCR4/CXCL12 signaling. Migration of NALM6 cells toward N6-MSC co-cultures (leukemic niche, blue bars) is compared to migration toward MSC mono-cultures (normal niche, grey bars) in absence or presence of AMD3100 (10 μM) after 48 hours using a 3.0 μm transwell system (n = 4; one-tailed t-test, paired). For this experiment we combined the data of four distinct primary MSCs (MSC#1-4). Data is shown as fold induction compared to migration towards MSC mono-culture. (G) Plots showing the secreted levels of CXCL12 by primary BCP-ALL cells and MSCs in mono-culture (circles represent the sum of cytokine secretion in mono-culture of BCP-ALL and mono-culture of MSC) compared to ALL-MSC co-culture (squares). Data was determined using a multiplexed fluorescent bead-based immunoassay. Boxes represent p25-p75 intervals.
Data are means ± SEM; * $p \leq 0.05$, ** $p \leq 0.01$, *** $p \leq 0.001$, N6 = NALM6. See also supplementary Figure 1.

We hypothesized that BCP-ALL cells alter the chemoattractive properties of their microenvironment once they have homed to the bone marrow via the CXCR4/CXCL12 axis. To address this hypothesis, GFP-negative BCP-ALL cells (NALM6) were cultured with MSCs in the bottom compartment of a transwell system as a model of the leukemic niche. Migration of GFP-positive BCP-ALL cells (NALM6) from the upper to the bottom compartment was determined (Figure 1D). GFP-positive BCP-ALL cells migrated significantly more toward ALL-MSC co-cultures (annotated as leukemic niche) than toward MSCs in mono-culture (annotated as normal niche; grey bars versus blue bars, $p < 0.01$; Figure 1E and supplementary Figure 1C-D). The leukemic niche induced migration of BCP-ALL cells by 2.2-fold compared to the healthy microenvironment (Figure 1F, $p < 0.001$). Surprisingly, CXCR4 inhibition by AMD3100 did not affect the preferential migration of BCP-ALL cells towards the leukemic niche (2.2-fold versus 2.5-fold, $p = 0.52$, Figure 1F and supplementary Figure 1E). In addition, we compared CXCL12 levels in the supernatant of mono- and co-cultures of primary BCP-ALL cells derived from 10 different patients representing major BCP-ALL subgroups and 4 primary MSCs. CXCL12 levels were high in mono-cultures of MSCs, and below detection level in mono-cultures of primary BCP-ALL cells (supplementary Figure 2A-B). Co-culture of primary BCP-ALL cells and MSCs did not increase CXCL12 levels compared to the secreted levels in mono-culture (Figure 1G). These results suggest that BCP-ALL cells create a leukemic niche that attracts leukemic cells in a CXCR4/CXCL12 independent manner.

ALL-MSC co-cultures reduce migration of healthy CD34+ HPCs

Since human HSCs migrate almost exclusively toward CXCL12[17], we hypothesized that healthy HSCs do not have an increased migration toward ALL-MSC co-cultures. To this aim, we assessed the migration of healthy $CD34^+$ hematopoietic progenitor cells (HPCs) toward primary MSCs cultured with or without BCP-ALL cells. As expected, $CD34^+$ HPCs migrated more abundantly toward MSCs than to control medium (1.8-fold, $p < 0.05$; Figure 2). However, migration of $CD34^+$ HPCs toward

ALL-MSC co-cultures was significantly reduced compared to migration toward MSCs in mono-cultures (20% reduction, $p < 0.05$; Figure 2). This implies that ALL-MSC co-cultures produce factors that more specifically attract BCP-ALL cells than healthy CD34$^+$ HPCs.

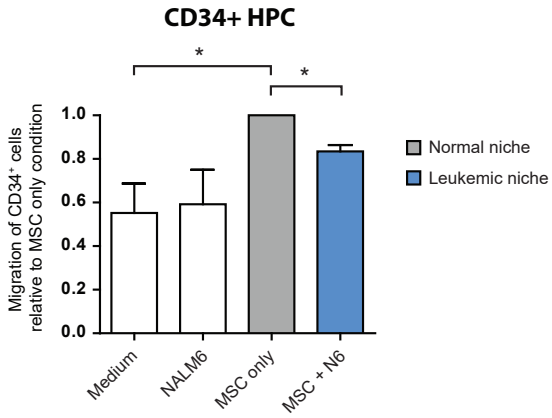

Figure 2. ALL-MSC co-cultures reduce migration of healthy CD34$^+$ HPCs.
Graph showing the migration of umbilical cord blood-derived healthy CD34$^+$ progenitor cells after 48 hours in a 3.0 µm transwell system. Bars represent migration toward culture medium, NALM6 cells, MSCs and NALM6-MSC cultures (n = 3; one-tailed t-test; paired). Migration towards MSC mono-culture was used to calculate the fold-change migration.
Data are means ± SEM; * $p \leq 0.05$, HPC = hematopoietic progenitor cell.

BCP-ALL cells recruit MSCs to create a leukemic microenvironment

Much effort is put into understanding the migration of malignant cells. However, less is known about the migratory behavior of healthy MSCs. Can leukemic cells actively recruit stromal cells toward tumor sites? If so, this would allow leukemic cells to create a niche to provide nutrients and survival factors without migrating. To address this hypothesis, we performed a transwell migration assay in which primary MSCs were allowed to migrate toward BCP-ALL cells or other MSCs in the bottom compartment. We observed that MSC migration was induced toward other MSCs compared to control medium ($p < 0.05$; Figure 3A-B). Strikingly, MSCs also actively migrated to BCP-ALL cells illustrating that BCP-ALL cells are able to recruit MSCs ($p < 0.001$; Figure 3A-B). However, MSC migration was significantly inhibited toward the leukemic niche (ALL-MSC co-cultures) compared to a bottom compartment containing only BCP-ALL cells (2-3 fold reduction, $p < 0.001$, Figure 3C-E). Interestingly, increasing the amount of ALL cells (up to 16-fold) in ALL-MSC co-cultures did not re-induce MSC migration (Figure 3D-E). These results show that ALL-MSC co-cultures efficiently attract leukemic cells, but reduce migration of MSCs similar to what was observed for healthy CD34$^+$ HPCs (Figure 2 and 3).

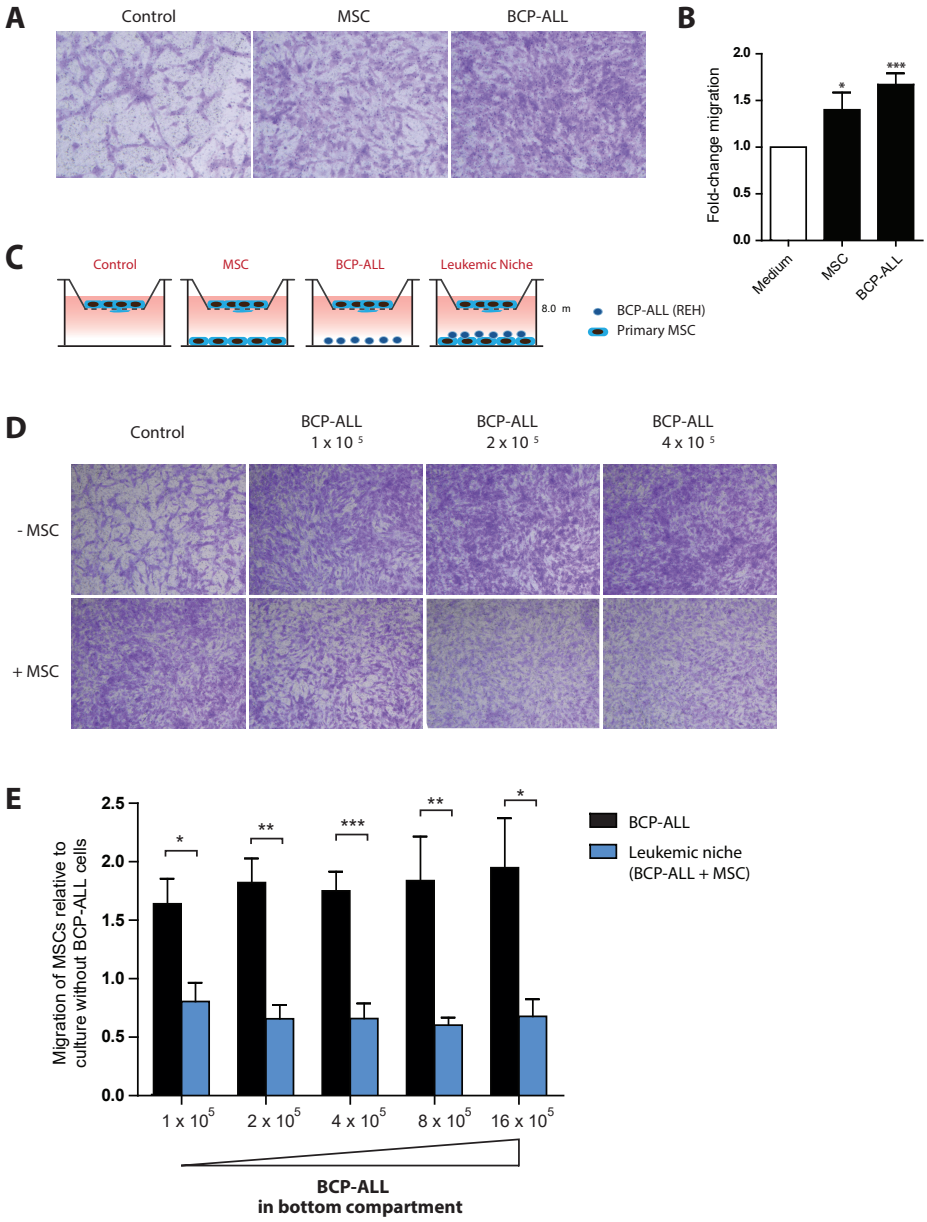

Figure 3. BCP-ALL cells recruit MSCs to create a leukemic microenvironment.
(A) Images of a representative experiment showing MSCs that migrated to the other side of a 8.0 μm transwell insert for 16 hours. Cells were fixed and subsequently stained with crystal violet. Images show MSCs migrated toward a bottom compartment containing culture medium, MSCs or BCP-ALL cells (REH) (n = 4). (B) Quantification of the migration of MSCs toward a bottom compartment containing MSCs or BCP-ALL cells (as exemplified in Figure 3A). The amount of migrated cells was measured by spectrophotometry of crystal violet stained cells (n = 4; one-tailed t-test; paired). Migration towards MSC mono-culture was used to calculate the fold-change migration.

Figure 3. BCP-ALL cells recruit MSCs to create a leukemic microenvironment. (continued)
(C) Schematic overview of experimental conditions used in Figure 2D-E (D) Images of a representative experiment showing that MSCs migrate to the other side of a 8.0 μm transwell insert for 16 hours toward an increasing amount of BCP-ALL cells (REH) in mono-culture (upper panels) or in co-culture with MSCs (MSC + REH; lower panels). (E) Quantification of MSC migration toward REH cells (BCP-ALL, black bars) or REH-MSC co-cultures (leukemic niche, blue bars), as exemplified in Figure 3D. Data was obtained by spectrophotometry of crystal violet stained cells (n = 4; one-tailed t-test, paired).
Data are means ± SEM; * $p \leq 0.05$, ** $p \leq 0.01$, *** $p \leq 0.001$.

Chemokine profiles of primary ALL-MSC co-cultures reveal recurrent induction of CCR4 and CXCR1/2 ligands

We hypothesized that the secretion of soluble factors within the leukemic microenvironment induces the migratory phenomena described above. To address which cytokines/chemokines may be altered in the leukemic niche, we quantified the levels of 64 cytokines known to be important in immunology/hematology in the supernatant of *ex vivo* co-cultures of patient-derived BCP-ALL cells (n = 10) and MSCs (n = 4) using a multiplexed fluorescent bead-based immunoassay (supplementary Table 1). We used primary leukemic cells derived from 10 different patients representing major BCP-ALL subgroups. Cytokine/chemokine profiles of primary BCP-ALL cells and primary MSCs in mono-culture are depicted in supplementary figure 2. Co-cultures of BCP-ALL cells with MSCs revealed the induction of unique secretion patterns per patient. These patterns were not affected by changing the source of MSC. Instead, each BCP-ALL patient induced the secretion of a specific set of factors, suggesting that leukemic cells govern the observed cytokine secretion (Figure 4, supplementary Figure 3 and supplementary Table 2). Surprisingly, all ALL-MSC co-cultures showed increased levels of CCL2/MCP-1 and/or CCL22/MDC (Figure 4A and supplementary Table 2), both ligands for the CCR4 receptor[18,19]. This chemokine receptor is implicated in T cell leukemia and lymphoma, but has not been implicated as an important factor for BCP-ALL[20]. In addition, analysis of previously published microarray-based gene expression data showed that CCR4 expression levels in pediatric ALL cells were significantly higher compared to healthy hematopoietic cells (Figure 4B)[21,22].

Further, we observed recurrent induction of CXCL8/IL-8 and CXCL1/GRO secretion, ligands of the CXCR1 and CXCR2 receptor[23]. CXCR1/2 ligands were induced by BCP-ALL cells from six out of ten patients. BCP-ALL cells from patients #1 and #2 induced the secretion of both CXCL8/IL-8 and CXCL1/GRO, while in co-cultures of four other patient samples (patient #5, #6, #9, and #10) the secretion of one of these cytokines was induced (Figure 4C). In contrast to CCR4 expression, CXCR1 and CXCR2 expression levels were lower in pediatric ALL compared to healthy hematopoietic cells (figure 4D). Finally, BCP-ALL cells from two out of ten

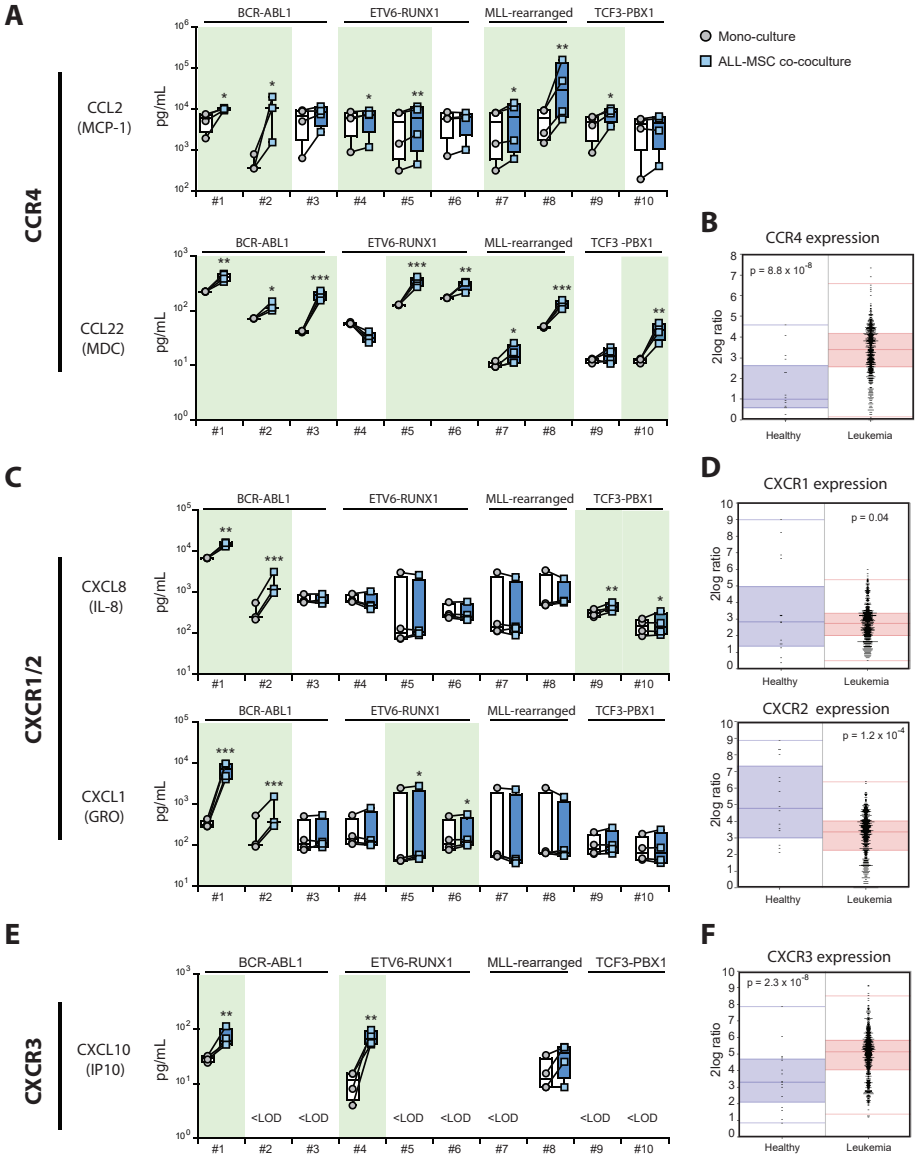

Figure 4. Chemokine profiles of primary ALL-MSC co-cultures reveal recurrent induction of CCR4 and CXCR1/2 ligands.

(A) Plots showing the secretion of CCL2/MCP-1 and CCL22/MDC of primary MSCs and primary BCP-ALL cells in mono-culture (circles represent the sum of cytokine secretion in mono-culture of BCP-ALL and mono-culture of MSC) compared to ALL-MSC co-cultures (squares). Data was obtained using a multiplexed fluorescent bead-based immunoassay. Boxes represent p25-p75 intervals. (B) Gene expression levels of the CCR4 receptor in healthy hematopoietic cells[21] and pediatric ALL cells[22]. Data was visualized using R2: microarray analysis and visualization platform. (C) Same as (A) for CXCL8/IL-8 and CXCL1/GRO secretion. (D) Same as (B) for CXCR1 and CXCR2 expression.

Figure 4. Chemokine profiles of primary ALL-MSC co-cultures reveal recurrent induction of CCR4 and CXCR1/2 ligands. (continued)
(E) Same as (A) for CXCL10/IP10 expression. (F) Same as (B) for CXCR3 expression. Raw data was logarithmically transformed to obtain a normal distribution of the data and upregulation of cytokines was tested using a one-tailed paired t-test * $p \leq 0.05$, ** $p \leq 0.01$, *** $p \leq 0.001$. See also supplementary Figure 2 and 3 and supplementary Table 1 and 2.

patients (patient #1 and #4) upregulated secretion of CXCL10/IP10, which is a ligand for the CXCR3 receptor. Gene expression levels of CXCR3 are higher in leukemic cells compared to healthy hematopoietic cells (Figure 4F).

These experiments show that primary BCP-ALL cells induce unique secretion patterns in co-culture with MSCs. Importantly, we found that CCR4 ligands CCL2/MCP-1 and CCL22/MDC were recurrently upregulated in MSC-ALL co-cultures, possibly revealing a common target for disruption of the BCP-ALL niche.

Recurrent induction of CCR4 and CXCR1/2 ligands in bone marrow aspirates of BCP-ALL patients

We validated the cytokine/chemokine patterns identified in our co-culture model using serum derived from bone marrow aspirates from 10 ALL patients at diagnosis. We compared the cytokine/chemokine patterns in these samples with serum obtained from bone marrow aspirates of the same patients taken at the end of induction chemotherapy (day 79 of the Dutch Childhood Oncology Group ALL-10 protocol). At this stage of treatment the patients were in remission. Furthermore, we used bone marrow aspirates of 7 healthy controls to analyze cytokine/chemokine patterns of the healthy niche. All bone marrow aspirates were analyzed using a multiplexed fluorescent bead-based immunoassay (supplementary Table 1). Levels of the CCR4 ligand CCL2/MCP-1 were significantly higher in the bone marrow of untreated, newly diagnosed BCP-ALL patients compared to healthy controls (2.0-fold increase, $p < 0.01$; Figure 5A). Interestingly, after induction therapy, the CCL2/MCP-1 levels in the bone marrow of ALL patients decreased to levels observed in healthy controls (2.2 fold decrease, $p < 0.01$; Figure 5A). This suggests that the induced CCL2/MCP-1 levels at diagnosis are causally linked to the presence of leukemic cells. CCL22/MDC levels were similar between BCP-ALL patients and healthy controls (Figure 5B). Like CCL2/MCP-1, CXCL1/GRO levels were also increased in the bone marrow of BCP-ALL patients (2.3-fold increase, $p < 0.05$; Figure 5C) and CXCL8/IL8 levels showed a trend towards upregulation (2.5-fold, $p = 0.052$; Figure 5D). Similar to CCL2/MCP-1 levels, the secreted levels of these CXCR1/2 ligands were significantly reduced after induction chemotherapy (2.3 fold and 3.1-fold respectively, $p < 0.05$; Figure 5C-D), again suggesting causality between the presence of leukemic cells and the upregulation of these cytokines. Finally, IP10 levels were similar between

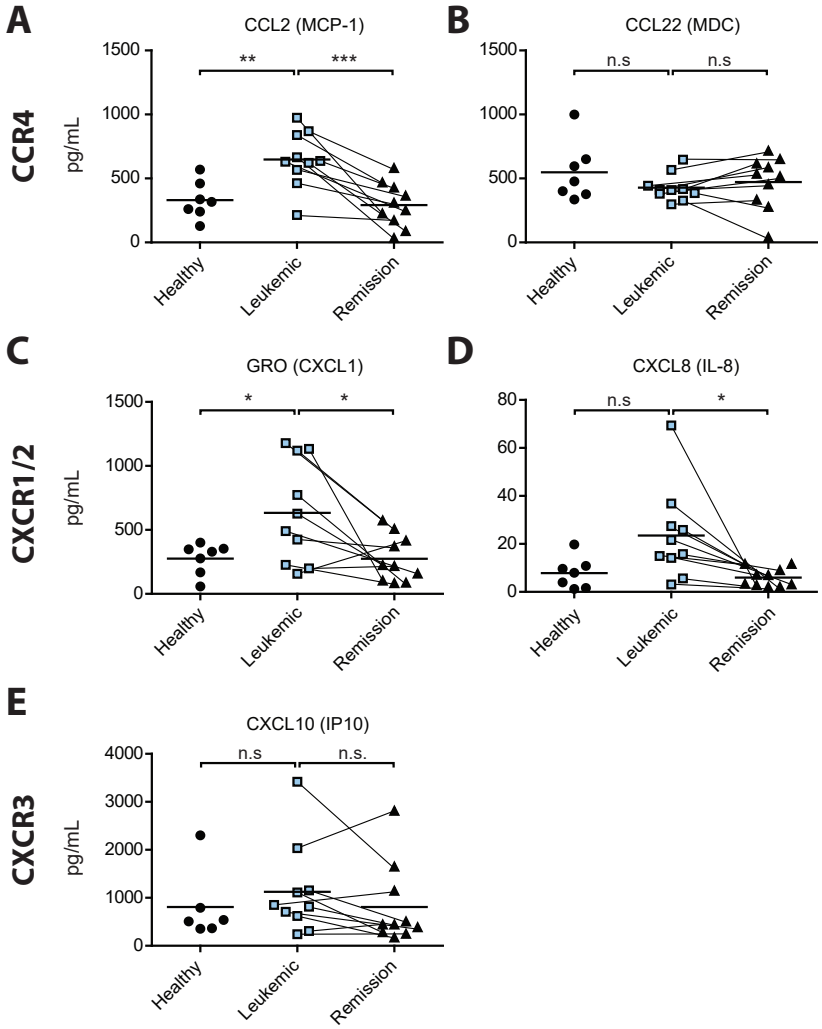

Figure 5. Recurrent induction of CCR4 and CXCR1/2 ligands in bone marrow aspirates of BCP-ALL patients.

Plots showing the serum levels of cytokines in bone marrow aspirates from healthy controls (n = 7, circles), from untreated BCP-ALL patients at diagnosis (n = 10, blue squares) and from BCP-ALL patients after induction treatment (n = 10, triangles; lines indicate paired samples). Data was obtained using a multiplexed fluorescent bead-based immunoassay in which we measured the levels of 64 cytokines. All cytokines upregulated in leukemic bone marrow are shown in Figure 5.

(A) Plot showing the serum levels of CCL2/MCP-1. (B) Plot showing the serum levels of CCL22/MDC. (C) Plot showing the serum levels of GRO/CXCL1. (D) Plot showing the serum levels of CXCL8/IL-8. (E) Plot showing the serum levels of CXCL10/IP10.

Healthy (circles) and leukemic samples (blue squares) were compared using a two-tailed unpaired t-test. Leukemic samples before and after induction therapy (blue squares versus triangles) were compared using a one-tailed paired t-test * $p \leq 0.05$, ** $p \leq 0.01$, *** $p \leq 0.001$. See also supplementary Table 1.

ALL patients and healthy controls (Figure 5E). These data implicate that CCR4 and CXCR1/2 signaling are affected in the bone marrow of ALL patients.

DISCUSSION

Several studies have tried to target the leukemic niche by inhibiting the most important chemokine signal produced by the hematopoietic niche: CXCL12[10]. These studies are mainly focused on acute myeloid leukemia (AML) and decrease CXCL12 levels by G-GSF treatment or block CXCR4/CXCL12 interaction with antagonists such as AMD3100/Plerixafor. Disruption of the CXCR4/CXCL12 axis led to mobilization of leukemic cells, increased sensitivity to therapeutic agents and prolonged survival in AML mouse models[16,24-31]. In addition, Phase 1/2 clinical trials have shown the feasibility of using CXCR4 antagonists during chemotherapeutic treatment of patients[32-35]. In ALL however, recent data suggests that blocking CXCL12-mediated migration is insufficient to completely disrupt leukemic niches. Although administration of CXCR4 antagonists to mice suffering from ALL resulted in mobilization of leukemic cells into the peripheral blood, leukemic cell count in the bone marrow was unaffected[13]. In addition, CXCL12 expression was remarkably downregulated in murine bone marrow regions of extensive leukemia growth[1]. Likewise, CXCL12 levels in the bone marrow of patients diagnosed with BCP-ALL were lower compared to those in the same patients at the time of remission and healthy controls[11]. The data in this study suggests that CXCR4/CXCL12 signaling is not driving the leukemic niche in BCP-ALL. Instead of changing CXCL12 production, we found that primary leukemic cells induce the release of a unique and patient-specific secretome in their niche. The induction of these patient-specific chemokines suggests that the leukemic cell instructs the stromal microenvironment to produce signals that are important for their migration and maintenance, thereby creating a self-reinforcing niche. Our study is the first to identify the alternative chemokines that might be important for the formation and maintenance of a leukemic niche in BCP-ALL. We used a biased approach to identify these pathways by focusing on the secretion of 64 cytokines known to be important in immunology/hematology. Unbiased approaches, like RNA sequencing and mass-spectrometry could further reveal which other molecular pathways are important for the formation of the BCP-ALL niche.

The unique cytokine/chemokine profiles for each patient suggests the need for patient-specific approaches to disrupt the leukemic niche. However, we also found recurrently induced signaling pathways: namely CCR4 and CXCR1/2 signaling. We found upregulation of ligands of these cytokine receptors in *ex vivo* leukemic co-

cultures, and importantly in bone marrow aspirates of patients with BCP-ALL. This suggests that CCR4 or CXCR1/2 inhibition might be an alternative or additional way to disrupt the BCP-ALL niche. Clinical trials have been initiated with monoclonal antibodies to CCR4 (mogamulizumab) in patients with lymphoma[36,37]. Unfortunately, mogamulizumab requires antibody-dependent cellular cytotoxicity mechanisms to eliminate CCR4$^+$ cells which may be less effective at the time of overt leukemia. Development of CCR4 antagonists similar to AMD3100 (Plerixafor) would be of utmost interest for ALL[37]. Our data warrant further investigation of the efficiency of such agents in disrupting the leukemic niche.

In conclusion, our data indicate that the BCP-ALL niche is highly potent in attracting BCP-ALL cells and repelling the influx of healthy hematopoietic cells and MSCs in a CXCL12 independent manner (Figure 6). Instead, we show the recurrent induction of CCR4 and CXCR1/2 ligands by BCP-ALL cells in the leukemic niche. Our data point to CCR4 and CXCR1/2 as valuable future therapeutic targets to interfere with the leukemic niche in ALL.

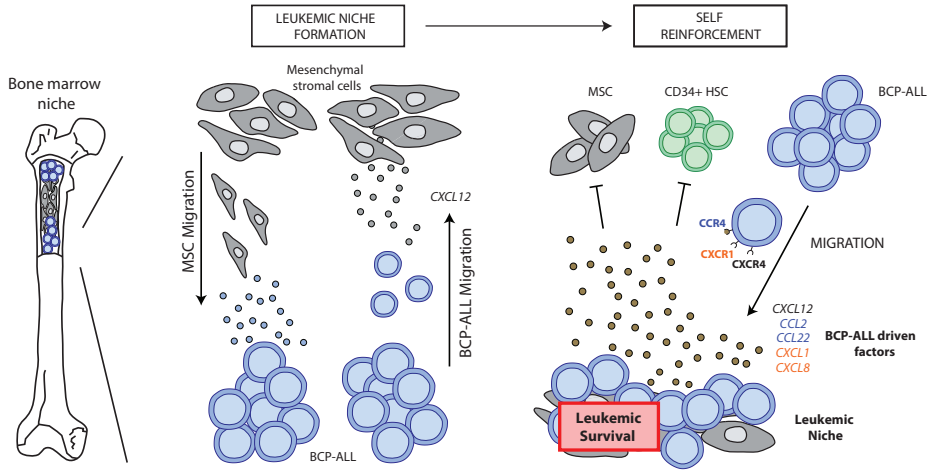

Figure 6. Model of the self-reinforcing BCP-ALL niche.
Proposed model for the formation of a leukemic niche by BCP-ALL cells. BCP-ALL cells actively migrate toward MSCs in a CXCL12 dependent manner. Simultaneously, MSC migration is induced by BCP-ALL cells. When BCP-ALL cells and MSCs are in close proximity, a leukemic microenvironment is created that specifically attracts other BCP-ALL cells and inhibits the migration of MSCs and healthy CD34$^+$ cells. This process is CXCR4/CXCL12 independent and is characterized by the secretion of patient-unique cytokines.

Acknowledgements
we thank all members of the research laboratory Pediatric Oncology of the Erasmus MC for their help in processing leukemic and mesenchymal stromal cell samples; M. Buitenhuis for critical discussions and reading of the manuscript; the Vlietland Ziekenhuis for collecting and providing cord blood; the Amsterdam Medical Center for providing the R2 gene genomic analysis and visualization platform. The work described in this paper was funded by the KiKa Foundation (Stichting Kinderen Kankervrij – Kika-39), the Dutch Cancer Society (UVA 2008; 4265, EMCR 2010; 4687), the Netherlands Organization for Scientific Research (NWO – VICI M.L. den Boer) and the Pediatric Oncology Foundation Rotterdam.

Author contributions
co-first authors B. de Rooij and R. Polak contributed equally to the study. B. de Rooij and R. Polak designed the study, performed the experiments, collected and analyzed all data, and wrote the paper. L. van den Berk performed the experiments shown in figure 5. F. Stalpers isolated MSCs and leukemic cell samples. M.L. den Boer and R. Pieters analyzed data and wrote the paper. All authors discussed the results and approved the submitted manuscript.

REFERENCES

1. Colmone, A., *et al.* Leukemic cells create bone marrow niches that disrupt the behavior of normal hematopoietic progenitor cells. *Science* **322**, 1861-1865 (2008).
2. Arai, F., *et al.* Tie2/angiopoietin-1 signaling regulates hematopoietic stem cell quiescence in the bone marrow niche. *Cell* **118**, 149-161 (2004).
3. Fujisaki, J., *et al.* In vivo imaging of Treg cells providing immune privilege to the haematopoietic stem-cell niche. *Nature* **474**, 216-219 (2011).
4. McMillin, D.W., *et al.* Tumor cell-specific bioluminescence platform to identify stroma-induced changes to anticancer drug activity. *Nat Med* **16**, 483-489 (2010).
5. Nakasone, E.S., *et al.* Imaging tumor-stroma interactions during chemotherapy reveals contributions of the microenvironment to resistance. *Cancer Cell* **21**, 488-503 (2012).
6. Schepers, K., *et al.* Myeloproliferative neoplasia remodels the endosteal bone marrow niche into a self-reinforcing leukemic niche. *Cell Stem Cell* **13**, 285-299 (2013).
7. Manabe, A., Coustan-Smith, E., Behm, F.G., Raimondi, S.C. & Campana, D. Bone marrow-derived stromal cells prevent apoptotic cell death in B-lineage acute lymphoblastic leukemia. *Blood* **79**, 2370-2377 (1992).
8. Polak, R., de Rooij, B., Pieters, R. & den Boer, M.L. B-cell precursor acute lymphoblastic leukemia cells use tunneling nanotubes to orchestrate their microenvironment. *Blood* **126**, 2404-2414 (2015).
9. Aiuti, A., Webb, I.J., Bleul, C., Springer, T. & Gutierrez-Ramos, J.C. The chemokine SDF-1 is a chemoattractant for human CD34+ hematopoietic progenitor cells and provides a new mechanism to explain the mobilization of CD34+ progenitors to peripheral blood. *The Journal of experimental medicine* **185**, 111-120 (1997).
10. Peled, A., *et al.* Dependence of human stem cell engraftment and repopulation of NOD/SCID mice on CXCR4. *Science* **283**, 845-848 (1999).
11. van den Berk, L.C., *et al.* Disturbed CXCR4/CXCL12 axis in paediatric precursor B-cell acute lymphoblastic leukaemia. *Br J Haematol* **166**, 240-249 (2014).
12. Flomenberg, N., *et al.* The use of AMD3100 plus G-CSF for autologous hematopoietic progenitor cell mobilization is superior to G-CSF alone. *Blood* **106**, 1867-1874 (2005).
13. Juarez, J., *et al.* CXCR4 antagonists mobilize childhood acute lymphoblastic leukemia cells into the peripheral blood and inhibit engraftment. *Leukemia* **21**, 1249-1257 (2007).
14. Sipkins, D.A., *et al.* In vivo imaging of specialized bone marrow endothelial microdomains for tumour engraftment. *Nature* **435**, 969-973 (2005).
15. Parameswaran, R., Yu, M., Lim, M., Groffen, J. & Heisterkamp, N. Combination of drug therapy in acute lymphoblastic leukemia with a CXCR4 antagonist. *Leukemia* **25**, 1314-1323 (2011).
16. Burger, J.A. & Peled, A. CXCR4 antagonists: targeting the microenvironment in leukemia and other cancers. *Leukemia* **23**, 43-52 (2009).
17. Wright, D.E., Bowman, E.P., Wagers, A.J., Butcher, E.C. & Weissman, I.L. Hematopoietic stem cells are uniquely selective in their migratory response to chemokines. *J Exp Med* **195**, 1145-1154 (2002).
18. Craig, M.J. & Loberg, R.D. CCL2 (Monocyte Chemoattractant Protein-1) in cancer bone metastases. *Cancer Metastasis Rev* **25**, 611-619 (2006).

19. Imai, T., *et al.* Macrophage-derived chemokine is a functional ligand for the CC chemokine receptor 4. *J Biol Chem* **273**, 1764-1768 (1998).
20. Nakagawa, M., *et al.* Gain-of-function CCR4 mutations in adult T cell leukemia/lymphoma. *J Exp Med* **211**, 2497-2505 (2014).
21. Andersson, A., Eden, P., Olofsson, T. & Fioretos, T. Gene expression signatures in childhood acute leukemias are largely unique and distinct from those of normal tissues and other malignancies. *BMC Med Genomics* **3**, 6 (2010).
22. Den Boer, M.L., *et al.* A subtype of childhood acute lymphoblastic leukaemia with poor treatment outcome: a genome-wide classification study. *Lancet Oncol* **10**, 125-134 (2009).
23. Murdoch, C. & Finn, A. Chemokine receptors and their role in inflammation and infectious diseases. *Blood* **95**, 3032-3043 (2000).
24. Petit, I., *et al.* G-CSF induces stem cell mobilization by decreasing bone marrow SDF-1 and up-regulating CXCR4. *Nat Immunol* **3**, 687-694 (2002).
25. Becker, P.S. Targeting the CXCR4 Pathway: Safety, Tolerability and Clinical Activity of Ulocuplumab (BMS-936564), an Anti-CXCR4 Antibody, in Relapsed/Refractory Acute Myeloid Leukemia. *ASH Abstract 386* (2014).
26. Fierro, F.A., *et al.* Combining SDF-1/CXCR4 antagonism and chemotherapy in relapsed acute myeloid leukemia. *Leukemia* **23**, 393-396 (2009).
27. Azab, A.K., *et al.* CXCR4 inhibitor AMD3100 disrupts the interaction of multiple myeloma cells with the bone marrow microenvironment and enhances their sensitivity to therapy. *Blood* **113**, 4341-4351 (2009).
28. Burger, M., *et al.* Small peptide inhibitors of the CXCR4 chemokine receptor (CD184) antagonize the activation, migration, and antiapoptotic responses of CXCL12 in chronic lymphocytic leukemia B cells. *Blood* **106**, 1824-1830 (2005).
29. Heuser, M., *et al.* Priming reloaded? *Blood* **114**, 925-926; author reply 926-927 (2009).
30. Tavor, S., *et al.* CXCR4 regulates migration and development of human acute myelogenous leukemia stem cells in transplanted NOD/SCID mice. *Cancer Res* **64**, 2817-2824 (2004).
31. Tavor, S., *et al.* The CXCR4 antagonist AMD3100 impairs survival of human AML cells and induces their differentiation. *Leukemia* **22**, 2151-5158 (2008).
32. Borthakur, G. BL-8040, a Peptidic CXCR4 Antagonist, Induces Leukemia Cell Death and Specific Leukemia Cell Mobilization in Relapsed/Refractory Acute Myeloid Leukemia Patients in an Ongoing Phase IIa Clinical Trial. *ASH abstract 950* (2014).
33. Cooper, T.M. Chemosensitization and Mobilization Of AML/ALL/MDS With Plerixafor (AMD 3100), a CXCR4 Antagonist: A Phase I Study Of Plerixafor + Cytarabine and Etoposide In Pediatric Patients With Acute Leukemia and MDS. *ASH Abstract 2680* (2013).
34. Lowenberg, B., *et al.* Effect of priming with granulocyte colony-stimulating factor on the outcome of chemotherapy for acute myeloid leukemia. *N Engl J Med* **349**, 743-752 (2003).
35. Uy, G.L., *et al.* A phase 1/2 study of chemosensitization with the CXCR4 antagonist plerixafor in relapsed or refractory acute myeloid leukemia. *Blood* **119**, 3917-3924 (2012).
36. Duvic, M., *et al.* Phase 1/2 study of mogamulizumab, a defucosylated anti-CCR4 antibody, in previously treated patients with cutaneous T-cell lymphoma. *Blood* **125**, 1883-1889 (2015).
37. Pease, J.E. & Horuk, R. Recent progress in the development of antagonists to the chemokine receptors CCR3 and CCR4. *Expert Opin Drug Discov* **9**, 467-483 (2014).

SUPPLEMENTARY FIGURES

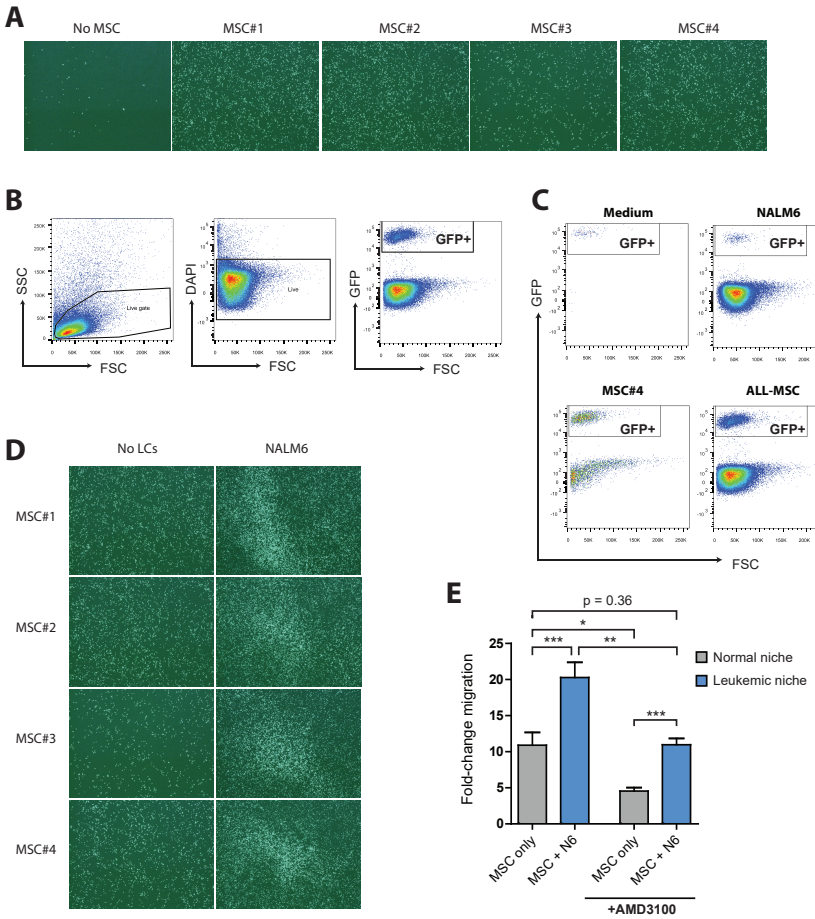

Supplementary Figure 1. ALL-MSC co-cultures induce leukemic cell migration.
(A) Representative microscope images depicting migrated GFP-positive NALM6 cells after 48 hours in a 3.0 μm transwell system. GFP-positive NALM6 cells were allowed to migrate toward a bottom compartment containing either culture medium, GFP-negative NALM6 cells or primary MSCs (n = 4). (B) Gating strategy for quantification of migrated GFP-positive NALM6 cells. (C) Representative flow cytometry plots showing the migration of GFP-positive NALM6 cells toward GFP-negative NALM6 cells, MSCs and GFP-negative ALL-MSC co-cultures. (D) Representative microscope images showing the migration of GFP-positive NALM6 cells toward GFP-negative ALL-MSC co-cultures (right panel) or migration to a bottom compartment containing only MSCs (left panel; n = 4). No LCs = no leukemic cells in the bottom compartment. (E) Graph showing the effect of CXCR4 inhibition by AMD3100 (10 μM) on migration of NALM6 cells towards MSC mono-cultures (normal niche, grey bars) and ALL-MSC co-cultures (leukemic niche, blue bars). Migration towards culture medium is used to calculate the fold-change migration. CXCR4 inhibition decreases migration of NALM6 cells towards the healthy and leukemic niche in a similar manner. However, the leukemic niche still induces migration of NALM6 cells in the presence of AMD3100.
Data are means ± SEM; * $p \leq 0.05$, ** $p \leq 0.01$, *** $p \leq 0.001$, N6 = NALM6. See also Figure 1.

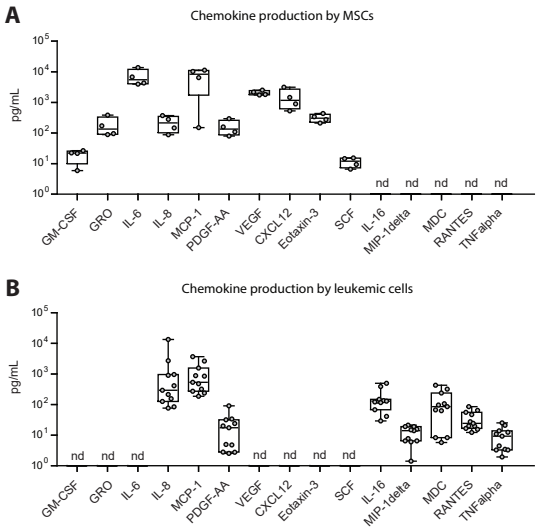

Supplementary Figure 2. Cytokine secretion of primary MSCs and BCP-ALL cells in mono-culture.
(A) Graph showing the cytokine production of MSCs from four donors after 5 days of mono-culture. (B) Graph showing the cytokine production of BCP-ALL cells from 10 different donors after 5 days of mono-culture.
Data was obtained using a multiplexed fluorescent bead-based immunoassay. Secreted levels of 64 cytokines/chemokines were analyzed. Cytokines/chemokines that were not detected in mesenchymal stromal cells or ALL cells were not depicted in this figure. nd = not detected

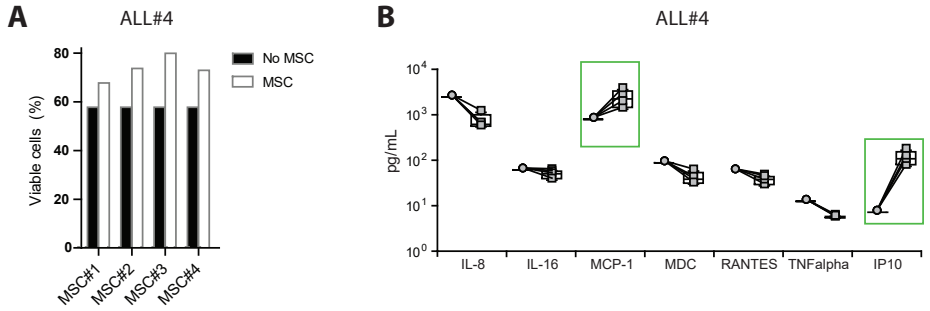

Supplementary Figure 3. Increased cytokine secretion is not explained by enhanced viability of leukemic cells in co-culture.
(A) Graph showing the viability of leukemic cells from patient ALL#4 cultured in absence or in presence of primary MSCs. (B) Plots showing the secretion of cytokines by BCP-ALL cells from patient ALL#4 in mono-culture (grey circles) and the secretion of cytokines by ALL#4 cells in ALL-MSC co-culture corrected for the secretion of MSCs (grey boxes). The dashed boxes indicate significantly upregulated cytokines shown in Figure 4.

Supplementary Table 1. Cytokine and chemokine screening panel.

Cytokine tested	Receptor	Cytokine tested	Receptor
VEGF	VEGFR	MIP-1α	CCR1
sCD40L	C40 and αIIbβ3 and α5β1	MIP-1β	CCR1 and CCR5
EGF	EGFR	PDGF-AA	PDGFR
Eotaxin	CCR2 and CCR3 and CCR5	PDGF-AB/BB	PDGFR
FGF-2	FGFR1	RANTES	CCR5
Flt-3 ligand	Flt-3	TGF-α	EGFR
Fractalkine	CX3CR1	TNF-α	TNFR1
G-CSF	GCSFR	TNF-β	LTB
GRO	CXCR2	TSLP	CRLF2 and IL7-R complex
IFNα2	IFNAR	6Ckine	CCR7
IFN-γ	IFNGR1 and IFNGR2	BCA-1	CXCR5
IL-1α	IL1R	CTACK	CCR10
IL-1β	IL1R	ENA-78	CXCR2
IL-1ra	IL1R	Eotaxin-2	CCR3
IL-2	IL2R	Eotaxin-3	CCR3
IL-3	IL3R	I-309	CCR8
IL-4	IL4R	IL-16	CD4
IL-5	IL5R	IL-20	IL20R
IL-6	CD 126 and CD130 complex	IL-21	IL21R
IL-7	IL7R	IL-23	IL23R
IL-8	CXCR1 and CXCR2	IL-28A	IL28R
IL-9	IL9R	IL-33	IL1RL1
IL-10	IL10R1-IL10R2 complex	LIF	LIFR
IL12 (p40)	IL12R	MCP-2	CCR1 and CCR2a and CCR5
IL12 (p70)	IL12R	MCP-4	CCR2 and CCR3 and CCR5
IL-13	IL13R	MIP-1d	CCR1 and CCR3
IL-15	IL15RaR	SCF	c-Kit
IL17A	IL17R	CXCL12	CXCR4 and CXCR7
IP-10	CXCR3	TARC	CCR4
MCP-1	CCR2 and CCR4	TPO	CD110
MCP-3	CCR2	TRAIL	TRAILR-complex
MDC (CCL22)	CCR4		

Supplementary Table 2. Overview of cytokines upregulated in BCP-ALL/MSC co-cultures.

	ID	G-CSF CSF3	GM-CSF CSF2	GRO CXCL1	IP10 CXCL10	MCP-1 CCL2	MCP-3 CCL8	MDC CCL22	ENA-78 CXCL5	I-309 CCL1	IL-6	IL-8 CXCL8
BCR-ABL1	#1											
	#2											
	#3											
ETV6-RUNX1	#4											
	#5											
	#6											
MLL	#7											
	#8											
TCF3-PBX1	#9											
	#10											

Supplementary Table 3. Primary mesenchymal stromal cells used in this study.

Name	Derived from	Subtype
MSC #1	Healthy BM	-
MSC #2	Healthy BM	-
MSC #3	Leukemic BM	B-Other
MSC #4	Leukemic BM	ETV6-RUNX1

Chapter 7

GENERAL DISCUSSION

This final chapter aims to discuss the work presented in this thesis. We put our findings in perspective; discuss the possible implications for leukemia treatment and future research, and present future plans derived from our studies.

TARGETED THERAPY FOR ETV6-RUNX1 POSITIVE LEUKEMIA

During the past decades, cancer research has focused on the development of more effective and less toxic anti-cancer therapies. A key example of targeted anti-cancer drugs are BCR-ABL1 inhibitors. These inhibitors are designed to block the constitutive activation of the tyrosine kinase domain of BCR-ABL1, a fusion protein resulting from translocation t(9;22), which is present in a subgroup of patients with CML and ALL. The addition of BCR-ABL1 inhibitors, such as Imatinib or Dasatinib, to treatment protocols significantly increased the survival of patients with BCR-ABL1 positive leukemia[1-5]. Regrettably, such a targeted approach is not available for the majority of children suffering from leukemia. In fact, every Dutch child with newly diagnosed ALL, except for infants (age < 365 days) and children with BCR-ABL1 positive ALL, initially receives the same treatment with classical chemotherapeutic agents according to the Dutch Childhood Oncology Group ALL11 protocol (see Figure 1)[6]. Subsequent phases of treatment are risk-directed and their intensity depends on several clinical features such as disease progression (central nervous system or testicular involvement), molecular features (such as the presence of the MLL-AF4 fusion gene), and early treatment response (measured by the initial response to prednisolone, achievement of cytomorphological complete remission after induction treatment, and the level of minimal residual disease)[6]. These risk-directed treatment protocols have significantly improved the clinical outcome of

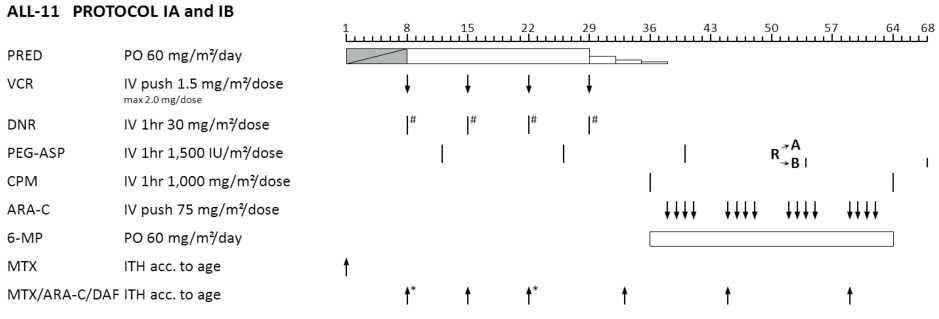

Figure 1. An overview of the initial treatment phase of ALL patients in the Netherlands
This overview represents the initial treatment phase of ALL patients in the Netherlands according to the Dutch Childhood Oncology Group ALL11 protocol[6].

children with ALL. However, children are treated with intensive chemotherapy regimens that induce significant side effects, such as severe infections, and have several late adverse effects, such as heart problems, osteonecrosis, psychological problems, and secondary tumors[3,7-11].

Fortunately, due to the improvement of molecular screening techniques, including gene expression profiling and next generation sequencing, the number of genetic drivers and driver mutations found in leukemic cells have increased dramatically[12-18]. This knowledge has led to the initiation of multiple phase I/II clinical trials that study the efficacy of drugs targeting these molecular drivers in refractory disease (e.g. PI3K/PKB inhibitors discussed in **chapter 2**). These studies have revealed that leukemia is a highly heterogeneous disease that is driven by multiple combinations of genetic lesions. Even within one leukemia patient a complex clonal diversity occurs, resulting in the presence of multiple subclones[18-22]. Therefore, targeted therapy for leukemia patients should not be directed to secondary mutations/hits, since these therapies will not eliminate all subclones effectively. Precision therapies directed against the first hit or initial drivers of leukemogenesis allow targeting of all leukemic cells and might not affect healthy cells that lack such alterations. Hence, these therapies will be more efficient and side effects may be less severe.

Similar to the BCR-ABL1 fusion protein, the ETV6-RUNX1 fusion protein might be a perfect candidate for precision therapies, since translocation t(12;21) is considered to be a first hit in leukemogenesis. Before leukemia occurs, this early genetic lesion is followed by a small number of alterations that are acquired independently and without preferential order, thereby generating a dynamic clonal architecture[18]. ETV6-RUNX1 positive leukemic cells are still highly dependent on the expression of the fusion protein for their survival[23,24]. ETV6-RUNX1 positive leukemia represents 20% of all children with acute lymphoblastic leukemia and is therewith one of the largest subgroups of pediatric leukemia. Despite the fact that event-free survival rates of children with ETV6-RUNX1 positive leukemia reach 90-95% in recent treatment protocols, the absolute number of relapse, death, and (long-term) side effects is still high among this large group of patients. The primary goal of the research described in the first part of this thesis is to identify and subsequently target biological drivers of ETV6-RUNX1 positive leukemia.

Model systems to study ETV6-RUNX1 positive ALL

Several laboratories have previously studied ETV6-RUNX1 positive leukemia and identified important features of this subtype of ALL. These studies showed the importance of the ETV6-RUNX1 fusion protein in cell lines[24-29], human progenitor cells[30-32] and mouse models[33-38].

The ETV6-RUNX1 fusion gene occurs in the human hematopoietic progenitor cell[30]. The laboratory of Tariq Enver and Mel Greaves for the first time showed that ETV6-RUNX1 transduced human cord blood-derived $CD34^+$ progenitors produce an abnormal lymphoid progenitor subgroup ($CD34^+CD38^{low}CD19^+$) with enhanced survival properties and increased self-renewal potential that is reminiscent of pre-leukemic progenitors observed in patients[30-32]. In addition, preliminary gene expression analysis of these cells revealed that ETV6-RUNX1 positive pre-leukemic cells display a gene expression signature that contains both hematopoietic stem cell (HSC) and pro-B cell associated genes[30]. However, the small number of replicate experiments hampered the authors to further analyze the molecular drivers of this phenotype.

In order to find molecular regulators of ETV6-RUNX1 positive leukemia, the laboratory of Renate Panzer-Grümayer performed siRNA silencing experiments in which ETV6-RUNX1 expression was abrogated in ETV6-RUNX1 positive human cell lines[23-26]. The silencing of ETV6-RUNX1 induced programmed cell death and significantly reduced proliferation of these cells, suggesting that ETV6-RUNX1 drives a pro-survival and pro-proliferative phenotype[23,24]. In contrast, the laboratory of Jan Trka did not find altered survival or proliferation of ETV6-RUNX1 positive cell lines after siRNA mediated knockdown of ETV6-RUNX1[29]. These contradicting results could be explained by differences in siRNA design, siRNA biosynthesis, or knockdown efficiency. The above-mentioned studies were performed in immortalized cancer cell lines. Since cell lines are genetically manipulated and cultured over an extended period of time, genotypic and phenotypic variation occurs. This raises the question whether these cells are a good representation of a primary human (pre-) leukemic cell. Although such studies might give insight in the cellular phenotype driven by ETV6-RUNX1, the acquired genetic variation makes the analysis of molecular drivers important for human disease challenging and possibly incorrect.

The phenotype of ETV6-RUNX1 expressing progenitors was further elucidated using several mice models. For example, the laboratory of Owen Williams performed ETV6-RUNX1 overexpression studies in fetal liver-derived murine hematopoietic progenitors[36,37]. These experiments were performed in healthy progenitor cells, thereby modeling the effects of the appearance of a 'first hit' in such a cell population. Similar to the studies performed in human cord blood derived hematopoietic progenitors, ETV6-RUNX1 transduced murine progenitors showed enhanced self-renewal *in vitro* and enhanced hematopoietic reconstitution *in vivo*, suggesting activation of pro-proliferative and pro-survival pathways[36]. In addition, expression of ETV6-RUNX1 altered the differentiation of murine progenitors by skewing B cell development[36]. In a study using ETV6-RUNX1 overexpression in

bone marrow-derived murine hematopoietic progenitors, a similar increase in early B cells was observed. In addition, the authors reported that these cells were unable to differentiate beyond the pro-B stage[33]. These data suggest that ETV6-RUNX1 also alters differentiation pathways in pre-leukemic progenitors. Furthermore, ectopic expression of ETV6-RUNX1 in a murine pro-B cell line changed cytoskeletal regulatory genes and altered migration properties[38]. These experiments performed in murine models attempt to recapitulate human disease. However, critical differences in phenotype and molecular mechanisms regulating stem cell maintenance and lineage differentiation exist between murine and human hematopoiesis[39-41]. For example, the transcription factor *Hoxb4* drives hematopoietic differentiation of murine embryonic stem cells (ESCs) and induced expansion of murine HSCs by nearly 1000 fold[42,43], while in contrast *HOXB4* did not alter self-renewal properties of ESC-derived human HSCs and only moderately induced HSC numbers by 2-4 fold[40,44]. Hence, although murine models add significant insight in understanding the initiation and evolutionary process of leukemogenesis driven by the ETV6-RUNX1 fusion protein[31,35], it is difficult to translate these findings to human leukemogenesis. Murine models are therefore not optimal for studies aiming to find therapeutic targets for ETV6-RUNX1 positive leukemia.

In order to identify targets of the ETV6-RUNX1 fusion protein relevant for human leukemia, several laboratories (including our own laboratory) used gene expression profiling of leukemic blasts of pediatric ALL patients[12,45-48]. These studies uncovered some promising downstream effectors of the ETV6-RUNX1 fusion protein, such as the erythropoietin receptor[27,47]. However, these studies used gene expression analysis of leukemic blasts in which ETV6-RUNX1 expression is already coupled to multiple secondary mutations. Therefore, this approach risks to reveal molecular targets that are not (directly) driven by the ETV6-RUNX1 fusion protein and hence are not important for all subclones within the leukemia.

To overcome the limitations of previous models, we compared gene expression profiling of primary leukemic blasts of 654 ALL patients with gene expression profiling of human cord blood-derived CD34-positive HPCs (CB-CD34$^+$) that ectopically expressed the ETV6-RUNX1 fusion protein (**chapter 3 and 4**). This approach allowed us to study ETV6-RUNX1 driven target genes that are still important in leukemic cells. We analyzed gene expression of ETV6-RUNX1 positive CB-CD34$^+$ cells at early time points (20 hours and 40 hours after transduction), since the disadvantage of using ectopic expression models is the risk of inducing gene expression levels above wild-type levels, not reflecting the normal biological effects. In addition, the simultaneous differential expression of genes in leukemic blasts of ETV6-RUNX1 positive ALL patients makes an overexpression artefact unlikely. Since we used a

retroviral vector, we primarily investigated the effects of ETV6-RUNX1 expression on dividing but not quiescent CB-CD34$^+$ cells. This population of progenitors is likely to be the population of interest since several reports support the hypothesis that ETV6-RUNX1 positive ALL originates in the CD34$^+$ lymphoid progenitor fraction[30,49,50].

Our studies revealed that ectopic expression of ETV6-RUNX1 in healthy human progenitors indeed induced transcriptional networks positively regulating survival, proliferation and migration of blood cells (**chapter 3 and 4**). Some of the molecular pathways found to be regulated by ETV6-RUNX1 in human progenitor cells were also identified in the above-described cell line and mouse models. For example, several genes that are affected by the erythropoietin receptor and by TGFβ signaling were induced in our data set. Interestingly, we found a novel network of differentially regulated transcription factors that induced autophagy in ETV6-RUNX1 positive cells via upregulation of Vps34 expression. This suggests that autophagy maybe a target for therapeutic interference. Indeed, we found that inhibition of the autophagy pathway affected the viability and proliferation of ETV6-RUNX1 positive leukemic cells and sensitized these cells to conventional cytotoxic drugs (**chapter 3**).

Autophagy: driving proliferation, survival and drug resistance in ETV6-RUNX1 positive leukemia

Macroautophagy, or shortly autophagy, is a cellular recycling system in which unwanted or damaged cellular components are degraded and recycled. All mammalian cells use autophagy both in normal and stress conditions. Levels of autophagy can rapidly enhance during cellular stress or starvation. During stress, autophagy provides the necessary free nucleotides, amino acids, and fatty acids to ensure the production of new essential proteins. Although autophagy can sustain cell survival during stress conditions, it can also result in cell death due to progressive cellular consumption[51-53]. Whether autophagy generally plays an initiating or tumor-suppressive role in cancer is still under debate and is most likely dependent on the cellular context[54-58]. Autophagy can promote survival of cancer cells by eliminating damaged mitochondria and other organelles, buffering oxidative stress, and thereby preventing apoptosis[54,59]. In addition, autophagy can cause resistance of cancer cells to chemotherapeutic drugs[57,60]. However, autophagy can also be an important tumor-suppressive mechanism that eliminates oncogenic proteins[54-57]. For example, both the PML-RARα fusion protein in acute promyelocytic leukemia[61,62] and the BCR-ABL1 fusion protein in CML[63] are degraded by autophagy during chemotherapeutic treatment. In this setting, autophagy inhibition would hamper the efficacy of treatment, since it decreases the therapy-induced degradation of leukemic fusion proteins. However, not all leukemic fusion proteins are degraded in this

manner. In RUNX1-RUNX1T1 positive AML, the fusion protein was not degraded by autophagy and autophagy inhibition increased the efficacy of therapy[64]. The apparent dual role of autophagy in cancer highlights the importance of investigating the context-specific role and the functional role of autophagy in a certain cancer before the start of autophagy-based therapeutic interventions.

In **chapter 3** of this thesis, we show that the ETV6-RUNX1 fusion protein enhanced levels of autophagy in pre-leukemic and leukemic cells. These enhanced levels of autophagy appeared to be an important pro-survival feature and encompasses an essential characteristic of ETV6-RUNX1 positive leukemic cells. Inhibition of autophagy by hydroxychloroquine (HCQ) induced cell death and sensitized ETV6-RUNX1 positive leukemic cells to L-Asparaginase *in vitro*. These experiments were performed in human cell line models and in primary human ALL cells. In addition, we showed that these effects were still present in an *ex vivo* niche setting in which we co-cultured primary leukemic cells with primary mesenchymal stromal cells. These pre-clinical findings indicate that patients with ETV6-RUNX1 positive leukemia might benefit from the inclusion of autophagy inhibitors in their treatment protocols. The efficacy of autophagy inhibitors during cancer treatment is currently examined in phase I/II clinical trials in a heterogeneous group of advanced tumors (reviewed in e.g. [57,65]). Initial results indicate that autophagy inhibition with HCQ is safe, tolerated at high concentrations, and might be effective in some patients with advanced solid tumors[66-68]. In addition, autophagy-independent "off-target" effects of chloroquines, like HCQ, were reported to enhance response to chemotherapy[69,70], strengthening the point to use chloroquines in clinical practice. However, more specific and more potent autophagy inhibitors are currently developed and preclinical studies with these novel inhibitors (e.g. Lys05) show promising improved antitumor activity compared to chloroquines[71].

In addition, the recent characterization of the crystal structure of Vps34[72] allowed the development of specific Vps34 inhibitors[73-75]. Since Vps34 plays an essential role in the induction of autophagy in ETV6-RUNX1 positive BCP-ALL, these patients may be the perfect candidates for the use of such an inhibitor. However, before initiating clinical trials in patients with ETV6-RUNX1 positive leukemia, the efficacy and specificity of autophagy inhibition (including Vps34 inhibitors) should be confirmed in *in vivo* models. The most widely used *in vivo* model for the validation of the efficacy of human leukemia treatment is the immune compromised NOD/SCID/gamma (NOD.Cg-*Prkdc*^{scid} *Il2rg*^{tm1Wjl}/SzJ; NSG) knockout mouse model[76-78]. In this model, leukemic cell lines and primary leukemic cells engraft significantly better than in other immune compromised mouse strains and can develop overt leukemia *in vivo*[76]. ETV6-RUNX1 positive cell lines engraft in NSG mice and can therefore function as a model system to further test the efficacy

of autophagy inhibitors. However, as mentioned earlier, cell lines might not be a good representation of a primary human leukemic cell. Unfortunately, the use of the NSG xenotransplantation model in studies with primary ETV6-RUNX1 positive leukemic cells is often hampered due to impaired engraftment or low rate of leukemia development within the lifespan of a mouse[79,80]. Further, the leukemic microenvironment in the NSG model consists of murine stromal cells, which do not represent the human bone marrow microenvironment[81]. To overcome these problems, xenotransplantation approaches are developed in which extramedullary human microenvironments are created in scaffolds seeded with human MSCs and transplanted in immune-deficient mice[82-84]. These models allow the engraftment of ETV6-RUNX1 positive primary human leukemic cells (van de Ven *et al*. unpublished data) and allow drug testing to be performed in a "humanized" microenvironment. Before introducing autophagy inhibitors to clinical protocols, it is recommended to perform additional *in vivo* experiments in such a human bone marrow-like xenograft model using primary leukemic cells.

LARG/RhoA signaling: driving migration of ETV6-RUNX1 positive leukemia

Previous gene expression studies in ETV6-RUNX1 positive BCP-ALL cells showed significant enrichment of genes involved in the regulation of migration[85,86]. Furthermore, the ETV6-RUNX1 fusion protein induced expression of genes involved in cytoskeletal regulation in a murine cell line, and enhanced the migratory capacity of murine B cells[28]. In **chapter 4,** we revealed the transcriptional program inducing the pro-migration phenotype in ETV6-RUNX1 positive CB-CD34$^+$ cells and primary leukemic cells, and found that leukemia-associated Rho guanine nucleotide exchange factor (LARG)/RhoA signaling is a master regulator of the described pro-migration phenotype.

Targeting the interaction between leukemic cells and their microenvironment has been focus for leukemia researchers for years. Several studies use growth factors disrupting the CXCR4/CXCL12 axis (G-CSF or GM-CSF) or CXCR4 antagonists to target leukemic niches. These studies imply that niche disruption may enhance therapy efficiency during leukemia treatment[87-97]. However, recent data argues that leukemia stem cells are not mobilized by CXCR4 inhibition[98], suggesting that CXCR4 inhibition is not sufficient to completely disrupt leukemic niches. Importantly, CXCR4 inhibition does not only interrupt the leukemic, but also the healthy hematopoietic niche[99,100]. The importance of the leukemic niche for ETV6-RUNX1 positive BCP-ALL became apparent in our *ex vivo* co-culture studies. Primary ETV6-RUNX1 positive BCP-ALL cells showed a significant induction of survival and drug resistance when co-cultured with primary MSCs (Figure 2). **Chapter 4** of this thesis provides the first pre-clinical evidence that inhibition of an intracellular signaling route can reduce

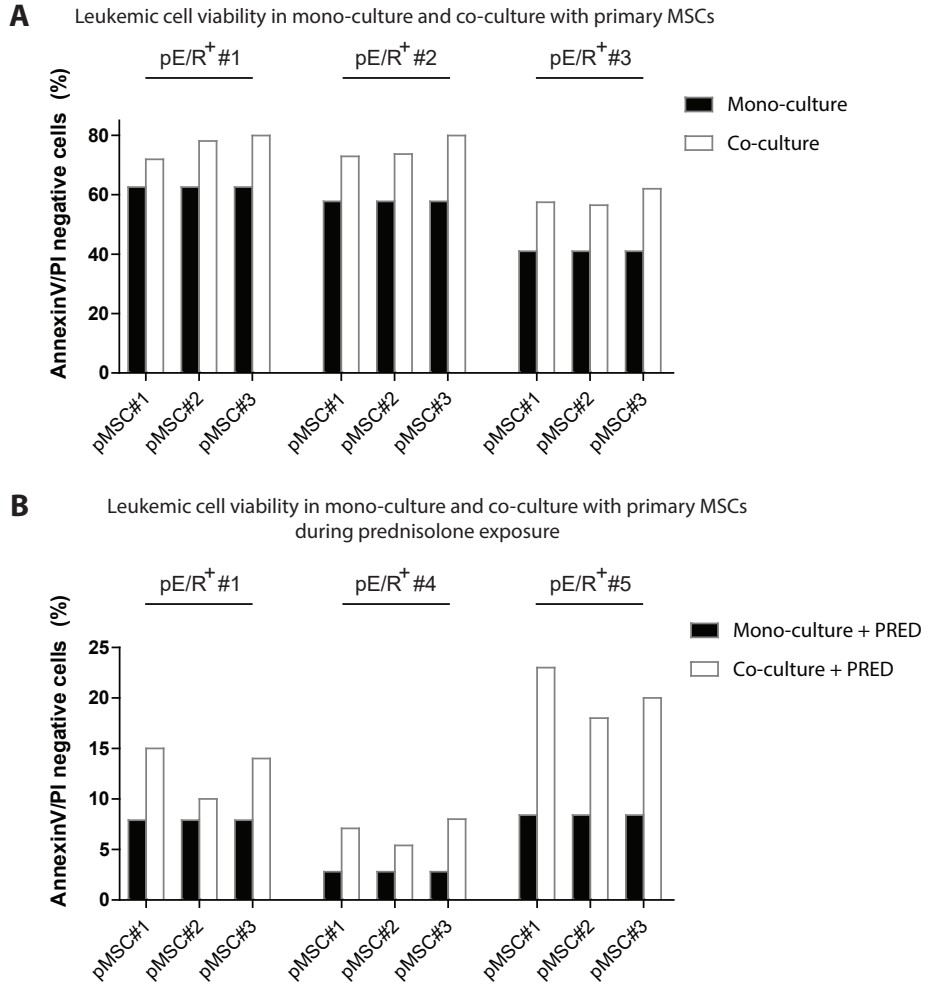

Figure 2. Survival analysis of primary ETV6-RUNX1 positive leukemic blast in mono-culture or co-culture with primary MSCs

In these experiments, we used 3 different primary human MSCs isolated from bone marrow (pMSC#1-#3). Black bars represent the percentage of annexin-PI negative cells in mono-culture. White bars represent the percentage of annexin-PI negative cells in co-culture with MSCs.

(**A**) Primary blasts were isolated from 3 ETV6-RUNX1 positive BCP-ALL patients and subsequently cultured for 3 days in absence or presence of primary MSCs. (**B**) Primary blasts were isolated from 3 ETV6-RUNX1 positive BCP-ALL patients and subsequently cultured for 3 days in absence of presence of primary MSCs during exposure to prednisolone. Abreviations: pMSC, primary mesenchymal stromal cell; pE/R$^+$, primary ETV6-RUNX1 positive leukemic cells; PRED, prednisolone.

migration of leukemic cells even in the presence of strong chemokine signals from the microenvironment. The discovery of the intracellular signaling pathway driving migration in ETV6-RUNX1 positive leukemia, namely the LARG/RhoA signaling

pathway, opens the exciting possibility of selectively inhibiting migration of cells that express the ETV6-RUNX1 fusion protein. The recent development of small molecule inhibitors for LARG and RhoA[101-103] allowed us to test this hypothesis. Indeed, we show that small molecule inhibition of LARG/RhoA blocks migration of ETV6-RUNX1 positive leukemic cells, while the migration of leukemic cells without the fusion gene was unaffected by LARG/RhoA inhibition. Therefore, we speculate that LARG/RhoA inhibition specifically targets the niche of ETV6-RUNX1 positive leukemic cells without affecting healthy hematopoietic niches. This could significantly increase effectivity and reduce toxicity of niche-disrupting approaches. However, to test this hypothesis and translate these findings to future clinical application, studies investigating the effects of small molecule inhibition of LARG/RhoA on both the healthy microenvironment and the ETV6-RUNX1 positive leukemic niche *in vivo* are essential. We recommend to perform such *in vivo* experiments in a humanized bone marrow xenograft model using primary leukemic cells. In addition, these experiments may reveal whether inhibition of ETV6-RUNX1 positive cell migration sensitizes cells to chemotherapy.

Gene expression analysis of ETV6-RUNX1 driven leukemia

The first part of this thesis has focused on the cellular pathways that are regulated by ETV6-RUNX1 in human progenitors and simultaneously are differentially expressed in ETV6-RUNX1 positive BCP-ALL. This approach revealed several genes that are likely to be important and specific for ETV6-RUNX1 positive leukemia (**chapter 3**). Therefore, this gene list provides an important tool for future research on the biology of ETV6-RUNX1 positive leukemia and reveals possible additional targets for precision therapeutic strategies.

The ectopic expression studies of ETV6-RUNX1 in CB-CD34$^+$ cells were performed simultaneously with ectopic expression studies of RUNX1-RUNX1T1 (AML1-ETO), allowing us to compare genes driven by two fusion proteins with the RUNT DNA binding domain. Both ETV6-RUNX1 and RUNX1-RUNX1T1 are known to downregulate RUNX1 target genes[104,105]. We indeed found several genes (32/556 differentially expressed genes) that were regulated both by expression of ETV6-RUNX1 and by expression of RUNX1-RUNX1T1 (Figure 3). However, the majority of these genes was induced by the fusion proteins. The vast majority of differentially expressed genes (524/556 genes) was either differentially regulated in RUNX1-RUNX1T1 positive progenitors or in ETV6-RUNX1 positive progenitors, suggesting that these fusion proteins not only function as dominant negative inhibitors of RUNX1 transcription, but also act as unique transcription factors. This is in line with several reports showing that these fusion proteins not only bind to RUNX1-bound promoter regions, but also bind to fusion protein specific promoter

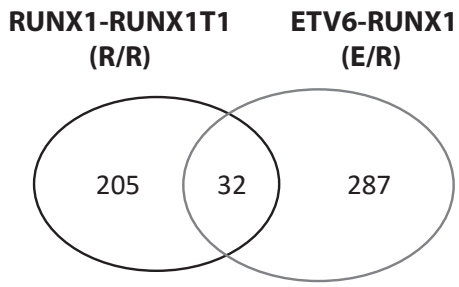

Figure 3. Gene expression analysis of CB-CD34$^+$ cells ectopically expressing oncogenic fusion proteins
(**A**) Comparison of differentially expressed genes at 20 hours and 40 hours after transduction between RUNX1-RUNX1T1 and ETV6-RUNX1 positive progenitors revealed that most genes are differentially regulated by RUNX1-RUNX1T1 and ETV6-RUNX1. (**B**) 41 probe sets representing 32 genes were similarly regulated by the RUNX1-RUNX1T1 and ETV6-RUNX1 fusion protein of which the top 25 most differentially regulated genes are depicted in this heatmap.

regions[106-108]. Interestingly, RUNX1 and activating protein 1 (AP1) were shown to play an important role in the formation of an activating or repressing complex by the RUNX1-RUNX1T1 fusion protein on these distinct promoter regions[109]. Whether this interplay is also important for the ETV6-RUNX1 fusion protein remains to be investigated.

Future perspectives for ETV6-RUNX1 positive BCP-ALL

The first part of this thesis shows that the exploration of genes that are driven by a first hit during leukemogenesis and that persist in the leukemic phase, provides a promising strategy to find targets for tailored therapy. The interference with such downstream targets was shown to effectively reverse important hallmarks of cancer[110]: inhibiting the Vps34/autophagy pathway effectively reduced proliferation and induced cell death of ETV6-RUNX1 positive cells *in vitro*, while targeting the LARG/RhoA pathway blocked migration of ETV6-RUNX1 positive cells. The major challenge is now to translate this knowledge into precision therapy for leukemia patients. In order to make this ultimate step, the results of the experiments in **chapter 3** and **chapter 4** must be reproduced in *in vivo* models. These models will answer a number of key questions that need to be answered before starting clinical trials using ETV6-RUNX1 targeted therapy. For example, it will be interesting to see whether Vps34/autophagy inhibition will have single agent effectivity *in vivo* and will improve the anti-leukemia effects of chemotherapy (e.g. L-asparaginase) without inducing more toxicity. In addition, it is still unclear which autophagy inhibitor is best in the setting of ETV6-RUNX1 positive leukemia. Keeping the study presented in **chapter 3** in mind, Vps34 inhibitors are likely to be the most specific agents for this subtype of leukemia. However, the autophagy-independent effects of the broadly used chloroquines might boost the efficacy of this group of agents. Likewise, it is still unclear whether inhibiting LARG/RhoA signaling *in vivo* results in the disruption of the leukemic niche and will improve the cytotoxic effects of

chemotherapy without inducing more toxicity. In addition, the combination of niche disrupting agents might enhance the efficacy of targeted agents, such as autophagy inhibitors in ETV6-RUNX1 positive BCP-ALL. Niche disrupting agents might also enhance the effectivity of another promising manner to target leukemic cells: immunotherapeutics, such as tumor specific monoclonal antibodies (e.g. anti-CD19), bi-specific T cell engagers, adoptive cellular therapies (e.g. CAR T cells), and immune checkpoint blockade (e.g. PD1/PD-L1 blockade and CTLA4 blockade)[111]. Although the combination of such targeted approaches might be the ideal way to abandon the necessity of toxic chemotherapy, their effectivity must first be tested in combination with classical chemotherapeutic agents, since jeopardizing the current excellent survival rates of patients with ETV6-RUNX1 positive BCP-ALL is unacceptable. Once these targeted approaches are shown to be safe, a good first step would be to add tailored agents in current treatment protocols and decrease the cumulative dose of toxic chemotherapeutic drugs, using innovating patient-centric trial designs[112].

UNDERSTANDING AND TARGETING THE LEUKEMIC NICHE

Next to the classical hallmarks of cancer[110] that include sustained proliferation, evasion of growth suppressors, resistance to cell death and replicative immortality, the formation of a tumor microenvironment is now recognized as a key feature of cancer[113]. The leukemic bone marrow microenvironment protects leukemic cells from elimination by immune responses and chemotherapeutic agents[114,115], and can even facilitate the development of drug resistance to both classical chemotherapeutic agents and newly developed targeted therapies[116-122]. Several studies show the importance of interaction between leukemic cells and their bone marrow microenvironment by convincingly reporting the modulation of the microenvironment by leukemic or pre-leukemic cells in murine models[123-126]. However, the functional mechanisms mediating crosstalk between leukemic cells and their local niche remain to be investigated. In the second part of this thesis, we aimed to better understand the mechanisms by which leukemic cells create a supportive microenvironment. In addition, we presented novel strategies aiming to disrupt this leukemic niche.

Cell-to-cell communication within the leukemic niche: the discovery of tunneling nanotubes

Cell-to-cell communication in the complex microenvironment of a leukemia can take place in multiple ways. Humoral factors, such as secreted growth factors, cytokines and chemokines, and extracellular vesicles are important for both normal

and leukemic cells[127-129]. Also direct cell-to-cell contact and subsequent signaling via integrins and gap junctions is reported to be an important means of communication between leukemic cells and their microenvironment[130-137]. In **chapter 5** of this thesis, we describe a novel way of functional connectivity within the leukemic niche: signaling via tunneling nanotubes (TNTs). Our study reveals that this type of interaction can take place between several cell types in the leukemic niche and is important for leukemic cell survival and niche-induced drug resistance. We developed an unbiased, quantitative, flow cytometry-based method to quantify TNT signaling by which we explored TNT signaling between several cellular counterparts (see **chapter 5**). TNT signaling occurred both between leukemic cells and MSCs. However, we predominantly observed TNT signaling from leukemic cells towards MSCs. Since the bone marrow microenvironment consists of multiple stromal cell types, we also explored whether TNT signaling is present between leukemic cells and osteoblast or adipocyte progenitors. Indeed, leukemic cells signal to osteoblast progenitors, adipocyte progenitors, mature osteoblasts and mature adipocytes (Figure 4). In addition, we show that leukemic cells signal equally effective toward bone marrow-derived MSCs from leukemia patients as toward MSCs derived from bone marrow of healthy volunteers (**chapter 5**). These data indicate that TNT signaling occurs between leukemic cells and a multitude of stromal counterparts in the niche. Since leukemic cells use TNTs to communicate with their microenvironment, the inhibition of TNTs might be a promising way to disrupt the leukemic niche. Therefore, we performed co-culture experiments in which TNT signaling was inhibited. Since no TNT specific inhibitors are currently available, we used a combination of two rather aspecific controls (**chapter 5**). TNTs need prolonged cell contact to signal efficiently. Therefore, we used gentle shaking of co-cultures to reduce the lifespan of TNTs, while allowing direct contact between BCP-ALL cells and MSCs. However, flow-derived shear forces (like in gentle shaking conditions) induce integrin-mediated intracellular signaling[138,139]. To exclude the effects of increased integrin signaling in shaking conditions, we physically separated ALL cells and MSCs using a transwell system. This transwell system allowed humoral communication via growth factors, cytokines, chemokines and extracellular vesicles (3μm inserts were used that allow transfer of extracellular vesicles including exosomes (ranging from 30nm-100nm) and microvesicles (ranging from 100nm- 1μm)), but inhibited direct cell-to-cell communication via TNTs, integrins and gap junctions. The combination of these controls allowed us to investigate the role of TNT signaling in co-cultures, since their common inhibitory feature is TNT inhibition (Table 1). However, shaking and transwell conditions did not exclusively inhibit TNTs while leaving other signaling modules unaffected. Evidently, a specific inhibitor of TNTs would be a key addition to these studies.

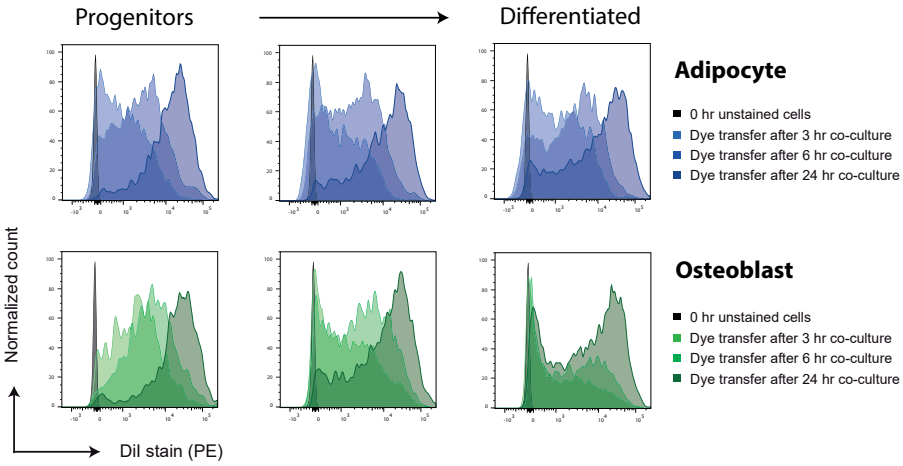

Figure 4. TNT signaling from leukemic cells toward osteoblast and adipocyte lineages
Primary bone marrow-derived MSCs were differentiated toward the adipocyte and osteoblast lineages (see **chapter 5** for details) and subsequently co-cultured with DiI-stained BCP-ALL cells (REH cell line). Dye transfer was measured 3, 6, and 24 hours after start of co-culture. We assessed dye transfer at three individual time-points during differentiation: 1 week (osteoblast and adipocyte progenitors), 2 weeks, and 3 weeks (differentiated adipocytes and osteoblasts) of differentiation.

One approach to find a TNT specific inhibitor is to decipher the molecular machinery that regulates TNT formation. Recently, this molecular machinery is starting to be unraveled. MSEC, HIV-Nef, and LST1 were reported to induce the formation of TNTs[140-143]. These molecules trigger intracellular signaling pathways, such as Rho GTPases and the Ral/exocyst complex, that are known to be important for actin remodeling and are associated with filopodia/lamelipodia formation. Also the PI3K/PKB signaling pathway may be involved in the formation of TNTs[144,145]. Inhibition of the machinery regulating the actin cytoskeleton offers an alternative promising approach to inhibit TNTs. The actin inhibitors cytochalasin D and latrunculin B were shown to effectively reduce dye transfer from leukemic cells toward MSCs (**chapter 5** and Figure 5), but were not suitable for functional experiments since the observed effects were only temporary due to a relatively short half-time. In addition, these inhibitors are generally very toxic to cells. To study whether actin inhibitors affect TNT formation directly or inhibit TNT formation due to toxicity, we performed additional dye transfer experiments with another class of toxic agents: tubulin inhibitors. In contrast to actin inhibition, tubulin inhibition did not affect dye transfer from leukemic cells toward MSCs, although tubulin inhibitors also significantly induced cell death of leukemic cells (Figure 5). This is in concordance with reports showing that TNTs contain F-actin, but do not contain microtubule/tubulin structures[146]. Thus, inhibition of the actin cytoskeleton might be a promising approach to inhibit TNT signaling. Several classes of actin inhibitors

Table 1. Effects of TNT inhibiting controls

	Shaking	Insert
Tunneling nanotubes	*inhibition*	*inhibition*
Soluble factors	∅	∅
Microvesicles	∅	∅
Exosomes	∅	∅
Integrins	*stimulation*	*inhibition*

Table visualizing the effects of gentle shaking or culture in a 3 μm transwell system on important intracellular communication mechanisms. ϴ = no effect.

have been reported, including small molecules that target the actin polymerization machinery[147]. Currently, we are performing experiments with several actin inhibitors to find an agent or a combination of agents that offers prolonged and efficient inhibition of TNT signaling and simultaneously shows low toxicity in healthy hematopoietic and niche cells (de Rooij *et al.* submitted).

Although the majority of studies on TNTs were performed *in vitro*, recently several studies have visualized the formation of TNTs *in vivo*[148-150]. For example, brain tumor cells create a functional network of TNT-connected tumor cells in the brain that was shown to be important for tissue repair and radioresistance[150]. However, whether TNTs are formed *in vivo* in the human bone marrow microenvironment is still an unanswered question. The laboratory of David Scadden and Charles Lin developed a method to track hematopoietic stem cells in a murine bone marrow niche by intravital imaging of transplanted HPCs in mouse calvarium bone marrow[151-153]. Since intravital microscopy is a rapidly developing field and imaging quality is improving fast, it is possible that in the near future also the formation of TNTs and TNT signaling can be visualized in the *in vivo* bone marrow niche.

Which molecules or organelles are transported via TNTs between leukemic cells and MSCs is still unclear. Studies report transfer of organelles, including mitochondria[146] and lysosomes[154], but also oncogenic proteins[155-157] and oncogenic microRNAs[158], and even exosomes and lipid nanoparticles[159]. For example, TNTs have been shown to transport drug-efflux pumps such as P-glycoproteins[157]. Recently, the transfer of mitochondria via TNTs was shown to be important for the survival of tumor cells. Tan *et al.* showed that mitochondrial DNA was transferred from the tumor microenvironment to tumor cells depleted of mitochondrial DNA, thereby restoring the respiratory function and tumorigenicity of these cells *in vivo*[160].

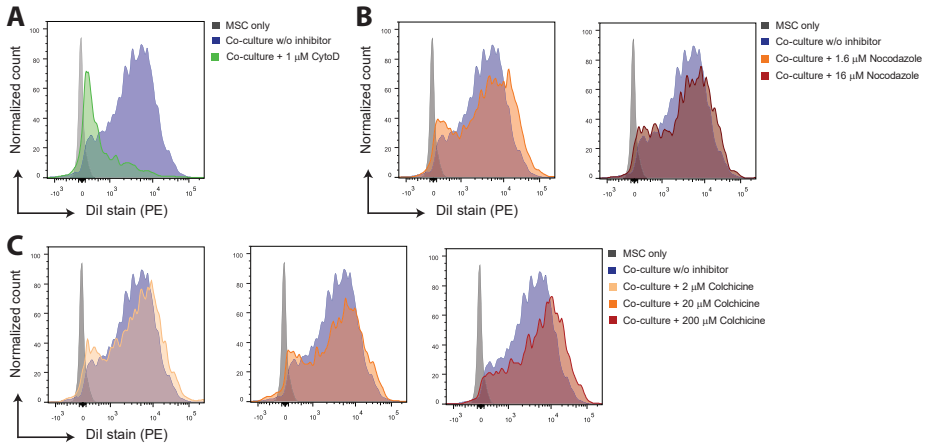

Figure 5. Tubulin inhibitors do not reduce TNT signaling from leukemic cells toward MSCs
DiI-stained CD19-positive BCP-ALL cells (NALM6) were co-cultured with unstained CD19-negative primary MSCs. Transfer of DiI staining to pMSCs was analyzed by flow cytometry 16 hours after start of co-culture. Gray graphs represent staining of MSCs at start of the experiment. Blue graphs represent dye transfer toward MSCs without the addition of an inhibitor.
(**A**) Dye transfer from DiI–stained BCP-ALL cells toward unstained MSCs was decreased by inhibition of F-actin by Cytochalasin D. (**B / C**) Dye transfer from DiI–stained BCP-ALL cells toward unstained MSCs was not affected by microtubule inhibition with Nocodazol (**B**) or Colchicine (**C**).

Similarly, the transfer of mitochondria from healthy cells toward cancer cells via TNTs was suggested to induce chemoresistance[161] and reduce cell death in early apoptotic cells[162]. In our study (**chapter 5**), we report TNT-dependent induction of survival and increase of chemoresistance in BCP-ALL cells in co-culture with MSCs. Transfer of mitochondria from MSCs toward leukemic cells might be responsible for these effects. However, we found a preferential transfer of lipophilic dye (labeling organelles and membrane components) from leukemic cells towards MSCs. In addition, a pilot experiment (**chapter 5**) shows that cytokine production in co-cultures of BCP-ALL cells and MSCs is driven by the leukemic cell. This suggests that leukemic cells use TNTs to direct stromal cells to produce appropriate survival factors. However, our study did not uncover the mediators that are transported via TNTs. Do leukemic cells use TNTs to send entire organelles, such as mitochondria or lysosomes, or (membrane-associated) proteins, nucleic acids or micro-RNAs toward MSCs? To answer this question, we initiated a study in which we overexpressed fluorescently tagged proteins that are markers for organelles, cytoskeletal proteins, exosomes, or important transmembrane or intracellular signaling molecules (see addendum). A more unbiased approach to reveal TNT-transported proteins is the use of trans-SILAC. Trans-SILAC was recently developed to study the non-cell-autonomous proteome exchange among cells of multicellular organisms[163] and was used to show that melanoma cells transfer Ras oncoproteins to healthy T cells to

modulate their effector function[164]. This approach combines stable-isotope labeling of amino acids in cell culture (SILAC) with mass spectrometry and high-purity cell sorting. These studies did not focus on the intercellular way of protein transport. However, since in these studies, the actin inhibitor Latrunculin B was used to exclude actin cytoskeleton-dependent transfer[163], it is likely that the observed transfer of proteins was mediated via TNTs. Alternatively, novel technologies that are able to quantify newly synthesized proteins, could be used to study the effects of TNT signaling between leukemic cells and MSCs on protein level (Click-iT technology, Life Technologies). This approach could also be used to study newly synthesized mRNA. These experiments might also provide insight into the molecular pathways that are activated within the stromal cells and explain the distinct patient-unique cytokine excretion patterns reported in **chapter 5 and 6**. Mass-spectrometry approaches might help in understanding how and why different leukemic cells induce distinct secretomes and which molecules are involved in these processes. In addition, the further identification of the transported cargo might hold clues for druggable targets.

The study presented in **chapter 5** focused on TNT formation and signaling in the BCP-ALL niche. During these experiments, we wondered whether TNT signaling is a unique characteristic of the BCP-ALL niche. Therefore, we performed pilot experiments with healthy human hematopoietic cells (isolated from umbilical cord blood) and leukemic cells from other acute leukemias. TNT signaling also occurred between healthy hematopoietic cells and MSCs (supplementary Figure 1), supporting the view that TNT signaling represents a widely used mechanism of cell-to-cell communication[165]. However, stromal support differentially affects survival of healthy hematopoietic cells from different lineages. Especially CD19-positive B-cells are dependent on TNT-driven stromal support *ex vivo* (supplementary Figure 2). Similarly, we observed that the effect of stromal support on leukemic cells depends on the phenotypic background (lymphoid or myeloid) and differentiation status of the leukemic cell. While primary BCP-ALL cells *ex vivo* are partially or completely dependent on TNT-driven stromal support, only a subgroup of primary T-ALL and primary AML cells is supported in such manner. This suggests that TNT inhibition will not be beneficial for all patients with acute leukemia (supplementary Figure 3).

The introduction of TNT inhibitors is far away from clinical practice. As discussed above, several important steps should be taken before TNT inhibitors may be used in therapy for ALL patients. If a non-toxic specific TNT inhibitor is available, *in vivo* confirmation of the experiments presented in **chapter 5** and this discussion are essential. These experiments would also allow studying the effects of TNT inhibition on normal hematopoiesis. We recommend to perform such experiments

in a human bone marrow-like xenograft model using primary leukemic cells with different phenotypic and genetic background.

The BCP-ALL niche revised

Several studies have tried to target the leukemic niche by inhibiting the most important chemokine signal produced by the hematopoietic niche: CXCL12[100]. Treatment with G-CSF, decreasing CXCL12 levels in the bone marrow, and CXCR4 antagonists, blocking CXCR4/CXCL12 interaction, led in leukemic mice models to mobilization of leukemic cells, increased sensitivity to therapeutic agents, and prolonged survival[88-97,166]. Phase 1/2 clinical trials have shown the feasibility of using CXCR4 antagonists during chemotherapeutic treatment[167-171]. However, recent data suggests that blocking CXCL12-mediated migration is insufficient to completely disrupt leukemic niches[98,172]. Furthermore, CXCR4/CXCL12 blockade does not only interrupt the leukemic, but also the healthy hematopoietic niche[99,100]. As discussed in paragraph 5.2 of **chapter 1**, leukemic cells disrupt the healthy bone marrow microenvironment in multiple ways. Whether migration and anchorage signals are changed in such a leukemic niche is largely unknown, especially in the context of BCP-ALL. In **chapter 6**, we show that BCP-ALL cells indeed affect the migration potential of their microenvironment by inducing migration of leukemic counterparts and inhibiting migration of healthy hematopoietic cells and mesenchymal stromal cells. This process is completely independent of the CXCR4/CXCL12 axis: CXCL12 levels were not altered, and CXCR4 inhibition did not affect this process. These data are in line with earlier reports showing that CXCL12 expression is not up-regulated in leukemic niches *in vivo*. CXCL12 expression was actually downregulated in murine bone marrow regions of extensive leukemia growth[123]. Likewise, CXCL12 serum levels of patients diagnosed with BCP-ALL were lower compared to healthy controls and patients in remission[173]. Instead of changes in CXCL12 production, we found that primary leukemic cells induce a unique and patient-specific secretome in co-culture with primary MSCs. This induction was independent of the origin of primary MSCs, which suggests that the leukemic cell instructs the stromal microenvironment to produce signals that are important for their migration and maintenance, thereby creating a self-reinforcing niche. In addition, these data show that CXCR4 blockade is not sufficient to disrupt the leukemic niche. Our study is the first in which alternative chemokine pathways that might be important for the formation and maintenance of a leukemic niche are identified. We used a biased approach to identify these pathways by focusing on the secretion of 64 cytokines known to be important in immunology/hematology. Unbiased approaches, such as RNA sequencing and mass-spectrometry focusing on newly synthesized RNA/proteins (Click-iT technology, Life Technologies), could further reveal which

molecular pathways are important for the formation of a leukemic niche. Our pilot study identified unique cytokine secretomes for each patient, suggesting the need for patient-specific approaches to disrupt the leukemic niche. However, primary cells of 10/10 BCP-ALL patients induced the production of CCR4 ligands (CCL2 and/or CCL22), suggesting that CCR4 inhibition might be a promising additional way to disrupt the BCP-ALL niche. Induction of CCR4 ligands were also found to be higher in bone marrow samples of leukemia patients, compared to bone marrow of the same patients after induction therapy or healthy controls (**chapter 6**). Since monoclonal antibodies to CCR4 (mogamulizumab) are available[174,175], this hypothesis could be tested in pre-clinical *in vivo* models. We recommend to perform such studies in a humanized bone marrow xenograft model using primary leukemic cells.

Future perspectives for niche-disrupting therapeutic strategies

The second part of this thesis aimed to better understand the molecular drivers behind the leukemic niche in BCP-ALL. The discovery of an important signaling module driving this niche (TNT signaling, **chapter 5**) and the discovery of the migratory changes induced by leukemic cells to create a self-reinforcing leukemic niche (**chapter 6**) provides significant insight into the biology of BCP-ALL. In addition, these studies revealed novel approaches to disrupt the leukemic niche in BCP-ALL. Potentially, niche disruption improves the anti-leukemic effects of chemotherapy, targeted therapy, and immunotherapy without inducing more toxicity. However, several essential steps have to be taken before the approaches presented in **chapter 5** (TNT inhibition) and **chapter 6** (specific disruption of the leukemic niche) can be implemented in clinical protocols. First, specific non-toxic inhibitors should be developed. Second, proof-of-principal experiments should be conducted in *in vivo* models, using humanized bone marrow niches and primary human leukemic cells. In these models, the safety and effectivity of niche-disrupting agents must be confirmed. Such agents must be safe as single agent and should enhance the anti-leukemic effects of chemotherapy, targeted therapy, or immunotherapy without inducing more toxicity. Only if these criteria are met, phase I/II trials can be conducted to test the safety of niche-disrupting agents. If these trials are successful, trials in which such agents are implemented in standard treatment protocols can be initialized, aiming to improve overall survival rates and reduce the amount of chemotherapeutic drugs administered without affecting outcome negatively.

Although implementation of niche-disrupting strategies in clinical protocols is far from reality, a better understanding of the BCP-ALL niche is the first step in this process. The second part of this thesis represents a small step in this journey.

REFERENCES

1. Savage, D.G. & Antman, K.H. Imatinib mesylate--a new oral targeted therapy. *N Engl J Med* **346**, 683-693 (2002).
2. Thompson, C.B. Attacking cancer at its root. *Cell* **138**, 1051-1054 (2009).
3. Wasilewski-Masker, K., *et al.* Bone mineral density deficits in survivors of childhood cancer: long-term follow-up guidelines and review of the literature. *Pediatrics* **121**, e705-713 (2008).
4. Biondi, A., *et al.* Imatinib after induction for treatment of children and adolescents with Philadelphia-chromosome-positive acute lymphoblastic leukaemia (EsPhALL): a randomised, open-label, intergroup study. *Lancet Oncol* **13**, 936-945 (2012).
5. Zwaan, C.M., *et al.* Dasatinib in children and adolescents with relapsed or refractory leukemia: results of the CA180-018 phase I dose-escalation study of the Innovative Therapies for Children with Cancer Consortium. *J Clin Oncol* **31**, 2460-2468 (2013).
6. Pieters, R., *et al.* Protocol ALL11. Treatment study protocol of the Dutch Childhood Oncology Groupo for children and adolescents (1-19 year) with newly diagnosed acute lymphoblastic leukemia. (SKION, 2014).
7. Jacobs, L.A. & Pucci, D.A. Adult survivors of childhood cancer: the medical and psychosocial late effects of cancer treatment and the impact on sexual and reproductive health. *J Sex Med* **10 Suppl 1**, 120-126 (2013).
8. Tonorezos, E.S., *et al.* Screening and management of adverse endocrine outcomes in adult survivors of childhood and adolescent cancer. *Lancet Diabetes Endocrinol* (2015).
9. Huang, T.T., *et al.* Pulmonary outcomes in survivors of childhood cancer: a systematic review. *Chest* **140**, 881-901 (2011).
10. Armenian, S.H., *et al.* Recommendations for cardiomyopathy surveillance for survivors of childhood cancer: a report from the International Late Effects of Childhood Cancer Guideline Harmonization Group. *Lancet Oncol* **16**, e123-136 (2015).
11. Sugden, E., Taylor, A., Pretorius, P., Kennedy, C. & Bhangoo, R. Meningiomas occurring during long-term survival after treatment for childhood cancer. *JRSM Open* **5**, 2054270414524567 (2014).
12. Den Boer, M.L., *et al.* A subtype of childhood acute lymphoblastic leukaemia with poor treatment outcome: a genome-wide classification study. *Lancet Oncol* **10**, 125-134 (2009).
13. Genovese, G., *et al.* Clonal hematopoiesis and blood-cancer risk inferred from blood DNA sequence. *N Engl J Med* **371**, 2477-2487 (2014).
14. Roberts, K.G., *et al.* Targetable kinase-activating lesions in Ph-like acute lymphoblastic leukemia. *N Engl J Med* **371**, 1005-1015 (2014).
15. Ley, T.J., *et al.* DNMT3A mutations in acute myeloid leukemia. *N Engl J Med* **363**, 2424-2433 (2010).
16. Mullighan, C.G., *et al.* Deletion of IKZF1 and prognosis in acute lymphoblastic leukemia. *N Engl J Med* **360**, 470-480 (2009).
17. Mullighan, C.G., *et al.* Genome-wide analysis of genetic alterations in acute lymphoblastic leukaemia. *Nature* **446**, 758-764 (2007).
18. Anderson, K., *et al.* Genetic variegation of clonal architecture and propagating cells in leukaemia. *Nature* **469**, 356-361 (2011).
19. Kim, T., *et al.* Clonal dynamics in a single AML case tracked for 9 years reveals the complexity of leukemia progression. *Leukemia* (2015).

20. Beekman, R., *et al.* Sequential gain of mutations in severe congenital neutropenia progressing to acute myeloid leukemia. *Blood* **119**, 5071-5077 (2012).
21. Shlush, L.I., *et al.* Identification of pre-leukaemic haematopoietic stem cells in acute leukaemia. *Nature* **506**, 328-333 (2014).
22. Paguirigan, A.L., *et al.* Single-cell genotyping demonstrates complex clonal diversity in acute myeloid leukemia. *Sci Transl Med* **7**, 281re282 (2015).
23. Diakos, C., *et al.* RNAi-mediated silencing of TEL/AML1 reveals a heat-shock protein- and survivin-dependent mechanism for survival. *Blood* **109**, 2607-2610 (2007).
24. Fuka, G., *et al.* Silencing of ETV6/RUNX1 abrogates PI3K/AKT/mTOR signaling and impairs reconstitution of leukemia in xenografts. *Leukemia* **26**, 927-933 (2012).
25. Fuka, G., Kauer, M., Kofler, R., Haas, O.A. & Panzer-Grumayer, R. The leukemia-specific fusion gene ETV6/RUNX1 perturbs distinct key biological functions primarily by gene repression. *PLoS One* **6**, e26348 (2011).
26. Diakos, C., *et al.* TEL-AML1 regulation of survivin and apoptosis via miRNA-494 and miRNA-320a. *Blood* **116**, 4885-4893 (2010).
27. Torrano, V., Procter, J., Cardus, P., Greaves, M. & Ford, A.M. ETV6-RUNX1 promotes survival of early B lineage progenitor cells via a dysregulated erythropoietin receptor. *Blood* **118**, 4910-4918 (2011).
28. Palmi, C., *et al.* Cytoskeletal Regulatory Gene Expression and Migratory Properties of B Cell Progenitors are Affected by the ETV6-RUNX1 Rearrangement. *Mol Cancer Res* (2014).
29. Zaliova, M., Madzo, J., Cario, G. & Trka, J. Revealing the role of TEL/AML1 for leukemic cell survival by RNAi-mediated silencing. *Leukemia* **25**, 313-320 (2011).
30. Hong, D., *et al.* Initiating and cancer-propagating cells in TEL-AML1-associated childhood leukemia. *Science* **319**, 336-339 (2008).
31. Ford, A.M., *et al.* The TEL-AML1 leukemia fusion gene dysregulates the TGF-beta pathway in early B lineage progenitor cells. *J Clin Invest* **119**, 826-836 (2009).
32. Fan, D., *et al.* Stem cell programs are retained in human leukemic lymphoblasts. *Oncogene* (2014).
33. Tsuzuki, S., Seto, M., Greaves, M. & Enver, T. Modeling first-hit functions of the t(12;21) TEL-AML1 translocation in mice. *Proc Natl Acad Sci U S A* **101**, 8443-8448 (2004).
34. Bernardin, F., *et al.* TEL-AML1, expressed from t(12;21) in human acute lymphocytic leukemia, induces acute leukemia in mice. *Cancer Res* **62**, 3904-3908 (2002).
35. van der Weyden, L., *et al.* Modeling the evolution of ETV6-RUNX1-induced B-cell precursor acute lymphoblastic leukemia in mice. *Blood* **118**, 1041-1051 (2011).
36. Morrow, M., Horton, S., Kioussis, D., Brady, H.J. & Williams, O. TEL-AML1 promotes development of specific hematopoietic lineages consistent with preleukemic activity. *Blood* **103**, 3890-3896 (2004).
37. Mangolini, M., *et al.* STAT3 mediates oncogenic addiction to TEL-AML1 in t(12;21) acute lymphoblastic leukemia. *Blood* **122**, 542-549 (2013).
38. Palmi, C., *et al.* Cytoskeletal regulatory gene expression and migratory properties of B-cell progenitors are affected by the ETV6-RUNX1 rearrangement. *Mol Cancer Res* **12**, 1796-1806 (2014).
39. Iwasaki, H. & Akashi, K. Hematopoietic developmental pathways: on cellular basis. *Oncogene* **26**, 6687-6696 (2007).
40. Doulatov, S., Notta, F., Laurenti, E. & Dick, J.E. Hematopoiesis: a human perspective. *Cell Stem Cell* **10**, 120-136 (2012).

41. Parekh, C. & Crooks, G.M. Critical differences in hematopoiesis and lymphoid development between humans and mice. *J Clin Immunol* **33**, 711-715 (2013).
42. Antonchuk, J., Sauvageau, G. & Humphries, R.K. HOXB4-induced expansion of adult hematopoietic stem cells ex vivo. *Cell* **109**, 39-45 (2002).
43. Kyba, M., Perlingeiro, R.C. & Daley, G.Q. HoxB4 confers definitive lymphoid-myeloid engraftment potential on embryonic stem cell and yolk sac hematopoietic progenitors. *Cell* **109**, 29-37 (2002).
44. Wang, L., *et al.* Generation of hematopoietic repopulating cells from human embryonic stem cells independent of ectopic HOXB4 expression. *The Journal of experimental medicine* **201**, 1603-1614 (2005).
45. Gefen, N., *et al.* Hsa-mir-125b-2 is highly expressed in childhood ETV6/RUNX1 (TEL/AML1) leukemias and confers survival advantage to growth inhibitory signals independent of p53. *Leukemia* **24**, 89-96 (2010).
46. Vaskova, M., *et al.* High expression of cytoskeletal protein drebrin in TEL/AML1pos B-cell precursor acute lymphoblastic leukemia identified by a novel monoclonal antibody. *Leuk Res* **35**, 1111-1113 (2011).
47. Inthal, A., *et al.* Role of the erythropoietin receptor in ETV6/RUNX1-positive acute lymphoblastic leukemia. *Clin Cancer Res* **14**, 7196-7204 (2008).
48. Yeoh, E.J., *et al.* Classification, subtype discovery, and prediction of outcome in pediatric acute lymphoblastic leukemia by gene expression profiling. *Cancer Cell* **1**, 133-143 (2002).
49. Hotfilder, M., *et al.* Immature CD34+CD19- progenitor/stem cells in TEL/AML1-positive acute lymphoblastic leukemia are genetically and functionally normal. *Blood* **100**, 640-646 (2002).
50. le Viseur, C., *et al.* In childhood acute lymphoblastic leukemia, blasts at different stages of immunophenotypic maturation have stem cell properties. *Cancer Cell* **14**, 47-58 (2008).
51. Levine, B. & Klionsky, D.J. Development by self-digestion: molecular mechanisms and biological functions of autophagy. *Dev Cell* **6**, 463-477 (2004).
52. Mizushima, N. & Komatsu, M. Autophagy: renovation of cells and tissues. *Cell* **147**, 728-741 (2011).
53. Baehrecke, E.H. Autophagy: dual roles in life and death? *Nat Rev Mol Cell Biol* **6**, 505-510 (2005).
54. Guo, J.Y., Xia, B. & White, E. Autophagy-mediated tumor promotion. *Cell* **155**, 1216-1219 (2013).
55. Mathew, R., Karantza-Wadsworth, V. & White, E. Role of autophagy in cancer. *Nat Rev Cancer* **7**, 961-967 (2007).
56. Levine, B. & Kroemer, G. Autophagy in the pathogenesis of disease. *Cell* **132**, 27-42 (2008).
57. White, E. Deconvoluting the context-dependent role for autophagy in cancer. *Nat Rev Cancer* **12**, 401-410 (2012).
58. Gump, J.M., *et al.* Autophagy variation within a cell population determines cell fate through selective degradation of Fap-1. *Nat Cell Biol* **16**, 47-54 (2014).
59. Degenhardt, K., *et al.* Autophagy promotes tumor cell survival and restricts necrosis, inflammation, and tumorigenesis. *Cancer Cell* **10**, 51-64 (2006).
60. Rubinsztein, D.C., Codogno, P. & Levine, B. Autophagy modulation as a potential therapeutic target for diverse diseases. *Nat Rev Drug Discov* **11**, 709-730 (2012).
61. Isakson, P., Bjoras, M., Boe, S.O. & Simonsen, A. Autophagy contributes to therapy-induced degradation of the PML/RARA oncoprotein. *Blood* **116**, 2324-2331 (2010).

62. Wang, Z., *et al.* Autophagy regulates myeloid cell differentiation by p62/SQSTM1-mediated degradation of PML-RARalpha oncoprotein. *Autophagy* **7**, 401-411 (2011).
63. Goussetis, D.J., *et al.* Autophagic degradation of the BCR-ABL oncoprotein and generation of antileukemic responses by arsenic trioxide. *Blood* **120**, 3555-3562 (2012).
64. Torgersen, M.L., Engedal, N., Boe, S.O., Hokland, P. & Simonsen, A. Targeting autophagy potentiates the apoptotic effect of histone deacetylase inhibitors in t(8;21) AML cells. *Blood* **122**, 2467-2476 (2013).
65. Amaravadi, R.K., *et al.* Principles and current strategies for targeting autophagy for cancer treatment. *Clin Cancer Res* **17**, 654-666 (2011).
66. Rosenfeld, M.R., *et al.* A phase I/II trial of hydroxychloroquine in conjunction with radiation therapy and concurrent and adjuvant temozolomide in patients with newly diagnosed glioblastoma multiforme. *Autophagy* **10**, 1359-1368 (2014).
67. Rangwala, R., *et al.* Combined MTOR and autophagy inhibition: Phase I trial of hydroxychloroquine and temsirolimus in patients with advanced solid tumors and melanoma. *Autophagy* **10**, 1391-1402 (2014).
68. Vogl, D.T., *et al.* Combined autophagy and proteasome inhibition: A phase 1 trial of hydroxychloroquine and bortezomib in patients with relapsed/refractory myeloma. *Autophagy* **10**, 1380-1390 (2014).
69. Maes, H., *et al.* Tumor Vessel Normalization by Chloroquine Independent of Autophagy. *Cancer Cell* **26**, 190-206 (2014).
70. Eng, C.H., *et al.* Macroautophagy is dispensable for growth of KRAS mutant tumors and chloroquine efficacy. *Proc Natl Acad Sci U S A* (2015).
71. McAfee, Q., *et al.* Autophagy inhibitor Lys05 has single-agent antitumor activity and reproduces the phenotype of a genetic autophagy deficiency. *Proc Natl Acad Sci U S A* **109**, 8253-8258 (2012).
72. Miller, S., *et al.* Shaping development of autophagy inhibitors with the structure of the lipid kinase Vps34. *Science* **327**, 1638-1642 (2010).
73. Bago, R., *et al.* Characterization of VPS34-IN1, a selective inhibitor of Vps34, reveals that the phosphatidylinositol 3-phosphate-binding SGK3 protein kinase is a downstream target of class III phosphoinositide 3-kinase. *Biochem J* **463**, 413-427 (2014).
74. Ronan, B., *et al.* A highly potent and selective Vps34 inhibitor alters vesicle trafficking and autophagy. *Nat Chem Biol* **10**, 1013-1019 (2014).
75. Dowdle, W.E., *et al.* Selective VPS34 inhibitor blocks autophagy and uncovers a role for NCOA4 in ferritin degradation and iron homeostasis in vivo. *Nat Cell Biol* **16**, 1069-1079 (2014).
76. Shultz, L.D., Ishikawa, F. & Greiner, D.L. Humanized mice in translational biomedical research. *Nat Rev Immunol* **7**, 118-130 (2007).
77. Shultz, L.D., *et al.* Human lymphoid and myeloid cell development in NOD/LtSz-scid IL2R gamma null mice engrafted with mobilized human hemopoietic stem cells. *J Immunol* **174**, 6477-6489 (2005).
78. Shultz, L.D., *et al.* Multiple defects in innate and adaptive immunologic function in NOD/LtSz-scid mice. *J Immunol* **154**, 180-191 (1995).
79. Meyer, L.H. & Debatin, K.M. Diversity of human leukemia xenograft mouse models: implications for disease biology. *Cancer Res* **71**, 7141-7144 (2011).

80. Meyer, L.H., *et al.* Early relapse in ALL is identified by time to leukemia in NOD/SCID mice and is characterized by a gene signature involving survival pathways. *Cancer Cell* **19**, 206-217 (2011).
81. Schepers, K., Campbell, T.B. & Passegue, E. Normal and Leukemic Stem Cell Niches: Insights and Therapeutic Opportunities. *Cell Stem Cell* **16**, 254-267 (2015).
82. Chen, Y., *et al.* Human extramedullary bone marrow in mice: a novel in vivo model of genetically controlled hematopoietic microenvironment. *Blood* **119**, 4971-4980 (2012).
83. Groen, R.W., *et al.* Reconstructing the human hematopoietic niche in immunodeficient mice: opportunities for studying primary multiple myeloma. *Blood* **120**, e9-e16 (2012).
84. Reinisch, A., *et al.* A humanized bone marrow ossicle xenotransplantation model enables improved engraftment of healthy and leukemic human hematopoietic cells. *Nat Med* (2016).
85. Spencer, J.A., *et al.* Direct measurement of local oxygen concentration in the bone marrow of live animals. *Nature* **508**, 269-273 (2014).
86. Gandemer, V., *et al.* Five distinct biological processes and 14 differentially expressed genes characterize TEL/AML1-positive leukemia. *BMC Genomics* **8**, 385 (2007).
87. Lowenberg, B., *et al.* Effect of priming with granulocyte colony-stimulating factor on the outcome of chemotherapy for acute myeloid leukemia. *N Engl J Med* **349**, 743-752 (2003).
88. Burger, M., *et al.* Small peptide inhibitors of the CXCR4 chemokine receptor (CD184) antagonize the activation, migration, and antiapoptotic responses of CXCL12 in chronic lymphocytic leukemia B cells. *Blood* **106**, 1824-1830 (2005).
89. Burger, J.A. & Peled, A. CXCR4 antagonists: targeting the microenvironment in leukemia and other cancers. *Leukemia* **23**, 43-52 (2009).
90. Juarez, J., *et al.* CXCR4 antagonists mobilize childhood acute lymphoblastic leukemia cells into the peripheral blood and inhibit engraftment. *Leukemia* **21**, 1249-1257 (2007).
91. Juarez, J., Bradstock, K.F., Gottlieb, D.J. & Bendall, L.J. Effects of inhibitors of the chemokine receptor CXCR4 on acute lymphoblastic leukemia cells in vitro. *Leukemia* **17**, 1294-1300 (2003).
92. Tavor, S., *et al.* The CXCR4 antagonist AMD3100 impairs survival of human AML cells and induces their differentiation. *Leukemia* **22**, 2151-5158 (2008).
93. Azab, A.K., *et al.* CXCR4 inhibitor AMD3100 disrupts the interaction of multiple myeloma cells with the bone marrow microenvironment and enhances their sensitivity to therapy. *Blood* **113**, 4341-4351 (2009).
94. Nervi, B., *et al.* Chemosensitization of acute myeloid leukemia (AML) following mobilization by the CXCR4 antagonist AMD3100. *Blood* **113**, 6206-6214 (2009).
95. Parameswaran, R., Yu, M., Lim, M., Groffen, J. & Heisterkamp, N. Combination of drug therapy in acute lymphoblastic leukemia with a CXCR4 antagonist. *Leukemia* **25**, 1314-1323 (2011).
96. O'Callaghan, K., *et al.* Targeting CXCR4 with cell-penetrating pepducins in lymphoma and lymphocytic leukemia. *Blood* **119**, 1717-1725 (2012).
97. Tavor, S., *et al.* CXCR4 regulates migration and development of human acute myelogenous leukemia stem cells in transplanted NOD/SCID mice. *Cancer Res* **64**, 2817-2824 (2004).
98. Heuser, M., *et al.* Priming reloaded? *Blood* **114**, 925-926; author reply 926-927 (2009).
99. Aiuti, A., Webb, I.J., Bleul, C., Springer, T. & Gutierrez-Ramos, J.C. The chemokine SDF-1 is a chemoattractant for human CD34+ hematopoietic progenitor cells and provides a new mechanism to explain the mobilization of CD34+ progenitors to peripheral blood. *The Journal of experimental medicine* **185**, 111-120 (1997).

100. Peled, A., *et al.* Dependence of human stem cell engraftment and repopulation of NOD/SCID mice on CXCR4. *Science* **283**, 845-848 (1999).
101. Shang, X., *et al.* Small-molecule inhibitors targeting G-protein-coupled Rho guanine nucleotide exchange factors. *Proc Natl Acad Sci U S A* **110**, 3155-3160 (2013).
102. Shang, X., *et al.* Rational design of small molecule inhibitors targeting RhoA subfamily Rho GTPases. *Chem Biol* **19**, 699-710 (2012).
103. Vigil, D., Cherfils, J., Rossman, K.L. & Der, C.J. Ras superfamily GEFs and GAPs: validated and tractable targets for cancer therapy? *Nat Rev Cancer* **10**, 842-857 (2010).
104. Elagib, K.E. & Goldfarb, A.N. Oncogenic pathways of AML1-ETO in acute myeloid leukemia: multifaceted manipulation of marrow maturation. *Cancer Lett* **251**, 179-186 (2007).
105. Zelent, A., Greaves, M. & Enver, T. Role of the TEL-AML1 fusion gene in the molecular pathogenesis of childhood acute lymphoblastic leukaemia. *Oncogene* **23**, 4275-4283 (2004).
106. Saeed, S., *et al.* Chromatin accessibility, p300, and histone acetylation define PML-RARalpha and AML1-ETO binding sites in acute myeloid leukemia. *Blood* **120**, 3058-3068 (2012).
107. Linka, Y., *et al.* The impact of TEL-AML1 (ETV6-RUNX1) expression in precursor B cells and implications for leukaemia using three different genome-wide screening methods. *Blood Cancer J* **3**, e151 (2013).
108. Bakshi, R., *et al.* The leukemogenic t(8;21) fusion protein AML1-ETO controls rRNA genes and associates with nucleolar-organizing regions at mitotic chromosomes. *J Cell Sci* **121**, 3981-3990 (2008).
109. Li, Y., *et al.* Genome-wide studies identify a novel interplay between AML1 and AML1/ETO in t(8;21) acute myeloid leukemia. *Blood* (2015).
110. Hanahan, D. & Weinberg, R.A. The hallmarks of cancer. *Cell* **100**, 57-70 (2000).
111. Bachireddy, P., Burkhardt, U.E., Rajasagi, M. & Wu, C.J. Haematological malignancies: at the forefront of immunotherapeutic innovation. *Nat Rev Cancer* **15**, 201-215 (2015).
112. Biankin, A.V., Piantadosi, S. & Hollingsworth, S.J. Patient-centric trials for therapeutic development in precision oncology. *Nature* **526**, 361-370 (2015).
113. Hanahan, D. & Weinberg, R.A. Hallmarks of cancer: the next generation. *Cell* **144**, 646-674 (2011).
114. Fujisaki, J., *et al.* In vivo imaging of Treg cells providing immune privilege to the haematopoietic stem-cell niche. *Nature* **474**, 216-219 (2011).
115. Arai, F., *et al.* Tie2/angiopoietin-1 signaling regulates hematopoietic stem cell quiescence in the bone marrow niche. *Cell* **118**, 149-161 (2004).
116. Konopleva, M.Y. & Jordan, C.T. Leukemia stem cells and microenvironment: biology and therapeutic targeting. *J Clin Oncol* **29**, 591-599 (2011).
117. McMillin, D.W., Negri, J.M. & Mitsiades, C.S. The role of tumour-stromal interactions in modifying drug response: challenges and opportunities. *Nat Rev Drug Discov* **12**, 217-228 (2013).
118. Pallasch, C.P., *et al.* Sensitizing protective tumor microenvironments to antibody-mediated therapy. *Cell* **156**, 590-602 (2014).
119. McMillin, D.W., *et al.* Tumor cell-specific bioluminescence platform to identify stroma-induced changes to anticancer drug activity. *Nat Med* **16**, 483-489 (2010).
120. Straussman, R., *et al.* Tumour micro-environment elicits innate resistance to RAF inhibitors through HGF secretion. *Nature* **487**, 500-504 (2012).
121. Wilson, T.R., *et al.* Widespread potential for growth-factor-driven resistance to anticancer kinase inhibitors. *Nature* **487**, 505-509 (2012).

122. Manshouri, T., *et al.* Bone marrow stroma-secreted cytokines protect JAK2(V617F)-mutated cells from the effects of a JAK2 inhibitor. *Cancer Res* **71**, 3831-3840 (2011).
123. Colmone, A., *et al.* Leukemic cells create bone marrow niches that disrupt the behavior of normal hematopoietic progenitor cells. *Science* **322**, 1861-1865 (2008).
124. Medyouf, H., *et al.* Myelodysplastic Cells in Patients Reprogram Mesenchymal Stromal Cells to Establish a Transplantable Stem Cell Niche Disease Unit. *Cell Stem Cell* (2014).
125. Schepers, K., *et al.* Myeloproliferative neoplasia remodels the endosteal bone marrow niche into a self-reinforcing leukemic niche. *Cell Stem Cell* **13**, 285-299 (2013).
126. Zhang, B., *et al.* Altered microenvironmental regulation of leukemic and normal stem cells in chronic myelogenous leukemia. *Cancer Cell* **21**, 577-592 (2012).
127. Majka, M., *et al.* Numerous growth factors, cytokines, and chemokines are secreted by human CD34(+) cells, myeloblasts, erythroblasts, and megakaryoblasts and regulate normal hematopoiesis in an autocrine/paracrine manner. *Blood* **97**, 3075-3085 (2001).
128. Kaushansky, K. Lineage-specific hematopoietic growth factors. *N Engl J Med* **354**, 2034-2045 (2006).
129. Ratajczak, J., Wysoczynski, M., Hayek, F., Janowska-Wieczorek, A. & Ratajczak, M.Z. Membrane-derived microvesicles: important and underappreciated mediators of cell-to-cell communication. *Leukemia* **20**, 1487-1495 (2006).
130. Miller, P.G., *et al.* In Vivo RNAi screening identifies a leukemia-specific dependence on integrin beta 3 signaling. *Cancer Cell* **24**, 45-58 (2013).
131. Hsieh, Y.T., *et al.* Integrin alpha4 blockade sensitizes drug resistant pre-B acute lymphoblastic leukemia to chemotherapy. *Blood* **121**, 1814-1818 (2013).
132. Chen, Y.Y., Malik, M., Tomkowicz, B.E., Collman, R.G. & Ptasznik, A. BCR-ABL1 alters SDF-1alpha-mediated adhesive responses through the beta2 integrin LFA-1 in leukemia cells. *Blood* **111**, 5182-5186 (2008).
133. Bendall, L.J., Kortlepel, K. & Gottlieb, D.J. Human acute myeloid leukemia cells bind to bone marrow stroma via a combination of beta-1 and beta-2 integrin mechanisms. *Blood* **82**, 3125-3132 (1993).
134. Foss, B., Tronstad, K.J. & Bruserud, O. Connexin-based signaling in acute myelogenous leukemia (AML). *Biochim Biophys Acta* **1798**, 1-8 (2010).
135. Zhang, X., *et al.* Effect of Cx43 gene-modified leukemic bone marrow stromal cells on the regulation of Jurkat cell line in vitro. *Leuk Res* **36**, 198-204 (2012).
136. Yang, J., Darley, R.L., Hallett, M. & Evans, W.H. Low connexin channel-dependent intercellular communication in human adult hematopoietic progenitor/stem cells: probing mechanisms of autologous stem cell therapy. *Cell Commun Adhes* **16**, 138-145 (2009).
137. Paraguassu-Braga, F.H., Borojevic, R., Bouzas, L.F., Barcinski, M.A. & Bonomo, A. Bone marrow stroma inhibits proliferation and apoptosis in leukemic cells through gap junction-mediated cell communication. *Cell Death Differ* **10**, 1101-1108 (2003).
138. Alon, R. & Dustin, M.L. Force as a facilitator of integrin conformational changes during leukocyte arrest on blood vessels and antigen-presenting cells. *Immunity* **26**, 17-27 (2007).
139. Alon, R. & Ley, K. Cells on the run: shear-regulated integrin activation in leukocyte rolling and arrest on endothelial cells. *Curr Opin Cell Biol* **20**, 525-532 (2008).
140. Kimura, S., Hase, K. & Ohno, H. The molecular basis of induction and formation of tunneling nanotubes. *Cell Tissue Res* **352**, 67-76 (2013).
141. Hase, K., *et al.* M-Sec promotes membrane nanotube formation by interacting with Ral and the exocyst complex. *Nat Cell Biol* **11**, 1427-1432 (2009).

142. Xu, W., *et al.* HIV-1 evades virus-specific IgG2 and IgA responses by targeting systemic and intestinal B cells via long-range intercellular conduits. *Nat Immunol* **10**, 1008-1017 (2009).
143. Schiller, C., *et al.* LST1 promotes the assembly of a molecular machinery responsible for tunneling nanotube formation. *J Cell Sci* **126**, 767-777 (2013).
144. Lou, E., *et al.* Tunneling nanotubes provide a unique conduit for intercellular transfer of cellular contents in human malignant pleural mesothelioma. *PLoS One* **7**, e33093 (2012).
145. Wang, Y., Cui, J., Sun, X. & Zhang, Y. Tunneling-nanotube development in astrocytes depends on p53 activation. *Cell Death Differ* **18**, 732-742 (2011).
146. Rustom, A., Saffrich, R., Markovic, I., Walther, P. & Gerdes, H.H. Nanotubular highways for intercellular organelle transport. *Science* **303**, 1007-1010 (2004).
147. Peng, G.E., Wilson, S.R. & Weiner, O.D. A pharmacological cocktail for arresting actin dynamics in living cells. *Mol Biol Cell* **22**, 3986-3994 (2011).
148. Chinnery, H.R., Pearlman, E. & McMenamin, P.G. Cutting edge: Membrane nanotubes in vivo: a feature of MHC class II+ cells in the mouse cornea. *J Immunol* **180**, 5779-5783 (2008).
149. Seyed-Razavi, Y., Hickey, M.J., Kuffova, L., McMenamin, P.G. & Chinnery, H.R. Membrane nanotubes in myeloid cells in the adult mouse cornea represent a novel mode of immune cell interaction. *Immunol Cell Biol* **91**, 89-95 (2013).
150. Osswald, M., *et al.* Brain tumour cells interconnect to a functional and resistant network. *Nature* **528**, 93-98 (2015).
151. Sipkins, D.A., *et al.* In vivo imaging of specialized bone marrow endothelial microdomains for tumour engraftment. *Nature* **435**, 969-973 (2005).
152. Lo Celso, C., *et al.* Live-animal tracking of individual haematopoietic stem/progenitor cells in their niche. *Nature* **457**, 92-96 (2009).
153. Lo Celso, C., Lin, C.P. & Scadden, D.T. In vivo imaging of transplanted hematopoietic stem and progenitor cells in mouse calvarium bone marrow. *Nat Protoc* **6**, 1-14 (2011).
154. Naphade, S., *et al.* Brief reports: Lysosomal cross-correction by hematopoietic stem cell-derived macrophages via tunneling nanotubes. *Stem Cells* **33**, 301-309 (2015).
155. Rainy, N., *et al.* H-Ras transfers from B to T cells via tunneling nanotubes. *Cell Death Dis* **4**, e726 (2013).
156. Arkwright, P.D., *et al.* Fas stimulation of T lymphocytes promotes rapid intercellular exchange of death signals via membrane nanotubes. *Cell Res* **20**, 72-88 (2010).
157. Pasquier, J., *et al.* Different modalities of intercellular membrane exchanges mediate cell-to-cell p-glycoprotein transfers in MCF-7 breast cancer cells. *J Biol Chem* **287**, 7374-7387 (2012).
158. Thayanithy, V., Dickson, E.L., Steer, C., Subramanian, S. & Lou, E. Tumor-stromal cross talk: direct cell-to-cell transfer of oncogenic microRNAs via tunneling nanotubes. *Transl Res* **164**, 359-365 (2014).
159. Kristl, J., Plajnsek, K.T., Kreft, M.E., Jankovic, B. & Kocbek, P. Intracellular trafficking of solid lipid nanoparticles and their distribution between cells through tunneling nanotubes. *Eur J Pharm Sci* **50**, 139-148 (2013).
160. Tan, A.S., *et al.* Mitochondrial genome acquisition restores respiratory function and tumorigenic potential of cancer cells without mitochondrial DNA. *Cell Metab* **21**, 81-94 (2015).
161. Pasquier, J., *et al.* Preferential transfer of mitochondria from endothelial to cancer cells through tunneling nanotubes modulates chemoresistance. *J Transl Med* **11**, 94 (2013).
162. Wang, X. & Gerdes, H.H. Transfer of mitochondria via tunneling nanotubes rescues apoptotic PC12 cells. *Cell Death Differ* **22**, 1181-1191 (2015).

163. Rechavi, O., *et al.* Trans-SILAC: sorting out the non-cell-autonomous proteome. *Nat Methods* **7**, 923-927 (2010).
164. Vernitsky, H., *et al.* Ras oncoproteins transfer from melanoma cells to T cells and modulate their effector functions. *J Immunol* **189**, 4361-4370 (2012).
165. Gerdes, H.H., Bukoreshtliev, N.V. & Barroso, J.F. Tunneling nanotubes: a new route for the exchange of components between animal cells. *FEBS Lett* **581**, 2194-2201 (2007).
166. Petit, I., *et al.* G-CSF induces stem cell mobilization by decreasing bone marrow SDF-1 and up-regulating CXCR4. *Nat Immunol* **3**, 687-694 (2002).
167. Uy, G.L., *et al.* A phase 1/2 study of chemosensitization with the CXCR4 antagonist plerixafor in relapsed or refractory acute myeloid leukemia. *Blood* **119**, 3917-3924 (2012).
168. Fierro, F.A., *et al.* Combining SDF-1/CXCR4 antagonism and chemotherapy in relapsed acute myeloid leukemia. *Leukemia* **23**, 393-396 (2009).
169. Borthakur, G. BL-8040, a Peptidic CXCR4 Antagonist, Induces Leukemia Cell Death and Specific Leukemia Cell Mobilization in Relapsed/Refractory Acute Myeloid Leukemia Patients in an Ongoing Phase IIa Clinical Trial. *ASH abstract 950* (2014).
170. Becker, P.S. Targeting the CXCR4 Pathway: Safety, Tolerability and Clinical Activity of Ulocuplumab (BMS-936564), an Anti-CXCR4 Antibody, in Relapsed/Refractory Acute Myeloid Leukemia. *ASH Abstract 386* (2014).
171. Cooper, T.M. Chemosensitization and Mobilization Of AML/ALL/MDS With Plerixafor (AMD 3100), a CXCR4 Antagonist: A Phase I Study Of Plerixafor + Cytarabine and Etoposide In Pediatric Patients With Acute Leukemia and MDS. *ASH Abstract 2680* (2013).
172. Ottmann, O.G., Bug, G. & Krauter, J. Current status of growth factors in the treatment of acute myeloid and lymphoblastic leukemia. *Seminars in hematology* **44**, 183-192 (2007).
173. van den Berk, L.C., *et al.* Disturbed CXCR4/CXCL12 axis in paediatric precursor B-cell acute lymphoblastic leukaemia. *Br J Haematol* **166**, 240-249 (2014).
174. Pease, J.E. & Horuk, R. Recent progress in the development of antagonists to the chemokine receptors CCR3 and CCR4. *Expert Opin Drug Discov* **9**, 467-483 (2014).
175. Duvic, M., *et al.* Phase 1/2 study of mogamulizumab, a defucosylated anti-CCR4 antibody, in previously treated patients with cutaneous T-cell lymphoma. *Blood* **125**, 1883-1889 (2015).

SUPPLEMENTARY FIGURES

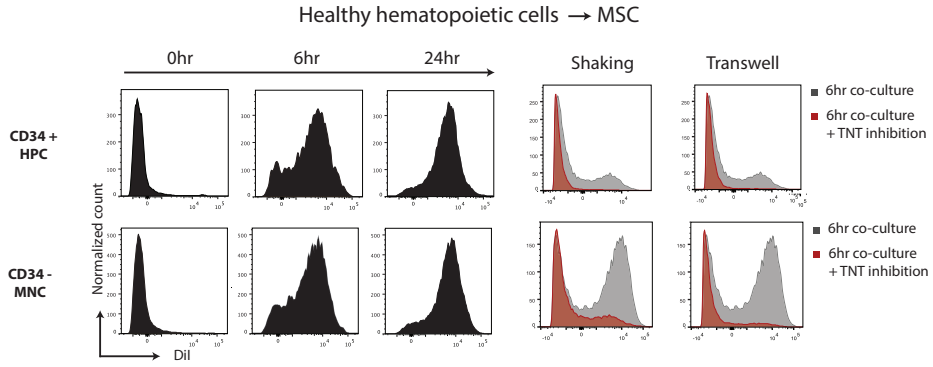

Supplementary Figure 1. TNT signaling from cord blood-derived healthy hematopoietic cells toward primary MSCs

Primary mononuclear cells (CD34 negative MNCs) and CD34^{+} hematopoietic progenitors (CD34 positive HPCs) were isolated from cord blood, stained with DiI and subsequently co-cultured with primary MSCs. Gentle shaking and transwell controls were used to inhibit TNT signaling.

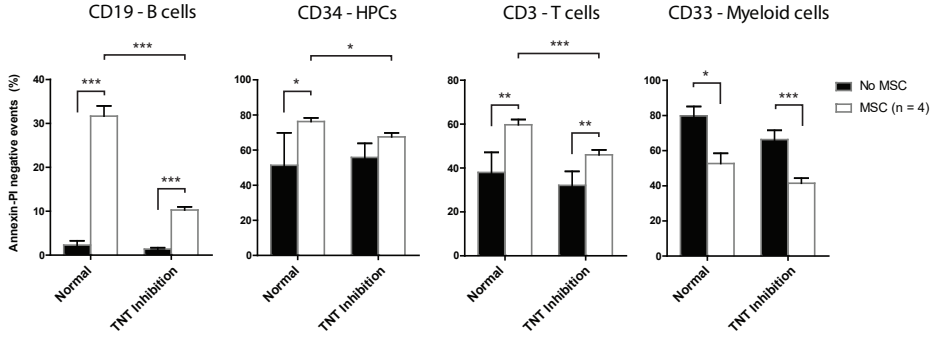

Supplementary Figure 2. TNT-dependent survival survival of healthy hematopoietic cells in co-culture with primary MSCs

CD19-positive cells (B-cells), CD3-positive cells (T-cells), CD33-positive cells (myeloid cells), and CD34-positive cells (HPCs) were isolated from umbilical cord blood and subsequently cultured for 5 days in absence (black bars) or presence (white bars) of primary MSCs. Survival analysis was performed using FACS. Hematopoietic cells were distinguished from MSCs by CD45 surface marker expression. Survival was quantified using Annexin V – Propidium Iodide staining. All experiments were performed with or without TNT inhibition. TNTs were inhibited by gentle shaking or culture in a 3 μm transwell system. TNT inhibition in this figure represents the average of TNT inhibiting controls. All experiments were performed at least 3 times with different cord blood donors and with 4 different primary MSCs. Error bars represent SEM. *, $p \leq 0.05$, **, $p \leq 0.01$, ***, $p \leq 0.001$.

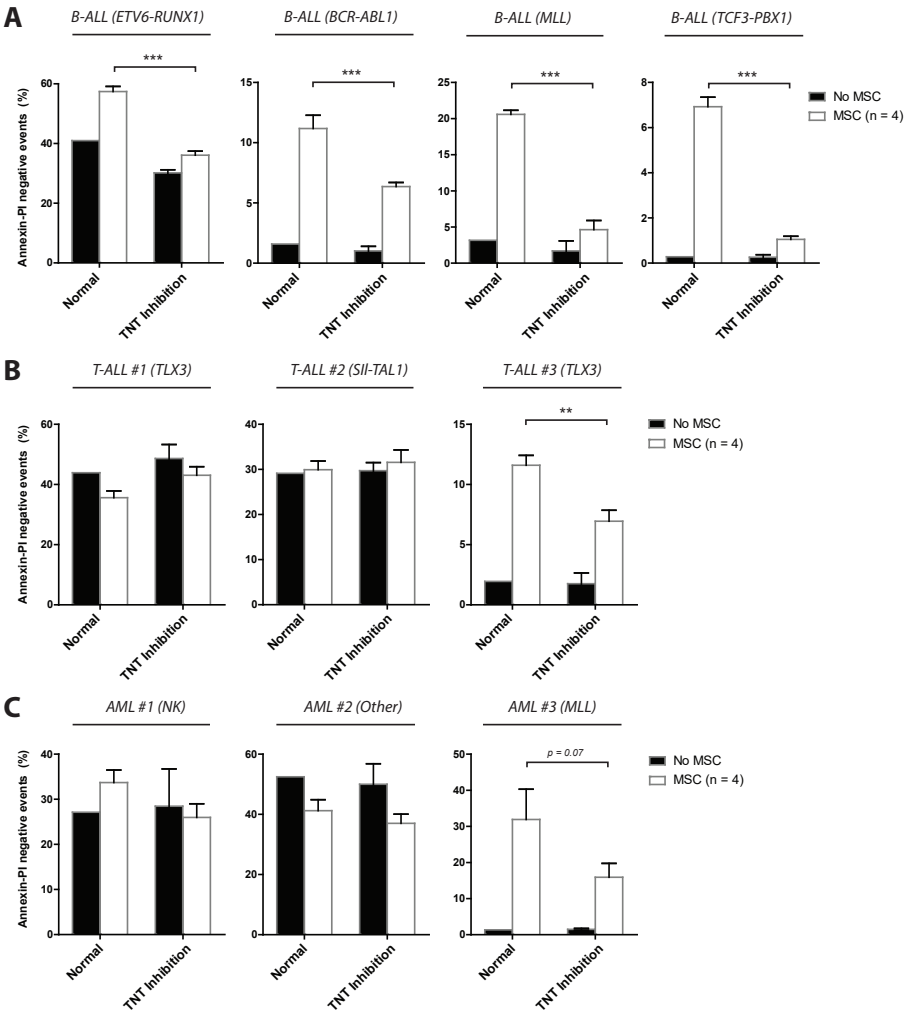

Supplementary Figure 3. TNT-dependent survival of primary BCP-ALL, T-ALL, and AML cells in co-culture with primary MSCs.

(A) Primary BCP-ALL cells from different cytogenetic subgroups (namely ETV6-RUNX1 (n = 3), BCR-ABL1 (n = 3), MLL-rearranged (n = 2), and TCF3-PBX1 (n = 2)) were isolated from bone marrow of pediatric patients. Cells were cultured for 5 days in absence (black bars) or presence (white bars) of primary MSCs. All experiments were performed with or without TNT inhibition. TNTs were inhibited by gentle shaking or culture in a 3 μm transwell system. TNT inhibition in this figure represents the average of TNT inhibiting controls. Experiments were performed with 4 different primary MSCs. A representative experiment was shown for each subgroup. Error bars represent SEM. *, $p \leq 0.05$, **, $p \leq 0.01$, ***, $p \leq 0.001$. (**B / C**) Primary T-ALL (**B**) and primary AML cells (**C**) were cultured for 5 days in absence (black bars) or presence (white bars) of primary MSCs. All experiments were performed with or without TNT inhibition. TNTs were inhibited by gentle shaking or culture in a 3 μm transwell system. TNT inhibition in this figure represents the average of TNT inhibiting controls. Experiments were performed with 4 different primary MSCs. Error bars represent SEM. **, $p \leq 0.01$.

Chapter 8

ADDENDUM

Tunneling nanotubes facilitate autophagosome transfer in the leukemic niche

Bob de Rooij[1], Roel Polak[1], Femke Stalpers[1], Rob Pieters[1,2] & Monique L. den Boer[1]

[1] Dept. of Pediatric Oncology, Erasmus MC-Sophia Children's Hospital, Rotterdam, The Netherlands.

[2] Princess Máxima Center for Pediatric Oncology, Utrecht, The Netherlands.

Leukemia. 2017 Jul;31(7):1651-1654

ABSTRACT

Acute lymphoblastic leukemia (ALL) cells create a leukemic niche with mesenchymal stromal cells (MSCs). Cytoskeletal structures called tunneling nanotubes (TNTs) facilitate communication between ALL cells and MSCs by transporting molecules and inducing the secretion of pro-survival cytokines. The identity of the molecules driving these malignant processes are currently unknown. Here we investigate which structures are transported from ALL cells toward MSCs by quantifying the transfer of ectopically expressed fluorescent marker proteins using flow cytometry. Our results indicate that actin, endoplasmatic reticulum, ICAM1, autophagosomes, mitochondria, and endosomes are contact-dependently transferred from leukemic cells toward MSCs. Transfer of mitochondria, adhesion molecule ICAM1, and autophagosomes were significantly reduced (≤ 9.6-fold) when TNT signaling was inhibited. Autophagosomes and mitochondria are known inducers of cytokine signaling and hence their transfer might unveil an important mechanism that ALL cells use to affect their microenvironment. Importantly, transfer of autophagosomes was 3.0-fold greater than the other molecules tested in ALL-MSC co-cultures, and has not been previously associated with TNT signaling. These data provide insight into intercellular signaling in the leukemic niche and implicate autophagosomes as novel TNT cargo.

Acute lymphoblastic leukemia (ALL) cells disrupt the healthy bone marrow microenvironment to create a leukemic niche that is crucial for facilitating leukemogenesis and protects leukemic cells from chemotherapeutic agents and immune cells[1,2]. However, the functional mechanisms that regulate this malignant process are largely unknown. Recently, we showed that tunneling nanotubes (TNTs) play an important role in the communication between leukemic cells and bone-marrow derived mesenchymal stromal cells (MSCs)[3,4]. TNTs are thin membrane protrusions that are driven by the actin cytoskeleton[5]. We recently showed that ALL cells use TNTs to signal toward MSCs and subsequently induce the secretion of pro-survival cytokines, leukemic cell survival and drug resistance[4]. B-cell precursor ALL (BCP-ALL) cells and MSCs exchange lipophilic molecules using TNTs[4]. However, the identity of the transported cargo needs further elucidation. In this study, we describe that autophagosomes, mitochondria and the transmembrane protein ICAM1 are transferred from B-cell precursor ALL (BCP-ALL) cells toward MSCs in a TNT-dependent manner.

To identify which structures are transferred from leukemic cells to MSCs via TNTs, we ectopically (i.e. non-endogenously) expressed fluorescently tagged proteins that mark specific cellular structures in BCP-ALL cells (NALM6) using lentiviral vectors (Figure 1A and supplementary Figure 1). After lentiviral transduction, we obtained stable BCP-ALL cell clones expressing turbo RFP (tRFP)-tagged marker proteins. The tRFP-positive BCP-ALL cells were stained with a nucleus specific dye (NucBlue), after which specific subcellular localization of fluorescent marker proteins was confirmed by confocal microscopy (Figure 1B). For example, CALR, which marks the endoplasmatic reticulum (ER), was expressed at the nuclear border (Figure 1B second panel from the top).

Next, we co-cultured tRFP-marker protein expressing BCP-ALL cells with tRFP-negative MSCs (Figure 1C) and quantified the transfer of tRFP by flow cytometry (Figure 1D). The B-cell marker CD19 was used to distinguish between BCP-ALL cells and MSCs (Figure 1D, second panel). Actin, ER, cytoplasm, ICAM1, autophagosomes, mitochondria, and early/late/recycle endosomes were transferred from BCP-ALL cells to MSCs, since MSCs became increasingly positive for tRFP signal after co-culture with tRFP-tagged leukemic clones for 24, 48, and 72 hours (Figure 2A). To exclude that tRFP transfer was nonspecific, we plotted the intensity of tRFP in BCP-ALL cells, that differed 6.9-fold between the brightest and dimmest clone (cytoplasm versus ER; supplementary Figure 2), against the intensity of tRFP in MSCs after co-culture for 48 hours (Figure 2B). No correlation was found between the amount of transfer and the intensity of the tRFP signal in the leukemic clone from which the tRFP-tagged molecule originated (Figure 2B; $p = 0.48$, Pearson correlation test), showing that the observed transfer is not explained by nonspecific leakage

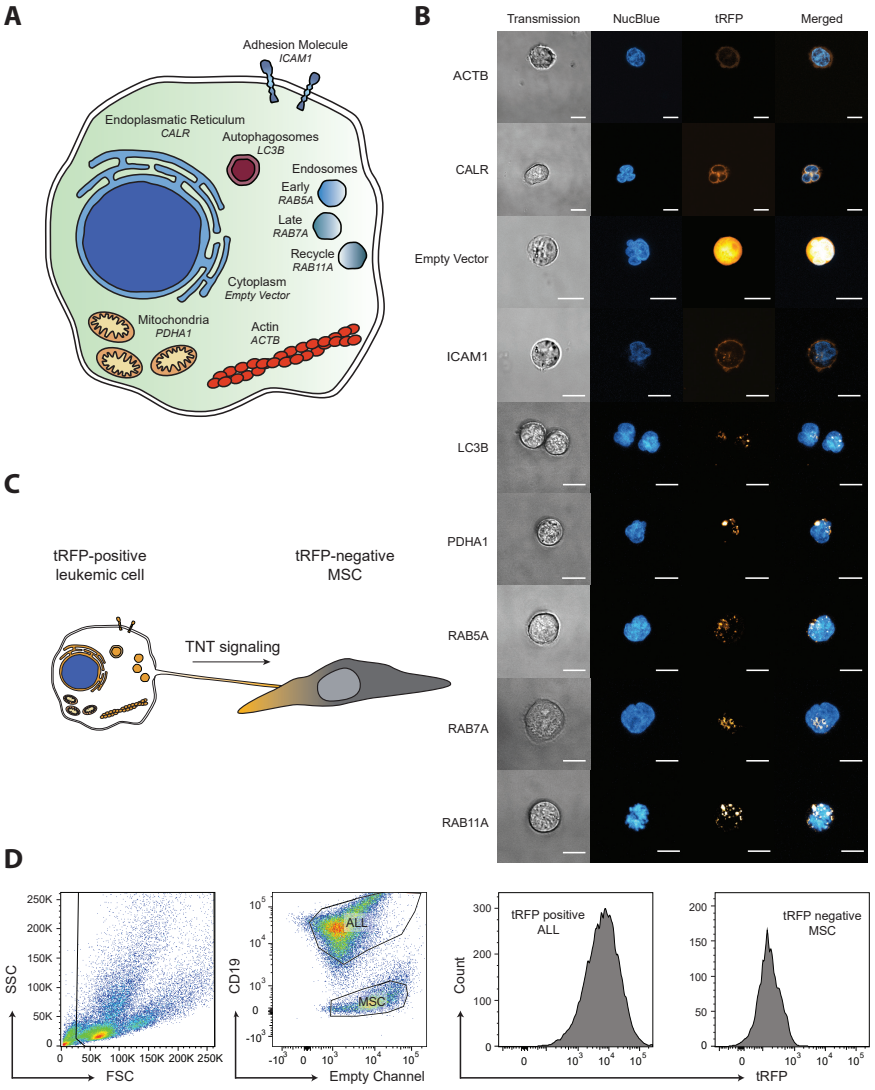

Figure 1. Identifying TNT cargo using fluorescently tagged proteins

(A) Schematic overview of ectopically expressed marker proteins that were used to visualize specific cellular structures in BCP-ALL cells (NALM6). (B) Representative confocal images showing the subcellular localization of tRFP-positive marker proteins relative to the nucleus in live NALM6 cells. A transmission image is provided to show the shape of the leukemic cell (left panel). (C) Experimental setup for visualizing protein transfer from BCP-ALL cells toward MSCs. Leukemic clones that express tRFP-positive marker proteins were co-cultured with tRFP-negative MSCs and transfer of protein toward was quantified by flow cytometry. (D) Gating strategy that was used to quantify transfer of tRFP-positive marker protein from leukemic cells toward MSCs by flow cytometry. BCP-ALL cells and MSCs are gated based on their forward and sideward scatter (first panel) and separated based on CD19 expression (second panel). Finally, the median tRFP signal in MSCs was quantified with the PE-channel and used as a measure of tRFP-positive marker protein transfer (last panel).

See also supplementary Figure 1.

of tRFP label. This implies that tRFP transfer from BCP-ALL cells toward MSCs is representative for transfer of tagged cellular structures. Autophagosomes appeared to be the most highly transported structure from BCP-ALL cells to MSCs (3.0-fold more than other proteins after 48 hours; Figure 2C). To assess the contribution of TNTs to the transfer of cellular structures, we performed ALL-MSC co-cultures in the absence or presence of TNT inhibiting conditions for 48 hours. TNTs were inhibited by two established approaches in literature: mechanical disruption of TNTs through gentle shaking of cell cultures and physical separation of BCP-ALL cells and MSCs using a transwell system (3.0 μm pore size)[4,6]. While actin inhibitors are often used to inhibit TNTs, their short half-time and high cytotoxicity prevented their use in these experiments[4]. Transfer of actin (ACTB), endoplasmatic reticulum (CALR), cytoplasmic content (Empty Vector), and endosome markers (RAB family) were inhibited by transwell conditions, but not by gentle shaking (Figure 2D). This implicates that transfer of these proteins is driven by cell-cell signaling modules other than TNTs. For example by gap junctional protein Cx43, which has been shown to be involved in transfer of extracellular vesicles[7]. Interestingly, transfer of transmembrane protein ICAM1, autophagosomes (LC3B), and mitochondria (PDHA1) were significantly inhibited by both TNT inhibiting conditions (shaking and transwell; $p < 0.05$, Figure 2D). Transmembrane proteins and mitochondria have previously been observed to be transferred via TNTs by other cell types[8,9]. Our data show that this is also true for TNT signaling between BCP-ALL cells and MSCs. Strikingly, transfer of autophagosomes was 3.0-fold higher than ICAM1 and PDHA1 transfer (Figure 2C). To our knowledge, this is the first time that autophagosome transfer is observed between ALL cells and MSC in a TNT-dependent manner.

Autophagy is a process that degrades and recycles unwanted or damaged cellular components, like proteins and organelles[10]. This process has been implicated as an important regulator of both tumor-initiation and tumor-suppression[11]. Autophagy is driven by double-membraned vesicles known as autophagosomes, which are shaped through the actin cytoskeleton[12]. TNT formation is also dependent on actin[4,5] and this co-dependence might be important for autophagosome transport through the TNT machinery. Interestingly, autophagy induction through starvation of cells has been shown to increase the formation of TNTs[13], suggesting a correlation between these processes. Recently, we observed that TNT signaling induces the secretion of pro-survival cytokines[4]. Autophagy is a known regulator of cytokine signaling and this process is influenced by mitochondrial reactive oxygen species and/or mitochondrial DNA[14].The transfer of mitochondria and autophagosomes from leukemic cells toward MSCs might therefore explain the release of supportive factors by the tumor microenvironment, as we recently reported elsewhere (Figure 2E)[4]. Interestingly, the transcription of ICAM1, a transmembrane protein involved

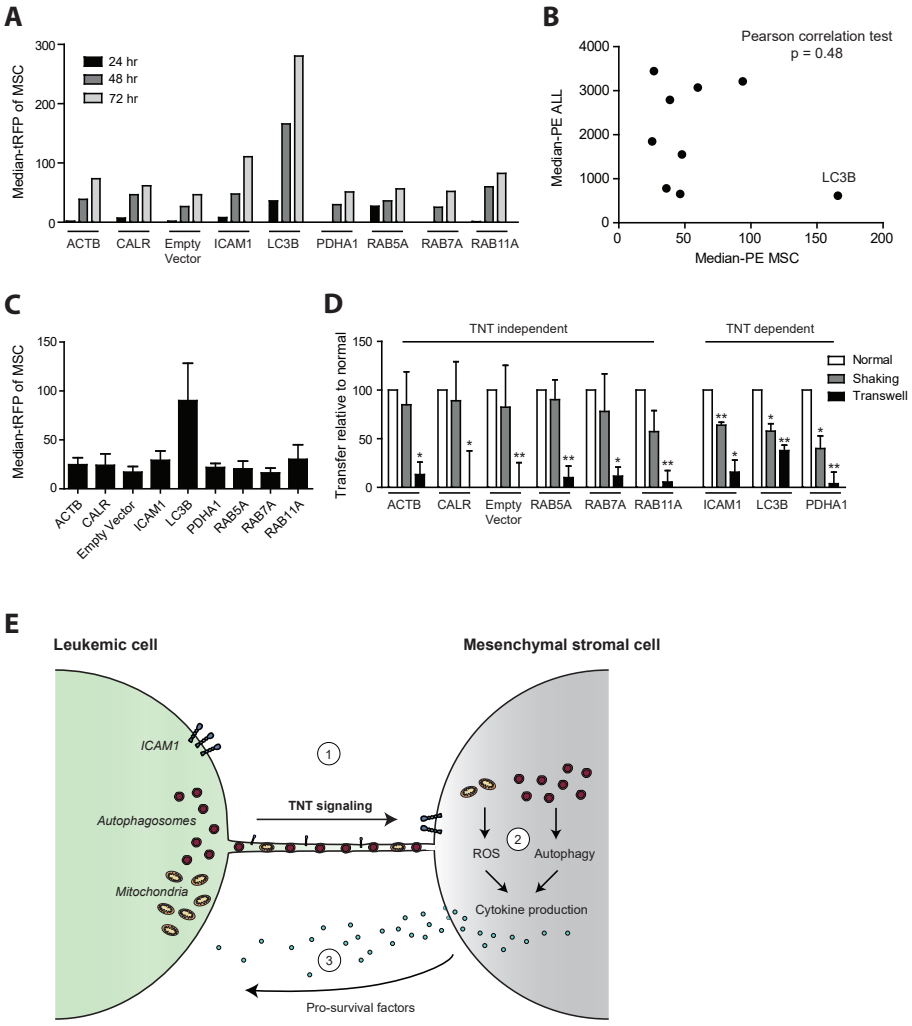

Figure 2. Autophagosomes, mitochondria and ICAM1 are transferred via tunneling nanotubes

(A) BCP-ALL cells expressing tRFP-markers were co-cultured with tRFP-negative MSCs for 24 (black bars), 48 (dark-grey bars), and 72 hours (light-grey bars). Median intensity of MSCs for tRFP is shown. (B) Graph showing the median tRFP intensity of MSCs (X-axis) compared to BCP-ALL tRFP intensity (Y-axis) after co-culture for 48 hours as depicted in Figure 2A. No correlation was found indicating that transfer of tRFP was protein specific (n = 3, p = 0.48, Pearson correlation test). (C) Graph showing the transfer of tRFP from BCP-ALL cells toward MSCs after 48 hours of co-culture (n = 3). (D) Graph showing the transfer of tRFP from BCP-ALL cells toward MSCs after TNT inhibition (grey and black bars), compared to normal co-culture conditions (white bars; n = 3; one-tailed t-test, paired). (E) Model of TNT signaling in the leukemic niche:

1: Leukemic cells use TNT signaling to transfer autophagosomes, mitochondria and ICAM1 toward MSCs in their microenvironment.

2: Increased reactive oxygen species (ROS) and autophagy in MSCs induces the production of cytokines

3: Supportive and nurturing factors are released into the tumor microenvironment, which induce survival and drug resistance in leukemic cells.

Data are means ± SEM; * $p \leq 0.05$, ** $p \leq 0.01$. See also supplementary Figure 2.

in cell-cell adhesion, is known to be upregulated in response to cytokine signaling and reactive oxgen species[15]. Its transport toward MSCs may provide anchorage to facilitate TNT function.

In conclusion, these data show the potential of using fluorescently labeled marker proteins to characterize which cellular structures are transported by TNT signaling from ALL cells to MSCs. Our study confirmed several known TNT cargo (i.e. mitochondria and transmembrane proteins)[8,9] and revealed novel structures (autophagosomes) that are transported through TNTs. The TNT-dependent transfer of autophagosomes and mitochondria from ALL cells toward MSCs might unveil an important mechanism that leukemic cells use to affect their microenvironment. Our study suggests that instead of upregulating autophagy in an indirect manner, leukemic cells transfer autophagosomes to MSCs in order to enhance autophagy-induced cytokine secretion. In addition, our study identifies autophagosomes, ICAM1 and mitochondria as important structures that are actively transported from leukemic cells toward their microenvironment via TNTs.

Acknowledgements

We thank all members of the research laboratory Pediatric Oncology of the Erasmus MC for their help in processing mesenchymal stromal cell samples, in particular F. Meijers-Stalpers; The Erasmus Optical Imaging Centre for providing support of CLSM, in particular G. Kremers; The work described in this paper was funded by the KiKa Foundation (Stichting Kinderen Kankervrij – Kika-39), the Dutch Cancer Society (UVA 2008; 4265, EMCR 2010; 4687), the Netherlands Organization for Scientific Research (NWO – VICI M.L. den Boer) and the Pediatric Oncology Foundation Rotterdam.

Author contributions

B. de Rooij and R. Polak designed the study, performed the experiments, collected and analyzed all data, and wrote the paper. F. Stalpers performed additional experiments. M.L. den Boer and R. Pieters analyzed data and wrote the paper. All authors discussed the results and approved the submitted manuscript.

REFERENCES

1. Colmone, A., *et al.* Leukemic cells create bone marrow niches that disrupt the behavior of normal hematopoietic progenitor cells. *Science* **322**, 1861-1865 (2008).
2. Nakasone, E.S., *et al.* Imaging tumor-stroma interactions during chemotherapy reveals contributions of the microenvironment to resistance. *Cancer Cell* **21**, 488-503 (2012).
3. Morrison, S.J. & Scadden, D.T. The bone marrow niche for haematopoietic stem cells. *Nature* **505**, 327-334 (2014).
4. Polak, R., de Rooij, B., Pieters, R. & den Boer, M.L. B-cell precursor acute lymphoblastic leukemia cells use tunneling nanotubes to orchestrate their microenvironment. *Blood* **126**, 2404-2414 (2015).
5. Rustom, A., Saffrich, R., Markovic, I., Walther, P. & Gerdes, H.H. Nanotubular highways for intercellular organelle transport. *Science* **303**, 1007-1010 (2004).
6. Sowinski, S., *et al.* Membrane nanotubes physically connect T cells over long distances presenting a novel route for HIV-1 transmission. *Nat Cell Biol* **10**, 211-219 (2008).
7. Soares, A.R., *et al.* Gap junctional protein Cx43 is involved in the communication between extracellular vesicles and mammalian cells. *Sci Rep* **5**, 13243 (2015).
8. Wang, X. & Gerdes, H.H. Transfer of mitochondria via tunneling nanotubes rescues apoptotic PC12 cells. *Cell Death Differ* **22**, 1181-1191 (2015).
9. Rainy, N., *et al.* H-Ras transfers from B to T cells via tunneling nanotubes. *Cell Death Dis* **4**, e726 (2013).
10. Mizushima, N. & Komatsu, M. Autophagy: renovation of cells and tissues. *Cell* **147**, 728-741 (2011).
11. Mathew, R., Karantza-Wadsworth, V. & White, E. Role of autophagy in cancer. *Nat Rev Cancer* **7**, 961-967 (2007).
12. Mi, N., *et al.* CapZ regulates autophagosomal membrane shaping by promoting actin assembly inside the isolation membrane. *Nat Cell Biol* **17**, 1112-1123 (2015).
13. Lou, E., *et al.* Tunneling nanotubes provide a unique conduit for intercellular transfer of cellular contents in human malignant pleural mesothelioma. *PLoS One* **7**, e33093 (2012).
14. Harris, J. Autophagy and cytokines. *Cytokine* **56**, 140-144 (2011).
15. Hubbard, A.K. & Rothlein, R. Intercellular adhesion molecule-1 (ICAM-1) expression and cell signaling cascades. *Free Radic Biol Med* **28**, 1379-1386 (2000).

SUPPLEMENTARY DATA

METHODS

Cell lines

BCP-ALL cell line NALM6 (B-Other) and human embryonic kidney cell line HEK293T were obtained from DSMZ (Braunschweig, Germany), used at low cell passages, and routinely verified by DNA fingerprinting.

Isolation and characterization of MSCs

Mesenchymal stromal cells (MSCs) were isolated from bone-marrow aspirates and characterized as previously described[1,2]. In short, MSCs were confirmed to have multilineage potential for adipocyte, osteocyte and chondrocyte differentiation and characterized using positive (CD44/ CD90/CD105/CD54/CD73/CD146/CD166/ STRO-1) and negative surface markers (CD19/CD45/CD34).

Leukemic clones containing fluorescent cellular markers

HEK293T cells were transfected with lentiviral vectors coding for tRFP-positive marker proteins (Cellpainter™ Organelle Markers; Origene, USA), together with the helper plasmids VSVG and pPAX, using X-tremegene 9 (Sigma-Aldrich; Saint Louis, USA). Turbo-RFP (tRFP) was added either C- or N-terminally to the marker proteins, to minimize its influence on protein structure (supplementary Figure 1). Lentiviral particles produced by the HEK293T cells were collected by harvesting supernatant for three consecutive days and purified using a 0.45 μm cellulose acetate filter (GE Healthcare Life Sciences, Buckinghamshire, United Kingdom) and ultra-centrifugation (32.000 rounds per minute (RPM) for 2 hours at room temperature).

BCP-ALL cells (NALM6) were transduced with a serial dilution of lentivirus to ensure optimal cell viability and virus transduction. Subsequently, BCP-ALL cells were centrifuged at 1800 RPM for 45 minutes at room temperature and incubated overnight. Afterwards, single cells were plated out and positive leukemic clones were selected based on tRFP positivity using a MACSQuant analyzer (Miltenyi Biotec, Gladbach Germany). The proliferation capacity of leukemic clones was confirmed to be unaffected compared to wildtype cells, by prolonged cell culture.

Confocal laser scanning microscopy

Leukemic clones expressing tRFP-positive marker proteins were visualized using a confocal laser scanning microscope (Leica SP5). The nucleus of leukemic cells was

stained using live cell stain "Nucblue", according to the manufacturer's protocol (Life Technologies, Breda, The Netherlands). Cells were imaged without fixation to retain optimal tRFP signal. Confocal images were acquired using sequential scanning of different channels at a resolution of 1024 x 1024 pixels in the x ^{x} y plane and 0.15 μm steps in z-direction. Nucblue and tRFP-positive marker proteins were excited with a 405-nm ultraviolet laser and a 561-nm Diode-Pumped Solid-State laser, respectively. Image processing was done with Fiji software[3].

Transfer of tRFP protein markers

tRFP-positive BCP-ALL cells (NALM6) were co-cultured with tRFP-negative MSCs in a 4:1 ratio for 24, 48 or 72 hours with and without TNT inhibition. TNTs were inhibited by mechanical disruption via gentle shaking of cell cultures (250 RPM), or by physical separation of leukemic cells (cultured in a 3.0 μm pore-sized insert) and MSCs (cultured in the bottom compartment of a transwell system; Corning, New York, USA). BCP-ALL cells and MSCs were separated using Brilliant Violet 421 labeled anti-human CD19 antibody (Biolegend, San Diego, USA). Median intensity of MSCs for the PE-channel was used as a measure of tRFP protein transfer and was determined using flow cytometry (BD Biosciences, California, USA; see Figure 1D for gating strategy).

Statistical analysis

Student's t-test was used as a statistical test and a Student's paired t-test was used when applicable (indicated in figure legends). Pearson correlation testing was used to compare the median tRFP intensity of MSCs and BCP-ALL cells after co-culture. Error bars show as standard error of the mean (SEM). Sample size and statistical test methods are reported in the figure legends. Variance between groups that are statistically compared is similar.

SUPPLEMENTARY FIGURES

A

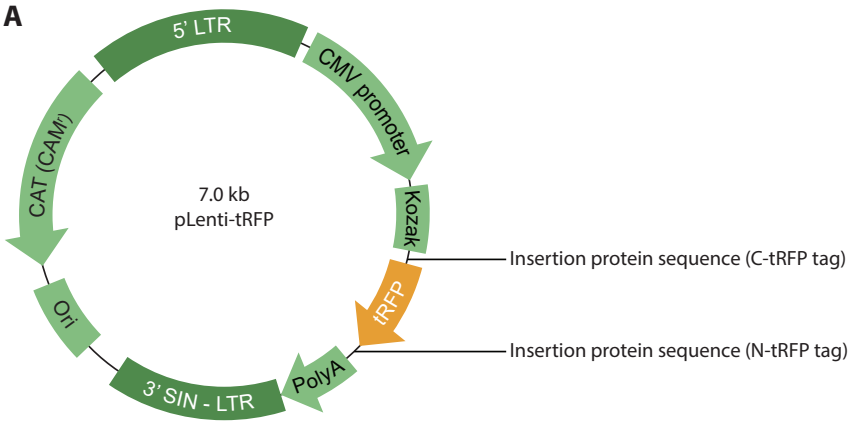

B

Marker protein	Cellular structure	GENENAME	Base pairs	Tag
Actin, beta	Actin filaments	ACTB	1852 bp	N-tRFP tag
Calreticulin	Endoplasmatic reticulum	CALR	1929 bp	C-tRFP tag
Empty vector	-	-		C-tRFP tag
Intercellular adhesion molecule 1	Integrin signalling	ICAM1	3249 bp	C-tRFP tag
Microtubule-associated protein 1 light chain 3 beta	Autophagosomes	MAP1LC3B	2304 bp	N-tRFP tag
Pyruvate dehydrogenase alpha 1	Mitochondria	PDHA1	3390 bp	C-tRFP tag
RAB5A, member RAS oncogene family	Early endosome	RAB5A	2548 bp	N-tRFP tag
RAB7A, member RAS oncogene family	Late endosome	RAB7A	2240 bp	N-tRFP tag
RAB11A, member RAS oncogene family	Recycle endosome	RAB11A	4943 bp	N-tRFP tag

Supplementary Figure 1. Transduction of leukemic cells with lentiviral vectors encoding for specific cellular markers

(A) Schematic overview of the lentiviral vector backbone in which specific cellular marker proteins were cloned. Two insertion sites were used in order to position the tRFP tag C or N-terminally. (B) Overview of the marker proteins depicting which cellular structures they visualize, their gene name, their length in base pairs (bp), and the position of the tRFP tag.

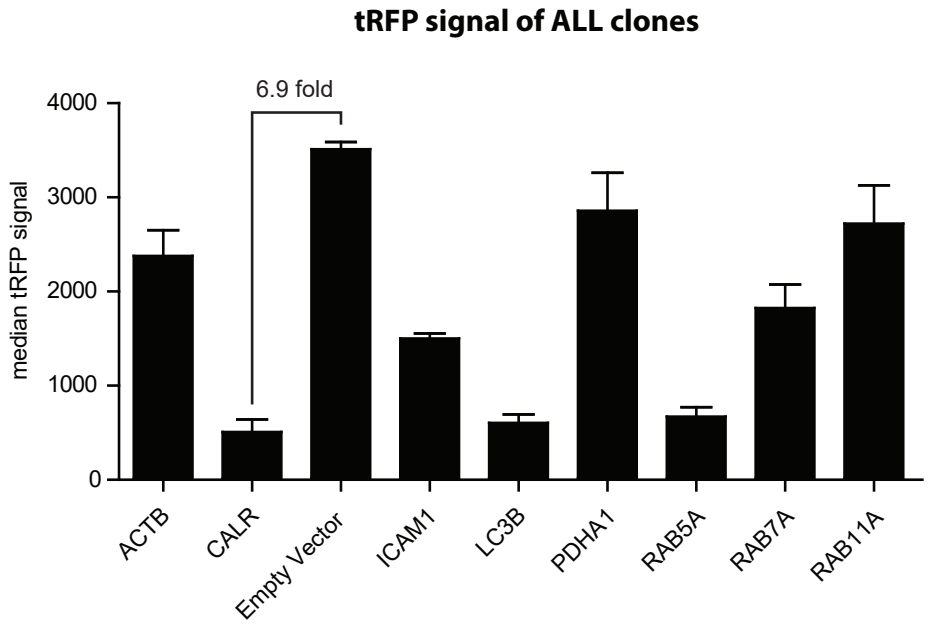

Supplementary Figure 2. tRFP positivity of BCP-ALL clones differs between markers
Graph showing the median tRFP intensity of tRFP-positive BCP-ALL cells for each cellular marker (n = 3). tRFP signal differs between clones and therefore transfer of tRFP protein from BCP-ALL cells toward MSCs should be corrected for the intensity of leukemic cells.

REFERENCES

1. Polak, R., de Rooij, B., Pieters, R. & den Boer, M.L. B-cell precursor acute lymphoblastic leukemia cells use tunneling nanotubes to orchestrate their microenvironment. *Blood* (2015).
2. van den Berk, L.C., *et al.* Disturbed CXCR4/CXCL12 axis in paediatric precursor B-cell acute lymphoblastic leukaemia. *Br J Haematol* **166**, 240-249 (2014).
3. Schindelin, J., *et al.* Fiji: an open-source platform for biological-image analysis. *Nat Methods* **9**, 676-682 (2012).

Chapter 9

SUMMARY

Acute lymphoblastic leukemia (ALL) is the most common pediatric malignancy. During the last decades, the overall survival rates of pediatric ALL have improved significantly. This is primarily due to optimization of conventional chemotherapeutic drug regimens combined with risk-directed stratification. However, to date, still 20% of pediatric ALL cases relapse due to resistance to therapy. In addition, short-term and long-term treatment-induced side effects remain considerable. New treatment regimens increasingly aim to target specific intrinsic characteristics and extrinsic signals important for leukemia. This approach has, for example, led to the successful development of targeted tyrosine kinase inhibitors that drastically improved the outcome of BCR-ABL1 positive leukemia patients. However, the majority of pediatric patients with leukemia is treated with non-specific classic chemotherapy regimens. This thesis identified leukemia-specific processes that can be used to target leukemic cells or the leukemic microenvironment.

The first part of this thesis focuses on intrinsic cellular processes that are important for proliferation, survival and/or drug resistance in ALL. Subsequently, we aimed to inhibit these biological processes in order to selectively target leukemic cells.

In **chapter 2**, we review the PI3K/protein kinase B (PKB/Akt) signaling module, an important mediator of cytokine signaling implicated in regulation of hematopoiesis. Constitutive activation of this signaling module has been observed in a large group of leukemia patients. Because activation of this signaling pathway has been demonstrated to be sufficient to induce hematologic malignancies and is thought to correlate with poor prognosis and enhanced drug resistance, it is considered to be a promising target for therapy. A large number of pharmacologic inhibitors directed against either individual or multiple components of this pathway have already been developed. Single-specificity inhibitors, targeting individual components of the PI3K/PKB signaling module, were shown to affect the survival of leukemic cells, but their anti-leukemic effect in patients appears to be modest. Compared to such inhibitors, dual-specificity inhibitors targeting the PI3K/PKB pathway at multiple levels or the combination of PI3K/PKB pathway inhibitors with classic chemotherapeutic regimens appear to have more promising anti-leukemic activity and are highly effective in preclinical leukemia models. Further research is warranted to examine the safety and efficacy of these regimens in leukemia patients.

In **chapter 3 and 4**, we study leukemia driven by the translocation t(12;21), resulting in the ETV6-RUNX1 fusion protein. This fusion gene, which is present in 25% of pediatric patients with B-cell precursor acute lymphoblastic leukemia (BCP-ALL), is considered a first hit in leukemogenesis. We focused on the biological processes that are affected by the ETV6-RUNX1 fusion protein by studying the effect of ectopic expression in healthy hematopoietic progenitor cells. This approach revealed a

transcriptional network that positively regulates proliferation, survival, migration, and cellular homeostasis in ETV6-RUNX1 positive cells. In **chapter 3,** we report an important role for autophagy, a cellular recycling system important for homeostasis and proliferation, in ETV6-RUNX1 positive BCP-ALL. Vps34, an important regulator of autophagy, was found to be up-regulated in ETV6-RUNX1 positive BCP-ALL patient cells. Induction of Vps34 was transcriptionally regulated by ETV6-RUNX1 and correlated with high levels of autophagy. Inhibition of autophagy reduced cell viability in both BCP-ALL cell lines and primary patient-derived BCP-ALL cells and selectively sensitized ETV6-RUNX1 positive leukemic cells to L-asparaginase. These findings reveal a causal relationship between ETV6-RUNX1 and autophagy, and provide the first preclinical evidence for the efficacy of autophagy inhibitors in ETV6-RUNX1 driven leukemia.

In **chapter 4,** we describe the role of Leukemia-Associated Rho Guanine nucleotide exchange factor (LARG) in the pro-migratory phenotype induced by the ETV6-RUNX1 fusion protein. We revealed that LARG is selectively up-regulated in ETV6-RUNX1 positive leukemic cells and induced by ectopic expression of ETV6-RUNX1 in healthy hematopoietic progenitors. Pharmacological small molecule inhibition of LARG and its downstream effector RhoA significantly inhibited the migration of ETV6-RUNX1 positive cells toward mesenchymal stromal cells (MSCs) and CXCL12, while proliferation and drug resistance remained unaffected. In contrast, migration of ETV6-RUNX1 negative cells was not altered by LARG/RhoA inhibition. These data show that enhanced LARG/RhoA signaling is important for migration of ETV6-RUNX1 positive leukemic cells. The specificity of this process for ETV6-RUNX positive cells may enable selective targeting of the leukemic microenvironment with small molecule inhibitors. Since leukemic cells are nurtured and protected against chemotherapy and immune responses in the leukemic bone marrow microenvironment, disruption of this leukemic niche is considered to be a promising approach to target leukemia.

The second part of this thesis aims to better understand and subsequently target extrinsic signals from the leukemic microenvironment by studying the crosstalk between leukemic cells and their niche. **Chapter 5 and 6** focus on the dynamic interplay between leukemic cells and MSCs, the best-studied component of the leukemic niche, in order to find novel strategies to disrupt leukemic niches. **Chapter 5** describes the discovery of tunneling nanotubes (TNTs) in the leukemic niche. TNTs have been described as a novel mode of intercellular communication, but their presence and importance in the leukemic microenvironment were so far unknown. We showed that primary BCP-ALL cells use TNTs to signal to primary MSCs. This signaling resulted in secretion of pro-survival cytokines, such as IP10/CXCL10,

IL8/CXCL8 and MCP-1/CCL2. In addition, TNT inhibiting conditions enabled us to analyze the functional importance of TNTs in an *ex vivo* model. TNT signaling was found to be important for the viability of patient-derived BCP-ALL cells and induction of stroma-mediated prednisolone resistance in leukemic cells. Disruption of TNTs significantly inhibited these leukemogenic processes. Our findings establish TNTs as a novel communication mechanism by which ALL cells modulate their bone marrow microenvironment. The identification of TNT signaling in ALL-MSC communication gives insight into the pathobiology of ALL and opens new avenues to develop alternative therapies that interfere with the leukemic niche.

Several studies have tried to target the leukemic niche by inhibiting CXCR4/CXCL12 signaling. However, recent data suggest that blocking CXCL12-mediated migration is insufficient to completely disrupt leukemic niches. In **chapter 6**, we aim to identify alternative factors for leukemic niche disruption. We used a patient-derived co-culture model in which the leukemic niche was represented by BCP-ALL cells and MSCs. Leukemic co-cultures inhibited migration of healthy hematopoietic progenitor cells and MSCs, but significantly induced migration of leukemic counterparts. This induction of leukemic cell migration was not affected by CXCR4 blockade. Moreover, CXCL12 levels were unaltered in co-cultures of primary BCP-ALL cells and MSCs, showing that BCP-ALL cells modify their niche without affecting the CXCR4/CXCL12 axis. Instead, patient-unique secretion patterns affecting alternative chemokine pathways, including CCR4, CXCR1/2, and CXCR3 ligands, were found to be induced. Also in serum of bone marrow aspirates from BCP-ALL patients, we observed a significant increase of CCR4 and CXCR1/2 ligands compared to bone marrow of the same patients in remission and healthy controls. These data show that BCP-ALL cells modify the migration properties of their niche without altering the CXCR4/CXCL12 axis, and warrant further research on CCR4 and CXCR1/2 signaling as candidate factors for leukemic niche disruption.

The studies described in this thesis identify both intrinsic characteristics (part 1) and extrinsic signals (part 2) driving BCP-ALL in children. Our results contribute to a conceptual revision of therapies for BCP-ALL in which besides targeting of leukemic cells also targeting of the interaction with the microenvironment needs to be considered. In **chapter 7**, we discuss the promising preclinical results described in this thesis and highlight the important next steps that need to be taken to realize our dream: a tailored, non-toxic therapy for children with leukemia.

Chapter 10

APPENDIX

NEDERLANDSE SAMENVATTING

Moleculaire determinanten van acute lymfatische leukemie bij kinderen
Op weg naar precisie therapie voor kinderen met acute lymfatische leukemie

Acute lymfatische leukemie (ALL) is de meest voorkomende kanker bij kinderen. Zonder behandeling is de ziekte dodelijk. Door de optimalisatie van behandeling met chemotherapie is de algehele overleving van kinderen met ALL in de afgelopen decennia aanzienlijk verbeterd. Hierbij wordt de intensiteit en duur van de therapie aangepast aan de hand van het risico op overlijden. Ondanks deze verbeteringen komt bij ongeveer 20% van de kinderen met ALL de leukemie terug (recidief). Ook heeft chemotherapie, die alle cellen in het lichaam aanvalt, ernstige bijwerkingen bij een aanzienlijk percentage kinderen. Wetenschappers zijn daarom op zoek naar nieuwe behandelingen voor leukemie die een recidief voorkomen en minder bijwerkingen geven. Deze therapieën zouden gericht moeten zijn tegen eigenschappen die uniek zijn voor de leukemiecel. Voor een kleine groep patiënten is een dergelijke therapie beschikbaar: kinderen met BCR-ABL1 positieve leukemie. Deze soort leukemie wordt veroorzaakt door een genetische fusie van het *BCR* gen en het *ABL1* gen. Het extra behandelen van deze kinderen met medicijnen tegen het product van dit fusie-gen, het fusie-eiwit BCR-ABL, heeft de overleving van deze groep kinderen drastisch verbeterd. Echter, voor de meeste kinderen met leukemie is zo'n doelgerichte therapie niet beschikbaar. Zij worden nog altijd alleen behandeld met aspecifieke chemotherapie. Dit proefschrift focust zich op het vinden van leukemie-specifieke processen die kunnen worden gebruikt om leukemiecellen doelgericht te behandelen.

In het eerste deel van dit proefschrift onderzoeken we moleculaire processen binnenin de leukemische cel, die belangrijk zijn voor hun groei, overleving en / of resistentie tegen geneesmiddelen. Vervolgens proberen we deze processen in de leukemiecel te blokkeren om de leukemiecellen selectief te doden.

Belangrijke processen binnenin een cel, zoals groei en overleving, worden aangestuurd door netwerken van eiwitten. Die netwerken worden ook wel signaleringsroutes genoemd. In **hoofdstuk 2**, bespreken we de beschikbare literatuur over het belang van de PI3K / proteïne kinase B (PKB / Akt) signaleringsroute in leukemie. Deze signaleringsroute is onder andere belangrijk voor het ontstaan van gezonde bloedcellen (hematopoiese). Echter, in een grote groep leukemiepatiënten is activatie van deze signaleringsroute waargenomen. Voortdurende activatie van PI3K / PKB lijkt zelfs voldoende te zijn voor de ontwikkeling van leukemie en

lijkt tevens te correleren met een slechte prognose en een verhoogde resistentie tegen chemotherapie. Daarom wordt deze signaleringsroute beschouwd als een veelbelovend doelwit voor therapie. De eerste stappen in het ontwikkelen van medicijnen die deze signaleringsroute remmen zijn genomen. Er zijn al meerdere farmacologische remmers ontwikkeld die gericht zijn tegen één of meerdere eiwitten in deze signaleringsroute. Vooral farmacologische remmers die de PI3K / PKB route op verschillende niveaus aanpakken of een combinatie van PI3K / PKB route remmers met chemotherapie zijn zeer effectief gebleken in preklinische leukemiemodellen en lijken daarom veelbelovend. Echter, verder onderzoek is nodig om de veiligheid en werkzaamheid van deze behandelingen bij leukemiepatiënten te onderzoeken.

In **hoofdstuk 3 en 4** gaan we zelf op zoek naar nieuwe aangrijpingspunten voor de behandeling van leukemie. In deze hoofdstukken bestuderen we leukemie veroorzaakt door het ETV6-RUNX1 (of TEL-AML1) fusie-eiwit. Dit fusie-eiwit komt voor bij 25% van de kinderen met voorloper B-cel acute lymfatische leukemie (BCP-ALL). Het ontstaan van dit fusie-eiwit wordt gezien als een eerste stap in het proces dat van een gezonde cel tot een kankercel maakt ('first hit'). We weten dat dit fusie-eiwit belangrijk is voor de overleving van kankercellen, maar het is nog onbekend welke signaleringsroutes in de cel hierbij betrokken zijn. Het begrijpen hiervan zou de mogelijkheid bieden om leukemiecellen met het fusie-eiwit specifiek aan te vallen. Daarom hebben we de biologische processen die worden aangestuurd door het ETV6-RUNX1 fusie-eiwit onderzocht. Dit doen we door het fusie-eiwit in te brengen in gezonde stamcellen van het bloed. Het inbrengen van het fusie-eiwit zorgde voor de activatie van genen die belangrijk zijn voor groei, overleving, beweging (migratie) en evenwicht (homeostase) in deze cellen. In **hoofdstuk 3**, beschrijven we dat autofagie een belangrijke rol speelt in ETV6-RUNX1 positieve leukemie. Autofagie is het recycling systeem van een cel. Dit systeem is belangrijk voor het evenwicht in de cel, maar ook voor overleving en groei van cellen. Vps34, een belangrijk eiwit die dit recycling proces aan en uit kan zetten, bleek door het ETV6-RUNX1 fusie-eiwit te worden geactiveerd. Hierdoor wordt autofagie in leukemiecellen aangezet. Remming van autofagie of Vps34 verminderde dan ook de overleving van ETV6-RUNX1 positieve cellen. Daarnaast werden ETV6-RUNX1 positieve leukemiecellen gevoeliger voor L-asparaginase, een belangrijk medicijn in de behandeling van leukemie. Dit alles was niet het geval voor ETV6-RUNX1 negatieve leukemiecellen. Deze bevindingen laten een oorzakelijk verband tussen ETV6-RUNX1 en autofagie zien, en leveren het eerste preklinische bewijs voor de werkzaamheid van autofagie-remmers in deze vorm van leukemie.

Leukemiecellen bevinden zich in patiënten voornamelijk in het beenmerg, de bloedfabriek van het lichaam. Deze omgeving beschermt niet alleen gezonde bloedcellen; ook leukemiecellen worden hier beschermd, bijvoorbeeld tegen

chemotherapie. Wetenschappers proberen dan ook dit micro-milieu (niche) te ontwrichten om leukemiecellen gevoeliger te maken voor therapie. In **hoofdstuk 4** laten we zien dat het ETV6-RUNX1 fusie-eiwit genen activeert die belangrijk zijn voor migratie (beweging) richting hun micro-milieu. We beschrijven de centrale rol van Leukemia-Associated Rho Guanine nucleotide exchange factor (LARG) en RhoA in dit proces. LARG zorgt voor activatie van RhoA, een eiwit dat belangrijk is voor migratie van cellen. LARG bleek niet alleen geactiveerd te zijn in ETV6-RUNX1 positieve leukemiecellen, maar werd ook geactiveerd door ETV6-RUNX1 in gezonde bloed voorlopercellen te plaatsen. Remming van LARG en RhoA verminderde de migratie van ETV6-RUNX1 positieve cellen naar een van de belangrijkste bouwstenen van het beenmerg, de mesenchymale stromacel (MSC). Daarnaast weten we dat het eiwit CXCL12 belangrijk is voor het behouden van leukemiecellen in het beenmerg. In onze studie werd migratie van ETV6-RUNX1 positieve leukemiecellen richting CXCL12 significant geremd. Daarentegen werd de migratie van ETV6-RUNX1 negatieve cellen niet beïnvloed door LARG / RhoA remming. Dit laat zien dat de activatie van LARG en RhoA alléén belangrijk is voor de migratie van ETV6-RUNX1 positieve cellen. De specificiteit van dit proces maakt het hopelijk in de toekomst mogelijk om het leukemische micromilieu selectief te remmen.

In het tweede deel van dit proefschrift bestuderen we de interactie tussen leukemiecellen en hun micromilieu in meer detail. We proberen de signalen vanuit het micro-milieu beter te begrijpen en proberen uiteindelijk nieuwe strategieën te ontwikkelen om dit micro-milieu te verstoren.

Hoofdstuk 5 en 6 bestuderen de dynamische interactie die plaatsvindt tussen leukemiecellen en MSCs, de best onderzochte bouwsteen van het leukemische micro-milieu. **Hoofdstuk 5** beschrijft de ontdekking van tunneling nanotubes (TNTs) in de leukemische niche. TNTs zijn zeer dunne verbindingskanaaltjes waardoor cellen onderling met elkaar kunnen communiceren. In hoofdstuk 5 laten we zien dat BCP-ALL cellen TNTs gebruiken om te communiceren met MSCs. Deze interactie zorgde voor de uitscheiding van meerdere belangrijke overlevingsfactoren (cytokines) in het micro-milieu (o.a. IP10, IL8 en MCP-1). Ook bleek de interactie belangrijk voor de overleving van leukemiecellen en zorgde de communicatie via TNTs ervoor dat leukemiecellen resistenter werden tegen chemotherapie (zoals Prednison en L-Asparaginase). Het verbreken van TNTs remde deze leukemische processen significant. Onze bevindingen laten zien dat TNT-signalering een belangrijk communicatiemechanisme is waarmee ALL cellen hun micro-milieu reguleren. De ontdekking van het belang van TNT-signalering kan daarom mogelijk worden gebruikt om effectievere therapieën te ontwikkelen die interfereren met de leukemische niche.

Zoals al eerder beschreven bestaan er eiwitten die essentieel zijn voor het behouden van bloedcellen in het beenmerg. Remming van CXCL12 zorgt bijvoorbeeld voor het uittreden van zowel gezonde bloedcellen als leukemiecellen uit het beenmerg. Verschillende studies hebben geprobeerd om het leukemische micro-milieu te verstoren door het remmen van CXCL12-gestuurde migratie. Echter, recente data suggereren dat het blokkeren van CXCL12 onvoldoende is om leukemische niches volledig te verbreken. In **hoofdstuk 6** zijn we op zoek gegaan naar de eiwitten die specifiek belangrijk zijn voor het behouden van leukemiecellen in hun micro-milieu. Om een leukemisch micro-milieu te simuleren gebruikten we een co-kweek model waarbij de leukemische niche werd vertegenwoordigd door BCP-ALL cellen en MSCs. We ontdekten dat deze leukemische niche zorgde voor een verhoogde migratie van leukemiecellen richting hun eigen niche en daarentegen een verminderde migratie van gezonde bloedcellen en MSCs. Dit proces werd niet beïnvloed wanneer CXCL12-gestuurde migratie werd geremd. Bovendien bleef de excretie van CXCL12 onveranderd in co-kweken van meerdere leukemie patiënten. In plaats daarvan zagen we dat in iedere patiënt een specifieke combinatie van migratie-bevorderende eiwitten (chemokines) werd geproduceerd. Opvallend was dat in iedere patiënt tenminste één eiwit werd geproduceerd die migratie bevorderde via de receptor-eiwitten CCR4 of CXCR1/2. Ook in het beenmerg van BCP-ALL patiënten zagen we een aanzienlijke toename van CCR4- en CXCR1/2-activerende eiwitten vergeleken met het beenmerg van dezelfde patiënten in remissie (na behandeling, dus zonder leukemiecellen) en vergeleken met gezonde controles. Deze data tonen aan dat BCP-ALL cellen de migratie eigenschappen van hun niche veranderen zonder CXCL12 te beïnvloeden, en suggereren dat remming van CCR4 en CXCR1/2 signalering belangrijke kandidaten kunnen zijn voor het verstoren van de leukemische niche.

De studies beschreven in dit proefschrift identificeren zowel intrinsieke kenmerken (deel 1) als extrinsieke signalen (deel 2) die belangrijk zijn voor BCP-ALL bij kinderen. Onze resultaten dragen bij aan een nieuwe visie op therapie voor BCP-ALL waarin therapie specifiek gericht is tegen moleculaire processen in de leukemiecel, maar ook tegen de interactie van leukemiecellen met hun micro-milieu. In **hoofdstuk 7**, bespreken we de in dit proefschrift beschreven pre-klinische resultaten en de belangrijke vervolgstappen die kunnen worden genomen om een op maat gemaakte, niet-toxische therapie voor kinderen met leukemie te verwezenlijken.

PHD PORTFOLIO

Name PhD student: drs. R. Polak	**PhD period: September 2010 – December 2014**
Erasmus MC Department: Hematology (2010-2012) and Pediatric Oncology (2013-2014)	**Promotors:** Prof. dr. M.L. den Boer, Prof. dr. R. Pieters
Research School: Molecular Medicine	**Supervisor:** Dr. M. Buitenhuis, Dr. M.B. Bierings

1. PhD training	**Year**	**ECTS**
General courses		
Basic course on R	2010	1.4
Basic workshop on Endnote	2010	0.3
Research management for PhD-students	2011	1.0
Workshop on Photoshop and Illustrator C6	2012	0.3
In depth courses		
Erasmus MC Hematology lectures	2010-2012	2.0
Course on Biomedical Research Techniques VIII	2010	1.6
Course on Molecular Medicine	2011	0.7
Course on Analysis of Microarray Gene Expression Data using R/BioC	2011	2.0
Course on Basic and Translational Oncology	2012	1.5
Annual Molecular Medicine Day	2012-2013	0.4
Seminars , workshops and congresses		
Scientific workshop Acute Myeloid Leukemia "Molecular"	2011	1
5th Dutch Hematology congress, Arnhem	2011	1
Research Retraite SKION-Princess Maxima Center	2013	0.6
Daniel den Hoed day	2013	0.2
KIKA promovendi dag	2014	1
Presentations		
Weekly Hematology Research Meetings (8x oral presentation)	2010-2012	3.5
AIO/Post-doc Hematology Meetings (2x oral presentation)	2010-2012	1
Weekly Pediatric Oncology Research Meetings (8x oral presentation)	2012-2014	3.5
Journal Club (Hematology and Pediatric Oncology; 3x oral presentation)	2010-2014	1.5
National conferences		
6th Dutch Hematology congress, Arnhem (1x oral presentation)	2012	2
16th Molecular Medicine Day, Rotterdam (1x poster presentation)	2012	1
Research Retraite SKION-Princess Maxima Center (1x oral presentation)	2015	1
International conferences		
56th American Society of Hematology Congress, San Francisco, CA, USA (2x oral presentation)	2014	3
9th Biennial Childhood Leukemia Symposium, Prague, Czech Republic (1x poster presentation)	2014	2
57th American Society of Hematology Congress, Orlando, FL, USA (2x poster presentation)	2015	2
Tunneling Nanotubes (TNTs) – Cell-to-Cell Social Networking in Disease	2016	2
2. Teaching		
Supervising		
Co-supervising master student (Biology and Science-based Business, LUMC)	2011	2
Supervising bachelor student (Life Science Research, Hogeschool Rotterdam)	2014	10
Supervising practicals		
3x practical on oncology/hematology for 2nd year medical students	2010-2012	0.5
TOTAL		**50**

PUBLICATIONS

1. De Rooij B*, **Polak R***, Stalpers F, van den Berk LCJ, Pieters R, Den Boer ML. Acute lymphoblastic leukemia cells create a leukemic niche without affecting the CXCR4/CXCL12 axis. *Haematologica.* 2017 Oct; 102(10):e389-e393.

2. De Rooij B, **Polak R**, Pieters R, Den Boer ML. Tunneling nanotubes facilitate autophagosome transfer in the leukemic niche. *Leukemia.* 2017 Jul;31(7):1651-1654.

3. Ariazi J*, Benowitz A*, De Biasi V*, Den Boer ML*, Cherqui S*, Cui H*, Douillet N*, Eugenin EA*, Favre D*, Goodman S*, Gousset K*, Hanein D*, Israel D*, Kimura S*, Kirkpatrick R*, Kuhn N*, Jeong C*, Lou E*, Mailliard R*, Maio S*, Okafo G*, Osswald M*, Pasquier J*, **Polak R***, Pradel G*,de Rooij B*,Schaeffer P*,Skeberdis A*, Smith IF*, Tanveer A*, Volkmann N*, Wu Z* and Zurzulo C*. Tunneling nanotubes and Gap junctions – their role in long-range intercellular communication during development, health, and disease conditions. *Frontiers in Molecular Neuroscience 2017.*

4. **Polak R***, De Rooij B*, Pieters R, Den Boer ML. B-cell precursor acute lymphoblastic leukemia cells use tunneling nanotubes to orchestrate their microenvironment. *Blood.* 2015 Nov;126(21):2404-14.

5. **Polak R** and Buitenhuis M. The PI3K/PKB signaling module as key regulator of hematopoiesis: implications for therapeutic strategies in leukemia. *Blood.* 2012 Jan;119(4):911-23.

6. **Polak R** and Buitenhuis M. The PI3K/PKB Signaling Module in Normal and Malignant Hematopoiesis. *Acute Leukemia - The Scientist's Perspective and Challenge*, 2011, ISBN: 978-953-307-553-2.

7. **Polak R***, Bours PH*, Hoepelman AI, Delgado E, Jarquin A, Matute AJ. Increasing resistance in community- acquired urinary tract infections in Latin America, five years after the implementation of national therapeutic guidelines. *Int J Infect Dis.* 2010 Sep;14(9):e770-4.

8. **Polak R**, Huisman A, Sikma MA, Kersting S. Spurious hypokalaemia and hypophosphataemia due to extreme hyperleukocytosis in a patient with a haematological malignancy. *Ann Clin Biochem.* 2010 Mar;47(Pt 2):179-81.

9. **Polak R,** Bierings MB, van der Leije CS, Sanders MA, Roovers O, Marchante JRM, Boer JM, Cornelissen JJ, Pieters P, den Boer ML & Buitenhuis M. Autophagy inhibition as targeted therapy for ETV6-RUNX1 driven B-cell precursor acute lymphoblastic leukemia. *Submitted.*

10. **Polak R**, Bierings MB, van den Dungen RES, de Rooij B, Pieters P, Buitenhuis M & den Boer ML. Small molecule inhibition of LARG/RhoA signaling blocks migration of ETV6-RUNX1 positive B-cell precursor acute lymphoblastic leukemia. *Submitted.*

11. E.M.P. Steeghs, **R. Polak**, B. de Rooij, L.C.J van den Berk, J.M. Boer, C. van de Ven, F. Stalpers, M. Bakker, R. Pieters, and M.L. den Boer. B-cell precursor acute lymphoblastic leukemia cells manipulate the gene expression profile of mesenchymal stromal cells. *Submitted.*

12. de Rooij B, **Polak R**, Stalpers F, Pieters R & den Boer ML. Disrupting tunneling nanotube signaling in the leukemic niche using actin inhibitors. *Submitted.*

13. Bartels M, **Polak R**[*]**,** Mokry M[*], Vervoort S, van Boxtel R, Govers A, Pals C. Bierings MB, van Solinge W, Egberts T, Nieuwenhuis E, Coffer PJ. Megakaryocyte and erythroid lineage development is controlled by modulation of protein acetylation. *Submitted.*

[*] authors contributed equally to this work

ABOUT THE AUTHOR

Roel Polak was born on February 24, 1985 in Alkmaar and grew up in De Rijp, a small village in the northern parts of the Netherlands. After graduating from the Murmellius Gymnasium in Alkmaar, he started Medical School at Utrecht University in 2003. During his study he participated in several extracurricular organizations including a rowing association and an educational committee. In addition, he completed a minor Spanish Language and Culture at Utrecht University in 2007. Hereafter, he travelled to León, Nicaragua for a scientific and clinical internship in pediatric and adult infection diseases and tropical medicine at the Universidad Nacional Autónoma de Nicaragua (under supervision of prof. dr. I.M. Hoepelman and dr. A.J. Matute). His passion for molecular research started with a scientific elective in the laboratory of Molecular Immunology at University Medical Center Utrecht in which he studied the effects of histone deacetylase inhibitors on megakaryopoiesis (under supervision of dr. M. Bartels and prof. dr. P.J. Coffer). He finished Medical School with a clinical elective in pediatrics at the Meander Medical Center in Amersfoort (under supervision of dr. D.A. van Tijn), and graduated from Utrecht University in 2010.

Being fascinated by fundamental cancer research, he started his PhD training in the laboratory of Hematology at the Erasmus University Medical Center in Rotterdam in the group of dr. M. Buitenhuis (co-supervised by dr. M.B. Bierings) in 2011. In these years he focused on researching the molecular drivers of ETV6-RUNX1 positive acute lymphoblastic leukemia. From 2013, he continued his training in the laboratory of Pediatric Oncology at the Erasmus University Medical Center in the group of prof. dr. M.L. den Boer and prof. dr. R. Pieters. In this period he got the opportunity to extend his molecular research with translational studies and, in addition, explored cellular interactions within the leukemic microenvironment. During his training he supervised a number of scientific BSc and MSc projects. The work performed during his PhD training is described in this thesis and has been presented at several national and international congresses.

After finishing his PhD research, being intrigued by care and research for pediatric patients with cancer, he started his residency in pediatrics at the St. Antonius Hospital in Nieuwegein in 2016 (under supervision of dr. W.A.F. Balemans, drs. I.M.A. Lukkassen, and drs. M. ten Berge). Currently he is a resident in the University Medical Center Utrecht (under supervision of dr. J Frenkel and prof. dr. E.S. Nieuwenhuis). In combination with his clinical work, he is still involved in research projects focusing on pediatric leukemia and aims to combine his clinical experience with extending his knowledge on fundamental and translational research.

DANKWOORD

If you never try you'll never know
Coldplay

Jaren van onderzoek met passie en inzet van vele mensen hebben geleid tot de inhoud van dit schrijven. Het is dan ook met veel trots en plezier dat ik dit proefschrift presenteer. En ondanks het feit dat mijn naam op de voorkant staat, zou dit werk er nooit geweest zijn zonder de hulp en inzet van anderen. Het is een genoegen jullie via deze weg te mogen bedanken.

Ten eerste wil ik mijn grote dankbaarheid betuigen aan de leukemiepatiënten en hun ouders voor het beschikbaar stellen van onderzoeksmateriaal. Gedurende een onbeschrijfelijk moeilijke periode in jullie leven, kiezen jullie ervoor wetenschappelijk onderzoek te steunen in de hoop toekomstige lotgenoten een betere behandeling te gunnen.

Prof.dr. M.L. den Boer, beste **Monique**, ik weet nog goed dat ik eind 2012 bij jou op kantoor zat en je vertrouwen in mij en mijn project voelde. Wat was ik blij dat je fiducie zag in mijn plannen en ik mijn promotie in jouw groep heb mogen afmaken. Het heeft me een scala aan nieuwe vaardigheden en denkrichtingen opgeleverd. De vrijheid die ik als PhD student in jouw groep heb gekregen was bijzonder en heeft uiteindelijk tot mooie wetenschappelijke resultaten geleid. Ontzettend bedankt voor je vertrouwen, steun en geduld.

Prof.dr. R. Pieters, beste **Rob**, jij bent de drijvende kracht achter het leukemie onderzoek in Nederland en het is dan ook een eer met je te mogen samenwerken. Je scherpte, denkvermogen en visie tijdens onze research meetings waren indrukwekkend. En de glinstering in je ogen bij de uitspraak "dit is goud" zal ik nooit vergeten (dat vonden wij nou ook). Ik respecteer je hoofdrol in het creëren van het Prinses Máxima Centrum voor Kinderoncologie enorm en denk dat je daarmee een grote stap hebt gezet in échte vooruitgang voor de patiënt. Bedankt voor de mogelijkheid me wetenschappelijk te ontwikkelen onder jouw supervisie.

Dr. M. Buitenhuis, beste **Miranda**, bij jou begon mijn wetenschappelijke carrière. Wat een eer was het om bij die jonge getalenteerde groepsleider in het Erasmus MC te mogen beginnen. Ik heb ongelofelijk veel van je geleerd, van de grondbeginselen van de moleculaire biologie tot verfijning van moleculaire technieken tot wetenschappelijke denken en ethiek, je hebt me als wetenschapper gevormd en ik

respecteer je enorm als onderzoeker en als mens. Het is voor mij heel bijzonder dat onze samenwerking steeds meer op gelijkwaardig niveau is plaats gaan vinden. Dank voor je inzet, vertrouwen, steun en betrokkenheid tot de laatste letter van dit proefschrift.

Dr. M.B. Bierings, beste **Marc**, ook jij bent vanaf het begin belangrijk geweest voor mijn onderzoek. Je zette met Miranda de beginselen van mijn project op papier en bent 'along the way' altijd een essentiële sparring partner geweest. Dank voor je scherpe visie, het inbrengen van klinisch perspectief (als we weer eens te moleculair afdwaalden), en je aansturing van het project waar dat nodig was.

Prof.dr. B. Löwenberg, prof.dr. P.J. Coffer en prof.dr. S.S. Sleijfer wil ik van harte bedanken voor het deelnemen aan mijn leescommissie en hun kritische blik op het finale manuscript. Beste **Bob**, het was maar al te bijzonder dat ik je voor twee jaar "mijn kamergenoot" mocht noemen. Ondanks je ongelofelijke staat van dienst, ben je altijd bereikbaar gebleven voor beginnende wetenschappers. Ik heb jouw aanwezigheid altijd als grote steun ervaren, zeker toen er lastige keuzes gemaakt dienden te worden. Dank dat je er was. Beste **Paul**, als medisch student mocht ik voor het eerst proeven aan de wetenschap in jouw lab. Ik had me geen betere plek kunnen bedenken. De goede sfeer, de oprechte interesse in "het waarom" en de gedegenheid van je onderzoek zijn nog altijd een voorbeeld voor mij als wetenschapper. Dank voor die mooie start! Beste **Stefan**, dank voor je inzet en deelname aan mijn kleine commissie, ik kijk uit naar de verdediging.

Prof.dr. I.P. Touw, prof.dr. J.J. Schuringa en prof.dr. P.M. Hoogerbrugge dank ik hartelijk voor het plaatsnemen in mijn corona. Beste **Ivo**, dank voor je adviezen en wetenschappelijk raad tijdens mijn tijd op de afdeling Hematologie. Deze hebben mijn onderzoek in de beginfase de nodige richting en realiteitszin gebracht. Beste **Jan Jacob** en **Peter**, laten we de discussies die op congressen al zijn begonnen op 22 november continueren, ik kijk er naar uit.

Mijn onderzoek was niet mogelijk geweest zonder de adequate verzameling en sampling van het verkregen patiënten-materiaal. Veel dank gaat dan ook naar de kinderoncologen die patiënten uitleggen waarom wetenschappelijk onderzoek zo belangrijk is voor de toekomst, maar ook naar de verpleegkundigen, het secretariaat van de afdeling kinderoncologie en het hematologisch laboratorium specieel, die samen ons onderzoek mogelijk maken. Daarnaast dank ik SKION en de COALL studiegroep voor het beschikbaar stellen van materiaal voor onze studies. Het feit dat jullie de zaken zo goed voor elkaar hebben legt de grondslag voor veel van ons

werk. En dan de toppers van de "patiëntendienst": **Aurelie**, **Femke**, **Myrte**, **Rosanna**, **Jessica**, **Wilco**, **Yvette**, **Pauline**, **Lonneke**, **Susan**, **Patty**, **Sandrita** en **Mereltjuh** (en voorgangers): veel dank voor jullie geweldige werk. Dankzij jullie konden wij knallen.

Zoals al eerder gezegd begon mijn PhD periode op de 13e verdieping, afdeling Hematologie. De bijzondere en mooie tijd die ik daar gehad heb is te danken aan de volgende mensen.

De "Buitenhuis groep": we waren maar een klein groepje, maar we waren er voor elkaar. Dank voor jullie steun en inzet bij mijn experimenten. **Georgi**, de 'founding father' van onze clone database, dank voor al je hulp en humor. **Aysegül**, I got to know you as a hard worker with a lot of passion for science. I wish you all the best in your future endeavors and with your family. **Cindy**, jij bent in het bijzonder belangrijk geweest om verder te komen met het ETV6-RUNX1 project. Niet alleen door al je experimentele werk, maar vooral ook door je kritische blik en waardevolle bijdragen aan ons onderzoek. We moeten nog steeds dat potje tennissen trouwens!

Mijn kamergenoten: **Lucia**, vanaf het eerste moment dat we elkaar zagen wist ik dat we vrienden gingen worden. Je Rotterdamse nuchterheid, directheid en humor zijn ongeëvenaard en je bent vooral een fantastische vrouw. Ik ben heel blij dat we elkaar blijven zien. Katarzyna, **Kasia**, you rock girl! We had so much fun in and out the lab and it was very special to be there during special and sometimes hard times in your life. I am so happy that you found yourself; be proud! **Patricia**, my Spanish tutor, it was nice to dream in Spanish about traveling the world. Enjoy Switzerland. **Davine** en **Avinash**, wat was het fijn om af en toe de frustraties van ons onderzoek met elkaar te kunnen delen, dank daarvoor.

De andere 'PhD-warriors': **Farshid**, I respect you in so many ways. Good luck at the NKI. **Marshall**, your Halloween parties became "signature-parties" and I enjoyed every minute of them. **Noemi**, your Italian temperament and bright mind will get you a long way in science, I'm sure we'll meet again. **Roberto**, we had so much fun in the lab together, even at the late hours. Thanks for your friendship. Let's keep in touch. **Mathijs**, zonder jouw expertise in bioinformatica en "out-of-the-box" denken was er niets uit onze CD34 data gekomen. Dank voor al je hulp! **Eric**, mijn beste Vroegindewijsneus, door jou hoor ik elke ochtend bij het wakker worden een liedje van Dries Roelvink..bedankt man..we gaan jou en **Helen** zien in Zeist!

Mijn lab-straatgenoten: **Onno**, zonder jou waren de 'deconcolved' plaatjes in het autofagie paper nooit zo mooi geworden. Dank voor je hulp. Je hebt ongelofelijk veel talent op veel verschillende vlakken. **Marijke**, dank voor het tot buikpijn toe lachen op werk en tijdens de Roparun. **Paulette**, onze klik is iets bijzonders. Je was mijn steun en toeverlaat in die eerste jaren op het lab. Dank voor je eerlijke, oprechte

zelf. Never change! **Eric**, Bindelsie! Wat had ik zonder jou moeten doen? Het is een oprechte vraag en ik weet het antwoord: niets. Dank voor alles Eric, je hulp vóór en tijdens experimenten, je onbegrensde expertise, het af en toe gebruik maken van je razendsnelle brein. Je bent een bijzonder onzelfzuchtig persoon die ik ontzettend waardeer.

Verder zou de flowcytometrie niet zo soepel draaien zonder de onvermoeibare inzet van **Elwin** en **Peter**, zou de afdeling niets zijn geweest zonder de planning en organisatie van **Ans** en **Leenke** en zouden de computers uit elkaar vallen zonder **Jan**. Dank ook aan **François**, **Joyce**, **Annelieke**, **Jasper**, **Nathalie, Isabel**, **Wendy**, **Pauline**, **Sonja**, **Marloes**, **Chantal**, **Antoinette**, **Remco**, **Rowan**, **Erdogan**, **Stefan**, **Marije**, **Claudia**, **Renée**, **Mark**, **Hansieeeeh**, **Tomasia**, **Menno**, **Anita**, **Niken**, **Monica**, **Kerim**, **Leonie**, **Yvette**, **Egied**, **Si**, **Jana**, **Keane** en **Julia** voor alle mooie momenten binnen en buiten het lab.

En natuurlijk dank aan alle groepsleiders, postdocs, PhD studenten en analisten die hebben bijgedragen aan de wetenschappelijk discussies tijdens de research meetings. In het bijzonder: **Jan Cornelissen**, **Tom Cupedo**, **Eric Braakman**, **Bob Löwenberg**, **Ivo Touw**, **Ruud Delwel**, **Pieter Sonneveld**, **Mojca Jongen-Lavrencic**, **Peter Valk**, **Marc Raaijmakers**, **Stefan Erkeland** en **Ferry Cornelissen**.

Mijn PhD periode vervolgde twee verdiepingen hoger: afdeling Pediatrische Oncologie. De volgende mensen hebben mijn laatste jaren als PhD student geweldig gemaakt.

Ten eerste mijn kamergenoten van (met trots) "the little boys room": man o man wat hebben we gelachen. **Mark**, jou imitaties en lach doen wonderen op mijn lachspieren en humeur en vermoeien nooit, succes met jouw laatste loodjes! **João**, you are awesome man, still every time we meet in Rotterdam, we connect so easily. It's been great working with and alongside you and I'll never forget all the amazing lab, soccer and MTB moments. Let there be more! **Lieneke**, je hebt wat te verdragen gehad bij ons op de kamer, maar die zachte gniffel links van me zei gelukkig alles. Wat ben ik blij dat je een mooie nieuwe baan gevonden hebt. Succes met het afronden van je thesis. **Judith**, je hebt een bijzondere rol in de groep, maar ook daarbuiten. Dank voor je wetenschappelijke en biostatistische adviezen, maar vooral ook voor je ongebreidelde enthousiasme op een mountainbike. **Alex**, achter het roze folie zat jij verscholen achter twee beeldschermen te R-en. Dank dat je er was, binnen én buiten de groep. **Priscilla**, mooi hoe jij gegroeid bent vanuit je rol als student tot volwaardig PhD student. Dank voor het organiseren van de escape-room uitjes.

De andere leden van de "B-ALL groep": **Rosanna**, je hebt me enorm geholpen om het LARG verhaal van de grond te krijgen. Dank voor al je hulp en tijd! **Isabel**, your German gründlichkeit is combined with a nice dose of chaos, I love it, thanks

for the great moments in and out the lab. **Femke**, het was eigenlijk best dapper van je om op onze sneltrein te springen, maar je hebt je geweldig staande gehouden. Dank voor je inzet en betrokkenheid. **Aurelie**, ik heb je besmet met het mountainbike virus en sindsdien ben je dé drijvende kracht achter onze MTB avonturen, dank voor je fijne aanwezigheid in en buiten het lab. **Lieke**, dank voor je inzet bij het opzetten van de MSC database, zonder jou was die niet zo bruikbaar geweest. Ik herinner me de goede momenten tijdens het congres in Praag. **Myrte**, ook jij was een essentiële schakel in het opzetten van de MSC databank, hartelijk dank daarvoor én voor je Brabantse gezelligheid. **Farhad**, I still remember the huge bacterial culture flasks you used for the microvesicle project and especially the face of Theo when he found out about it. **Ingrid** en **Cesca**, dank voor jullie opbouwende kritiek tijdens de wekelijke research meetings.

Mijn ML I/II lab-maatjes: **Rui**, we had a great time together in the lab. It was really nice to have someone at the same phase of his PhD period, just knowing that you're not alone helps. Thanks for all the fun. **Dirk**, je bent denk ik de grootste fan van ons onderzoek. Wat hebben we veel naast elkaar gezeten tijdens alle mega-experimenten die langs zijn gekomen. Je bent een onderzoeker in hart en nieren en hebt een bijzonder talent. Veel dank dat we bij tijd en wijlen gebruik mochten maken van je brein en met je konden sparren over onze dwaze ideeën. Zoals al eerder benoemd zijn de analisten van de oncologie groepen die de "patiëntendienst" runnen een essentieel onderdeel van ons lab. Maar dat geldt ook voor de inzet van de andere analisten: **Ad**, **Theo** (ik kom zeker nog een keer naar die stem van je luisteren), **Dicky**, **Lilian**, **Lisette**, **Rolien**, **Sylvia** (door jouw aanwezigheid is het lab een stuk veiliger), **Ytje**, **Lisette**, bedankt! En zonder **Marcel** en **Ram** was het lab in elkaar gestort, dank voor jullie inzet voor het algemene belang van iedereen in het lab.

Veel dank ook aan de groepsleiders, postdocs en PhD studenten van het lab kindergeneeskunde voor jullie bijdragen aan het wetenschappelijke klimaat en de feedback op mijn studies: **Eddy**, **Patricia**, **Arian**, **Jasmijn** en **Daria** (mijn ASH buddies), **Noorie**, **Askar**, **Nicole**, **Celia**, **Linda**, **Sharon**, **Marieke**, **Léa**, **Kirsten**, **Yunlei**, **Patrick**, **Janneke Samson**, **Cees Vink** en in het bijzonder **Maarten Fornerod**, **Michel Zwaan**, **Marry van den Heuvel-Eibrink**, **Ronald Stam**, en **Jules Meijerink.**

Na het doen van al die experimenten en het bouwen van de papers, moet er nog een proefschrift tot stand komen. Naast een full time baan als kinderarts in opleiding is dat een hele kluif en heb je de steun vanuit de kliniek nodig. Daarom heel veel dank aan de arts-assistenten en kinderartsen van het **Wilhelmina Kinderziekenhuis**, het **Prinses Máxima Centrum voor Kinderoncologie** en het **Sint Antonius Ziekenhuis** die me gesteund hebben gedurende deze periode. In het bijzonder mijn opleiders:

Walter Balemans, **Maartje ten Berge**, **Ingrid Lukkassen**, **Edward Nieuwenhuis** en **Joost Frenkel**, veel dank voor jullie altijd aanwezige vertrouwen en steun.

Vrienden en familie zijn het fundament waar alles op rust. Jullie waardering, liefde en zijn maken mij wie ik ben en maken het leven geweldig.

De **America's**, ultieme levensgenieters, onverslaanbaar in goede diners en gierende lachen, laten er nog velen komen! De **Polakken**, een liefdevol en prachtig gezelschap met oma als stralend middelpunt. Het is zo jammer dat je dit net gemist hebt. En die familiedag, die komt er!

Steefie, mijn oudste en trouwste vriend, ik ken je al sinds de peuterspeelzaal en wat is het bijzonder dat ondanks onze totaal andere paden en levens, we zó belangrijk voor elkaar zijn. Dank voor je steun door dik en dun.

Loukie, **Jorie**, **Roos**(je) en **Birgit,** jullie maken ook van jongs af aan deel uit van mijn leven. Hoe bijzonder is het dat het bij ons niet uit maakt hoe lang er tussen diners zit, of wat er ook gebeurd is, de warmte en vriendschap is er direct en altijd.

Maarten, Mortimer, en **Daniel**, we kennen elkaar sinds de brugklas en hebben ons sindsdien nooit meer verveeld. Die legendarische fietsvakanties moeten we misschien toch nog een keer overwegen?

Anne-Lieke, we hebben een geweldige tijd gehad samen en je bent heel belangrijk geweest tijdens het eerste deel van mijn promotie. Dank voor je steun en liefde in die tijd.

Rolex, mannen van het goede leven, het is een geweldige ervaring jullie als vrienden te mogen hebben. **Dirk**, je out-of-the-box denken is een voorbeeld voor velen, zeker voor mij. **Gijs**, je humor en intense goedheid stralen uit op alles wat je doet en iedereen om je heen. **Arjan**, niet alleen roeiploeggenoot, maar ook werkgroepgenoot én huisgenoot; wat hebben we genoten! **Paul**, jij en **Renske** hebben een bijzondere plek in ons hart. Onze klik is heel speciaal denk ik. We hebben samen zoveel meegemaakt en ons Nicaragua avontuur staat ergens bovenaan de mooiste momenten van mijn leven.

Dan mijn paranimfen. Ik ben ontzettend trots dat jullie achter me staan op 22 november.

Maarten, vaak groeien goede vrienden van de middelbare school langzaam uit elkaar en heel soms gebeurt juist het tegenovergestelde. Sinds dat we elkaar kennen zijn we langzaam steeds dichter bij elkaar gekomen en stiekem ook steeds meer op elkaar gaan lijken. We denken op soms verbazingwekkend gelijke wijze, en kunnen elkaar daardoor op precies de juiste manier en op precies de juiste momenten scherp houden. Dank voor je ongelimiteerde vriendschap.

Bob, er zijn maar weinig mensen in je leven die wetenschappelijk denkend zo op één lijn zitten en die je blindelings vertrouwt in een wereld die niet altijd te vertrouwen is. Jij bent die persoon voor mij. Ons wetenschappelijk avontuur heeft me laten beseffen dat ik nooit meer zonder die 'rushes' wil. Dank voor alle mooie momenten, dat onvergetelijke gegrinnik, en vooral dank voor je vriendschap.

Lieve **Ton** en **Elly**, wat een geluk hebben wij met jullie aan onze zijde! Jullie hebben een essentiële rol in het functioneren van ons gezin. Het is fantastisch om te zien hoe jullie van Max genieten en, vice versa, hoe Max geniet en opfleurt van de oppasdagen bij opa Ton en oma Elly. Het is niet te beschrijven hoeveel dat waard is. Dank voor alles.

Lieve **Annemarie**, zussie! je bent een topper en wat ben ik trots op je! Jouw doorzettingsvermogen en vertrouwen in wie je bent verdienen een diepe buiging. Dank voor je liefde en dank voor het scherphouden van die broer van je.

Lieve **pappa en mamma**, zonder jullie was ik nooit gekomen waar ik nu ben en vooral nooit geweest wíe ik nu ben. Jullie zijn mijn basis, mijn grootste fans. Jullie kennen me als geen ander. Ik realiseer me dat mijn manier van leven jullie ook veel zorgen oplevert en het doet soms pijn om daar doorheen te walsen. Niet vergeten hoeveel ik van jullie hou. **Mam**, je bent de liefste 'self-made woman' die ik ken, op alle fronten, en het grappige is dat jij je dat niet eens realiseert. De intensiteit van ons gevoel is wat mij betreft een groot cadeau. **Pap**, je bent mijn grote voorbeeld vanaf kleine jongen tot op de dag van vandaag. Wij hebben samen altijd een heel speciale band gehad. Onuitgesproken, en dat hoeft ook niet. Een blik of zelfs minder dan dat is genoeg om elkaar te begrijpen. Zo bijzonder. Dank voor jullie onvoorwaardelijke liefde.

"Look at the stars, look how they shine for you and everything you do"
Lieve **Max**, wat een prachtig mooi ventje ben jij, ik ben zo trots op je! Ik geniet met volle teugen van jou 'zijn'. Je maakt het leven geweldig mooi.

Lieve **Merel**, mijn droomvrouw en mijn belangrijkste steunpilaar. Het is me nog steeds een raadsel waar ik je aan verdien. Je bent lief, je hebt humor, je bent getalenteerd en intelligent, je bent prachtig mooi, je bent de beste moeder van de wereld. Trots overspoelt me als ik aan je denk. Ik weet niet hoe ik het zonder je had moeten doen in de afgelopen jaren. Dank voor je alles betekenende liefde en steun. Dankzij jou kan ik zijn wie ik ben. Ik kijk ontzettend uit naar onze toekomst.